

**Katholieke Universiteit Leuven
Groep Biomedische Wetenschappen**

**Faculteit Bio-ingenieurswetenschappen
Departement Biosystemen, Afdeling Gentechnologie**



Molecular and mutational analysis of a wheat thaumatin-like xylanase inhibitor (TLXI)

Sigrid Rombouts

Doctoraal proefschrift in de Farmaceutische Wetenschappen

Leuven, 2007

**Katholieke Universiteit Leuven
Groep Biomedische Wetenschappen**

**Faculteit Bio-ingenieurswetenschappen
Departement Biosystemen, Afdeling Gentechnologie**



Molecular and mutational analysis of a wheat thaumatin-like xylanase inhibitor (TLXI)

Sigrid ROMBOOTS

Jury:

Promotor: Prof. Guido Volckaert
Copromotor: Prof. Anja Rabijns
Voorzitter: Prof. Arthur Van Aerschot
Leden: Prof. Ann Gils
 Prof. Johan Robben
 Prof. Luc Van Meervelt
 Dr. Ir. Kurt Gebruers

Leuven, 5 april 2007

Doctoraal proefschrift in de Farmaceutische Wetenschappen

Auditorium Heuts
Kasteelpark Arenberg 20
Leuven

Donderdag 5 april 2007, 17.00 uur

Promotor: Professor Guido Volckaert
Copromotor: Professor Anja Rabijns

Table of contents

Table of contents	i
Dankwoord	v
List of abbreviations	vii
Chapter 1 The players: arabinoxylans, xylanases and xylanase inhibitors	3
1.1 Introduction	3
1.2 The substrate: (arabino)xylan	3
1.3 The enzymes: xylanases	5
1.3.1 Classification of xylanases	6
1.3.2 Glycoside hydrolase family 10 xylanases	7
1.3.3 Glycoside hydrolase family 11 xylanases	8
1.3.4 <i>In vivo</i> functions and industrial applications of xylanases	9
1.4 The inhibitors: xylanase inhibitors	10
1.4.1 TAXI-type inhibitors	11
1.4.2 XIP-type inhibitors	15
1.4.3 A novel type of xylanase inhibitors: TLXI	20
1.4.4 Potential role of xylanase inhibitors in biotechnological applications	21
Chapter 2 Thaumatin-like proteins	23
2.1 Introduction	23
2.2 Thaumatin	23
2.3 Thaumatin-like proteins	26
2.3.1 Activities ascribed to TLPs	26
2.3.2 Potential applications of TLPs	32
Background and aims of the study	35
Chapter 3 Molecular identification of the TLXI encoding gene	39
3.1 Introduction	39
3.2 Materials and methods	40
3.2.1 Standard molecular biology techniques	40
3.2.2 Isolation of plant genomic DNA and mRNA	40
3.2.3 Rapid amplification of cDNA ends (RACE)	40
3.2.4 Polymerase chain reaction (PCR) on genomic DNA	41
3.2.5 Thermal asymmetric interlaced (TAIL) PCR	42
3.2.6 pCR [®] 4-TOPO cloning	44
3.2.7 Primers used in this chapter	44
3.3 Results	45
3.3.1 Identification of the <i>tlxi</i> gene in hexaploid wheat (<i>T. aestivum</i>)	45
3.3.2 Genetic variation	48
3.4 Discussion	53
3.5 Conclusions	59
Chapter 4 Recombinant expression of TLXI	61
4.1 Introduction	61
4.2 Materials and methods	62
4.2.1 Standard molecular biology techniques	62
4.2.2 <i>E. coli</i> and <i>P. pastoris</i> strains and growth media	62
4.2.3 Construction of expression plasmids	64
4.2.4 Transformation of host cell organism	66

4.2.5	Recombinant expression	68
4.2.6	Xylanase inhibition assay	70
4.2.7	Protein electrophoresis	71
4.2.8	Purification of recombinant TLXI by cation exchange chromatography (CEC)	71
4.2.9	TLXI content determination	72
4.2.10	Western blot analysis	72
4.2.11	Primers used in this chapter	73
4.3	Results	74
4.3.1	Expression of TLXI in <i>E. coli</i>	74
4.3.2	Expression optimization of recombinant TLXI in <i>P. pastoris</i>	75
4.3.3	Production of rTLXI in <i>P. pastoris</i>	81
4.3.4	Purification of rTLXI with CEC	82
4.4	Discussion	83
4.5	Conclusions	87
Chapter 5 Biochemical characterization of rTLXI		89
5.1	Introduction	89
5.2	Materials and methods	89
5.2.1	Materials	89
5.2.2	Iso-electric focusing and protein electrophoresis	90
5.2.3	Xylanase inhibition assay	90
5.2.4	Glycosylation analysis	92
5.2.5	Binding to polysaccharides	93
5.3	Results	94
5.3.1	Biochemical characteristics of rTLXI	94
5.3.2	Inhibition specificity	97
5.3.3	Binding of rTLXI to polysaccharides	99
5.4	Discussion	101
5.5	Conclusions	105
Chapter 6 Mutational analysis of TLXI to gain insight in its interaction with GH11 xylanases		107
6.1	Introduction	107
6.2	Materials and methods	107
6.2.1	Standard molecular biology techniques	107
6.2.2	Molecular biological techniques	108
6.2.3	Site-directed mutagenesis	108
6.2.4	Protein content determination	110
6.2.5	Gel permeation chromatography (GPC)	110
6.2.6	Circular dichroism (CD) measurements	111
6.2.7	Modeling	111
6.3	Results	111
6.3.1	Three-dimensional model of TLXI	111
6.3.2	Selection, construction and recombinant expression of the mutants	113
6.3.3	Inhibition activity of the mutants	115
6.3.4	Gel permeation chromatography (GPC)	118
6.3.5	CD analysis	120
6.3.6	Western blot	121
6.3.7	Docking model of the ExIA/TLXI complex	122
6.4	Discussion	123
6.5	Conclusions	126
Chapter 7 Recombinant expression and characterization of TLXI variants and related sequences		127
7.1	Introduction	127
7.2	Materials and methods	127
7.2.1	Standard molecular biology techniques	127
7.2.2	Molecular biology techniques	127

7.2.3	Isolation of the genes encoding the mature protein	128
7.3	Results	129
7.3.1	Recombinant expression and purification	129
7.3.2	Biochemical characterization	131
7.4	Discussion	133
7.5	Conclusion	136
Chapter 8 Recombinant expression and mutational analysis of <i>A. niger</i> xylanase to gain insight in the interaction with TLXI		139
8.1	Introduction	139
8.2	Materials and methods	140
8.2.1	Standard molecular biology techniques	140
8.2.2	Molecular biological techniques	140
8.2.3	Isolation of the <i>exlA</i> coding sequence and construction of the expression plasmid	140
8.2.4	Site-directed mutagenesis	140
8.2.5	Purification with anion exchange chromatography (AEC)	141
8.2.6	Protein content determination	141
8.2.7	Xylanase activity assay	141
8.2.8	Kinetic analysis of rExlA	142
8.2.9	Gel permeation chromatography (GPC)	143
8.2.10	Kinetic analysis of rTLXI	143
8.2.11	Primers used in this chapter	144
8.3	Results	144
8.3.1	Recombinant expression and purification of rExlA and rExlA _[D37A]	144
8.3.2	Xylanase activity assay and pH optimum	144
8.3.3	Kinetic analysis of rExlA	145
8.3.4	Xylanase inhibition assay	148
8.3.5	Gel permeation chromatography (GPC)	148
8.3.6	Kinetic analysis of rTLXI	150
8.4	Discussion	152
8.5	Conclusions	157
General conclusions and future prospects		159
Summary		163
Samenvatting		167
References		171
Curriculum Vitae		185

Dankwoord

Het is me gelukt... Heel gelukkig ben ik en ook fier dat 'mijn boekje' nu een plaatsje kan krijgen in onze boekenkast. Een heleboel mensen - het is een onbegonnen taak om deze allen bij naam te noemen - hebben de voorbije jaren hun rechtstreekse of onrechtstreekse bijdrage geleverd aan het tot stand komen van dit proefschrift. Hierbij wil ik hen van harte danken. Tot een aantal personen wil ik graag een persoonlijk woordje van dank richten omdat ze één voor één, op hun eigen specifieke manier, voor mij heel wat hebben betekend.

Mijn promotor, prof. Volckaert, wil ik graag bedanken omdat hij me de mogelijkheid heeft geboden om aan de slag te kunnen in het Labo voor Gentechnologie, eerst als medewerker van het 'Xylafun' project, daarna als doctoraatsstudent met 'mijn eigen' IWT-beurs. Mijn dank gaat ook uit naar mijn co-promotor, prof. Rabijns, omdat ze altijd klaarstond om allerlei vragen te beantwoorden.

Zonder de steun van mijn 'coach' Steven Van Campenhout, was dit werk nooit kunnen worden tot wat het nu is. Steven, jouw ideeën en niet aflatend enthousiasme hebben me telkens weer in de juiste richting geduwd en hebben me na elke tegenslag weer de moed gegeven om verder te gaan. Merci!

Of je je werk graag doet, hangt voor een groot deel ook af van je collega's. Hen wil ik dan ook bedanken voor de aangename jaren die ik op het labo heb mogen beleven. In het bijzonder denk ik hierbij aan mijn bureaugenootjes Tine, Stijn en Barbara voor de leuke babbels tussendoor over koetjes en kalfjes en voor de discussies over hoe deze inhibitor nu toch zou kunnen werken. Ook Gert en Tim, de andere 'Xylafunners' van het lab, zijn voor mij een grote steun geweest. Jullie 'peptalk' op momenten dat het minder goed ging, heeft enorm veel voor mij betekend. Al mijn andere collega's (het zou wat veel plaats vergen om hen allemaal persoonlijk te bedanken en het zou te gevaarlijk zijn om iemand te vergeten) wil ik stuk voor stuk bedanken. Ik wens hen allemaal nog veel succes toe in alles wat ze doen (doctoreren, trouwen, samenwonen, kindjes krijgen,...). 'Mijn' thesisstudenten John, Steve, Stan en Filip, merci voor al het werk dat jullie hebben verricht. Ik hoop dat jullie evenveel van mij hebben geleerd als ik van jullie.

Zonder de hulp van een aantal mensen van 'buitenaf' zou dit boekje een stuk dunner geweest zijn of zou het er zelfs helemaal niet zijn geweest. Van het Labo voor Levensmiddelenchemie denk ik hierbij aan prof. Delcour, die me een aantal jaren geleden heeft geïntroduceerd in de onderzoekswereld door me de mogelijkheid te geven om te werken op glucanasen. Kurt wens ik te bedanken omdat hij TLXI heeft 'ontdekt'. Kurt, ik moet toegeven dat ik je soms ook heb vervloekt omdat je het ding ontdekt had, maar al bij al ben ik toch blij dat ik dankzij jouw 'ontdekking' dit onderzoek heb kunnen doen. Samen met Ellen heb ik geprobeerd het mysterie van TLXI wat op te helderen. Ellen, bedankt voor de fijne samenwerking en voor alle hulp. Ik

vond het fijn dat we ondanks de 'miserie' er toch nog om konden blijven lachen (soms wel wat groen). Ik wens je nog veel succes toe en hoop dat je het komende jaar nog veel nieuwe dingen mag ontdekken over TLXI (maar liefst geen dingen die mijn hypothesen tegenspreken). Johnny Beaugrand wil ik graag bedanken voor het uitvoeren van de Western blots.

Elien van het Labo voor Biokristallografie ben ik zeer erkentelijk voor haar geduld en doorzettingsvermogen om TLXI en het complex te kristalliseren. Prof. De Maeyer en Arnout van het Labo voor Biomoleculaire Modelling ben ik zeer dankbaar voor het maken van de modelstructuur van TLXI en van het complex. Bedankt dat ik met al mijn vragen bij jullie terecht kon en dat jullie je geduld nooit hebben verloren ondanks jullie drukke bezigheden.

Ik kon ook altijd op de steun rekenen van mijn toekomstige schoonouders. Bedankt omdat ik bij jullie altijd welkom ben en voor het bijspringen bij het huishoudelijke werk in drukke tijden!

Het IWT wil ik graag bedanken voor de financiële steun die ze mij gaven als specialisatiebursaal. Alle juryleden ben ik erkentelijk voor het nalezen van dit doctoraatswerk en voor de suggesties die zij deden ter verbetering ervan.

Tot slot wil ik degenen bedanken die me het nauwst aan het hart liggen. Mama en papa, bedankt voor alle kansen die jullie me hebben gegeven. Zonder jullie stond ik niet waar ik nu sta. Geen woorden kunnen beschrijven hoe dankbaar ik jullie ben. Ook mijn 'broeder' mag ik natuurlijk niet vergeten te vermelden voor de interesse in mijn werk en voor de vele bemoedigende knuffels. Ik hoop, en ik twijfel er niet aan, dat je al je dromen kan waarmaken. Misschien word jij wel de tweede 'doctor' in ons gezin?

En dan, last but not least, mijn 'toekomstige', David. Zonder jou was me dit nooit gelukt. Eerst en vooral had zonder jou dit boekje er lay-out-gewijs niet zo mooi uitgezien. Maar daarenboven had ik zonder je troost, luisterbereidheid (ondanks het feit dat je er niks van snapte) en relativiseringsvermogen misschien al lang opgegeven. Bedankt om er altijd te zijn voor mij, schattie. Je bent er één uit de duizend!

Sigrid,

Maart 2007

List of abbreviations

Å	Ångström	LDL	low density lipoproteine
ABA	abscisic acid	LMW	low molecular weight
ABRE	abscisic acid -responsive element	LSLB	low salt LB (medium)
AD	arbitrary degenerate	Mal d 2	thaumatin-like protein from <i>Malus domestica</i> (apple)
AEC	anion exchange chromatography	Man	mannose
AOX1	alcohol oxidase 1 from <i>P. pastoris</i>	(m)AU	(milli) absorbance units
APS	ammonium peroxodisulphate	MBS	MYB binding site
as-1	activation sequence-1	milliQ water	deionized water (Millipore)
AX	arabinoxylan	MOE	The Molecular Operating Environment
AXOS	arabinoxyloligosaccharides	mRNA	messenger ribonucleic acid
A _{xnm}	absorbance at x nm	Mut	methanol utilization phenotype
BLAST	basic local alignment search tool	Mut ⁺	wild-type methanol utilization phenotype
BLASTp	protein-protein BLAST	Mut ^S	methanol utilization slow phenotype
BMGY	buffered glycerol-complex medium	4-MUX ₂	4-methylumbelliferyl-beta-D-xylobioside
BMMY	buffered methanol-complex medium	MWCO	molecular weight cut-off
bp	base pairs	MYB	myeloblastosis oncogene
BSA	bovine serum albumin	NCBI	National Center for Biotechnology Information
CAZy	Carbohydrate Active Enzymes database	N-terminal	amino-terminal
CBD	cellulose-binding domain	OD _{600nm}	optical density at 600 nm
CD	circular dichroism	P	product
cDNA	complementary deoxyribonucleic acid	PBS	phosphate-buffered saline
CEC	cation exchange chromatography	PCR	polymerase chain reaction
C-terminal	carboxy-terminal	PDB	Protein Data Bank
cv.	cultivar	PEG	polyethylene glycol
3D	three-dimensional	<i>Pfu</i>	<i>Pyrococcus furiosus</i>
DNA	deoxyribonucleic acid	pI	iso-electric point
DNS	dinitro salicylic acid	PlantCARE	plant cis-acting regulatory elements
dNTP	deoxynucleoside triphosphate	PNGaseF	peptide-N-glycosidase F
EDTA	ethylene diamine tetra-acetic acid	PR	pathogenesis-related
ER	endoplasmic reticulum	RACE	rapid amplification of cDNA ends
ERF	ethylene-response factor	RNA	ribonucleic acid
EST	expressed sequence tag	(r)AS-TLXI	(recombinant) TLXI from <i>Aegilops speltoides</i>
GH	glycoside hydrolase family	(r)TAXI	(recombinant) <i>Triticum aestivum</i> xylanase inhibitor
GlcNAc	N-acetylglucosamine	(r)TLXI	(recombinant) thaumatin-like xylanase inhibitor
GPC	gel permeation chromatography	S	substrate
HADDOCK	high ambiguity driven protein-protein docking	S.D.	standard deviation
I	inhibitor	S.E.M.	standard error of the mean
IC ₅₀	molar I/E ratio needed to obtain 50% inhibition of the tested xylanase	SC-TLXI	TLXI from <i>Secale cereale</i>
IPTG	isopropyl-1-thio-β-D-galactopyranoside	SDS	sodium dodecyl sulphate
IU	inhibition unit	SDS-PAGE	sodium dodecyl sulphate polyacrylamide gel electrophoresis
Jun a 3	thaumatin-like protein from <i>Juniperus ashei</i> (mountain cedar)	t	time
k	apparent first-order rate constant	TAIL-PCR	thermal asymmetric interlaced polymerase chain reaction
k _{cat}	catalytic constant		
kDa	kilodalton		
K _i	inhibition constant		
K _m	Michaelis-Menten constant		
LB	Luria-Bertani (medium)		

List of abbreviations

tBLASTn	protein query vs. translated database	v_0	initial velocity
TEMED	N,N,N',N'-tetramethylethylenediamine	V_{max}	maximal velocity
TFMSA	trifluoromethane sulfonic acid	v_S	steady state velocity
TIM	triosephosphate isomerase	WE-AX	water-extractable arabinoxylan
TLP	thaumatin-like protein	WRTL2P	winter rye thaumatin-like protein
TMV	tobacco mosaic virus	WU-AX	water-unextractable arabinoxylan
Tris	Tris-[hydroxymethyl]-amino methane	XIP	xylanase inhibitor protein
U	enzyme unit	YPD	yeast extract peptone dextrose (medium)
UTR	untranslated region	YPDS	yeast extract peptone dextrose sorbitol (medium)
UV	ultraviolet		

Xylanases

XylD	endo-1,4-xylanase D from <i>Cellulomonas fimi</i>
XynI	endo-1,4-xylanase 1 from <i>Trichoderma longibrachiatum/reesei</i>
XynII	endo-1,4-xylanase 2 from <i>Trichoderma longibrachiatum/reesei</i>
XynA	endo-1,4-xylanase A from <i>Bacillus subtilis</i>
XylI	endo-1,4-xylanase from <i>Streptomyces</i> sp. S38
XlnC	endo-1,4-xylanase from <i>Aspergillus nidulans</i>
XynC	endo-1,4-xylanase C from <i>Penicillium funiculosum</i>
(r)ExIA	(recombinant) endo-1,4-xylanase from <i>Aspergillus niger</i>

Amino acid abbreviations

A	Ala	Alanine
C	Cys	Cysteine
D	Asp	Aspartate
E	Glu	Glutamate
F	Phe	Phenylalanine
G	Gly	Glycine
H	His	Histidine
I	Ile	Isoleucine
K	Lys	Lysine
L	Leu	Leucine
M	Met	Methionine
N	Asn	Asparagine
P	Pro	Proline
Q	Gln	Glutamine
R	Arg	Arginine
S	Ser	Serine
T	Thr	Threonine
V	Val	Valine
W	Trp	Tryptophan
Y	Tyr	Tyrosine

PART I
INTRODUCTION

Chapter 1

The players: arabinoxylans, xylanases and xylanase inhibitors

1.1 Introduction

Arabinoxylans are the most important non-starch polysaccharides in wheat (*Triticum aestivum*) and have a strong impact on the functionality of wheat grains, or fractions thereof, in biotechnological processes. Their occurrence, structure and impact on human health will be discussed. Furthermore, this chapter focuses on endoxylanases, further referred to as xylanases, the biotechnologically most important xylolytic enzymes. The classification of this group of enzymes will be explained and special emphasis will be paid to family 10 and family 11 xylanases, and more particularly to their biochemical and structural features and substrate specificity. In addition, the industrial applications and *in vivo* functions of microbial xylanases will be highlighted. Finally, the characteristics, structures and *in vivo* functions of the two currently described proteinaceous inhibitors of xylanases will be presented including their potential use in biotechnological applications. Furthermore, the interaction of these inhibitors with xylanases and the factors governing their specificity will be explained. The molecular identification, recombinant expression, characterization and mutagenesis of a third, recently isolated, xylanase inhibitor forms the subject of this dissertation.

1.2 The substrate: (arabino)xylan

The plant cell is protected from its surrounding environment by the cell wall. Together with cellulose (1,4- β -glucan) and lignin (a complex polyphenolic compound), hemicellulose makes up the major polymeric constituent of plant cell walls (Kulkarni *et al.*, 1999). The term hemicellulose refers to a group of carbohydrates in which heteroxylan, a heteropolysaccharide with a backbone consisting of 1,4-linked β -D-xylopyranose units, forms the major class. Xylan varies in structure between different plant species and the homopolymeric backbone chain can be substituted to varying degrees with glucuronopyranosyl, 4-O-methyl-D-glucuronopyranosyl, α -L-arabinofuranosyl, acetyl, feruloyl and/or *p*-coumaroyl side-chain groups (Kulkarni *et al.*, 1999; Li *et al.*, 2000) (Figure 1-1). Xylans in grasses, like wheat, are typically arabinoxylans (Kulkarni *et al.*, 1999), substituted with arabinofuranosyl groups.

Although arabinoxylans can be divided in water-extractable (WE-AX) and water-unextractable (WU-AX) arabinoxylans, displaying different physicochemical properties, a common structure, as described above, exists.

Due to its heterogeneity and complexity, the complete hydrolysis of xylan requires a large variety of synergistically acting enzymes (Figure 1-1) (Subramaniyan and Prema, 2002). Endo-1,4- β -xylanases (EC 3.2.1.8) depolymerize xylan by the random hydrolysis of the xylan backbone. The side groups present in xylan are liberated by α -L-arabinofuranosidase (EC 3.2.1.55), α -D-glucuronidase (EC 3.2.1.139), phenolic acid (*p*-coumaric and ferulic acid) esterase (EC 3.1.1.- and 3.1.1.73, respectively) and acetyl xylan esterase (EC 3.1.1.72). 1,4- β -D-Xylosidases (EC 3.2.1.37) attack the non-reducing end of xylo-oligosaccharides that are generated by the action of endoxylanases and liberate xylose.

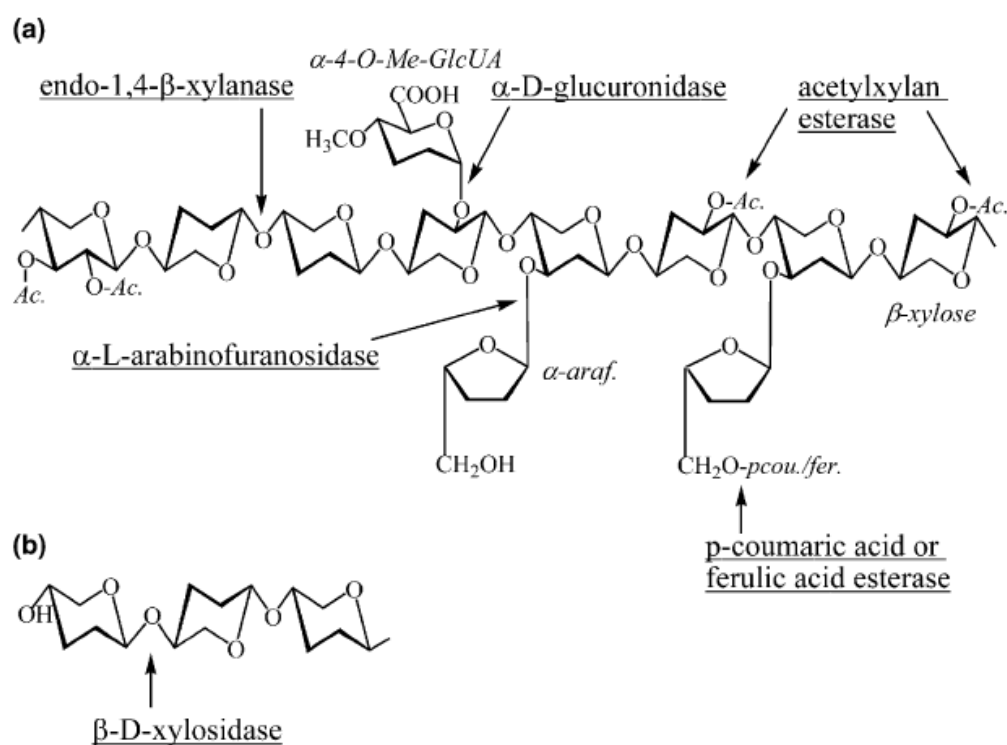


Figure 1-1: (a) Structure of heteroxylan and the sites of attack by xylanolytic enzymes. The backbone of the substrate is composed of 1,4- β -linked xylose residues. (b) Hydrolysis of xylo-oligosaccharides by β -xylosidase (Collins *et al.*, 2005).

Ac., acetyl group; α -araf., α -arabinofuranose; α -4-*O*-Me-GlcUA, α -4-*O*-methylglucuronic acid; pcou., *p*-coumaric acid; fer., ferulic acid.

Arabinoxylans are a major component of dietary fiber in cereal grains (Holloway *et al.*, 1980; Henry, 1985), which is a collective term for a variety of plant substances that are resistant to digestion by human gastrointestinal enzymes (Eastwood and Passmore, 1983). They are a source of soluble and insoluble fiber, displaying different physicochemical properties. These properties determine their physiological effect. Whereas soluble fiber forms viscous gels in the intestinal tract, insoluble fiber does not exhibit viscosity. The most widely recognized benefits of dietary fiber have been related to gastrointestinal function. These effects can mainly be attributed to the insoluble fibers. Insoluble fibers lead to laxation and decreased intraluminal pressure. By decreasing the intestinal transit time, the colon is protected from prolonged exposure to cytotoxic substances which may also be carcinogenic. The metabolic responses to dietary fibers are related to viscosity and fermentability which are more characteristic of soluble fiber. By forming viscous solutions, soluble fibers delay gastric emptying which contributes to appetite regulation, making it an important factor in the control of obesity (Brennan, 2005). Soluble fibers also lead to lower postprandial blood glucose levels (Brennan, 2005) and to a decrease in serum (LDL) cholesterol (Brown *et al.*, 1999). These effects improve glycaemic control in type II diabetes and lower the risk of cardiovascular disease, respectively. Fermentation of soluble fibers by the colonic microflora results in the release of short chain fatty acids (Davidson and McDonald, 1998). Acetate is utilized primarily as a fuel substrate by skeletal muscle. In addition, acetate and propionate affect hepatic cholesterol synthesis. For these reasons, cereals are an important component in the production of functional foods, foods that exert a beneficial effect on host health (Charalampopoulos *et al.*, 2002).

1.3 The enzymes: xylanases

Xylanases are hydrolytic enzymes which randomly cleave the β -1,4 backbone of the complex cell wall polysaccharide, heteroxylan. Xylanases occur in bacteria from marine and terrestrial environments, fungi, insects and plants (Dekker and Richards, 1976). Due to the heterogeneity and complexity of heteroxylan, diverse forms of these enzymes exist, displaying varying folds, mechanisms of action, substrate specificities, hydrolytic activities (yields, rates and products) and physicochemical characteristics. Furthermore, xylanases differ in their substrate selectivity, which has been defined as the relative activity of the xylanase towards WU-AX and WE-AX substrates (Moers *et*

al., 2003). Depending on the application, preferential attack of WU-AX or WE-AX by the xylanases is desired, while activity towards the other population is often undesirable.

The classification system of xylanases and glycoside hydrolases in general (EC 3.2.1.x.) is explained. Although xylanases have also been identified in glycoside hydrolase family (GH) 5, 7, 8 and 43 this paragraph only focuses on the characteristics of the xylanases belonging to the two most important families, GH10 and 11. A common feature of both enzyme families are their endo character and the double displacement mechanism of the hydrolysis of the glycosidic bond resulting in retention of anomeric configuration (Gebler *et al.*, 1992). In both families, the catalytic residues are two glutamate residues acting as a general acid/base catalyst and as a nucleophile, respectively (Biely *et al.*, 1997).

1.3.1 Classification of xylanases

In 1991 (Henrissat) a classification system was introduced which allowed the classification of not only xylanases, but glycoside hydrolases in general (EC 3.2.1.x), and which has now become the standard classification of these enzymes. This system is based on primary sequence comparison of the catalytic domains only and groups enzymes in families of related sequences. As the structure and molecular mechanism of an enzyme are related to the amino acid sequence, this classification system reflects both structural and mechanical features. To date, 106 glycoside hydrolase families exist according to the CAZy (Carbohydrate Active Enzymes database) web server (<http://afmb.cnrs-mrs.fr/CAZY/>) (Coutinho and Henrissat, 1999). Furthermore, divergent evolution has resulted in some of the families having related three-dimensional structures and thus the grouping of families into higher hierarchical levels, known as clans or superfamilies, has been introduced (Henrissat and Davies, 1997). Presently, 14 different clans have been proposed (GH-A to GH-N), with most clans encompassing two or three families, apart from clan GH-A which currently encompasses 17 families. Within this classification system, xylanases are normally reported as being confined to families 10 (clan GH-A) and 11 (clan GH-C). However, enzymes with xylanase activity have also been reported in GH5 (clan GH-A), 7 (clan GH-B), 8 (clan GH-M), and 43 (clan GH-F) (Collins *et al.*, 2005).

1.3.2 Glycoside hydrolase family 10 xylanases

Family 10 xylanases are produced by plants, bacteria and fungi and typically have a high molecular mass (≥ 30 kDa) and a low pI (Subramaniyan and Prema, 2002). They often contain substrate-binding domains (Jeffries, 1996) exhibiting specificity for cellulose (cellulose-binding domain, CBD) which are fused to the catalytic domain via linker sequences, often rich in proline, glycine and/or hydroxyamino acids (Gilbert and Hazlewood, 1993). Xylanases do not usually have xylan-specific binding domains, but one is present in the xylanase of *Cellulomonas fimi* (XylD) (Black *et al.*, 1995).

Enzymes belonging to family 10 exhibit greater catalytic versatility or lower substrate specificity than enzymes of family 11. They are capable of cleaving the main chain of the substrate closer to the substituents and can release shorter xylooligosaccharides than family 11 xylanases (Biely *et al.*, 1997). This greater catalytic versatility can be ascribed to differences in tertiary structures between xylanases belonging to family 10 and 11. Family 10 xylanases display an $(\alpha/\beta)_8$ barrel or TIM (triosephosphate isomerase)-barrel fold (Wierenga, 2001) (Figure 1-2). The catalytic acid-base and the nucleophilic residues are located at the end of β -strands 4 and 7, respectively (Jenkins *et al.*, 1995). The structure has been likened to a 'salad bowl' in which the substrate binds in the shallow groove. The fact that the substrate binding sites apparently are not such deep clefts as the substrate binding sites of family 11 xylanases together with a possible greater conformational flexibility of the larger family 10 xylanases, may account for the lower substrate specificity (Biely *et al.*, 1997).

Consistent with their endo-mode of action, the substrate binding cleft extends along the length of the proteins and can accommodate from four to seven xylose residues (Biely *et al.*, 1981; Charnock *et al.*, 1998). Each region that can accommodate a xylose moiety is known as a subsite. Subsites are given a negative or positive number depending on whether they bind the glycon or aglycon regions of the substrate, respectively. Glycosidic bond cleavage occurs between the -1 (glycon) and +1 (aglycon) subsites (Davies *et al.*, 1997). The crystal structures of several GH10 xylanases in complex with substrate or mechanistic inhibitors have revealed highly conserved amino acids, particularly in the -1 and -2 subsites, that play a key role in substrate recognition (Pell *et al.*, 2004). Although the three-dimensional structures of GH10 enzymes are highly conserved, the topology of their substrate binding clefts is very variable (Charnock *et al.*, 1998).

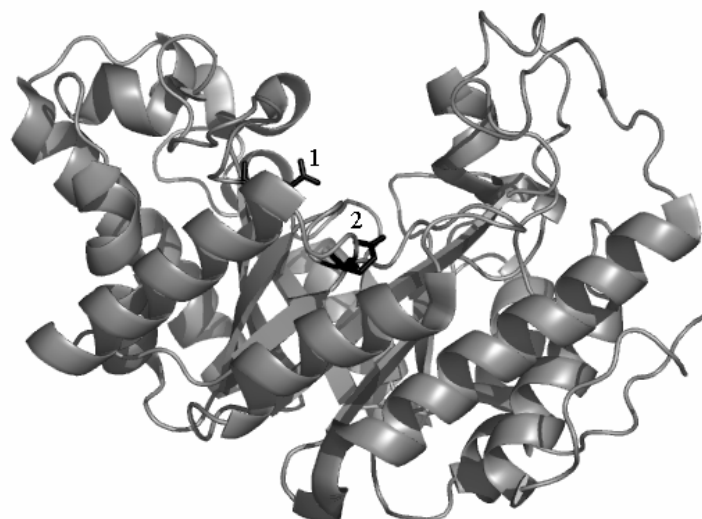


Figure 1-2: Three-dimensional structure of xylanase 10C from *Cellvibrio japonicus* (PDB entry 1us2; <http://www.rcsb.org/pdb/Welcome.do>) (Pell *et al.*, 2004).

The active site glutamates are indicated. 1 represents the acid/base glutamate and 2 the nucleophilic glutamate. The picture was generated with Pymol (Delano Scientific, San Francisco, CA, USA).

1.3.3 Glycoside hydrolase family 11 xylanases

The GH11 family is composed of highly specific low molecular mass xylanases (around 20 kDa) from eukaryotic and bacterial microorganisms sharing amino acid sequence identities varying from 40-90% (Törrönen and Rouvinen, 1997). GH11 xylanases have a lower catalytic versatility than GH10 xylanases and their reaction products can be further hydrolyzed by the GH10 xylanases (Biely *et al.*, 1997). Although family 11 is a very homologous group of enzymes, the pH optima of GH11 xylanases vary widely from acidic values as low as 2 to alkaline values as high as 11. Based on their pH optima, GH11 xylanases can be subdivided in two groups: those that exhibit a more acidic (<5.0) and those that exhibit a more alkaline (>5.0) pH optimum. The correlation between the presence of an Asn or an Asp residue at hydrogen-bonding distance from the acid-base catalyst and the alkaline or acidic pH optima of GH11 xylanases, respectively, is well recognized (Joshi *et al.*, 2000).

GH11 xylanases fold into a single ellipsoidal domain (β -jelly roll) comprising two β -sheets and a single three turn α -helix (Figure 1-3) and are described as a partially closed right hand (Törrönen and Rouvinen, 1997). The hydrophobic faces of the two β -sheets pack together to form a sandwich, which is described as ‘fingers’. The twisted parts of the β -sheets and the α -helix form the ‘palm’, while the concave face of the twisted β -sheets forms the substrate binding site. The long loop between two β -strands is

described as a ‘thumb’. The ‘cord’ runs across the mouth of the cleft, partly closing it at one side. The hydrophilic face of β -sheet A forms a flat surface with many Ser and Thr residues, which is called the Ser/Thr surface (Törrönen *et al.*, 1994). The two conserved catalytic glutamate residues are located opposite to each other in the open active site cleft. Major differences between the available crystal structures of GH11 xylanases are related to the position of the ‘thumb’ determining the width of the active site cleft (Törrönen and Rouvinen, 1995; Havukainen *et al.*, 1996). Unlike GH10 xylanases, only a few members of GH11 are reported to be modular proteins (Törrönen and Rouvinen, 1997).

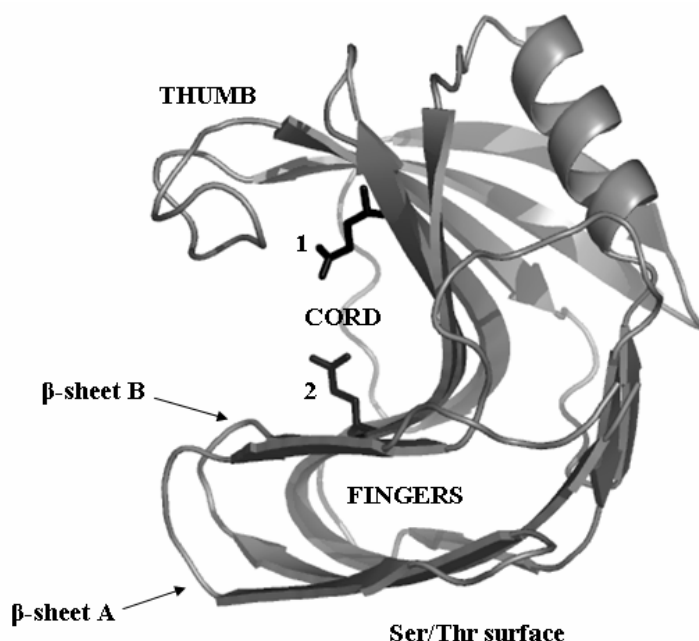


Figure 1-3: Three-dimensional structure of GH11 xylanase XynI of *Trichoderma reesei* (PDB entry 1XYN) (Törrönen and Rouvinen, 1995).

The active site glutamates are shown as sticks (1: nucleophile; 2: acid/base catalyst). The picture was generated with Pymol (Delano Scientific).

1.3.4 *In vivo* functions and industrial applications of xylanases

Plant xylanases, belonging solely to GH10, are involved in the depolymerization of the prominent cereal cell wall component, arabinoxylan, during germination (Fincher, 1989). Xylanases of microbial origin are important enzymes in phytopathogenesis because of their ability to hydrolyze the plant cell wall enabling the pathogenic organism to penetrate (Walton, 1994). They also have been implicated as signals that trigger plant defense responses (Enkerli *et al.*, 1999).

Xylanolytic enzymes from microorganisms, however, have also attracted a great deal of attention in the last decade because of their biotechnological potential in various industrial processes. Xylanases began to be used in the 1980s: initially in the preparation of animal feed and later in the food, textile and paper industries. Xylanases are used to improve the processibility of cereals and/or the quality of the end product by degrading and/or modifying the (arabino)xylan population. Currently, xylanases and cellulases, together with pectinases, account for 20% of the world enzyme market (Polizeli *et al.*, 2005).

In animal feed preparations, xylanases, which preferentially degrade WE-AX, are added to break down arabinoxylans in the ingredients of the feed, reducing the viscosity in the intestinal tract. This results in the improvement of the digestion of nutrients in the initial part of the digestive tract, resulting in a better use of energy. Additionally, xylanases increase the accessibility of nutrients to the animal's digestive system by degradation of the cell walls of endosperm cells (Bedford and Classen, 1992). Moreover, this kind of diet is found to reduce unwanted residues in the excreta (phosphorus, nitrogen, copper and zinc), an effect that could have a role in reducing environmental contamination (Polizeli *et al.*, 2005).

In bread-making, xylanases having a preference for WU-AX are almost routinely used in bread improver mixtures, to improve dough handling properties, oven spring texture and loaf volume (Rouau *et al.*, 1994; Courtin *et al.*, 2001; Sprössler, 1997; Courtin *et al.*, 1999). Also, a larger amount of arabinoxyloligosaccharides (AXOS) in bread would be beneficial to health (Campbell *et al.*, 1997; Hsu *et al.*, 2004; Polizeli *et al.*, 2005). Xylanases also have beneficial effects in the pulp and paper industry where they reduce the consumption of chlorine in the bleaching process (Suurnäkki *et al.*, 1997) and in gluten/starch separation (Frederix *et al.*, 2003).

1.4 The inhibitors: xylanase inhibitors

The discovery some years ago of xylanase inhibitors in cereals has profound implications on the industrial use of xylanases as they affect their efficiency and functionality. Two different types of xylanase inhibitors, showing neither sequence nor structural similarity, have been described in literature: TAXI (*Triticum aestivum* xylanase inhibitor)-type (Debyser *et al.*, 1997) and XIP (xylanase inhibitor protein)-type (McLauchlan *et al.*, 1999; Juge *et al.*, 2004) inhibitors. Their specificity towards

microbial xylanases suggests that both inhibitors are involved in plant defense mechanisms rather than in the regulation of the activity of plant xylanases.

1.4.1 TAXI-type inhibitors

TAXI-type inhibitors were first isolated from wheat flour. They have an experimental molecular mass of approximately 40.0 kDa and occur in two molecular forms, A and B, the latter resulting from proteolytic modification of the former (Debyser and Delcour, 1998; Debyser, 1999; Debyser *et al.*, 1999). After reduction with β -mercaptoethanol, the modified molecular form (B) dissociates into two fragments with molecular masses of approximately 10.0 and 30.0 kDa, whereas the molecular mass of the unmodified form (A) does not change upon reduction (Figure 1-4B). Gebruers *et al.* (2001) demonstrated that TAXI is in fact a mixture of two xylanase inhibitors, namely TAXI-I and TAXI-II, which differ from one another in pI and xylanase specificity and each consist of a molecular form A and B. Their pI values are approximately 8.8 and 9.3 or higher, respectively. Both TAXI-I and -II are only active against GH11 xylanases but not against GH10 xylanases (Gebruers, 2002; Gebruers *et al.*, 2004). Whereas TAXI-I inhibits *Aspergillus niger* xylanase (ExlA) to a greater extent than *Bacillus subtilis* xylanase (XynA), TAXI-II inhibits only XynA. TAXI-II activity seems to depend on the pH optimum of the xylanases (Gebruers, 2002). TAXI-I and TAXI-II were identified at the molecular level (Fierens *et al.*, 2003; Raedschelders *et al.*, 2005) (NCBI Accession numbers AJ438880 and AJ697849, respectively). A striking characteristic of TAXI-II sequences is the presence of extra C-terminal amino acids. Both TAXI isoforms were successfully expressed in *Pichia pastoris* (Fierens *et al.*, 2004; Raedschelders *et al.*, 2005). Their native counterparts, isolated from wheat whole meal, were subjected to crystallization experiments and their structures were resolved (Sansen *et al.*, 2003; Sansen, 2005). Despite local discrepancies, primarily confined to loop regions, both TAXIs display a highly similar structure (Figure 1-4A). The electron density map suggests an N-glycosylation site in both TAXI-type inhibitors.

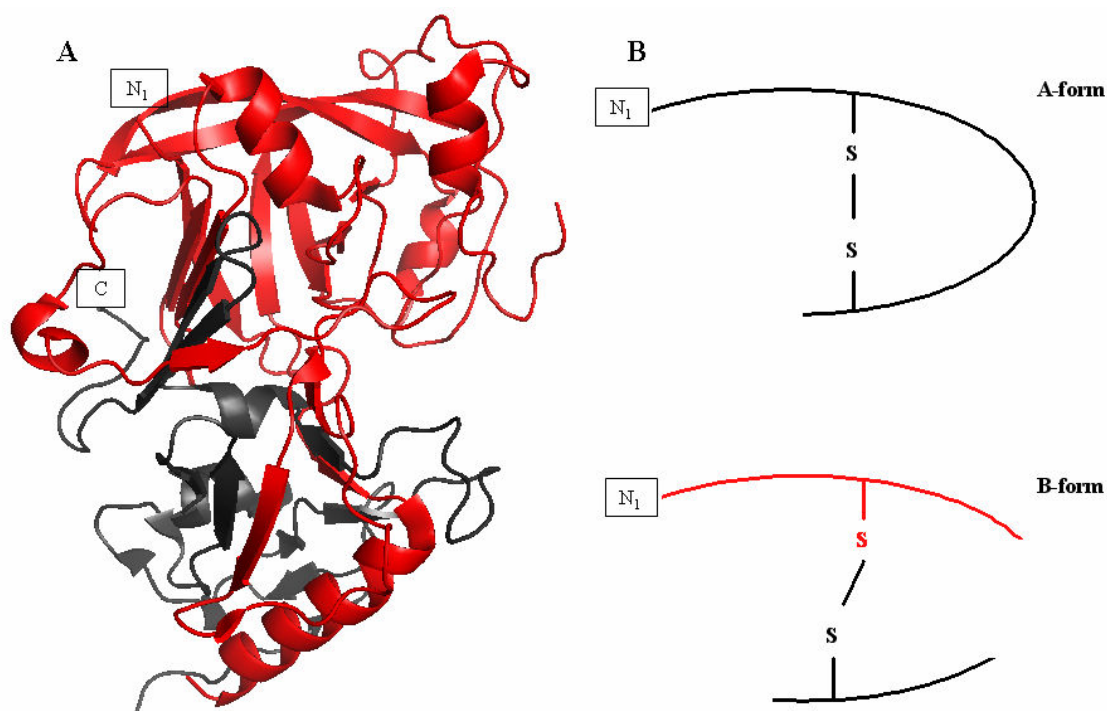


Figure 1-4: Ribbon representation of the overall structure of TAXI-I (PDB entry 1T6E) (A) and schematic representation of the TAXI-I molecular processing (B).

A) The picture was generated with Pymol (Delano Scientific). The 30 kDa and 10 kDa polypeptides are in red and grey, respectively. The N- and C-termini are labeled. B) The two molecular forms, A and B, are schematically represented and identical N-terminal ends are indicated. Upon reduction with β -mercaptoethanol, form B, resulting from proteolytic modification of form A, dissociates in the two fragments of 30 and 10 kDa (modified picture from Gebruers *et al.*, 2004). The 30 kDa polypeptide is in red.

TAXI-type inhibitors were purified from wheat (*T. aestivum*), barley (*Hordeum vulgare*), rye (*Secale cereale*) and durum wheat (*T. durum*) (Goesaert *et al.*, 2004). Multiple isoforms were obtained from wheat (Gebruers *et al.*, 2001; Gebruers *et al.*, 2002a) and rye (Goesaert *et al.*, 2002; Goesaert, 2002), while durum wheat and barley (Goesaert, 2002) contained two and one predominant TAXI-like inhibitors, respectively. Igawa *et al.* (2004) isolated mRNA transcripts of two new TAXI family members, *taxi-III* and *taxi-IV* (NCBI Accession numbers AB114627 and AB114628, respectively), from wheat, mainly from the root and older leaves. However, it must be noted that based on its inhibition specificity TAXI-III can be considered as TAXI-I-like (Raedschelders *et al.*, 2005), while the TAXI-IV inhibition specificity has not been reported yet. *taxi-III* and *taxi-IV* genes are induced upon infection with phytopathogens in contrast to *taxi-I* genes (Igawa *et al.*, 2004). The pathogen and wound inducibility

was confirmed by the presence of several promoter-elements often found in defense-related genes. The fact that endogenous wheat xylanases, belonging to family 10 (Simpson *et al.*, 2003), are not inhibited, indicates that TAXI-like proteins do not play a role as such in plant growth and development (Gebruers, 2002), but suggests again that they do play a role in plant defense.

1.4.1.1 Interaction between TAXI-type inhibitors and xylanases, and factors determining their specificity

Crystallographic data of the ExIA-TAXI-I complex (PDB entry 1T6G) revealed both a direct interaction of TAXI-I with the active site region of the enzyme as well as substrate-mimicking contacts filling the whole substrate-docking region (Sansen *et al.*, 2004). Whereas TAXI-I doesn't undergo a conformational change, the 'thumb' of the xylanase is displaced upon complex formation. His374_{TAXI-I} turned out to be the key residue for inhibition with its imidazole ring fitting in between and making direct contact with the two catalytic glutamate residues of the enzyme as well as with the pH optimum-determining Asp37_{ExIA} (Figure 1-5). The crucial role of this residue was confirmed by site-directed mutagenesis (Fierens *et al.*, 2005). Mutation to alanine, glutamine and lysine to a variable degree reduced the inhibition capacity of the inhibitor mainly due to higher complex dissociation rate constants. This finding suggests that His374_{TAXI-I} plays a critical role in the stabilization of the complex rather than in the docking of inhibitor onto enzyme. The fact that the mutations have variable effects on the inhibition of different xylanases is strong evidence for the existence of additional inhibition determinants. Furthermore, the abolition of the interaction between TAXI-I and a D37A mutant of ExIA corroborates the interaction of TAXI-I with this residue (Tahir *et al.*, 2004). As already mentioned, TAXI-I not only interacts with the active site of the enzyme, but also mimicks the substrate through binding to the substrate binding sites (Sansen *et al.*, 2004). In this context, Leu292_{TAXI-I} perfectly superimposes with xylose at subsite -2 (Tyr10_{ExIA}) (Figure 1-5). Additional interactions between ExIA and TAXI-I are located in the His374_{TAXI-I}-containing C-terminal loop of TAXI-I. More particularly, main chain atoms of Phe375_{TAXI-I} and Thr376_{TAXI-I} are hydrogen-bound to Gln129_{ExIA} and Arg115_{ExIA} in the xylanase glycon subsite -1. In addition, on the aglycon site, there is a clear hydrogen bond interaction between Gln187_{TAXI-I} and Trp172_{ExIA}, which interferes directly with subsites +1 and +2.

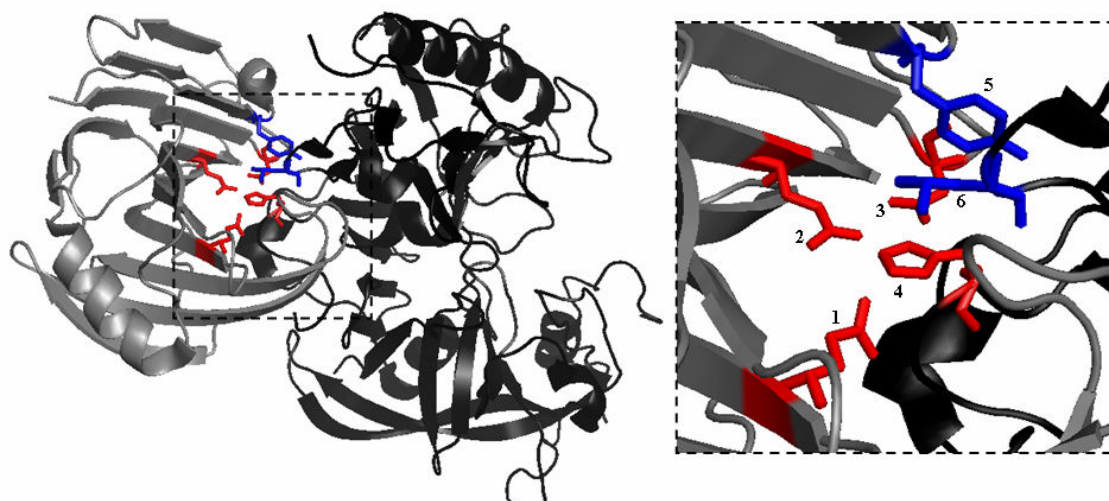


Figure 1-5: Three-dimensional structure of the ExIA-TAXI-I complex (PDB entry 1T6G).

ExIA is in grey while TAXI-I is in black. The main interacting residues are given in the enlarged picture on the right. The key TAXI-I residue His374_{TAXI-I} (4) forms an ionic interaction with the nucleophile Glu79_{ExIA} (1) and forms a hydrogen bond with Glu170_{ExIA} (2) and Asp37_{ExIA} (3). Leu292_{TAXI-I} (6) mimicks the substrate by stacking with Tyr10_{ExIA} (5) forming subsite -2. Residues interacting in the active site are in red, while residues interacting at the substrate binding site are in blue. The picture was generated with Pymol (Delano Scientific).

As already mentioned, TAXI-II inhibits only XynA and not ExIA as opposed to TAXI-I which inhibits both GH11 xylanases. Sansen *et al.* (2004) proposed that the C-terminal loop, which is longer in TAXI-II, is a possible determinant for xylanase specificity. However, a profound analysis of TAXI-II sequences and subsequent confirmation by site-directed mutagenesis (Raedschelders *et al.*, 2005) reveals that TAXI-II inhibition specificity bears solely on the identity of two key residues, namely the residue that interacts at subsite -2 of the xylanase, corresponding to Leu292_{TAXI-I}, and the residue that interacts at the active site of the xylanase, corresponding to His374_{TAXI-I}. Raedschelders and coworkers (2005) identified two sequences exhibiting TAXI-II activity, TAXI-IIA and TAXI-IIB.

Table 1-1: Overview of the specificity determinants of TAXI-I and TAXI-IIA and B.

	position 292*	position 374*
TAXI-I	Leu	His
TAXI-IIA	Pro	His
TAXI-IIB	Leu	Gln

* Residue numbering refers to TAXI-I

Whereas TAXI-IIA possesses a Pro and a His at the positions corresponding to Leu292_{TAXI-I} and His374_{TAXI-I}, respectively, TAXI-IIB has a Leu and a Gln at the corresponding positions (Table 1-1). Since TAXI-IIA is not able to inhibit ExlA, it was suggested that Pro is not able to mimick xylose at subsite -2 of ExlA. However, in the case of XynA, mimicking at this subsite can be realized by a Pro, resulting in an even stronger interaction than when a Leu is present since TAXI-IIA displays a stronger inhibition of this xylanase than the other TAXI forms and since the mutation of the Pro to a Leu decreases the inhibition activity towards this enzyme. A possible explanation could be the presence of a Trp at subsite -2 (Trp9_{XynA}), as is the case in all alkalophilic GH11 xylanases, instead of a Tyr (Tyr10_{ExlA}), like in all acidophilic xylanases. The fact that TAXI-IIB doesn't inhibit ExlA, indicates that there is no strong interaction possible between Gln, corresponding to His374_{TAXI-I}, and the Glu and Asp residues of the active site of the xylanase. Since the interaction of TAXI-IIB with XynA is comparable to the interaction of TAXI-I with this xylanase, it is suggested that the Asn present in XynA instead of Asp37_{ExlA} makes comparable contacts with Gln and His. As a conclusion it can be stated that ExlA is only inhibited by a TAXI-form that contains the Leu/His combination, while for inhibition of XynA the Pro/His, the Leu/Gln as well as the Leu/His combinations are suitable.

Although no crystallographic data have been published yet on the XynA-TAXI-I complex, several mutational experiments were already performed to gain insight in this interaction. Mutants of XynA, based on the known structure of the ExlA-TAXI-I complex (Bourgois *et al.*, 2006), not only confirmed that the interactions described for the latter complex are also present in the XynA-TAXI-I complex, but they also confirmed the specificity determining factors for TAXI-I and TAXI-II suggested by Raedschelders *et al.* (2005). Moreover, mutations located in the 'finger' region of XynA, resulted in sterical blocking of inhibitor binding whether or not accompanied by partial blocking of substrate entrance in the active site (Sørensen and Sibbesen, 2006; Bourgois *et al.*, 2006).

1.4.2 XIP-type inhibitors

XIP-I was first purified from wheat flour (McLauchlan *et al.*, 1999). By immunodetection, XIP-I was located predominantly in the grain tissue, where it appears at a late stage in grain development and persists after germination (Elliott *et al.*, 2003).

Purified XIP-I was found to be a glycosylated, monomeric, basic protein with a pI of approximately 8.8 and an experimental molecular mass of 29 kDa (McLauchlan *et al.*, 1999) inhibiting GH10 and GH11 xylanases provided they are from fungal origin (Flatman *et al.*, 2002). The only exception known up to now is *A. aculeatus* GH10 xylanase which is not inhibited despite its fungal origin. Moreover, some bacterial xylanases are also inhibited (see below). XIP-I was also demonstrated to possess dual target enzyme specificity (Sancho *et al.*, 2003). Next to xylanases, XIP-I also inhibits two barley α -amylase isozymes. The cDNA sequence encoding XIP-I has been identified (NCBI Accession number AJ422119) and successfully expressed in *Escherichia coli* (Elliott *et al.*, 2002). Recombinant XIP-I however rapidly lost its biological activity, probably due to the lack of appropriate glycosylation and disulfide bond formation (Juge *et al.*, 2004). The architecture of XIP-I, as determined by X-ray crystallography (Payan *et al.*, 2003), consists of a single elliptical $(\beta/\alpha)_8$ scaffold (PDB entry 1OMO). Although XIP-I appears to display sequence and structure homology to GH18 chitinases, the inhibitor itself has no intrinsic chitinase activity (McLauchlan *et al.*, 1999; Elliott *et al.*, 2002). However, the catalytic glutamate of GH18 chitinases is conserved in the XIP-I structure, but its side-chain is fully engaged in salt-bridges with neighboring residues. This homology is particularly relevant to its physiological role in the wheat plant since plant chitinases are regulated in response to fungal elicitors and they exhibit rapid evolution by acting as prime targets for the co-evolution of plant-pathogen interactions (Bischof *et al.*, 2000). It could thus be that, as part of this co-evolution process, XIP-I has evolved from chitinases, still responding to fungal attack, but interacting with xylanases rather than chitin (Bellincampi *et al.*, 2004).

Unlike *taxi-I*, *xip-I* is pathogen-inducible, and unlike *taxi-III* and *taxi-IV*, its expression depends on the type of the pathogen and/or infected tissue (Igawa *et al.*, 2005). Indeed, *xip-I* was not expressed in flowering spikelets inoculated with *Fusarium graminearum*, but transcription was greatly enhanced in *Erysiphe graminis*-infected leaves. Moreover, *xip-I* was expressed when the leaves were wounded and its expression was significantly elevated by treatment with methyl jasmonate. Thus, *xip-I* has the features of a plant defense gene regulated by a jasmonic acid-mediated signaling pathway. The finding that XIP-I does not inhibit endogenous wheat xylanase activity but does inhibit exogenous xylanases from fungal sources, also suggests that XIP-I is involved in protecting the grain from fungal attack during dormancy, when other plant defense

mechanisms, and in particular those that involve an active response, are inactive or less effective (Elliott *et al.*, 2003).

Affinity chromatography with immobilized ExIA yielded rye, durum wheat, barley and maize XIP-type inhibitors (Goesaert *et al.*, 2004). Multiple XIP-type iso-inhibitors are present in these cereals (Elliott *et al.*, 2003; Goesaert, 2002; Goesaert *et al.*, 2003). Much as in wheat, the observed heterogeneity may be partially due to modifications during storage and purification (Flatman *et al.*, 2002), although a large part may be the result of post-translational modifications and the presence of multiple *xip* genes (Elliott *et al.*, 2003; Gebruers *et al.*, 2002b). EST database screening revealed that several different EST sequences occurred in a variety of cereals. They appeared to be grouped in subfamilies (Elliott, 2002). Next to *xip-I*, found in wheat, *xip-II* and *xip-III* (NCBI Accession numbers AJ318884 and AB204556, respectively) were found in durum wheat and wheat, respectively.

1.4.2.1 Interaction between XIP-type inhibitors and xylanases, and factors determining their specificity

Based on activity measurements, XIP-I was originally suggested to inhibit both GH10 and GH11 xylanases as long as they are from fungal origin (McLauchlan *et al.*, 1999; Flatman *et al.*, 2002; Furniss *et al.*, 2002). Crystallographic analysis of XIP-I in complex with a GH10 xylanase from *A. nidulans* (XlnC) (PDB entry 1TA3) and of XIP-I in complex with a GH11 xylanase from *Penicillium funiculosum* (XynC) (PDB entry 1TE1) revealed that XIP-I has two independent binding sites for both families of xylanases that display a different fold (Payan *et al.*, 2004). In both cases, inhibition is caused by a combination of substrate mimicking interactions and interactions with the active site glutamates.

Interaction of XIP-I with GH10 xylanase XlnC mainly occurs through an α -helix of XIP-I (α_7) (Figure 1-6), which covers the central part of the substrate binding cleft resulting in an occlusion of the active site of the enzyme. Side-chains emerging from the helix point into the heart of the cleft and occupy the four central subsites. Tyr238_{XIP-I}, Lys234_{XIP-I}, Asn235_{XIP-I} and His232_{XIP-I} interact with subsites -2, -1, +1, +2, respectively, whereas Lys246_{XIP-I} sterically blocks access to subsite -3. Furthermore, Lys234_{XIP-I} forms a hydrogen bond with the acid/base catalyst and a water mediated hydrogen bond with the nucleophile of the xylanase (Figure 1-6). The heart of the

substrate binding site is occupied by an aromatic cluster of residues from the inhibitor (Tyr237, Tyr238, His232, Trp230 and Tyr273) and the enzyme (Trp269, His209, Trp277, Tyr174, Arg278). Several loops located around the active site of the XlnC xylanase are involved in the interaction with XIP-I (Figure 1-6).

To explain the inhibitor's apparent specificity for fungal GH10 xylanases, a comparison between fungal and bacterial GH10 xylanases was performed. Whereas there are no structural differences between the loop regions of fungal GH10 xylanases and XlnC, the structure of bacterial GH10 xylanases revealed insertions in the β/α -loop segments at the carboxyl side of the β -barrel, more specifically in the $\beta4$ - $\alpha4$ and $\beta8$ - $\alpha8$ loop regions (Figure 1-6), which interact with XIP-I in XlnC. However, the bacterial *Streptomyces olivaceoviridis* xylanase (PDB entry 1ISV) contains no substitutions in the loop regions causing sterical clashes with XIP-I and also contains no insertions in the loop regions. Therefore, it is suggested that this bacterial xylanase could be inhibited by XIP-I. Hence, XIP-I does not appear to display absolute specificity for fungal GH10 xylanases but is likely to target GH10 enzymes that lack the extended loops at the carboxyl side of the β -barrel.

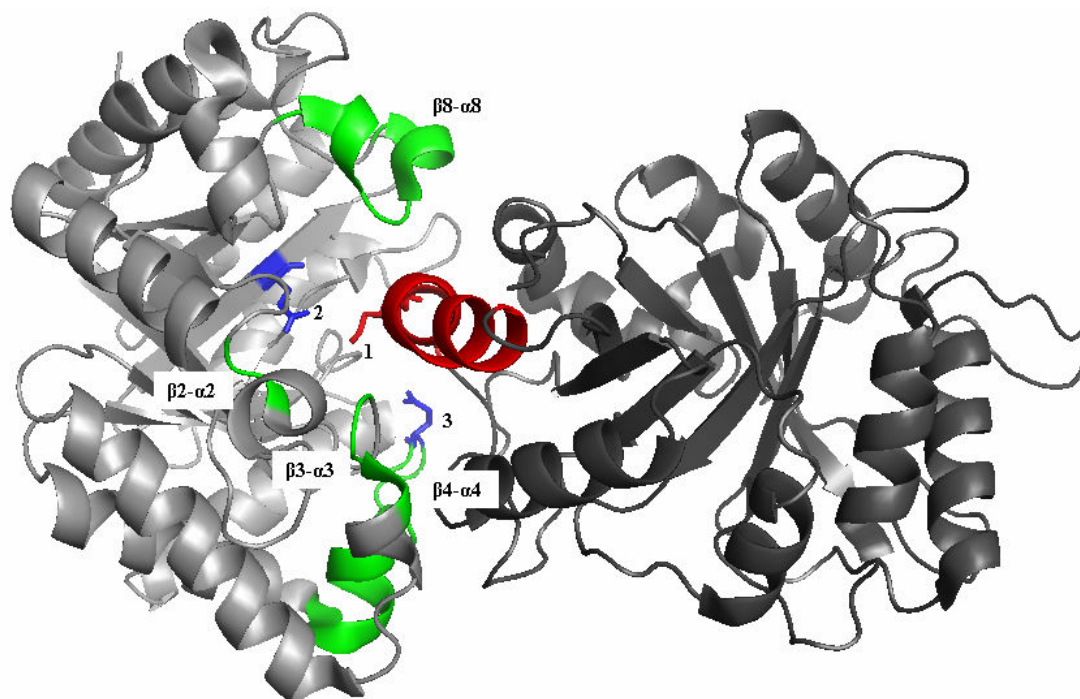


Figure 1-6: Three-dimensional structure of the XlnC (GH10)-XIP-I complex (PDB entry 1TA3).

XIP-I is in dark grey and XlnC is in light grey. The $\alpha7$ -helix from XIP-I is in red, whereas the interacting loops of the XlnC xylanase are in green. The names of the loops are indicated. Lys234_{XIP-I} (1) hydrogen bonds with the acid/base catalyst (3) and forms a water mediated hydrogen bond with the nucleophile (2) of the xylanase. The picture was generated with Pymol (Delano Scientific).

The crystal structure of the XynC-XIP-I complex (Payan *et al.*, 2004) reveals that inhibition of this xylanase, and probably of other GH11 xylanases, occurs through a loop of XIP-I that protrudes between the ‘thumb’ and the ‘palm’ of the enzyme blocking access to the active site (Figure 1-7). The interaction is associated with tight interactions with the ‘thumb’ and the ‘palm’ regions of the xylanase resulting in blocking of the three glycon subsites (-3, -2, -1). The close interaction with the ‘thumb’ region was confirmed by the insensitivity of an ExlA N117A mutant, located at the tip of the ‘thumb’, for inhibition by XIP-I (Tahir *et al.*, 2002). Since this Asn residue is conserved in most GH11 xylanases (bacterial and fungal), it is probably the environment of this amino acid in the structure that is responsible for the difference in binding suggesting that the ‘thumb’ region rather than a single residue is involved in XIP-I binding to GH11 xylanases. The main inhibition determinant is Arg149_{XIP-I} (Figure 1-7) that stacks with the aromatic Trp18_{XynC} at subsite -2 of the xylanase. Furthermore, this residue also forms a hydrogen bond with the acid/base catalyst.

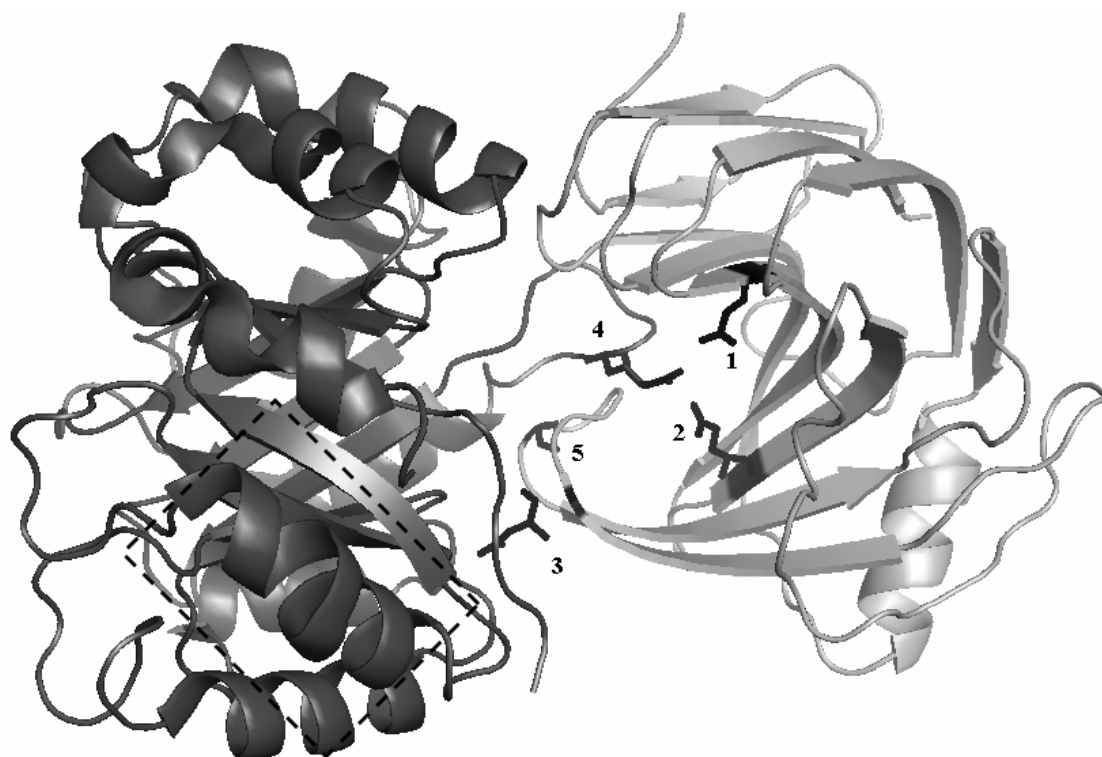


Figure 1-7: Three-dimensional structure of the XynC (GH11)-XIP-I complex (PDB entry 1TE1).

XIP-I is in dark grey and XynC is in light grey. The loop containing Arg149_{XIP-I} (4) protrudes in the active site of XynC (1: nucleophile; 2: acid/base catalyst). The Asn residue corresponding to Asn117 of ExlA is indicated (3). The XIP-I helix interacting with GH10 xylanases is boxed. Bacterial GH11 xylanases contain an insertion after Gly129_{XynC} (5) and the tip of the ‘thumb’ adopts a different conformation. The picture was generated with Pymol (Delano Scientific).

Since the overall shape and amino acid composition of the ‘thumb’ of the xylanase plays a particular important role in inhibitor binding, this region mainly determines the specificity of XIP-I towards fungal GH11 xylanases. The reason why several enzymes, like the bacterial GH11 xylanases of *B. subtilis* (XynA), *Neocallimastix patriciarum* and *B. circulans*, are not inhibited by XIP-I is that they show insertions in the region surrounding the tip of the ‘thumb’ at the highly conserved Gly129_{XynC} (Figure 1-7). The presence of an arginine instead of a threonine (XynC) after this insertion causes the loop to adopt a strikingly different conformation that would cause sterical clashes with XIP-I.

Tahir *et al.* (2004) demonstrated that a D37A mutant of ExlA lost its inhibition sensitivity towards XIP-I and its ability to form a complex with the inhibitor. As mentioned above, this residue is involved in acidophilic adaptation of xylanases and is at hydrogen-bonding distance of the acid/base catalyst. The loss of interaction of D37A with XIP-I is likely to be the result of a disruption of the hydrogen bonding network in the vicinity of the active site. Considering the effects of the N117A and D37A mutants, it is suggested that inhibition is the result of a sequence of events in which XIP-I interacts with Asn117 and later to the whole ‘thumb’ region, which would in turn direct the loop of XIP-I to the active site where it makes a strong contact with the acid/base catalyst and/or other active site residues.

1.4.3 A novel type of xylanase inhibitors: TLXI

In addition to TAXI- and XIP-type inhibitors, a novel type of xylanase inhibitor has been identified in wheat (Fierens *et al.*, 2007). TLXI (thaumatin-like xylanase inhibitor) was purified from wheat whole meal by a combination of ion exchange and affinity chromatography. The N-terminal sequence was determined and shows similarity with thaumatin-like proteins (TLPs) from various origins. The novel inhibitor is a basic, monomeric, glycosylated protein with an experimental molecular mass of 18 kDa occurring in different forms with varying extents of glycosylation (Fierens *et al.*, 2007). TLXI inhibits GH11 xylanases but is inactive towards GH10 xylanases. Except for zeamatin, which inhibits insect α -amylase and porcine pancreas trypsin, no enzyme inhibitor is currently known among the TLPs. Hence, TLXI represents a novel function within this group of proteins. The molecular identification, recombinant expression and mutagenesis of this inhibitor form the subject of this thesis.

1.4.4 Potential role of xylanase inhibitors in biotechnological applications

Since xylanase inhibitors present in cereals hamper the activity of microbial xylanases used as an additive in various cereal-based industrial applications, they have a rather negative effect in these processes. However, a positive role has been reported as well. During storage of refrigerated dough, the enzymatic hydrolysis of arabinoxylans by endogenous xylanases gives rise to a liquid layer at the dough surface, referred to as dough syrupe (Gys *et al.*, 2003; Courtin *et al.*, 2005). Addition of TAXI was shown to reduce this phenomenon (Courtin *et al.*, 2005; Courtin *et al.*, 2006) by inhibiting microbial xylanases present in the flour and hence delaying the occurrence of dough syrup upon prolonged storage of refrigerated doughs. Addition of a cocktail of inhibitors could be recommended to inhibit a large range of xylanases (Courtin *et al.*, 2006).

In addition, the reversible interaction between xylanases and their proteinaceous inhibitors has been utilized as a technological means to purify xylanases from microbial preparations (Gebruers, 2002). By coupling wheat TAXI and XIP inhibitors to resins and subsequent affinity chromatography, highly pure xylanases were obtained from an *A. niger* culture filtrate. This method may offer an alternative tool for screening novel commercial xylanases.

Chapter 2

Thaumatococcus-like proteins

2.1 Introduction

In the previous chapter, the group of xylanase inhibitor proteins was discussed, to which TLXI belongs from a functional point of view. However, the TLXI protein displays no sequence similarity with the other xylanase inhibitors identified up to now. This chapter therefore focuses on the group of proteins to which TLXI shows sequence similarity: the thaumatococcus-like proteins (TLPs). The name of this group of proteins is derived from the sweet tasting protein thaumatococcus, as all of the proteins belonging to it share a high degree of similarity to this protein. Due to their inducibility by pathogens, they are classified in group 5 of the pathogenesis-related (PR) proteins. However, some of these PR-proteins are not only induced *de novo* upon pathogen attack, wounding or other physical or chemical stress, but they are constitutively expressed in some organs or during developmental stages. These forms are called PR-like proteins and they are also thought to play a significant role in protecting seeds against fungal attack during storage or germination (Hejgaard *et al.*, 1991).

2.2 Thaumatococcus

Thaumatococcus is a sweet-tasting, basic protein extracted from the fruit of *Thaumatococcus daniellii*, a bushy plant that grows in West Africa (Van der Wel and Loeve, 1972). Thaumatococcus elicits a very sweet taste that is rated to be 1600 times and 100,000 times sweeter than sucrose on a weight basis and a molar basis, respectively. This makes thaumatococcus the sweetest known natural substance on earth. The biosynthesis of this protein by *T. daniellii* might help the host plant to mimic the sweetness of sucrose. This would make it more likely that wild animals ingest the plant, thus leading to more efficient seed dispersal (Faus, 2000). In 1983, it has been approved as a safe food ingredient (Faus, 2000) and it has been commercialized since then under the brand name “Talin”. Thaumatococcus is listed as food additive E957. It has found applications in animal feed, pet food, chewing gum and many staple food items. Since the protein is very effective at masking bitter notes, often associated with pharmaceuticals or vitamins, it is used as an excipient in pharmaceuticals covering strongly bitter

aftertastes and leaving a pleasant feeling in the mouth. As a non-caloric sweetener, thaumatin has attracted attention as a candidate for control of obesity, oral health and diabetic management (Faus, 2000). Thaumatin was also introduced into potato plants, and the protein with the intense sweet taste was detected in all organs of the regenerated plants (Witty and Harvey, 1990). In transgenic tomato plants it was used to modify tomato taste (Bartoszewski *et al.*, 2003). Thus, flavor and sweetness could be enhanced in a number of various transgenic fruits and vegetables by introducing the thaumatin-encoding sequence.

Thaumatin occurs as a mixture of two predominant forms: Thaumatin I and II (Van der Wel and Loeve, 1972). Both proteins are a single chain of 207 amino acids (Iyengar *et al.*, 1979), which differ from one another by only five amino acids. The molecular weight is close to 22 kDa. One of the striking features is the presence of eight disulfide bridges (Van der Wel *et al.*, 1984), which brings about a complex 3D-crosslinking that may be responsible for the heat- and pH-resistance of thaumatin. Thaumatin genes were shown to belong to a multigene family and possess very small introns situated at different positions in the various structural genes (Ledebouer *et al.*, 1984).

The three-dimensional structure of thaumatin I has been solved (De Vos *et al.*, 1985; Ogata *et al.*, 1992) and consists of three domains (domains I, II and III). The central part of the molecule is built as an 11-stranded β -sandwich (domain I). All β -strands of the sandwich are antiparallel except the N-terminal and C-terminal ones. To this main domain are attached two small domains rich in disulfide bonds (domains II and III). The thaumatin structure hence utilizes two kinds of building motifs: a folded β -sheet or a flattened “ β -barrel”, and the β ribbons and small loops stabilized by disulfide bonds. Since the second motif is found in venom toxin, bungarotocin, wheat germ agglutinin, cytotoxins and ragweed pollen allergens (Drenth *et al.*, 1980), all of which bind to membrane-bound receptors, it is tempting to speculate that this motif may be important for binding to the membrane-bound receptors (De Vos *et al.*, 1985). By modifying lysine residues, it was determined that some of these residues may play an important role in sweetness (Kim and Weickman, 1994; Kaneko and Kitabatake, 2001). More specifically, the basicity of the cleft region formed by domains I and II and the four lysine residues surrounding the cleft region seem likely to be structurally required for sweetness. The cleft region is highly acidic in several other TLPs (Koiwa *et al.*, 1999) (Figure 2-1), suggesting that these proteins don't have a sweet taste. Because multiple

lysine residues seem to be involved, sweetness could be determined by a multipoint interaction of thaumatin with the receptor, identified as the T1R2-T1R3 receptor (Temussi, 2002).

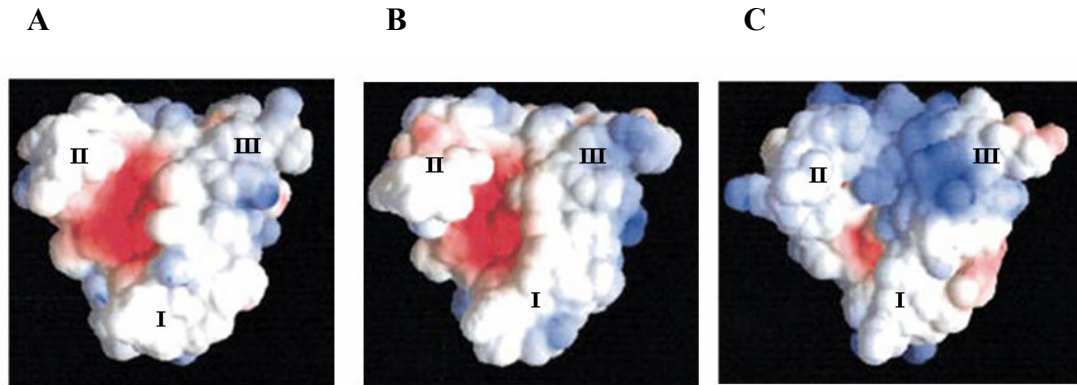


Figure 2-1: View of the surface topology of (A) PR-5d, (B) zeamatin and (C) thaumatin showing the solvent-accessible surface and surface electrostatic potential (adapted from Koiwa *et al.*, 1999).

The protein surface is colored according to the electrostatic potential, ranging from red (most negative) to white (neutral) to blue (most positive). The three domains constituting the proteins are indicated (I, II and III). The cleft region at the boundary of domains I and II is shown for each protein. Whereas the cleft regions of PR-5d and zeamatin are highly acidic (red), the cleft region of thaumatin is basic (blue).

The industrial use of thaumatin is hampered by the limited availability of raw material and the expensive extraction methods. Therefore, attempts have been made to produce recombinant thaumatin in several microorganisms and in transgenic plants (Witty, 1990), using either the cloned natural gene for thaumatin II or, alternatively, a synthetic gene that contains codons optimized for expression in the particular host being used (Lee *et al.*, 1988). Attempts have been made to produce thaumatin by using *E. coli* (Edens *et al.*, 1982), *Kluyveromyces lactis* (Edens and Van der Wel, 1985), *B. subtilis* (Illingworth *et al.*, 1988), *S. lividans* (Illingworth *et al.*, 1989), *S. cerevisiae* (Edens and Van der Wel, 1985; Lee *et al.*, 1988), *P. pastoris* (Masuda *et al.*, 2004), *Penicillium roquefortii* (Faus *et al.*, 1997) and *A. awamori* (Moralejo *et al.*, 1999; Moralejo *et al.*, 2000; Moralejo *et al.*, 2001; Moralejo *et al.*, 2002). So far, none of the attempts at expressing recombinant thaumatin have been capable of reaching expression levels that are economically feasible (1g/liter). Moreover, expression often resulted in a non-active (non-sweet) form of the protein.

2.3 Thaumatin-like proteins

PR proteins have been described as proteins that are encoded by the plant genome and that are induced specifically in response to infections by pathogens (fungi, bacteria, viruses) or by adverse environmental factors (Breiteneder, 2004). They represent a collection of unrelated protein families which function as part of the plant defense system. Originally, the PRs were grouped into five families, based on sequence characteristics (Van Loon, 1985). Nowadays, this group of proteins has been extended to 17 families (Van Loon and Van Strien, 1999; Christensen *et al.*, 2002). Based on their sequence similarity with the sweet-tasting thaumatin, all PR-5 proteins are designated TLPs, although none of these proteins has been described to have a sweet taste. According to their molecular mass, TLPs are grouped into two sections: one group of proteins has a size ranging from 22 to 26 kDa whereas the other group comprises proteins of 18 kDa or less due to an internal deletion of about 25% of the size of the high molecular weight members. Members of the first group usually accumulate in cell vacuoles as opposed to members of the second group which are mainly found extracellularly (Chan *et al.*, 1999). So far, TLPs from the substantially smaller group have been identified mainly in cereals. There are acidic, basic and neutral TLPs. All of the TLPs of the larger group contain 16 cysteine residues which are involved in the formation of 8 disulfide bridges, whereas the members of the smaller group have 10 cysteine residues involved in 5 disulfide bridges. The presence of those disulfide bridges make them resistant to proteases and pH- or heat induced denaturation. Recently, TLPs have also been discovered in animals, more specifically in nematodes and insects (Brandazza *et al.*, 2004; Shatters *et al.*, 2006), and in fungi (Grenier *et al.*, 2000; Greenstein *et al.*, 2006). As in plants, TLPs could play a defense role against pathogens in these organisms. This chapter only focuses on TLPs from plant origin.

2.3.1 Activities ascribed to TLPs

2.3.1.1 Antifungal activity

Some TLPs have been shown to display antifungal potential *in vitro* (Roberts and Selitrennikoff, 1990; Woloshuk *et al.*, 1991; Huynh *et al.*, 1992; Bryngelsson and Green, 1989) as well as in transgenic plants (Liu *et al.*, 1994). Zeamatin, a TLP isolated

from *Zea mays* (Roberts and Selitrennikoff, 1990), acts quickly as an antifungal agent by rupturing hyphal membranes in as little as 15 seconds. However, the precise mechanism behind the antifungal activity of some TLPs still remains unclear. Several hypotheses have been made though on the determinants of this activity.

Roberts and Selitrennikoff (1990) hypothesized that zeamatin forms a membrane pore causing water influx and subsequent osmotic rupture. However, the fact that the membrane permeabilizing activity is similar at room temperature and at 4°C, suggested that zeamatin is not simply inserted into the fungal membrane because the immobility of the membrane lipid at 4°C prevents the uptake of pore-forming compounds. Therefore, it is believed that zeamatin interacts with other components of the fungal membrane (Batalia *et al.*, 1996) (Figure 2-2) which results in an influx of water or ions through the membrane. This interaction may occur with a membrane ion channel, a water channel or an osmotic receptor, which destabilizes the pressure gradient maintaining the extending hyphal tip.

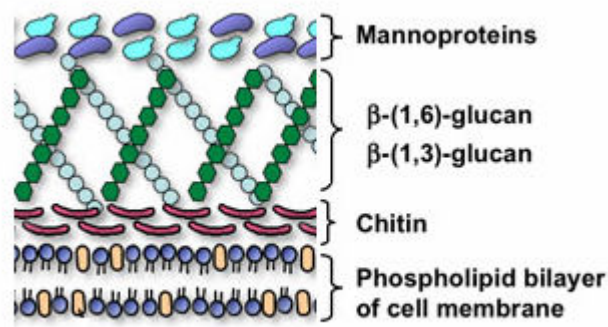


Figure 2-2: Schematic of the fungal cell wall.

An important observation in this context is the presence of a common structure in the antifungal TLPs (Koiwa *et al.*, 1999). Indeed, structural comparison of antifungal TLPs revealed the presence of an acidic cleft at the boundary of domains I and II of the protein (Figure 2-1). This negatively charged cleft is thought to be responsible for the interaction with the positively charged membrane proteins like water and ion channels (Menu-Bouaouiche *et al.*, 2003). For a tobacco TLP, ionic interaction has indeed been shown to be important in the establishment of the antifungal activity because the protein is inactive in the presence of salt (Koiwa *et al.*, 1997). It must be noted, however, that the presence of such an acidic cleft *per se* does not provide a TLP with

antifungal properties. For example, TLPs from apple and cherry don't possess antifungal activity despite the presence of a strongly acidic cleft. On the other hand does the absence of a cleft region, like in the low molecular mass TLPs, not necessarily mean that the protein is devoid of antifungal activity. An antifungal TLP from winter rye lacks the cleft region because of the absence of domain II, although the acidic residues from domain I are conserved (Chan *et al.*, 1999). Possibly, the acidic nature of this region is more important than the presence of a cleft region. In contrast, Anzlovar *et al.* (1998) showed that the incorporation of negative charge to the fungal liposome increased membrane permeabilization suggesting that initial interaction with the fungal cell surface may occur between the overall cationic TLP and the negatively charged cell surface.

In addition to the above, the cleft region is rich in hydrophilic residues, which is a characteristic fairly typical of carbohydrate binding sites. There is indeed strong evidence for the specific binding of several TLPs to water-insoluble β -1,3-glucans (Trudel *et al.*, 1998). Docking experiments of linear β -1,3-glucan revealed that the most favorable site for binding is in the cleft region (Osmond *et al.*, 2001). Several residues are present in the cleft that can form hydrogen bonds to the carbohydrate moieties, as well as aromatic residues that can be involved in stacking interactions. The binding of antifungal proteins to β -1,3-glucans (Figure 2-2) at specific sites of fungal cell walls could be one prerequisite to the subsequent membrane alteration. A possible two-step mechanism of action is proposed (Trudel *et al.*, 1998). In a first step, TLPs bind to the fungal cell wall β -1,3-glucan, the structure and configuration of which determines the extent of binding. This step is followed by the membrane permeabilization discussed above. Moreover, antifungal TLPs display a strict specificity for a particular target cell (Abad *et al.*, 1996). Presumably, in fungi resistant to particular TLPs initial binding is physically impeded by the presence of cell-wall associated proteins or polysaccharides. Yun *et al.* (1997) discovered that stress proteins on the yeast cell surface determine resistance to osmotin, a TLP from tobacco. Also the interaction of the antifungal TLP with the fungal membrane is specific since the enzymatic digestion of the cell wall of sensitive and resistant yeast cells rendered the spheroplasts equally susceptible to the cytotoxic action of osmotin, but not to other osmotin-like proteins. Another hypothesis on the biological significance of TLPs binding to fungal glucans is that they might act in concert with enzymes displaying glucanase activity, belonging to PR-2 (Hrmova and

Fincher, 1993), to disrupt the fungal cell wall glucans. They might also bind to nascent glucans during fungal cell wall synthesis preventing proper assembly during hyphal extension (Osmond *et al.*, 2001).

2.3.1.2 Antifreeze activity

Freezing-tolerant plants survive subzero temperatures by forming ice in extracellular spaces within their tissues (Marentes *et al.*, 1993). These ice crystals grow at the expense of water drawn from within the cells, and so the contents of the cells dehydrate and cool below the freezing point without freezing. The process of extracellular ice formation is controlled by antifreeze proteins, which modify the rate and pattern of growth of extracellular ice crystals by adsorbing onto ice crystals in order to reduce freezing injury and physical damage within tissues. In winter rye, which is an overwintering, freezing-tolerant cereal, these antifreeze proteins, induced during cold acclimation (Marentes *et al.*, 1993) and accumulating in the apoplast, show similarity to three classes of PR proteins: PR-2, PR-3 and PR-5, which represent β -1,3-glucanases, chitinases and TLPs, respectively (Hon *et al.*, 1995). The TLPs, together with the other antifreeze proteins, are assumed to adsorb onto the ice surface thereby blocking the binding of additional water molecules, which creates an ice-crystal surface with many highly curved fronts and a high surface free energy (Yu and Griffith, 1999). Consequently, the growth of these fronts is halted because it is less energetically favorable for water molecules to bind to this surface. The temperature must be lowered further to decrease free energy before crystal growth proceeds. As a result, the freezing point of the solution is depressed. Yu and Griffith (1999) discovered that antifreeze proteins form oligomeric complexes in the apoplast enabling them to block a larger area of the ice surface. As a result, the growth of ice crystals is inhibited to a greater extent and antifreeze activity increases. The expression of antifreeze proteins is induced by cold, drought, ethylene, but not by abscisic acid (Yu *et al.*, 2001; Yu and Griffith, 2001). The antifungal activity of TLPs is consistent with the fact that a number of freezing-tolerant grasses become more resistant to fungal disease (Tronsmo, 1984).

2.3.1.3 Enzyme inhibitors

The only enzyme inhibitor identified hitherto among the TLPs is zeamatin, isolated from *Zea mays* (Roberts and Selitrennikoff, 1990). Not only does this protein bind β -1,3-glucan (Trudel *et al.*, 1998) and permeabilize fungal cell walls (Roberts and

Selitrennikoff, 1990), it also displays inhibitory activity against some insect amylases and porcine pancreas trypsin (Schimoler-O'Rourke *et al.*, 2001). For the latter activity, however, high molar ratios of zeamatin to trypsin are required. Since zeamatin does not inhibit fungal α -amylase and fungi do not contain trypsin, zeamatin's antifungal activity is not the result of the inhibition of these enzymes, but proceeds as described in section 2.3.1.1. The mode of inhibition by zeamatin is not yet clarified.

2.3.1.4 β -1,3-glucanase activity

Some plant TLPs from various origins display β -1,3-glucanase activity (Grenier *et al.*, 1999) although they appeared to be less active than glucanases belonging to the PR-2 group of proteins. Based on the absence of sequence similarities, TLPs do not belong to any classified glycosyl hydrolase family (CAZy, <http://afmb.cnrs-mrs.fr/CAZY/>) and hence are said to represent a novel set of glycosyl hydrolases (EC 3.2.1.x). Since some TLPs display glucanase activity but no antifungal activity and vice versa, TLP glucanase activity cannot be regarded as the only and primary antifungal factor. Additionally, the glucanase activity of TLPs is so low that it seems unlikely that such activity plays a key role in the defense of plants against phytopathogenic fungi (Barre *et al.*, 2000). The physiological consequences and biological significance of the glucanase activity of TLPs are not yet fully understood. It is believed, however, that reaction products of their enzymatic activity act as elicitors and induce various defense responses of the plants (Menu-Bouaouiche *et al.*, 2003). TLPs with glucanase activity that accumulate in large quantities in ripening fruits are also suggested to degrade specifically cell wall β -1,3-glucans and hence may contribute to the softening of the pulp or flesh of e.g. banana, grape and cherry (Menu-Bouaouiche *et al.*, 2003). However, this proposed role in tissue softening during fruit ripening should be interpreted with care given the very low glucanase activity of TLPs as compared to that of genuine glucanases.

There is no doubt that the acidic cleft of the TLP plays an essential role in both the binding (Osmond *et al.*, 2001) (section 2.3.1.1.) and subsequent hydrolysis of the β -1,3-glucans (Menu-Bouaouiche *et al.*, 2003). However, besides the acidic character there are some other structural requirements the cleft needs to meet in order to acquire β -1,3-glucanase activity. An apparent crucial feature of the cleft is the presence of Asp and Glu residues that are correctly positioned to act as proton donor and nucleophile residue in a mechanism of glucan hydrolysis. The β -1,3-glucanase activity of a TLP also

requires a favorable positioning of the β -1,3-glucan towards the catalytically active acidic residues in order to be cleaved. In a cherry TLP endowed with β -1,3-glucanase activity the catalytically active acidic residues are located at the top of an extended cleft which is quite unusual among endoglucanases. The active site residues of endoglucanases currently occur in the center of a cleft that extends across the surface of the enzyme (Hrmova and Fincher, 2001). This could possibly explain the low activity of TLPs in comparison to genuine glucanases.

2.3.1.5 Plant allergens

The prevalence of allergy to fruit and vegetables increased over the last twenty years (Inschlag *et al.*, 1998). The allergic response can vary from local reactions to even life-threatening severe systemic reactions. A considerable percentage of the plant-derived allergens can be grouped to one of the families of PR proteins (Hoffmann-Sommergruber, 2000). Members of the PR-5 family (TLPs) represent food allergens present in various plant derived foods. The first allergen identified within this group of PR proteins was the Mal d 2 protein from apple (Hsieh *et al.*, 1995). Since then, several other allergenic TLPs were isolated from fruits like cherry (Inschlag *et al.*, 1998), kiwi (Gavrovic-Jankulovic *et al.*, 2002) and bell pepper (Leitner *et al.*, 1998). Due to their high water content and possibly sweet taste, fruits are very likely to be attacked by phytophagous fungi or insects. For this reason fruits constitutively express particular levels of TLPs in certain developmental stages making them able to elicit an allergic response in humans not only when they are attacked by a phytopathogen (Hoffmann-Sommergruber, 2000). Two allergenic pollen TLPs have also been isolated from mountain cedar (Midoro-Horiuti *et al.*, 2000) and Arizona cypress (Cortegano *et al.*, 2004). Since most of the allergenic TLPs identified so far contain a potential N-glycosylation site or are shown to be glycosylated (Gavrovic-Jankulovic *et al.*, 2002), there is an ongoing discussion whether the carbohydrate moiety of glycoallergens contributes to their IgE-binding capacity and ability to elicit IgE-mediated symptoms. Studies on the pollen allergen of mountain cedar revealed that the IgE-binding epitopes are on a helix-loop region on one side of the protein, accessible for interaction with macromolecules, such as immunoglobulins (Soman *et al.*, 2000). It is assumed that a large, solvent-exposed, hydrophobic area surrounded by charged residues contributes to both the binding affinity and specificity of the interaction with IgE.

2.3.2 Potential applications of TLPs

Due to its antifungal properties against human pathogens like *Candida albicans* (Roberts and Selitrennikoff, 1990), zeamatin has the potential to be used as a human therapeutic agent. The applicability of zeamatin in therapy of vaginal candidiasis was tested using a model organism (Stevens *et al.*, 2002). From the results it appeared that there was a synergistic action between zeamatin and nikkomycin Z, an inhibitor of the synthesis of the fungal cell wall component chitin, or clotrimazole, which blocks the synthesis of membrane sterol. Hence, zeamatin is believed to potentiate other agents in topical therapy of vaginal candidiasis although further studies are required. The same synergistic effect with nikkomycin Z was detected in an *in vitro* assay for two TLPs isolated from barley grains (Hejgaard *et al.*, 1991).

The antifungal activity of TLPs against plant pathogens on the other hand makes them attractive candidates for use in genetic engineering to produce disease resistant crop plants. Green house experiments have been performed to increase the resistance of wheat to *Fusarium* head blight (Chen *et al.*, 1999; Anand *et al.*, 2003; Mackintosh *et al.*, 2006), the resistance of rice to sheath blight (Datta *et al.*, 1999) and the resistance of potato to late blight disease (Liu *et al.*, 1994), plant diseases that cause serious economical losses. In all of the cases, resistance was increased or development of disease symptoms was delayed. Although expression of a single PR-protein seemed to have a beneficial effect on slowing disease progression, satisfactory levels of resistance were achieved only when combinations of PR-protein genes were introduced into the plant (Chen *et al.*, 1999). However, the first field evaluation of transgenic wheat plants expressing PR-proteins failed to show any improved resistance under heavy inoculum loads (Anand *et al.*, 2003). So although the production of transgenic plant by introduction of TLP-genes seems very promising in the green house, further optimization is required before these transgenic plants can be commercially used.

Antifreeze proteins, among which TLPs, have also attracted attention of food technologists interested in controlling the way ice crystals grow in frozen foods. The inhibition of ice recrystallization, which is the formation of larger ice crystals at the expense of smaller ones, may be an important factor determining the texture of frozen foods, especially foods such as ice cream that are eaten while frozen. The presence of

antifreeze proteins in these products may inhibit ice crystal growth and preserve the smooth and creamy texture of a high quality product (Griffith and Ewart, 1995; Breton *et al.*, 2000).

Background and aims of the study

Arabinoxylans are heteropolysaccharides that form the major constituents of the cereal plant cell wall. Due to their unique physicochemical properties, such as water-holding capacity and viscosity forming potential, they determine the functionality of the grain in several cereal-based applications such as bread-making (Courtin and Delcour, 1998), gluten-starch separation (Frederix *et al.*, 2004) and pasta production (Ingelbrecht *et al.*, 2001). Microbial xylanases, hydrolyzing arabinoxylans, can alter the physicochemical properties of these polysaccharides and, hence, are often used in these kinds of applications to improve processing properties, production yield and product quality (Rouau *et al.*, 1994; Courtin *et al.*, 2001; Sprössler, 1997; Courtin *et al.*, 1999; Frederix *et al.*, 2003; Ingelbrecht *et al.*, 2001). However, the presence of xylanase inhibitors in cereals often influences the functionality of added xylanases. Identification and characterization of these inhibitors, and more specifically insight into the interaction between xylanases and xylanase inhibitors, could help to develop a scientific basis for the tailor-made production of xylanases that are not or less inhibited by xylanase inhibitors. This would decrease the amounts of xylanases that need to be added during cereal processing, which would be economically advantageous.

The research work described in this dissertation can be situated within the IWT-GBOU project 'Xylafun', which aims at a better understanding of xylanases and factors governing their functionality. An important topic within this interdisciplinary project are the xylanase inhibitors. Hitherto, two structurally unrelated cereal xylanase inhibitors, TAXI and XIP, have been extensively characterized (Gebruers, 2002; McLauchlan *et al.*, 1999; Sancho *et al.*, 2003). Additionally, their genes were identified (Fierens *et al.*, 2003; Raedschelders *et al.*, 2005; Elliott *et al.*, 2002), they were expressed (Fierens *et al.*, 2003; Raedschelders *et al.*, 2005; Elliott *et al.*, 2002), their structures were resolved (Sansen *et al.*, 2003; Sansen, 2005; Payan *et al.*, 2003) and the crucial amino acids determining their inhibition activity and specificity were identified (Sansen *et al.*, 2004; Raedschelders *et al.*, 2005; Payan *et al.*, 2004). Recently, however, a new cereal xylanase inhibitor, TLXI, was isolated at the Laboratory of Food Chemistry and Biochemistry (Faculty of Bioscience Engineering, K.U.Leuven). Whereas the biochemical characterization of wheat TLXI is the scope of the latter

laboratory and more specifically of Ellen Fierens, this dissertation, performed at the Laboratory of Gene Technology of the same faculty, focuses on the molecular and mutational analysis of this inhibitor. Obviously, both research topics are complementary since they both aim at a better understanding of xylanase inhibitor functionality. Therefore, the work was performed in close collaboration with the Laboratory of Food Chemistry and Biochemistry.

The technical objectives of this study were:

1. The molecular identification of the TLXI encoding gene in wheat and variants of this gene in wheat and other cereals (Chapter 3).
2. Optimizing recombinant expression of this gene in *P. pastoris* to provide a straightforward production system of the protein (Chapter 4).
3. Biochemical characterization of the recombinant inhibitor and comparison with the TLXI protein isolated from wheat (Chapter 5).
4. Providing a first insight in the interaction between TLXI and the inhibited xylanases via a mutagenic approach and via comparison of the inhibition characteristics of TLXI and its variants (Chapter 6, 7 and 8).

PART II
EXPERIMENTAL WORK

Chapter 3

Molecular identification of the TLXI encoding gene

3.1 Introduction

In 2002, a new type of xylanase inhibitor was identified and isolated from wheat at the Laboratory of Food Chemistry and Biochemistry (K.U.Leuven). After TAXI- and XIP-type inhibitors, this was the third type of xylanase inhibitor purified from cereals. The experimental molecular mass of this native inhibitor was about 18 kDa and it was shown to inhibit only GH11 xylanases. The lack of knowledge about its precise identity, i.e. the complete amino acid sequence, urged to identify the TLXI encoding gene. The absence of knowledge about the interaction mechanism between xylanases and this new type of inhibitor necessitated to express the protein in recombinant organisms, a prerequisite for further mutational analysis and necessary to elucidate the structure-function relationship.

In this chapter the identification of a wheat gene, encoding this new type of inhibitor, is described. It is primarily based on the determination of the N-terminal peptide sequence (Fierens *et al.*, 2007) and an EST (expressed sequence tag) database search. Bioinformatic analysis of the newly identified gene indicated that the inhibitor belongs to a group of proteins showing homology to the sweet tasting protein, thaumatin, conferring the inhibitor its name, TLXI (thaumatin-like xylanase inhibitor). The fact that TLXI belongs to this group of structurally related proteins, suggested that TLXI is involved in the plant defense mechanism, a hypothesis that is further supported by analyzing the promoter region of the *tlxi* gene. Because, in addition to mutational analysis, naturally occurring variants can also shed light on the structure-function relationship, an attempt was made to identify TLXI encoding genes in other cereals and diploid wheat species.

3.2 Materials and methods

3.2.1 Standard molecular biology techniques

Agarose gel electrophoresis and DNA sequence analysis were performed as described by Sambrook and Russell (2001) unless specified otherwise. DNA sequences were analyzed on a 377 DNA Sequencer using ABI PRISM Big Dye Terminator chemistry (Applied Biosystems, Foster City, CA, USA). The Sequencher 4.1 package (Gene Codes Corporation, Michigan, USA) was used to correct and align the machine-read DNA sequences. Primers (Table 3-3) were purchased from Prologo Primers and Probes (Paris, France) unless specified otherwise.

3.2.2 Isolation of plant genomic DNA and mRNA

Genomic DNA was isolated from young leaves of hexaploid wheat cultivars (*T. aestivum* Estica and Soisson), diploid wheat species (*T. urartu*, *Aegilops squarrosa* and *A. speltoides*) and rye (*Secale cereale* cv. halo) using the DNeasy Plant Mini kit (Qiagen, Hilden, Germany). Total RNA was extracted from young embryos (3 weeks post anthesis) of cv. Estica by means of the Invisorb Spin-Plant-RNA Mini kit (Invitek, Berlin-Buch, Germany). mRNA was purified from the total RNA with the Oligotex mRNA Mini kit (Qiagen). All procedures were carried out according to the manufacturer's instructions.

3.2.3 Rapid amplification of cDNA ends (RACE)

3.2.3.1 3'RACE

3'RACE was performed starting from mRNA, isolated from young embryos of wheat cv. Estica. cDNA was obtained by reverse-transcribing the mRNA using the GeneRacer kit (Invitrogen, Carlsbad, USA) with the GeneRacer™ Oligo dT primer using conditions specified by the supplier. *T. aestivum* cDNA (cv. Estica) was subsequently used as a template for HotStarTaq DNA polymerase (Qiagen) mediated PCR amplification with gene specific primer I3race, designed on EST BE399034, in combination with GeneRacer™3' primer supplied with the kit. A nested 3'RACE was performed on this PCR product with gene specific primer I3 nested and GeneRacer™3'Nested primer. For both PCR reactions the following temperature

program was used: 15 min at 95°C (activation of the polymerase and initial denaturation); 1 min at 94°C (denaturation), 1 min 30 s at 58°C (primer annealing), 2 min at 72°C (primer extension) (30 cycles); 10 min at 72°C (final extension). The nested PCR product was purified using the PCRapid kit (Invitex) and cloned in a pCR[®]4-TOPO[®] vector (section 3.2.6.) (Invitrogen) followed by DNA sequencing (section 3.2.1.).

3.2.3.2 5'RACE

5'RACE was performed, according to the protocol supplied with the GeneRacer kit (Invitrogen), on mRNA with gene specific primer I5race and a nested 5'RACE with gene specific primer I5nested in combination with GeneRacer[™] 5' primer and GeneRacer[™] 5' Nested primer (Invitrogen), respectively, both annealing to the GeneRacer[™] RNA Oligo ligated at the 5' end of the decapped mRNA. The I5race and I5nested primers were both designed on the sequence obtained by PCR on genomic DNA (section 3.2.4.) and on corresponding EST sequences. The PCR product was purified using the PCRapid kit (Invitex). PCR products resulting from the 5'RACE reaction were directly sequenced (section 3.2.1.).

3.2.4 Polymerase chain reaction (PCR) on genomic DNA

Amplification on genomic DNA of wheat cv. Estica, isolated as described above, was performed using HotStarTaq DNA polymerase (Qiagen) (1.5 Unit) and specific primers Iintf, designed on EST sequence BE427320, and XI2, located in the 3'UTR (untranslated region) and designed based on the sequence obtained by 3'RACE. The PCR reaction was carried out with buffer supplied by the manufacturer, taking into account the recommended reaction volumes (30 µl), concentrations of dNTPs (Roche diagnostics, Brussels, Belgium) (200 µM each), primers (1 µM each) and template DNA (50 ng). To identify *tlxi* variants and related sequences, PCR on genomic DNA of *A. squarrosa*, *A. speltoides*, *T. urartu*, *S. cereale* cv. halo and *T. aestivum* cv. Soisson was performed in the same way as described above. The primers used for this purpose are specified in the related results sections.

The following temperature program was used unless specified otherwise: 15 min at 95°C (activation polymerase and initial denaturation); 1 min at 94°C (denaturation), 1 min 30s at 58°C (primer annealing), 2 min at 72°C (primer extension) (30-35 cycles);

10 min at 72°C (final extension). PCR products were purified using the PCRapid kit (Invitex) and directly sequenced (section 3.2.1.).

3.2.5 Thermal asymmetric interlaced (TAIL) PCR

TAIL-PCR (Thermal Asymmetric Interlaced PCR), developed by Liu and Whittier (1995), is an efficient technique for isolation of DNA segments adjacent to known sequences. This strategy uses nested sequence-specific primers together with 16-bp degenerate primers (AD-primers) in a multistep thermal cycling program. The degenerate primers used in this study are given in Table 3-3. The procedure consists of the alternation of lower-stringency and higher-stringency cycling to allow amplification of gene-specific flanking regions. This strategy uses two primers of different length and annealing stability (degenerate primer and gene-specific primer). PCR cycles at higher temperatures favor the annealing of the longer gene-specific primers, while lower temperature incubation allows annealing of both specific and degenerate primers. A typical thermal cycling program consists of 12-15 TAIL cycles containing 1 lower-stringency and 2 higher-stringency cycles. To preferentially amplify target sequences over non target-sequences, three TAIL reactions (hereafter called TAIL1, TAIL2 and TAIL3) are performed consecutively, each time with a nested gene-specific primer. For TAIL2, the forty-fold diluted product of TAIL1 was used as template. For TAIL3, the product of TAIL2 was used as a template in a twenty-fold dilution.

In this study, the TAIL reaction was applied for the identification of the 5' untranslated region. For the 5'TAIL reaction on genomic DNA of wheat cvs. Estica and Soisson, Iintr, I5race and I5nested (Table 3-3) were used as gene specific primers and AD3 was used as a degenerate primer (Table 3-3). Based on the newly identified 5' untranslated region of the *tlxi* gene encoded by Estica, new primers, 5TAIL1, 5TAIL2 and 5TAIL3 (Table 3-3) were developed and used in combination with the AD2 degenerate primer (Table 3-3) to identify the sequence more upstream, enabling us to gain further insight in the promoter region.

The reaction mixtures and the thermal cycling program are schematically given in Table 3-1 and 3-2, respectively. The cycling program was adapted from Liu *et al.* (1995). The use of HotStarTaq polymerase (Qiagen) urged to incorporate an extra 15 minutes activation step at the start of each individual PCR reaction. Final PCR products

were purified with the PCRapid kit (Invitex) and directly sequenced (section 3.2.1.) or sequenced following TOPO[®] cloning (section 3.2.6.).

Table 3-1: Reaction mixture composition in TAIL1, TAIL2 and TAIL3 reactions.

	TAIL1	TAIL2	TAIL3
	volume (µl)		
Template	3*	1**	1***
PCR buffer (10x)	2	2.5	5
dNTPs (2mM each)	2	1.25	2.5
Gene specific primer (20 µM)	0.15	0.25	0.5
AD primer (20 µM)	2	2.5	5
HotStarTaq polymerase (5U/µl)	0.2	0.16	0.3
Q solution (5x)	4	5	10
milliQ water	7.65	12.34	25.7
TOTAL volume	20	25	50

* genomic DNA is used as template (50 ng)

** a 40-fold dilution of TAIL1 PCR product is used as template

*** a 20-fold dilution of TAIL2 PCR product is used as template

Table 3-2: Thermal cycling program in TAIL1, TAIL2 and TAIL3.

TAIL1		
Temperature (°C)	Duration (min)	Number of cycles
95	15	
94	1	} 5
64	1	
72	3	
94	1	
27.5 to 72	3	
72	3	
94	0.5	} 2
64	1	
72	3	
94	0.5	
42	1	} 15
72	3	
72	3	

TAIL2 ^a and TAIL3 ^b		
Temperature (°C)	Duration (min)	Number of cycles
95	15	
94	0.5	} 2
64	1	
72	3	
94	0.5	
42	1	} 12 ^a /10 ^b
72	3	
72	3	

3.2.6 pCR[®]4-TOPO cloning

If after optimization of the PCR reaction and purification of the PCR product, still multiple bands appeared on agarose gel, PCR products were cloned in a pCR[®]4-TOPO[®] vector (Invitrogen). For this purpose the TOPO TA Cloning[®] Kit for Sequencing (Invitrogen) was used according to the manufacturer's instructions. In this way, the different obtained PCR products can be sequenced separately.

The pCR[®]4-TOPO[®] vector is supplied linearized with single 3' deoxythymidylate overhangs and topoisomerase covalently bound to the vector. Hence, PCR products containing 3' deoxyadenylate overhangs, due to the terminal transferase activity of *Taq* polymerase, can efficiently be ligated with the vector without the use of a ligase.

3.2.7 Primers used in this chapter

Table 3-3: Primers used in the different sections of this chapter.

primer	sequence	reference (section)
GeneRacer [™] OligodT primer	GCTGTCAACGATACGCTACGTAACGGCATGACAGTG(T) ₁₈	3.2.3.1
GeneRacer [™] 3' Primer	GCTGTCAACGATACGCTACGTAACG	3.2.3.1
GeneRacer [™] 3'Nested Primer	CGCTACGTAACGGCATGACAGTG	3.2.3.1
I3race	GTGCCAGACCGGCGACTG	3.2.3.1
I3nested	GTGGCAGCTCGCTGACTTG	3.2.3.1
GeneRacer [™] 5' Primer	CGACTGGAGCACGAGGACACTGA	3.2.3.2.
GeneRacer [™] 5'Nested Primer	GGACACTGACATGGACTGAAGGAGTA	3.2.3.2.
I5race	TTGGTGGAGCACGAGCGCCAC	3.2.3.2., 3.2.5
I5nested	CCGGCCACACCGTGAAGTG	3.2.3.2., 3.2.5
Iintf	CAAGCGCGGCACCGCTCACCATC	3.2.4.
XI2	AATACCTGACACACGTGTACGG	3.2.4.
XI301	AACACACACTGCAGACAATG	3.2.4.
XICON1	TTCACGGTGTGGCCGGCGGT	3.2.4.
XICON2	CGCTCATCATGGGCAGAAGAC	3.2.4.
XI1	GCTCATCATGGGCAGAAGACGA	3.2.4.
halo1	ACGGGCGCACACGTCGCAC	3.2.4.
halo2	TCCAGCACGGACACCTCGGC	3.2.4.
Ximatf	CACAGATCT GCACCGCTCACCATCACGAAC	3.2.4.
AD1	NTCGASTWTSWGTT	3.2.5.
AD2	NGTCGASWGANAWGAA	3.2.5.
AD3	WGTGNAGWANCANAGA	3.2.5.
Iintr	CAAGTCAGCGAGCTGCCAC	3.2.5.
5TAIL1	CAGTGTGTGTGGTGTCTAGAGAG	3.2.5.
5TAIL2	CGTGCTCAACATGTGTAAGCGAGCTAG	3.2.5.
5TAIL3	GTCAAAGATGGCGCCAAGATTTGGCTAC	3.2.5.

*Bgl*II restriction sites are indicated in bold.

3.3 Results

3.3.1 Identification of the *tlxi* gene in hexaploid wheat (*T. aestivum*)

The N-terminal amino acid sequence of TLXI, isolated from wheat, was determined as APLTITNRXHFTVXXAVALVLHQQG (with X referring to an unidentified amino acid) by Edman degradation (Fierens *et al.*, 2007). This sequence was used to screen *Triticeae* EST sequences with tBLASTn (Altschul *et al.*, 1997) yielding two partially overlapping EST sequences (BE427320 and BE399034). Assembly and manual editing resulted in a contiguous draft sequence. Based on this draft sequence, internally located primers I3race and I3nested (Table 3-3) were designed and used in a 3'RACE reaction on mRNA of wheat cv. Estica. After TOPO cloning and sequencing, clones that consistently overlapped with the draft sequence were found. Hence, assembly of the EST sequences and the 3'RACE sequences resulted in a new, extended draft sequence. Subsequently, new primers (Iintf and XI2) (Table 3-3) were designed and used to perform PCR on genomic DNA of wheat cv. Estica. The sequence of this product corresponded perfectly with the draft sequence and revealed that the *tlxi* sequence does not contain introns. At this point of the study, the mature sequence including the 3'UTR was identified. To determine the signal sequence and the 5'UTR, 5'RACE was performed using primers I5race and I5nested (Table 3-3). Sequencing of this product resulted in the determination of the complete cDNA sequence (Figure 3-1). The coding sequence consists of 534 bp, is G/C-rich (69.2%) and results, upon translation, in a protein of 177 amino acids (Figure 3-2). The DNA, mRNA and amino acid sequences were deposited in the NCBI database (Accession numbers AJ786602, AJ786601 and CAH10283, respectively).

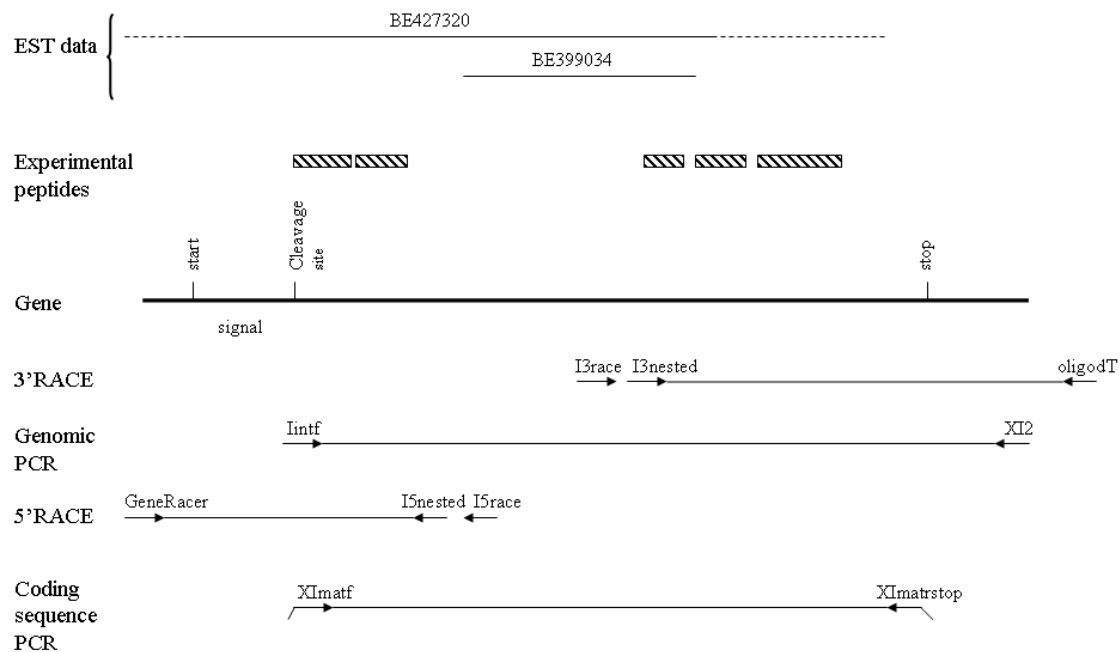


Figure 3-1: Schematic overview of *tlxi* sequence determination.

Schematic overview of *tlxi* sequence data and relative positions of primers used for characterization and cloning. Details are explained in the text. Flanking regions of EST BE427320 (dotted line) showed limited identity with the *tlxi* mRNA because of low quality. The coding sequence PCR will be discussed in chapter 4. Experimental peptides were determined from wheat TLXI by Fierens and coworkers (2007).

Using the SignalP program (Bendtsen *et al.*, 2004) for protein localization prediction, the highest score was given to the possibility that TLXI is secreted outside the plant cell. The predicted cleavage site between the signal sequence and the mature protein is situated between alanine -1 and alanine +1 (Figure 3-2). The latter alanine residue corresponds to the experimentally determined N-terminus of native TLXI. Hence, the open reading frame encodes a signal peptide of 26 amino acids followed by a mature protein of 151 amino acids. ScanProsite (Gattiker *et al.*, 2002) predicts an N-glycosylation recognition site (⁹⁵Asn-Tyr-Thr⁹⁷) indicating potential glycosylation of Asn95. Ten cysteine residues are present in the mature protein sequence, potentially resulting in five intramolecular disulfide bonds. The calculated molecular mass of the TLXI protein is 15633 Da and its theoretical pI-value is 8.38. Both parameters were obtained with ProtParam (Gill and Von Hippel, 1989).

```

-26           M A S P A R S A S A S P V L L
-94 ACACACACTGCAGACAATGGCGTCTCCAGCCAGAAGCGGAGCGCCTCTCCAGTCTCCTCT
-11  L L V V L A A G A S A A P L T I T N R C
-34 CTTGCTCGTCTCCTCGCCGCCGGGCAAGCGGGCACCGCTCACCATCACGAACCGGTG
 10  H F T V W P A V A L V L H Q G G G G T E
 26  CCACTTCACGGTGTGGCCGGCGGTGGCGCTCGTGTCCACCAAGGGGGCGGCGGCACCGA
 30  L H P G A S W S L D T P V I G S Q Y I W
 86  GCTCCACCCAGGGGCCAGCTGGAGCCTCGACACGCCGGTGATCGGCTCCCAGTACATATG
 50  G R T G C S F D R A G K G R C Q T G D C
146  GGGGCGCACGGGCTGCTCCTTCGACCGGGCCGCAAGGGGGCGGTGCCAGACCGGGCGACTG
 70  G G S S L T C G G N P A V P V T M A E V
206  CGGTGGCAGCTCGCTGACTTGGGGGGCAACCCGGCGGTGCCGGTGACCATGGCCGAGGT
 90  S V L Q G N Y T Y G V T S T L K G F N L
266  GTCCGTGCTCCAAGGCAACTATACCTACGGCGTACGTCGACGCTCAAGGGGTTCACCT
110  P M D L K C S S G D A L P C R K A G C D
326  GCCCATGGACCTGAAGTGCAGCTCCGGCGACGCGCTCCCGTGCCGGAAGGCTGGGTGCGA
130  V V Q P Y A K S C S A A G S R L Q I V F
386  CGTTGTCCAGCCGTACGCGAAGAGCTGCAGCGCGGCTGGAAGCCGGCTCCAGATCGTCTT
150  C P *
446  CTGCCATGATGAGCGGCAGAACATATATAGCACGTATACGCATGTAATAACCACCGCAC
506  GTACGGGTAGTAGTACCTCCGTATACCGTACACGTGTGTCAGGTATCCCAGCCGCGAGTG
566  CATACTCGAGCGAGGTTCCAATAAAGGTGCCATTACCTTTGGTGTAAAAA
626  AAAAAAAAAA

```

Figure 3-2: Complete cDNA and amino acid sequences of TLXI.

The first methionine of the signal sequence (italic) is at position -26. The mature protein starts at position 1, stops at position 151 and contains 10 cysteine residues (bold) and one possible *N*-glycosylation site (bold, italic) at position 95. Parts of the amino acid sequence were confirmed by sequencing of TLXI peptides obtained after cyanogen bromide cleavage of native protein (underlined) (Fierens *et al.*, 2007). The Prosite thaumatin family signature PS00316 is shaded.

At a later time, more wheat EST sequences were found in the database which showed 99-100% identity with the *tlxi* sequence. These EST sequences were isolated from root (CK199869), grain (CD915298) and ovary (CD914550). In addition, EST sequences from barley (CK124694) and durum wheat (AJ611730) were 76% and 59% identical, respectively, at the nucleotide level with the *tlxi* coding sequence and 60% and 44%, respectively, after translation.

BLASTp analysis (Altschul *et al.*, 1997) shows that the xylanase inhibitor contains a conserved domain and belongs to the thaumatin family (Pfam00314). This finding is further supported by the presence of the Prosite PS00316 thaumatin family signature. The consensus pattern for this family of proteins is: G-x-[GF]-x-C-x-T-[GA]-D-C-x(1,2)-G-x(2,3)-C. However, four residues precede the last cysteine of the pattern in the TLXI sequence instead of two or three. Similarities up to 68% were found with several thaumatin-like proteins from various origins (barley, rice, corn).

3.3.2 Genetic variation

In an attempt to find variance in the TLXI encoding genes, several strategies were applied. The isolation of variant coding sequences, subsequent recombinant expression and characterization can help to identify the amino acids that cause the inhibition specificity or the residues that contribute to other properties of the protein. For this reason, we tried to find variants of the TLXI coding sequence, isolated from *T. aestivum* cv. Estica (see section 3.3.1.), in another hexaploid wheat cultivar, *T. aestivum* cv. Soisson, in diploid wheat species (*T. urartu*, *A. speltoides* and *A. squarrosa*) and in another cereal, rye (*S. cereale* cv. halo). In addition, we also identified and compared the 5'UTR region of the *tlxi* gene in *T. aestivum* cvs. Estica and Soisson.

3.3.2.1 Variation of *tlxi* genes in hexaploid wheat cultivars

PCR on genomic DNA of wheat cv. Soisson was performed with primers XI301, located right before the translation start of the *tlxi* gene and XI2, located in the 3'UTR region (Table 3-3). Primers were based on the *tlxi* sequence isolated from cv. Estica. The sequence showed 100% sequence identity with the sequence obtained from wheat cv. Estica. To identify and compare the 5' untranscribed regions of *tlxi* genes from wheat cvs. Estica and Soisson, a 5'TAIL reaction was performed on both cultivars as described in section 3.2.5. Direct sequencing of the PCR products resulted in two different 5' untranscribed regions for Estica and Soisson. However, the variation is very limited. Both regions display 98% sequence identity. TOPO cloning of the PCR product of the 5'TAIL reaction on genomic DNA of cv. Soisson revealed that, next to the abundant sequence described above, a small fraction of the TOPO clones also contained a 5' untranscribed region that was 100% identical with the one isolated from cv. Estica. This finding indicates that the observed variance is not due to variation between the two cultivars, but is in fact due to orthologous or paralogous variation. This was also confirmed by the second TAIL reaction that was performed on genomic DNA of cv. Estica with gene specific nested primers 5TAIL1, 5TAIL2 and 5TAIL3. Comparison of the sequences showed that the newly generated sequence overlapped the 5' untranscribed region formerly amplified from genomic DNA of cv. Soisson meaning that both sequences occur in both cultivars. A contiguous sequence was made from the two sequences amplified with the two consecutive TAIL PCR reactions, and the program PlantCARE (Lescot *et al.*, 2002) was used to search for motifs in this

promoter region of the *tlxi* gene resulting in the identification of a putative TATA-box, CAAT box, ABRE (abscisic acid-responsive element) motif and MBS (MYB binding site) motif (Figure 3-3), located 151 bp, 161 bp, 289 bp and 75 bp upstream of the putative transcription start, as determined by 5'RACE, respectively.

```

-365 AGGTTTGTAAAGTGTACGCTATTGTGCCCGCTCCACCGTCGGCACGTCACGGTTGATACCA
-305 CCAGGGCCTTAATGGACACGTGTATTTTAGGGCGTCAAGATAAACTTTTTCTTTCTTTGG
      ABRE
-245 CCCATCATTATCTGATGGAGTCGTGTGGCACTACAGACGGTGGGAATTGTCGTCGATCTT
-185 CAACGGACGAAAGGGAAAAGCGGCCAATCTTGGCTATATTGGCGTCCAAGTAGGTAGTAG
      CAAT-box TATA-box
-125 GTACGTAGTAGCCAAATCTTGGCGCCATCTTTGACTTCAATGCTCCCACCCAACTGCTTG
      MBS
-65 TAGTCTAGCTCGCTTACACATGTTGAGCACGACAGATAAATAAGCATGCAGCCTCTCTAG
-5 ACACCAACACACACTGCAGACAAATGCGGTCTCCAGCCAGAAGCGCGAGCGCCTCTCCAGTC
      CTCTCTTTGCTCGTCTCTCGCCCGGGGCAAGCGCGGCACCGCTCACC

```

Figure 3-3: Promoter region of a *tlxi* gene including the translation start (ATG, bold) and the start of the mature protein (GCA, underlined).

The putative transcription start is boxed and the motifs, recognized by the program PlantCARE, are underlined and the respective names are indicated. Numbering is relative to the putative transcription start.

3.3.2.2 Identification of *tlxi* genes in diploid wheat species

While hexaploid wheat, like *T. aestivum*, contains the A, B and D genomes (AABBDD), diploid wheat species only have one genome. *T. urartu*, *A. speltoides* and *A. squarrosa* are diploid wheat species and contain the A genome (AA), the S genome (SS) and the D genome (DD), respectively. They are the progenitor species of hexaploid wheat. The S genome is most closely related to the B genome of hexaploid wheat. To clarify by which genome of hexaploid wheat the identified TLXI sequence is encoded, PCR with primers XI301 and XI2 (Table 3-3) was performed on the three diploid wheat species. For *A. speltoides* and *A. squarrosa*, one single band was detected by agarose gel electrophoresis. For *T. urartu* on the other hand, no PCR product was formed. Direct sequencing of the obtained PCR products, using the PCR primers, showed that the *tlxi* sequence identified earlier from wheat cv. Estica, is encoded by the D genome of hexaploid wheat because the sequence amplified from *A. squarrosa* was 100% identical with this sequence. The sequence amplified from *A. speltoides* (SS) was 90% identical to the sequence from *A. squarrosa*. The corresponding mature *A.*

speltooides protein (without signal sequence), further referred to as AS-TLXI, displays 90% identity (ClustalW, www.ebi.ac.uk/clustalw/) with the TLXI sequence encoded by the D genome, further referred to as TLXI. The signal sequence is two amino acids longer compared to the D genome sequence (Figure 3-4).

```

TLXI      MASPA--RSASASPVLLLLLVLAAGASAAPLTIITNRCHFTVWPAVALVLHQGGGGTELHP 32
AS-TLXI   MASAGSRCVSASPVLLLLFVVLAVGASAAPLTIITNRCPFTVWPAVALVLHQGGGGTELHP 32
          ***.* * .*****:****.***** *****
          *****

TLXI      GASWLDTPVIGSQYIWGRTGCSFDRAGKRCQTGDCGGSSSLTCGGNPAVPVTMAEVSVL 92
AS-TLXI   GASWTLDTFVIGSEYIWGRTGCSFDGSGKRCQTGDCGGSSLICGGNPAAPVTMAEVSVL 92
          ***:*****:***** .***** *****.*****

TLXI      QGNYTYGVTSTLKGFNLPMDLKSSGDALPCRKAGCDVVQPYAKSCSAAGSRLQIVFCP 151
AS-TLXI   EGNITYGVTSTFKGFNLAMDLTCSGDALRCRKAGCDVVRPHAKSCSAAGSRLQVVFPC 151
          :*****:*****.*.*.***** *****:*.*****:****

```

Figure 3-4: Sequence alignment (clustalW) of the TLXI sequences encoded by *A. speltooides* (AS-TLXI) and *A. squarrosa* (TLXI).

Signal sequences are in bold. Numbering refers to the mature sequence (without signal sequence).

Because the amplification of a PCR product from *T. urartu* with the above mentioned primers failed, new primers were designed, XICON1 and XICON2 (Table 3-3), situated right behind the start of the mature protein and at the stopcodon, respectively. These primers were designed in regions identical in D and the S genome sequences, which are also highly conserved in other TLPs. After TOPO cloning and sequencing, the obtained sequences could be classified in three groups. The majority of the clones contained a sequence that, upon translation, showed 62% identity (ClustalW) with TLXI and AS-TLXI. tBLASTn analysis (Altschul *et al.*, 1997) revealed a 99% identity with wheat EST BU607139. The second sequence that could be identified was 45% and 43% identical at the amino acid level with TLXI and AS-TLXI, respectively. However, there was a 99% amino acid sequence identity with translated EST sequences isolated from *T. aestivum* (CJ666849, CJ663167, CV777825, CV776413 and BE420142). A small fraction of the TOPO clones contained a sequence displaying 88% sequence identity (ClustalW) with *tlxi*. However, an internal stopcodon, caused by a frameshift due to an insertion (Figure 3-5), is present and interrupts translation, indicating the sequence to be a putative pseudogene. The insertion probably originates from a defective DNA replication event during evolution since the insertions are (imperfect) repeats from the flanking sequences. Some pseudogenes have also been reported in other gene families, like those encoding for LMW glutenin (Johal *et al.*, 2004) and α -gliadin (Van Herpen *et*

al., 2006). Noteworthy, also several pseudogenes related to the xylanase inhibitor TAXI have been found (G. Raedschelders, personal communication).

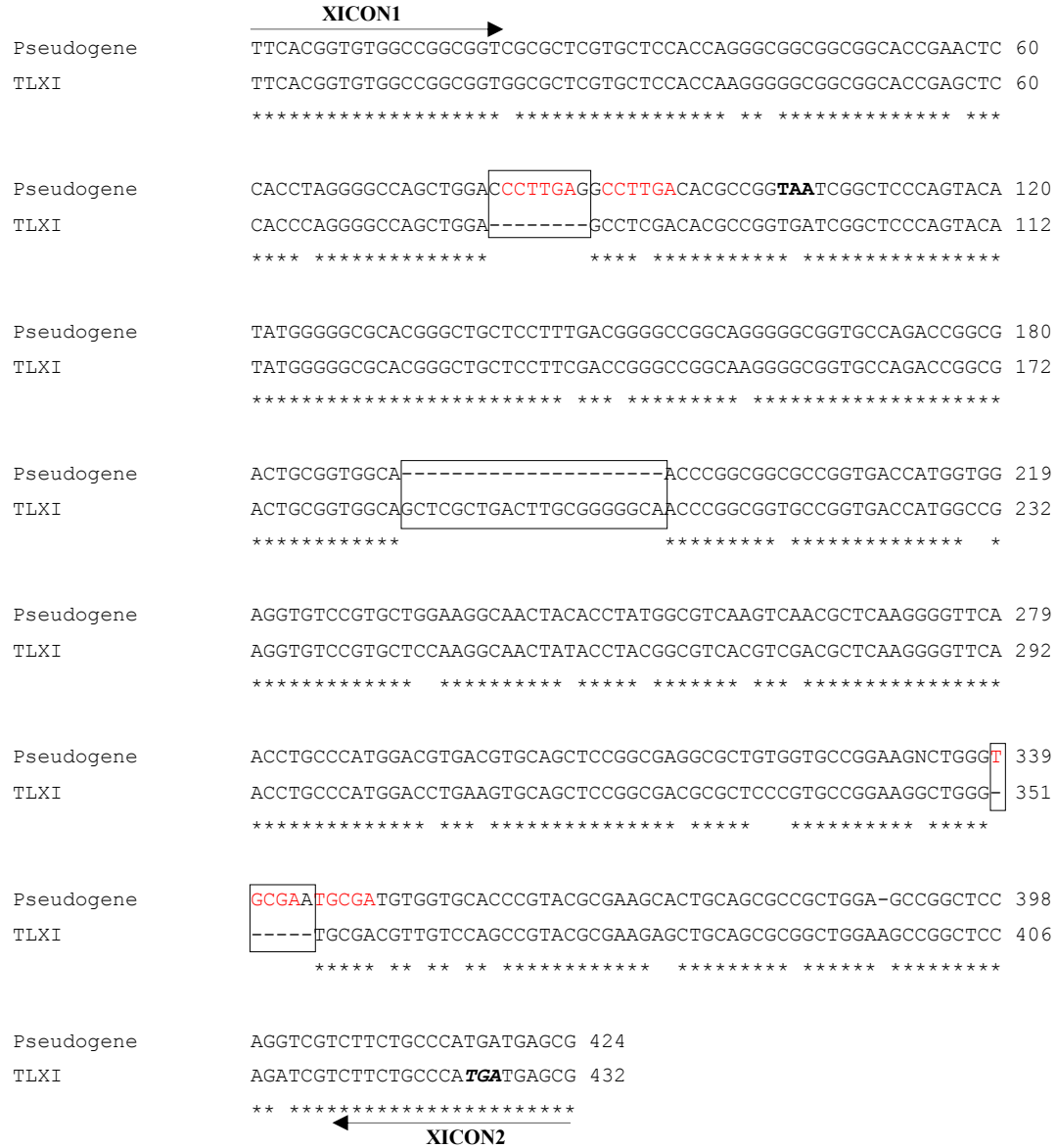


Figure 3-5: Sequence alignment (ClustalW) of a pseudogene amplified from genomic DNA of *T. urartu* (AA) with the corresponding part of the *tlxi* gene.

Primers (XICON1 and XICON2) used in the PCR reaction are indicated with arrows. The insertions and deletions (INDELs) are boxed. The internal stopcodon of the pseudogene is indicated in bold, while the normal stopcodon of the *tlxi* gene is bold and italic. The repeats are colored red.

3.3.2.3 Identification of *tlxi* genes in other cereals

A PCR reaction on genomic DNA of *S. cereale* cv. halo was performed with primer combination XICON1-XICON2 and I3race-XI1 (Table 3-3). The thermal cycling

program was as described in section 3.2.4., but the annealing temperature was 59°C. Only with primer combination I3race-XI1, amplifying only part of the *tlxi* sequence, a single band could be detected with agarose gel electrophoresis. After TOPO cloning and sequencing, a sequence was found that, upon translation, was 84% identical (ClustalW) to the corresponding sequence of TLXI from wheat. To complete the sequence, a reverse primer, halo1 (Table 3-3), was developed based on the newly identified sequence. A PCR reaction in combination with the XImatf forward primer, located at the start of the mature protein, resulted in a non-specific amplification product. Hence, a nested PCR was performed with primers XImatf and halo2 (Table 3-3) according to the protocol described in section 3.2.4., but at an annealing temperature of 63°C, resulting in a sequence that consistently overlapped with the I3race-XI1 PCR product. Assembly of the two sequences resulted in a sequence displaying 93% and 88% identity (Figure 3-6) with TLXI at the nucleotide level and the amino acid level, respectively. The most remarkable difference between the TLXI sequence from rye, further referred to as SC-TLXI, and from wheat is that, due to an insertion, the potential glycosylation site (N-x-S/T) is disrupted.

```

SC-TLXI      APLTITNRCHFTVWPAVALVLHQGGSGTELHPGASWTLDTPVIGSQYIWGRTGCSFDGAG 60
TLXI         APLTITNRCHFTVWPAVALVLHQGGGGTELHPGASWSLDTPVIGSQYIWGRTGCSFDGAG 60
*****.*****:***** **

SC-TLXI      KGRCQTGDCGGSSLICGGNPSALVTMAEVSVLEGNYYTYGVTSTLKGFNLPVDVTCSSGD 120
TLXI         KGRCQTGDCGGSSLTCGGNPAVPVTMAEVSVLQGN-YTYGVTSTLKGFNLPMDLKCSSGD 119
*****:*****:***** ** * *****:*. *****

SC-TLXI      ALRCGKAGCDVVRPYAKSCSATGSRLQVVFCEP 152
TLXI         ALPCRKAGCDVVQPYAKSCSAAGSRLQIVFCEP 151
** * *****:*****:*****:*****

```

Figure 3-6: Sequence alignment (ClustalW) of the amino acid sequences of SC-TLXI and TLXI.

The intact and disrupted N-glycosylation recognition sequence of TLXI and SC-TLXI, respectively, are shaded.

3.4 Discussion

The gene sequence encoding a new type of xylanase inhibitor, TLXI, has been identified. The TLXI coding sequence is 534 bp long and encodes a mature protein of 151 amino acids preceded by a signal peptide for secretion of 26 amino acids. The calculated molecular mass and pI are 15.6 kDa and 8.38, respectively, and the protein contains a potential N-glycosylation site at Asn95. The experimental determination of molecular mass and pI are discussed in chapter 5. The protein sequence derived from the gene sequence matches perfectly with the experimentally determined internal amino acid sequences of native TLXI. A database search (InterPro, www.ebi.ac.uk/interpro/) for the presence of catalogued motifs or patterns in the identified TLXI sequence revealed that the protein belongs to the thaumatin family of proteins (Pfam Accession Number: PF00314; Prosite Accession Number: PS00316), conferring the inhibitor its name, TLXI (thaumatin-like xylanase inhibitor). Proteins within this family are homologous to the intensely sweet tasting protein, thaumatin, found in the West African shrub *Thaumatococcus danielli*. Thaumatin-like proteins (TLPs) have been classified in class 5 of the pathogenesis-related proteins (PR-5) (Selitrennikoff, 2001), a group of proteins for which a defensive role in plant systems is suggested by their expression, which is generally induced by pathogens. The PR-5 family constitutes a group of unique proteins with diverse functions including antifungal activity, sweet taste and antifreeze activity. So far, the known TLPs are of molecular masses falling into two ranges, between 22-26 kDa, and below 18 kDa, respectively. The latter group, to which TLXI belongs, has members which have been identified in cereals (Reimmann and Dudler, 1993; Reiss *et al.*, 2006) and in chickpea (Hanselle *et al.*, 2001) and contains deletions corresponding to ~ 25% of the size of the high molecular mass members. Koiwa *et al.* (1999) found that TLPs with antifungal activity had a particular motif under the form of a negative charged surface cleft which may be the site of interaction between the TLP and the plasma membrane of the fungus. This cleft is situated at the boundary between domains I and II of the protein (Figure 3-7).

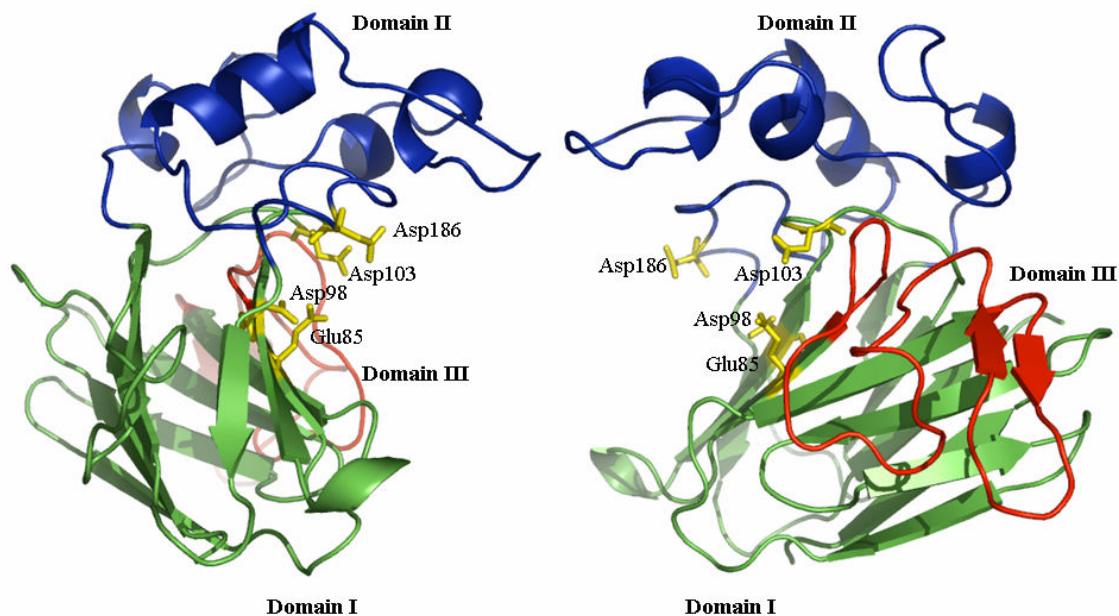


Figure 3-7: Structure of the tobacco PR-5d protein (PDB 1AUN) containing a conserved acidic cleft region (Koiwa *et al.*, 1999).

Both structures show a side view of the cleft region of PR-5d, but rotated 180°. The PR-5d protein consists of domain I (green), domain II (blue) and domain III (red). Domain II is absent in TLXI as shown by sequence alignment (Figure 3-8). Residues responsible for the acidic character of the cleft are represented as yellow sticks and residue names and numbers are indicated.

Like some other shorter TLPs, TLXI lacks domain II (Figure 3-8) resulting in the absence of the cleft region. This, however, does not exclude automatically that TLXI lacks antifungal activity. Indeed, a 17.6 kDa TLP (WRTLTP2) isolated from winter rye, lacking the cleft region, has been shown to possess antifungal activity (Chan *et al.*, 1999). In contrast to TLXI, however, this protein still possesses the conserved acidic residues conferring the negative charge to the cleft of high molecular mass TLPs as part of domain I, suggesting that it is not the presence of the cleft region that is determining for antifungal activity but the presence of the negative charge.

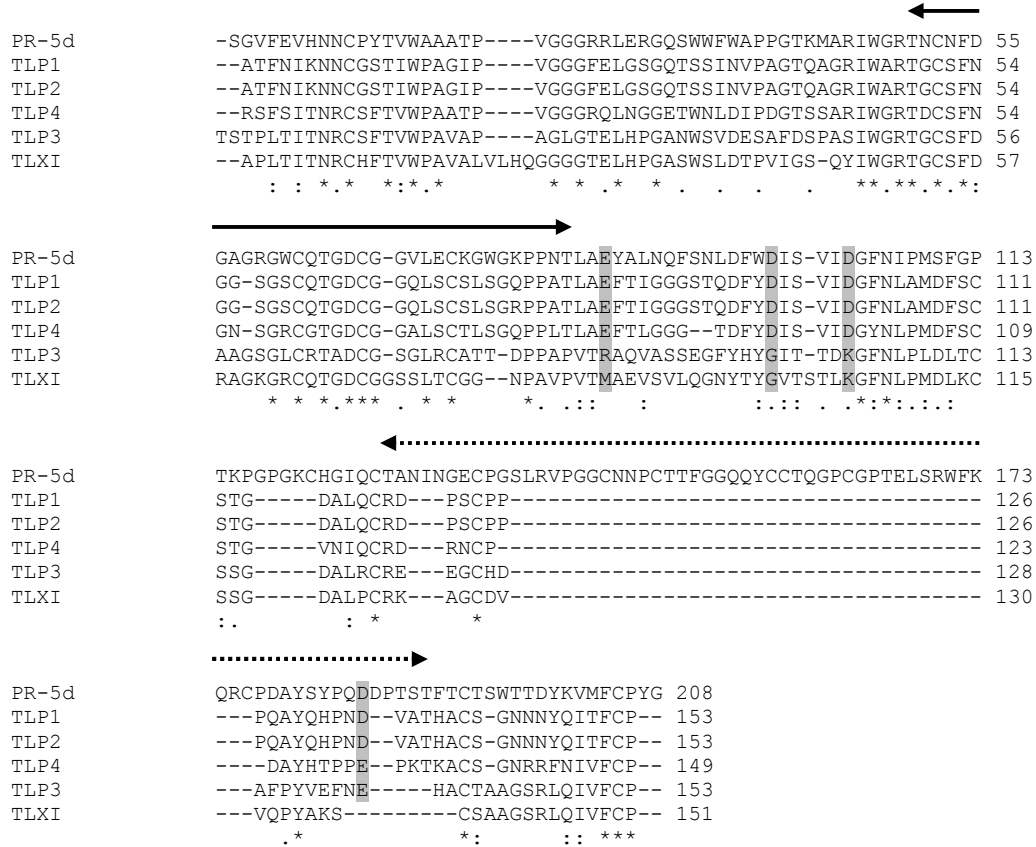


Figure 3-8: Sequence alignment (ClustalW) of short TLPs from barley (TLP 1, 2, 3 and 4, Reiss *et al.*, 2006) with one of the high molecular mass TLPs (PR-5d) and TLXI.

Domain III is indicated with a solid arrow, while domain II is indicated with a dashed arrow. The rest of the protein constitutes domain I. The residues corresponding to the acidic residues determining the negative charge cleft of PR-5d (Koiwa *et al.*, 1999) are shaded. TLXI, like TLP3, doesn't possess acidic residues at these positions indicating that it will probably not have antifungal activity by permeabilizing the fungal plasma membrane. TLP2 shows 96% identity to WRTLP2 from winter rye (Chan *et al.*, 1999).

Identifying TLXI as a xylanase inhibitor, may indicate that TLXI potentially exerts its role in the defense mechanism in another way than by permeabilizing the plasma membrane of the fungus. More especially, by inhibiting xylanases, secreted by pathogens to degrade the plant cell wall (Gomez-Gomez *et al.*, 2002), it could prevent the fungus from penetrating the plant. Only one other TLP, i.e. zeamatin, showing 43% identity (ClustalW) with TLXI, is known to inhibit enzymes, namely insect α -amylase and mammalian trypsin (Schimoler-O'Rourke *et al.*, 2001). Although the antifungal activity of zeamatin cannot be attributed to this inhibitory activity, but is due to its membrane permeabilizing activity, its inhibition of α -amylases from insects can contribute to the plant defense mechanism against this kind of plant enemies.

Analogously to TAXI and XIP, structurally related to the aspartic protease family (Sansen *et al.*, 2004) and the GH18 chitinases (McLauchlan *et al.*, 1999), respectively, a role in the plant defense mechanism can be suggested for TLXI based on its homology with PR-5 proteins. The three xylanase inhibitors indeed evolved from existing proteins produced by the plant as part of their defense system against microbes. Although a direct role in plant defense remains to be demonstrated and the precise mechanism needs to be elucidated, the specificity of TLXI towards microbial xylanases and its structural and sequence homology with PR-5 proteins suggest a role in plant defense.

Up to now, little is known about TLXI gene expression. Thanks to the rapidly growing number of publicly available EST sequences, it is possible to get an idea about the occurrence of particular proteins in specific plant tissues and developmental stages by consulting the available EST libraries. *tlxi*-like EST sequences are mainly found in wheat and some are expressed in abiotic stress conditions like salt and cold stress (Table 3-4).

Table 3-4: Wheat ESTs^a matching the *tlxi* sequence

GenBank Id	coverage	tissue	developmental stage	identity (%) ^b
CK199869	100	root*	n.s.	100
CD921496	100	grain	608 degrees per day after pollination	100
CD915298	100	grain	550 degrees per day after pollination	100
CD914871	100	grain	550 degrees per day after pollination	100
CD914550	100	grain	550 degrees per day after pollination	100
CD937830	100	ovary	n.s.	99
CD911344	100	grain	550 degrees per day after pollination	99
CD915745	100	grain	550 degrees per day after pollination	99
CD867627	100	grain	550 degrees per day after pollination	99
CD867628	100	root	n.s.	99
CD915744	96	root	n.s.	99
CD914060	94	grain	550 degrees per day after pollination	99
CD901330	93	grain	356 degrees per day after pollination	98
CD914870	84	grain	550 degrees per day after pollination	100
CD913334	88	grain	550 degrees per day after pollination	99
CD914059	85	grain	550 degrees per day after pollination	99
CD914549	82	grain	550 degrees per day after pollination	99
CD915299	78	grain	550 degrees per day after pollination	99
CK199529	82	root*	n.s.	99

^a ESTs covering more than 75% of the mature protein are shown (GenBank release 158.0).

^b Nucleotide identities in covering region.

* cold-acclimated and salt stressed.

n.s., not specified

tlxi-like genes are mainly expressed in the developing grain from wheat, explaining why the RACE reaction to identify the sequence could be performed on mRNA from young embryos. A minority of the EST sequences was isolated from root and ovary (Table 3-4). The EST sequences isolated from barley only show a limited similarity, displaying a maximum identity with TLXI of 60% at protein level.

In contrast, the occurrence of expressed TAXI orthologues was confirmed in different cereals (Fierens *et al.*, 2003), like barley and rye (e.g. BQ471743, BQ427163 and BE586568), from which TAXI-like xylanase inhibiting proteins were indeed isolated (Goesaert *et al.*, 2001; Goesaert *et al.*, 2002) and genetically identified (Raedschelders *et al.*, 2004). The wheat EST libraries suggest that the *taxi*-like genes are expressed in different plant tissues (e.g. seed, leaf, kernel and root) at different stages of plant development. TAXI is also expressed under plant stress conditions such as those induced by *Fusarium graminearum* infection and drought. Like for TAXI, EST sequences showing homology to the third xylanase inhibitor, XIP, were found in different plant tissues in different stages of development and in different cereals, like barley and wheat, but no EST sequences were found in rye that showed significant homology with the *xip*-like genes. However, purification of the rye homologue of XIP-I has already been established (Goesaert *et al.*, 2004). XIP expression is also induced by abiotic stress and by infection with *F. graminearum*. Hence, expression of the three inhibitors, occurring in different plant tissues in different developmental stages, is influenced by either environmental stress conditions or infection with pathogens.

The promoter region of a gene can also contain valuable information about the conditions in which a gene is expressed, about tissue-specific expression or concerning the factors inducing the expression. Next to the TATA-box, involved in positioning the RNA polymerase II for correct initiation, and the CAAT-box, a conserved sequence recognized by a large group of transcription factors, two other motifs were recognized by the PlantCARE program. The first motif, located at position -289 relative to the putative transcription start, is the ABRE motif (section 3.3.2.1.), a cis-element involved in abscisic acid (ABA) responsiveness. ABA is a plant hormone that is produced in response to various environmental conditions, including drought, low temperature and salinity and is able to regulate specific promoter elements, called ABRE motifs, containing an ACGT core sequence (Shen *et al.*, 2004). Hence TLXI could be produced under these abiotic stress conditions, which was also indicated by analysis of the EST

sequences. This does not exclude that TLXI is involved in pathogen resistance because for barley, induction of pathogen resistance by abiotic stress, including exogenous ABA, was proven (Wiese *et al.*, 2004).

In addition, ABA was also shown to be produced by phytopathogenic fungi (Kettner and Dörffling, 1995). There is increasing evidence that ABA is involved in the interaction between phytopathogenic microorganisms and their host plants. Increased levels of endogenous ABA have also been reported from various plant species in response to infection with fungi, bacteria and viruses (Tuomi *et al.*, 1993). Tuomi *et al.* (1993) showed that the phytopathogen *Botrytis cinerea* produces ABA and they also suggest that this organism induces ABA production by the mother plant as a response to physiological stress. Recently, it was shown that *B. cinerea* produces a xylanase, which is strongly inhibited by TAXI and XIP (Brutus *et al.*, 2005). Therefore it would be very interesting to verify if TLXI is able to inhibit this xylanase, because the presence of this pathogenic fungus would possibly induce TLXI expression. These findings are an indication that, due to the presence of the ABRE motif in the promoter region, TLXI expression is induced by the presence of phytopathogens.

Analysis with the program PlantCARE indicated the presence of a second motif, the MBS motif, located 75 bp upstream of the putative transcription start and involved in drought inducibility. The MBS motif is induced by the transcription factor MYB, shown to be involved in dehydration and salt stress of *Arabidopsis* (Urao *et al.*, 1993). Analogous to their function in animals, genes such as *myb*, encoding transcription factors, may also function in plant pathogenesis and defense responses (Yang and Klessig, 1996). It was shown that the tobacco mosaic virus (TMV) and *Pseudomonas syringae* pathovar *syringae*, also causing leaf blight in wheat, can induce a *myb* gene homolog in tobacco, which can trigger pathogenesis related genes. The MBS motif, recognized in the 5'UTR region of *tlxi*, is a type I MBS motif, characterized by the consensus sequence (T/C)AAC(T/G)G. Again, the presence of this motif is indicative for the inducibility of TLXI under stress conditions, either abiotic or biotic.

Also in the promoter region of the *taxi-III* gene, several consensus-sequences of *cis*-acting elements implicated in pathogen- and wound-inducible gene expression were found (Igawa *et al.*, 2004). GCC box, AGC box and W box sequences were identified, which are found in the promoters of many pathogenesis-related genes and are known as the DNA binding sites of ethylene-response factor (ERF) and WRKY transcription factor, respectively. In addition, the core sequence of *activation sequence-1* (*as-1*), a

functionally important element of a subgroup of salicylic acid-inducible defense genes, and consensus sequences of type I MBS motifs were found. So in both *tlxi* and *taxi-III* promoter regions, motifs were found that confer a role in plant pathogenesis to these inhibitors. More of these motifs were found in the 5' untranscribed region from *taxi-III* compared to *tlxi*, but this is due to the fact that the region identified upstream of the transcription start is larger for *taxi-III*. Possibly, the *tlxi* gene also contains more motifs more upstream than the identified sequence.

Since the TLXI encoding sequences amplified from wheat cv. Estica and from its diploid progenitor species *A. squarrosa* are identical, the *tlxi* gene is presumably located on the D genome of hexaploid wheat. However, the chromosomal location could not yet be determined. In an attempt to find variants of TLXI, we found a *tlxi* gene encoded by the diploid wheat species *A. speltoides*, showing 90% identity with TLXI after translation. Because no information is available yet about the interaction of TLXI with xylanases, expression and characterization of the variant AS-TLXI, would also be an interesting challenge since possible changes in inhibition specificity could shed light on which amino acids are responsible for the interaction (Chapter 7). Also from the rye genome, a *tlxi*-like sequence was isolated, displaying, upon translation, 88% identity with TLXI. The identified sequence would be very interesting for heterologous expression and characterization due to the lack of a potential glycosylation site. The absence of N-glycosylation could possibly influence inhibition specificity, protein stability or other characteristics. Attempts to express the rye recombinant *tlxi*-gene will be reported further (section 7.3.1.).

3.5 Conclusions

We identified the *tlxi* gene encoding a mature protein of 151 amino acids with a predicted molecular mass and pI of 15.6 kDa and 8.38, respectively. Bioinformatic analysis classified TLXI as a thaumatin-like protein. Like other TLPs, TLXI is most probably a very stable protein, due to the presence of several potential disulfide bonds, and probably plays a role in plant defense against pathogens, a role that is also attributed to the other xylanase inhibitors TAXI and XIP. Identification of the promoter region and subsequent analysis with the PlantCARE program demonstrated the presence of two conserved motifs in addition to the CAAT-box and the TATA-box, i.e.

an ABRE motif and a MBS motif, both referring to inducibility under stress conditions. These stress conditions can be either abiotic - abscisic acid and MYB proteins are produced during drought, low temperature and osmotic stress conditions – or biotic – abscisic acid and MYB production are also stimulated by the presence of pathogenic organisms.

A TLXI encoding gene was also isolated from rye (SC-TLXI) and *A. speltoides* (AS-TLXI). Both proteins displayed high sequence identity with the TLXI protein sequence from hexaploid wheat, making it interesting proteins to gain insight in the structure-function relationship of TLXI.

Chapter 4

Recombinant expression of TLXI

4.1 Introduction

In the previous chapter, the isolation of a putative *tlxi* gene sequence from wheat genomic DNA was described. To confirm whether the isolated sequence indeed encodes a xylanase inhibitor, the gene was expressed. In first instance, *E. coli* was used as a host organism for recombinant expression. Neither cytoplasmic nor periplasmic expression resulted in the production of active recombinant inhibitor. Therefore, an alternative expression host was used, *P. pastoris*. This methylotrophic yeast combines several advantages of both prokaryotic and animal cell expression systems. It is readily amenable to genetic manipulation, can be easily grown to high cell densities using minimal media, and is able to introduce some eukaryotic posttranslational modifications, like O- and N-glycosylation (Bretthauer and Castellino, 1999). *P. pastoris* is also capable of expressing heterologous genes to high levels under the control of the strong and tightly regulated alcohol oxidase 1 (*AOX1*) promoter. Additionally, foreign proteins in *P. pastoris* can be produced either intracellularly or extracellularly. Because this yeast secretes only low levels of endogenous proteins, the secreted heterologous protein constitutes the vast majority of total protein in the medium (Cereghino and Cregg, 2000) facilitating its purification.

Since considerable amounts of recombinant TLXI are needed for downstream applications, we report in this chapter on the optimization of the expression in *P. pastoris*. Several parameters, like pre-induction osmotic stress, medium pH, induction temperature, methanol concentration and aeration have been subjected to optimization. The optimal parameters have subsequently been applied in a large scale expression protocol followed by purification of the recombinant protein with cation exchange chromatography (CEC).

4.2 Materials and methods

4.2.1 Standard molecular biology techniques

Agarose gel electrophoresis and DNA sequence analysis were performed as described by Sambrook and Russell (2001) unless specified otherwise. DNA sequences were analyzed on a 377 DNA Sequencer using ABI PRISM Big Dye Terminator chemistry (Applied Biosystems). The Sequencher 4.1 package (Gene Codes Corporation) was used to correct and align obtained DNA sequences. Primers were ordered from Proligo Primers and Probes unless specified otherwise. PCR reactions were performed with *Pfu* DNA polymerase (Stratagene, La Jolla, CA, USA) applying the following temperature program, unless mentioned otherwise: 5 min at 95°C (initial denaturation); 1 min at 94°C (denaturation), 1 min 30s at 58°C (primer annealing), 2 min at 72°C (primer extension) (30-35 cycles); 10 min at 72°C (final extension). PCR products were purified using the PCRapid kit (Invitex). Electrocompetent *E. coli* cells were prepared according to the method of Tung and Chow (1995) with minor modifications while competent *P. pastoris* cells were prepared according to the instructions of the EasySelect *Pichia* Expression kit (Invitrogen). Plasmid DNA (up to 20 µg) was isolated from *E. coli* cells using the QIAprep Spin Miniprep Kit (Qiagen). Genomic DNA was isolated from *P. pastoris* according to the method of Fujimura and Sakuma (1993). All enzymatic reactions, like restriction, ligation and dephosphorylation, were performed according to the protocol supplied with the enzyme.

4.2.2 *E. coli* and *P. pastoris* strains and growth media

Electrocompetent *E. coli* XL1-Blue MRF' cells (Stratagene) and chemocompetent *E. coli* TOP10F' cells (Invitrogen) were used for DNA manipulations with *E. coli* expression vectors and *P. pastoris* expression vectors, respectively. For expression in *E. coli* cells, chemocompetent TOP10 cells and electrocompetent BL21 cells were used, while expression in *P. pastoris* was performed in X33 (genotype: wild-type; phenotype: Mut⁺), KM71H (genotype: *arg4 aox1::ARG4*; phenotype: Mut^S, Arg⁺) or SMD1168H (genotype: *pep4*; phenotype: Mut⁺, pep4⁻) cells. The genotypes of the different *E. coli* strains are presented in Table 4-1.

Table 4-1: Genotypes of the *E. coli* strains used in this study.

<i>E. coli</i> strain	Genotype
XL1-Blue MRF'	$\Delta(mcrA)183 \Delta(mcrCB-hsdSMR-mrr)173 endA1 supE44 thi-1 recA1 gyrA96 relA1 lac$ [F' <i>proAB lacI^q Z</i> $\Delta M15$ Tn10 (Tet ^r)]
TOP10F'	F' [<i>lacI^q Tn10</i> (Tetr)] <i>mcrA</i> $\Delta(mrr-hsdRMS-mcrBC)$ $\Phi 80lacZ\Delta M15$ $\Delta lacX74$ <i>recA1</i> <i>araD139</i> $\Delta(ara-leu)7697$ <i>galU galK rpsL endA1 nupG</i>
TOP10	F' <i>mcrA</i> $\Delta(mrr-hsdRMS-mcrBC)$ $\Phi 80lacZ\Delta M15$ $\Delta lacX74$ <i>recA1</i> <i>araD139</i> $\Delta(ara-leu)7697$ <i>galU galK rpsL</i> (Str ^r) <i>endA1 nupG</i>
BL21 (DE3)	F' <i>dcm ompT hsdS</i> (<i>r_B⁻ m_B⁻</i>) <i>gal</i> (DE3)

Growth and expression of *E. coli* cells was performed in Luria-Bertani (LB) medium containing 1% bacto-tryptone (BD Diagnostic Systems, Sparks, MD, USA), 0.5% yeast extract (BD Diagnostic Systems) and 1% sodium chloride (Acros Organics, Geel, Belgium). To obtain solid agarplates, 1.5% Select Agar (Invitrogen) was added. Following steam sterilization, the appropriate antibiotic was supplied. Ampicillin (Sigma-Aldrich, St. Louis, MO, USA) was used at a concentration of 100 $\mu\text{g/ml}$.

E. coli cells containing the *P. pastoris* expression vector, pPICZ α C, were grown in low salt LB-medium (LSLB), identical to LB-medium but containing 0.5% sodium chloride instead of 1%. For solid agarplates, 1.5% Select Agar (Invitrogen) was added. The antibiotic, zeocin (Invitrogen), was added to a final concentration of 25 $\mu\text{g/ml}$.

YPD (Yeast Extract Peptone Dextrose) medium, used during the transformation protocol of *P. pastoris*, consists of 1% yeast extract, 2% bacto-peptone (BD Diagnostic Systems) and 2% dextrose (Acros Organics). Transformed *P. pastoris* cells were plated on YPDS (Yeast Extract Peptone Dextrose Sorbitol medium)-agar plates with 100 $\mu\text{g/ml}$ ZeocinTM. YPDS-medium is composed of YPD medium supplemented with 1M sorbitol (Acros Organics). 2% Select Agar is added to obtain solid agarplates. Growth of transformed *P. pastoris* cells prior to induction was performed in BMGY (Buffered Glycerol-complex Medium)-medium supplemented with 0.35 M sodium chloride containing 1% yeast extract, 2% bacto-peptone, 100 mM potassium phosphate buffer (pH 6.0), 1.34% yeast nitrogen base without amino acids (Formedium, Norwich, England), 4×10^{-5} % biotin (Serva Electrophoresis GmbH, Heidelberg, Germany) and 1% glycerol (Acros Organics). BMMY (Buffered Methanol-complex Medium)-medium was used for induction of *P. pastoris* cells. The composition of this medium is identical to BMGY-medium but with 0.5% methanol instead of 1% glycerol.

4.2.3 Construction of expression plasmids

4.2.3.1 Construction of *E. coli* expression plasmids

The DNA sequence encoding mature TLXI was amplified by primer combination XImatf and XImatr (Table 4-3) using PCR product lintf/XI2 as template (Figure 3-1). Both primers contain *Bgl*III restriction sites. The PCR product was cloned in a pBAD/Thio-TOPO[®] vector (Invitrogen) for cytoplasmic expression according to the manufacturer's instructions after addition of 3' deoxyadenylate-overhangs with *SuperTaq* polymerase (SphaeroQ, Leiden, The Netherlands) (2.5 U, 72°C, 10 min) and purification (Invitex). This vector was used for subsequent subcloning of the *tlxi* gene as a *Bgl*III (Roche Diagnostics) fragment in the *Bgl*III site of periplasmic expression vectors pHOS31 (Hertveldt *et al.*, 2002) and pBAD/gIII B (Invitrogen) (Figure 4-1). The DNA sequence encoding mature TLXI including the stopcodon was also amplified. In this case, XImatf and XImatrstop were used as primers (Table 4-3) and PCR product lintf/XI2 was used as template (Figure 3-1). The PCR product was purified and cloned in the pCR[®]4-TOPO[®] vector (section 3.2.6.). After verification by DNA sequencing (section 4.2.1.) it was used for subcloning of the coding sequence in the *Bgl*III site of periplasmic vector pBAD/gIII B. Inclusion of the stopcodon enabled us to express the *tlxi* gene without C-terminal tags.

Restriction and dephosphorylation of the periplasmic vectors was performed as specified by the supplier of the restriction enzymes and the Calf Intestine Phosphatase (Roche Diagnostics), respectively, and both vectors were purified prior to ligation of the PCR product. DNA ligation of compatible ends was performed with T4-DNA ligase (Promega, Madison, USA) at a three to five times molar ratio insert:vector using the supplied protocol. The characteristics of the cytoplasmic and periplasmic vectors are given in Table 4-2.

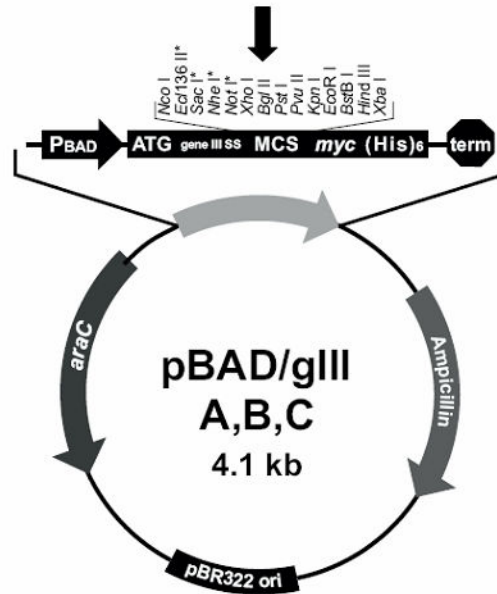


Figure 4-1: Schematic representation of periplasmic expression vector pBAD/gIII (adopted from the Invitrogen manual).

P_{BAD} : araBAD promoter; ATG: initiation ATG; gene III ss: gene III secretion signal; MCS: multiple cloning site; *myc*: C-terminal *myc* epitope tag; (His)₆: C-terminal polyhistidine region; term: *rrnB* transcription termination region; Ampicillin: ampicillin resistance gene (β -lactamase); pBR322 *ori*: origin of replication; *araC* gene: encodes the regulatory protein for tight regulation of the P_{BAD} promoter. The *Bgl*III restriction site for insertion of the *tlxi* gene is indicated with an arrow.

Table 4-2: Expression systems used for TLXI expression in *E. coli*

Plasmid	Promoter	Inducer	Recombinant protein	Cellular localization
pBAD/Thio-TOPO	P_{BAD}	arabinose	<i>E. coli</i> thioredoxin fusion**	cytoplasm
pHOS31	<i>lac</i>	IPTG*	non-fusion	periplasm
pBAD/gIII	P_{BAD}	arabinose	non-fusion	periplasm

* Isopropyl-1-thio- β -D-galactopyranoside

** Thioredoxin can potentially be removed by cleavage with enterokinase

4.2.3.2 Construction of *P. pastoris* expression plasmids

The DNA sequence encoding mature TLXI, including the stopcodon, was amplified with primer combination XImatf and XImatrstop (Table 4-3) using PCR product Intf/XI2 as template (section 3.3.1.). The resulting PCR product was cloned in a pCR[®]4-TOPO vector (section 3.2.6.), verified by DNA sequencing and subsequently subcloned as a *Bgl*III fragment in a *Bsm*BI restricted (New England Biolabs, Beverly, MA, USA), dephosphorylated pPICZ α C vector (Invitrogen). The gene encoding mature TLXI without stopcodon was subcloned as *Bgl*III fragment in pPICZ α C using a

pBAD/Thio-TOPO[®] vector, containing this sequence (section 4.2.3.1.), as template. Ligation was performed as described in section 4.2.3.1. The pPICZ α C vector (Figure 4-2) contains the secretion signal sequence of the *Saccharomyces cerevisiae* α -factor prepro-peptide, leading to secretion of the expressed protein. Expression is driven by the strong, highly-inducible P_{AOX1} promoter, the promoter regulating the production of alcohol oxidase and inducible with methanol.

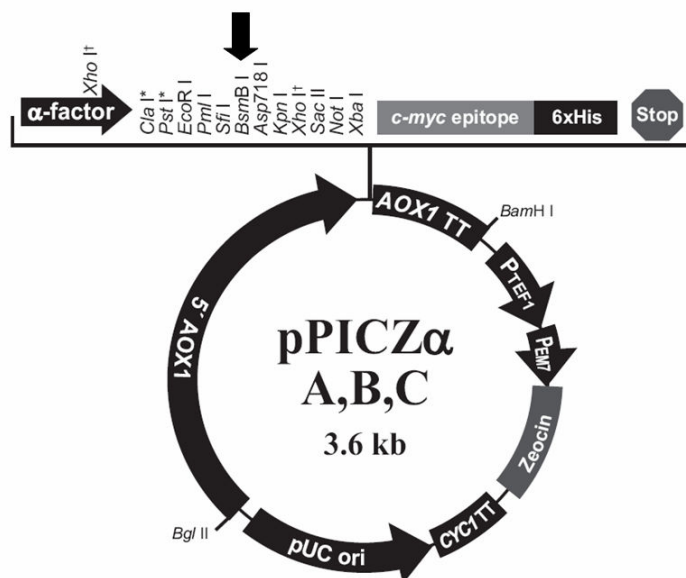


Figure 4-2: Schematic representation of *P. pastoris* expression vector pPICZ α (adopted from the Invitrogen manual).

5'*AOX1*: alcohol oxidase 1 promoter region; α -factor: native *S. cerevisiae* α -factor secretion signal; *c-myc* epitope: C-terminal *myc* epitope tag; 6xHis: C-terminal polyhistidine tag; stop: stopcodon; *AOX1* TT: *AOX1* Transcription Termination; P_{TEF1}: transcription elongation factor 1 gene promoter from *S. cerevisiae*; P_{EM7}: synthetic prokaryotic constitutive promoter; zeocin: *Streptoalloteichus hindustanus ble* gene (zeocin resistance gene); *CYC1* TT: *CYC1* transcription termination region; pUC ori: origin of replication. The *BsmBI* restriction site for insertion of the *tlx* gene is indicated with an arrow.

4.2.4 Transformation of host cell organism

4.2.4.1 Transformation of *E. coli*

Generally, transformation of *E. coli* cells was achieved by electroporation, except when using TOP10(F') cells (Invitrogen), which are commercial, chemocompetent cells and are transformed by heat shock according to the instructions of the manufacturer. For electroporation, 2 μ l of the above described ligation mixture was mixed with 40 μ l of

electrocompetent cells in prechilled electroporation cuvettes (Eurogentec, Seraing, Belgium) and subjected to a high voltage pulse (200 Ω , 25 μ F, 1.7 kV) using a Gene Pulser™ apparatus (Bio-Rad Laboratories, Hercules, CA, USA). Immediately after removal of the cuvette, 1 ml LB medium supplemented with 1% (w/v) glucose was added, followed by a one hour incubation period at 37°C allowing expression of the antibiotic resistance gene. Cells, transformed by heat shock or electroporation, were plated on selective medium containing ampicillin when *E. coli* expression vectors were used and zeocin when the pPICZ α C vector was used.

A vector containing the insert in the desired orientation was traced by means of clone analysis, consisting of a restriction digest on plasmid DNA isolated with the QIAprep Spin Miniprep kit (Qiagen), and the sequence was verified by DNA sequencing. A sequence verified construct was used to transform the appropriate *E. coli* or *P. pastoris* strain for expression.

4.2.4.2 Transformation of *P. pastoris*

Prior to transformation of the chemically competent *Pichia* cells, about 3 μ g of a sequence-verified pPICZ α C-*tlxi* construct was linearised with 20 U *PmeI* (New England Biolabs) (2h, 37°C) and subjected to ethanol precipitation using 1/10 volume 3 M sodium acetate and 2.5 volumes of 100% ethanol. The DNA was pelleted by centrifugation and the pellet was subsequently washed with 80% ethanol. The air-dried pellet was dissolved in 5 μ l of milliQ water. Transformation was performed as described in the EasySelect *Pichia* Expression kit manual (Invitrogen). Briefly, the construct, dissolved in 5 μ l milliQ water, was added to 50 μ l of competent *P. pastoris* cells (section 4.2.1.). 1 ml of Solution II (PEG solution) (Invitrogen) was added and the DNA/cell mixture was mixed by vortexing. The transformation reactions were incubated at 30°C for 1 hour and vortexed every 15 min. After heat shocking the cells at 42°C for 10 min, the cells were distributed in two microcentrifuge tubes and 1 ml of YPD medium was added to each tube. The cells were incubated at 30°C for 1 hour to allow expression of zeocin resistance. After 1 hour, the cells were pelleted by centrifugation (3000 x g, 5 min) at room temperature, the supernatant was discarded and each tube of cells was resuspended in 500 μ l of Solution III (salt solution) (Invitrogen) followed by combining the two tube contents. Again, the cell were centrifuged (3000 x g, 5 min) and the pellet was resuspended in 100 μ l of Solution III.

The entire transformation was then plated on a YPDS-plate, containing zeocin, and incubated for 3 to 10 days at 30°C.

Genomic DNA of zeocin-resistant *P. pastoris* transformants was isolated (section 4.2.1.) and the presence of the *tlxi* gene was confirmed by PCR with HotStarTaq DNA polymerase as described in chapter 3 (section 3.2.4.) and primers 5' *AOXI* and 3' *AOXI* (Invitrogen) (Table 4-3) with 50 ng of genomic DNA as template.

4.2.5 Recombinant expression

4.2.5.1 Recombinant expression in *E. coli*

Cells were grown in 4 ml LB medium supplemented with 100 µg/ml ampicillin and 2% glucose at 37°C with shaking until the absorbance at 600 nm (A_{600nm}) reached 0.5-0.6. After centrifugation at 2900 \times g (20 min), cell pellets were washed and resuspended in 4 ml fresh LB medium with ampicillin but without glucose. Protein expression was induced by adding 0.1 mM IPTG (in case of pHOS31) (Promega) or 0.02% (w/v) arabinose (in case of pBAD/Thio-TOPO and pBAD/gIII B) (Sigma-Aldrich) and cells were further grown at 37°C. After a 4 hour induction period, cells were harvested by centrifugation at 2900 \times g for 15 min and the cell pellets were kept at -20°C until further processing. As a negative control, non-induced cells were processed identically. In case of cytoplasmic expression, the thawed cell pellet was resuspended in 2 ml A-Trit solution (10% sucrose, 50 mM Tris, pH 8.0) containing 2.5% (w/v) lysozyme (Sigma-Aldrich). After 30 min incubation on ice and three freeze (-80°C)/thaw (25°C) cycles, the cells were sonicated (three bursts of 15 s with 1 min pause in between). A small fraction, containing the soluble as well as the insoluble proteins, was retained for analysis with protein electrophoresis. The rest of the sonicated cells was centrifuged (10 min, 16000 \times g) and the supernatant, containing the soluble protein fraction, was retained for further analysis. After washing the pellet with milliQ water, the pellet was resuspended in 150 µl A-Trit solution. This latter fraction contained the insoluble proteins.

For preparation of the periplasmic protein fraction a cold osmotic shock was used. For this purpose, the thawed cell pellet was resuspended in 30 mM Tris-HCl solution (pH 8.0) containing 20% (w/v) sucrose and EDTA was added to a final concentration of 1 mM. After 10 min of incubation at room temperature, the cells were pelleted (8000 \times g, 10 min, 4°C) and resuspended in ice-cold magnesium sulphate (5 mM). Following 10

min incubation on ice, the cells were again pelleted (10 min, 8000 \times g, 4°C). The supernatant contained the proteins released by the cold osmotic shock.

4.2.5.2 Small-scale expression in *P. pastoris*

Small-scale expression in *P. pastoris* was performed as described by Shi *et al.* (2003). 10 ml BMGY medium was inoculated with a single transformant and incubated at 30°C for 24h with shaking at 250 rpm. The cells were harvested by centrifugation at 2500 \times g for 5 min, resuspended in 1 ml BMMY medium and induced overnight at 30°C by adding methanol to a final concentration of 1% (v/v). The culture supernatant, obtained after 5 min of centrifugation at room temperature (16000 \times g), was kept for further analysis. Small-scale culture expression was used to screen for the *P. pastoris* strain that gave the best expression levels and to examine whether expression was better with or without a tag. Also the influence of the medium pH on expression levels was tested in this way. For this purpose, the BMMY medium was adjusted with phosphoric acid or potassium hydroxide to different pH values, i.e. pH 3.0, 5.0, 6.0, 6.5, 7.0, 7.5, 8.0.

4.2.5.3 Expression optimization in *P. pastoris*

The expression optimization procedure was adapted from Shi *et al.* (2003).

10 ml BMGY medium was inoculated with a single *P. pastoris* transformant. After an incubation period of 24h at 30°C (250 rpm), the volume was increased to 500 ml BMGY medium and the cell suspension was transferred to a 2 l flask covered with 2-3 sterile gauze layers. The cells were further incubated overnight (30°C, 250 rpm) after which a pre-induction transition phase was included whereby 1/10th volume of 10% (v/v) glycerol/13.4% (w/v) yeast nitrogen base (w/o amino acids) was added to the primary culture and allowed to incubate for an additional 3-5h until the A_{600nm} reached 10-12. The cell culture was harvested by centrifugation (2500 \times g, 10 min, room temperature) and the cells were resuspended in BMMY medium to an A_{600nm} of 50. 1% (v/v) methanol was added to the culture to induce expression and the total volume was divided in 10 ml fractions in 250 ml flasks covered with 2-3 sterile gauze layers. To optimize the induction temperature the 10 ml portions were incubated at 16°C, 20°C, 26°C and 30°C. To measure the effect of the methanol concentration, expression was induced with 0.75%, 1%, 1.25% and 1.5% methanol, added to different 10 ml portions. Because pre-induction osmotic stress can influence the expression level, BMGY medium was supplemented with either 0.35 M sodium chloride, 0.35 M potassium

acetate or 1.0 M sorbitol followed by normal induction in BMMY medium (10 ml portions). Every induction, incubated in a particular condition, was performed in triplicate and lasted approximately 20 hours. The flasks were always covered with 2-3 layers of sterile gauze.

The importance of good aeration of the culture during induction was examined by comparing expression levels from a culture, induced in normal flasks, with the expression levels in baffled flasks. For this purpose, the cells that were resuspended in BMMY medium to reach an $A_{600\text{nm}}$ of 50 were not divided in 10 ml fractions, but the total volume was transferred to a 1 l flasks, either baffled or not. 1 ml samples were taken at different time points to determine the optimal duration of induction.

4.2.6 Xylanase inhibition assay

Xylanase inhibition assays were determined by a variant of the colorimetric Xylazyme AX-method (Megazyme, Bray, Ireland) adapted from Gebruers and co-workers (2001). The substrate employed is azurine-crosslinked wheat arabinoxylan, which hydrates in water but is water insoluble. Hydrolysis by a xylanase produces water soluble dyed fragments. The rate of release of those fragments can be measured as an increase in $A_{590\text{nm}}$ and can be related directly to enzyme activity. *Trichoderma longibrachiatum* xylanase (Megazyme) (XynI, Swiss-Prot P36218) was used as enzyme. Enzyme solutions were prepared in sodium acetate buffer (250 mM, pH 5.0) with BSA (0.5 mg/ml) and contained 2.0 units per 0.5 ml. One enzyme unit corresponds to the amount of enzyme resulting in an increase of $A_{590\text{nm}}$ of 1.0 with the Xylazyme AX-method described below.

Dilutions of the culture supernatant, containing inhibitor, were prepared in 250 μ l 250 mM sodium acetate (pH 5.0). An equal volume of the XynI solution was added and the mixture was incubated at room temperature for 30 min. The mixtures were then moved to a water bath at 30 °C and after 10 min, an azurine-cross-linked wheat AX tablet (Megazyme) was added. They were then incubated for 60 min at 30 °C. The reaction was terminated by the addition of 2.0% (w/v) Tris solution (pH 9.0) (5.0 ml) and vigorous vortex-mixing. After 10 min at room temperature the tubes were shaken vigorously and the contents were filtered through a paper filter (VWR International, Leuven, Belgium) (diameter 90 mm). The $A_{590\text{nm}}$ values were measured with a Ultrospec III spectrophotometer (Pharmacia, Uppsala, Sweden) against a control, prepared by incubating the enzyme with buffer instead of inhibitor solution. In addition,

a blank was included containing 500 µl of buffer. The inhibition activity, expressed as a percentage reduction in xylanase activity, was calculated as follows:

$$\text{Inhibition(\%)} = \frac{((A_{280\text{nm}}^{\text{control}} - A_{280\text{nm}}^{\text{blank}}) - (A_{280\text{nm}}^{\text{sample}} - A_{280\text{nm}}^{\text{blank}}))}{(A_{280\text{nm}}^{\text{control}} - A_{280\text{nm}}^{\text{blank}})} \times 100$$

in which the control contains enzyme and buffer, the blank contains only buffer and the sample contains enzyme and inhibitor. One inhibition unit (IU) is defined here as the amount of recombinant TLXI needed to reduce the xylanase activity with 50% in the above described test.

4.2.7 Protein electrophoresis

Protein expression was verified by sodium dodecyl sulphate polyacrylamide gel electrophoresis (SDS-PAGE) according to Laemmli (1970). Loading buffer (50 mM Tris.HCl pH 6.8, 2 mM EDTA, 10% glycerol, 1% SDS, 0.1% bromophenol blue) was added to each protein sample. Then samples were boiled for 5 min, centrifuged (16000 \times g, 1 min) and loaded on a polyacrylamide gel. Proteins were first concentrated on a stacking gel (4% polyacrylamide, 125 mM Tris.HCl pH 6.8, 0.1% SDS, 0.1% TEMED and 0.034% APS) followed by separation according to molecular weight on a 15% separating gel (15% polyacrylamide, 375 mM Tris.HCl pH 8.8, 0.1% SDS, 0.05% TEMED and 0.034% APS). Electrophoresis was performed using the Mini Protean II electrophoresis system (Bio-Rad) at 150 V for approximately 1h. Running buffer contained 0.05 M Tris base, 1.44% glycine and 0.1% SDS. Proteins were coomassie stained with Simply Blue SafeStain (Invitrogen) according to the manufacturer's protocol. The low-molecular mass markers (GE Healthcare, Uppsala, Sweden) used as reference were α -lactalbumin (14.4 kDa), trypsin-inhibitor (20.1 kDa), carbonic anhydrase (30.0 kDa), ovalbumin (43.0 kDa), bovine serum albumin (67.0 kDa) and phosphorylase b (94.0 kDa).

4.2.8 Purification of recombinant TLXI by cation exchange chromatography (CEC)

Prior to isolation of the inhibitor from the culture supernatants, the medium was dialyzed overnight at 4°C with a Spectra/Por[®]4 membrane (MWCO 12000-14000) (Spectrum Laboratories Inc., Breda, the Netherlands) against sodium acetate buffer (25

mM, pH 5.0) to remove salts and to adjust the pH. The crude protein sample was purified with CEC using a SP-Sepharose Fast Flow column (15 x 160 mm, GE Healthcare) equilibrated with the same buffer. The matrix of this column exists of negatively charged sulfopropyl groups coupled to a highly cross-linked agarose matrix. Because the pI of recombinant TLXI is above 5, the protein is positively charged at pH 5.0 and binds to the negatively charged matrix through ionic interaction. The proteins were loaded at a flow rate of 2.0 ml/min and after a washing step (200 ml, 2.0 ml/min), the bound proteins were eluted in 2.0 ml fractions using a salt gradient of 0-1.0 M sodium chloride in 140 min (flow rate: 1.0 ml/min). The gradient was built up as follows: 0 to 0.3 M NaCl in 30 min; 0.3 M NaCl was kept for 30 min; 0.3 M to 0.6 M NaCl in 60 min; 0.6 M NaCl to 1 M NaCl in 0 min; 1 M NaCl was kept for 20 min. Increasing ionic strength displaces the bound proteins as ions in the buffer compete for binding sites. The purity of the protein was verified via protein electrophoresis (section 4.2.7.), the pure fractions were pooled and dialyzed overnight against sodium acetate buffer (25 mM, pH 5.0) to remove sodium chloride prior to further characterization (chapter 5).

4.2.9 TLXI content determination

TLXI concentrations were determined spectrophotometrically at 280 nm using a specific absorbance value of 1.402 AU for 1 mg/ml recombinant TLXI (1.000 cm UV-cell path length). To calculate this specific absorbance value following formula was used (Gill and von Hippel, 1989), taken into account that part of the multiple cloning site (SMNSRGPAGRLGS) was not cleaved from the protein.

$$A_{280nm} = \frac{(5500 \times \text{numb}(W)) + (1490 \times \text{numb}(Y)) + (125 \times \text{numb}(C))}{Mm}$$

where A_{280nm} is the specific absorbance value at 280nm and Mm is the molecular mass of the protein (g/mol). $\text{Numb}(W)$, $\text{numb}(Y)$ and $\text{numb}(C)$ are the number of tryptophan, tyrosine and cysteine residues, respectively, and 5500, 1490 and 125 are the extinction coefficients at 280 nm of these residues, respectively.

4.2.10 Western blot analysis

Samples (0.5 μ g native TLXI and 0.2 μ g recombinant TLXI) were separated by electrophoresis as described in section 4.2.7., but for 90 min at 130 V. BenchMark™

coloured molecular mass standards (Invitrogen) were used. Prior to transfer of the separated proteins onto activated nitrocellulose membranes (Protran Schleicher & Schuell, Dassel, Germany), the gels were equilibrated for 15 min in Towbin's buffer (Tris-glycine in 20 % ethanol) pH 9.2 (Towbin *et al.*, 1979). Electrotransfer was performed with a Trans-Blot semi-dry electrophoretic transfer cell (Bio-Rad) at room temperature for 25 min at 16 V. Free protein binding sites on the blot were then blocked via overnight incubation at 4 °C in casein solution (1.0 % in phosphate-buffered saline (PBS) containing 100 mM sodium chloride and 2 mM potassium chloride). Next, the membranes were incubated on a rotary plate shaker for 60 min at room temperature with affinity purified rabbit polyclonal antibodies (0.13 µg/ml) against TLXI in PBS-Tween (0.05% v/v) pH 7.4 (Beaugrand *et al.*, 2006). After extensive washing in PBS-Tween, the membranes were incubated under gentle rotary shaking for 60 min at room temperature with a solution of goat anti-rabbit IgG antibodies conjugated to horseradish peroxidase. The goat antibodies (Sigma-Aldrich) were diluted (30 000 times) in PBS-Tween according to the manufacturer's instructions. Subsequently, the membranes were washed again in PBS-Tween and incubated with 3,3', 5,5'-tetramethylbenzidine (Sigma-Aldrich) solution (4.0 ml for 10 × 10 cm membrane) as substrate for the horseradish peroxidase. After 10 min of development, the staining was stopped by washing the membrane for 5 min in deionised water and subsequent drying on filter paper.

4.2.11 Primers used in this chapter

Table 4-3: Primers used in the different sections of this chapter.

name	sequence	reference (section)
XImatf	CACAGATCTGCACCGCTCACCATCACGAAC	4.2.3.1. and 4.2.3.2.
XImatr	CAGAGATCTTGGGCAGAAGACGATCTG	4.2.3.1.
Ximatrstop	CACAGATCTTCATGGGCAGAAGACGATCTG	4.2.3.2.
5' <i>AOXI</i>	GACTGGTCCAATTGACAAGC	4.2.4.2.
3' <i>AOXI</i>	GCAAATGGCATTCTGACATCC	4.2.4.2.

*Bgl*III restriction sites are indicated in bold.

4.3 Results

4.3.1 Expression of TLXI in *E. coli*

To confirm that the identified gene codes for a functional xylanase inhibitor, the coding sequence was used for recombinant expression in *E. coli*. The mature TLXI coding sequence, without the stopcodon, was amplified with primers XImatf and XImatr (Table 4-3) using PCR product Iintf/XI2 (Figure 3-1) as template. The amplified product was inserted into the pBAD/Thio-TOPO[®] vector for cytoplasmic expression and used for transformation of chemocompetent TOP10 cells. In the presence of arabinose (final concentration of 0.02% w/v), expression from P_{BAD} was induced and the protein of interest produced as a C-terminal fusion with thioredoxin. After expression, the soluble and insoluble fractions were separated and analyzed with SDS-PAGE. We expected to see a protein band of 31.8 kDa, calculated with the ProtParam tool and comprising the thioredoxin sequence (11.7 kDa), the TLXI sequence (15.64 kDa), the linker sequence between these two proteins (1.25 kDa), the V5 epitope sequence (2.3 kDa) and the polyhistidine region (0.84 kDa). Such a protein band could only be detected in the total and the insoluble protein fraction of induced cultures and not in the soluble protein fraction of induced cultures (Figure 4-3). Xylanase inhibition assays, performed on the soluble protein fraction, indicated that no active protein was present as could be expected from SDS-PAGE analysis.

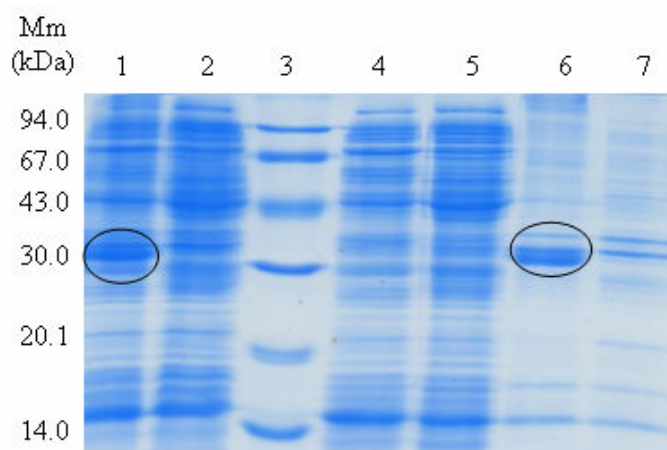


Figure 4-3: SDS-PAGE of expression of recombinant TLXI as a fusion with thioredoxin in *E. coli*.

Lane 1: total protein fraction, induced cells; lane 2: total protein fraction, uninduced cells; lane 4: soluble protein fraction, induced cells; lane 5: soluble protein fraction, uninduced cells; lane 6: insoluble protein fraction, induced cells; lane 7: insoluble protein fraction, uninduced cells. The values of the molecular mass (Mm) markers (lane 3) are indicated on the left. The fusion protein is circled.

Because cytoplasmic expression didn't result in the production of soluble, active TLXI, an attempt was made to perform periplasmic expression. Periplasmic expression vectors, like pBAD/gIII and pHOS31, contain the *gene III* and the *pelB* leader sequences, respectively, that direct the protein to the periplasm of *E. coli*. The TLXI coding sequence, isolated by a *Bgl*II cleavage from a *tlxi*-containing pBAD/Thio-TOPO[®] vector, was subcloned in the *Bgl*II sites of pBAD/gIII B and pHOS31 and used for transformation of chemocompetent TOP10 cells and electrocompetent XL1-Blue MRF' cells, respectively. Sequence-verified pBAD/gIII B and pHOS31 constructs were transformed to *E. coli* TOP10 cells and BL21 cells, respectively. BL21 (DE3) strains are protease-deficient and could therefore lead to increased expression levels. Since pHOS31 is a phagemid vector, expression with the pHOS31 vector would result in a fusion with the phage minor coat protein g3p. However, this fusion is avoided here by the use of a non-suppressor *E. coli* strain as host cell (BL21 (DE3)). Analysis of the periplasmic protein fraction with SDS-PAGE, revealed that no heterologously expressed protein was secreted in the periplasm, which was also confirmed by inhibition activity measurements. From the pBAD/gIII expression culture, a lysate was also prepared of the remaining pellet after isolation of the periplasmic protein fraction. No inhibition activity could be detected in the lysate.

TLXI with its stopcodon was also cloned in pBAD/gIII B. For this purpose, PCR was performed with primers XImatf and XImatstop, which includes the stopcodon (Table 4-3). A sequence-verified pCR[®]4-TOPO[®] construct, containing this PCR product, was used for subcloning in the *Bgl*II site of pBAD/gIII B. A sequenced pBAD/gIII B construct was used to transform *E. coli* BL21 (DE3) cells and expression and isolation of the periplasmic fraction was performed. Again, no protein band corresponding to the molecular mass of recombinant TLXI could be detected with SDS-PAGE and no inhibition activity could be measured in the periplasmic protein fraction (results not shown).

4.3.2 Expression optimization of recombinant TLXI in *P. pastoris*

The TLXI coding sequence, either with or without stopcodon, was ligated in the *Bsm*BI site of the pPICZ α C expression vector. These inserts were subcloned from a *tlxi* gene-containing pCR[®]4-TOPO[®] and pBAD/Thio-TOPO[®] vector, respectively. A sequence-verified pPICZ α C construct was used to transform *P. pastoris* cells X33 (Mut⁺), KM71H (Mut^S Arg⁺) and SMD1168H (Mut⁺ pep4⁻), the latter being a strain defective

in the vacuole peptidase A (*pep4*) and hence suited for expression of protease-sensitive proteins. Transformation of SMD1168H cells was only performed with constructs leading to expression of a non-tagged protein. Expression was performed in a small-scale culture per colony obtained from the transformation mixture. Subsequently, the inhibition activity of 250 µl of culture medium was determined against XynI. For the first time, inhibition activity could be measured, confirming that the isolated gene is indeed the TLXI encoding gene. The percentages of reduction of xylanase activity were compared between different *P. pastoris* strains and colonies. A comparison was also made between expression of tagged and non-tagged recombinant TLXI, further referred to as rTLXI (Table 4-4). Since this experiment is only used as a screening method to pick out the best colony, expressions and inhibition activity measurements were performed as single measurements.

Table 4-4: Inhibition activities in culture media of the different *P. pastoris* strains transformed with a *tlxi* gene-containing pPICZαC vector.

tag	colony	inhibition activity (%) ^a		
		X33	KM71H	SMD1168H
+	1	51	56	
	2		69	
	3		67	
	4		80	
-	1	57	87	0
	2	59	88	42
	3	67	82	53
	4			51
	5			63
	6			58
	7			58
	8			63

+: *P. pastoris* strain transformed with a pPICZαC vector containing the *tlxi* gene without stopcodon, resulting in rTLXI with tags (c *myc* epitope and 6 x His tag).

-: *P. pastoris* strain transformed with a pPICZαC vector containing the *tlxi* gene with stopcodon, resulting in rTLXI without tags (c *myc* epitope and 6 x His tag).

^a Inhibition activities as percentage reduction of xylanase-activity.

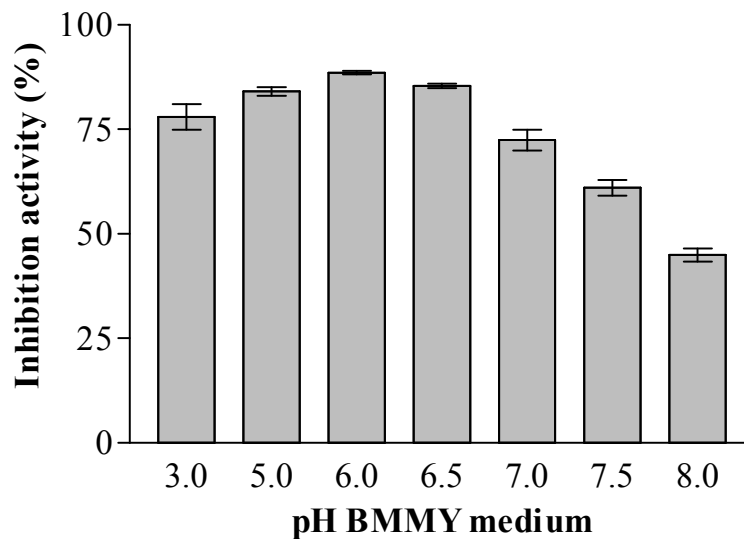
The inhibition activity of the colony giving the highest reduction of xylanase activity is shaded.

When the expression levels of active rTLXI were compared, a trend could be observed. Expression levels appeared to be higher when rTLXI was not fused to C-terminal tags while expression with strain KM71H gave the best results when compared to expression by X33 and SMD1168H. Although the three colonies of strain KM71H,

expressing rTLXI without tag, gave comparative expression levels, colony 2 was chosen for further expression experiments.

Small-scale expression was also used as a screening method to determine which pH conditions were optimal for expression of rTLXI and, hence, resulted in the highest expression levels of active inhibitor. For this purpose, cells were grown in BMGY medium at pH 6.0 while BMMY medium, adjusted to pH values ranging from 3.0 to 8.0, was used for induction. Inhibition activities were measured with culture medium of a non-transformed KM71H strain as a control (Figure 4-4A). 15 μ l samples of culture medium from each pH condition were also analyzed with SDS-PAGE (Figure 4-4B). The results indicate that rTLXI is most efficiently and/or most stably expressed when the culture is induced under lower pH conditions (pH 3.0-6.5) with pH 6.0 giving rise to the highest yields of active inhibitor. Further expression experiments were therefore performed at pH 6.0.

A



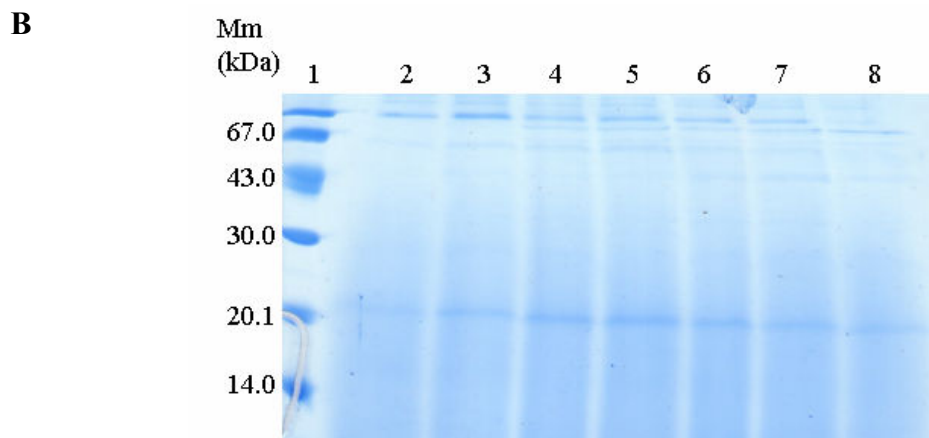


Figure 4-4: Inhibition activity measurements (A) and SDS-PAGE (B) of culture media of expression cultures induced under various pH conditions.

(A) Inhibition activity (%) is given as a function of the pH of the BMMY medium. Measurements were performed in triplicate. Error bars represent S.D.

(B) SDS-PAGE of 1 culture media of expression cultures induced under various pH conditions. Lane 2: pH 3.0; lane 3: pH 5.0; lane 4: pH 6.0; lane 5: pH 6.5; lane 6: pH 7.0; lane 7: pH 7.5; lane 8: pH 8.0. The values of the molecular mass (Mm) markers (lane 1) are indicated on the left.

The effect of induction temperature, pre-induction osmotic stress and methanol concentration on the expression level was examined. The results showed that expression levels of active rTLXI were higher at temperatures lower than 30°C (Figure 4-5A), which is the standard temperature for yeast induction. Induction temperatures between 20°C and 26°C were applied in subsequent experiments.

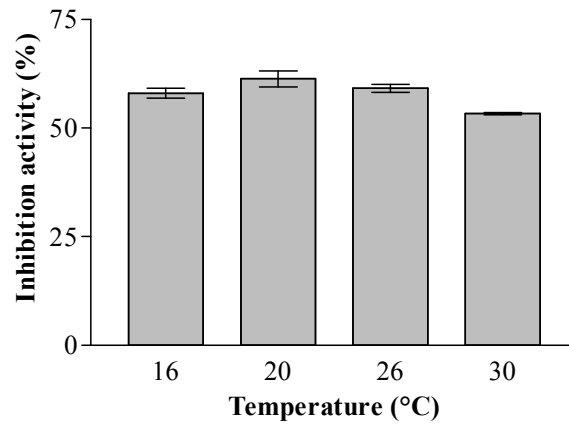
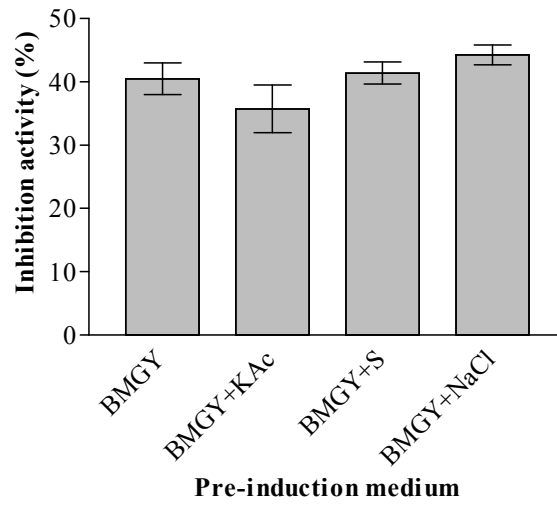
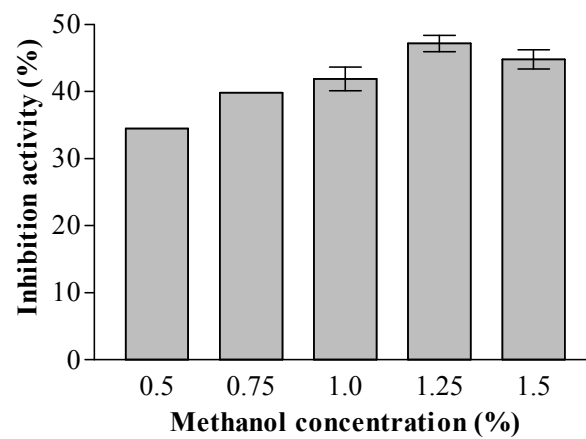
Figure 4-5 (opposite page): Effect of the induction temperature (A), pre-induction osmotic stress with potassium acetate (KAc), sorbitol (S) and sodium chloride (NaCl) (B) and methanol concentration (C) on expression levels of active rTLXI.

(A) Inhibition activity determined on 200 µl culture medium.

(B) Inhibition activity determined on 100 µl culture medium.

(C) Inhibition activity determined on 100 µl culture medium

As a control, an equal amount of culture medium of a non-transformed *P. pastoris* KM71H culture, incubated under the same conditions, was used. Expressions were performed in triplicate and the averages of the inhibition activities are plotted in the graph with their corresponding S.D.

A**B****C**

Because pre-induction osmotic stress can affect the yield of the produced protein, different osmotic compounds (0.35 M potassium acetate, 1.0 M sorbitol and 0.35 M sodium chloride) were added to the BMGY growth medium. Hereafter, induction was performed in standard BMMY medium in 10 ml fractions as described in section 4.2.5.3. The addition of potassium acetate and sorbitol appeared to have no, or even a rather negative affect in the case of potassium acetate, on protein production (Figure 4-5B) compared to the condition where cells were grown in BMGY medium without additives. On the other hand, the presence of sodium chloride in the BMGY medium led to a slight increase in rTLXI expression levels. In further experiments, the BMGY medium was supplemented with 0.35 M sodium chloride.

The methanol concentration, used for induction of expression, is also a parameter that is a possible subject for optimization. 10 ml fractions were induced with final methanol concentrations of 0.5%, 0.75%, 1.0%, 1.25% or 1.5%. Inhibition activity was measured on 100 μ l of culture medium using culture medium of non-transformed *P. pastoris* KM71H cells, induced under the same conditions, as control. Induction with 1.25% methanol resulted in significantly higher expression levels compared to lower or higher methanol concentrations (Figure 4-5C). Hence, expression was always induced with 1.25% methanol in following experiments.

In a last experiment, all the determined optimal expression conditions were applied in an expression experiment conducted to determine the effect of good aeration of the culture and to determine the optimal duration of induction. The total volume of cells, resuspended in BMMY medium, was transferred to a 1 l baffled flask, providing good aeration to the cells, or a non-baffled flask. The medium was resupplemented with 1.25% methanol every 24 hours and at different time points during the induction phase 1 ml samples were taken that were used to determine inhibition activity (Figure 4-6) and to follow cell growth. The latter was monitored by measuring the optical density at 600 nm (OD_{600nm}). A control was included existing of non-transformed *P. pastoris* KM71H cells, induced under the same conditions. Every expression, except for the control, was performed in duplicate. Inhibition activities were expressed as IU/ml.

The use of baffled flasks during induction seemed to significantly increase expression levels and was by far the most important factor in the determination of expression yields (Figure 4-6). Especially in the early hours of the induction phase, the difference in expression levels between baffled and non-baffled flasks is huge. Indeed, expression

of rTLXI in baffled flasks starts immediately after induction and increases rapidly. Until 49 hours after induction the expression levels (IU/ml) are approximately twice as high in baffled flasks compared to non-baffled flasks. After this time point, the production of rTLXI reaches a plateau in baffled flasks, while the expression in non-baffled flasks still increases. After 137 hours of induction, the difference between expression in baffled and non-baffled flasks, is smaller than in the early hours of the induction phase, but still expression levels are approximately 20% higher when there is a good aeration. Surprisingly, higher expression levels seemed to be independent of cell growth, because the OD_{600nm} of the control, the culture in baffled and non-baffled flasks are comparable (results not shown). So, although expression levels are higher in baffled flasks, the growth of the *P. pastoris* cells during the induction phase is unaffected by the aeration of the culture.

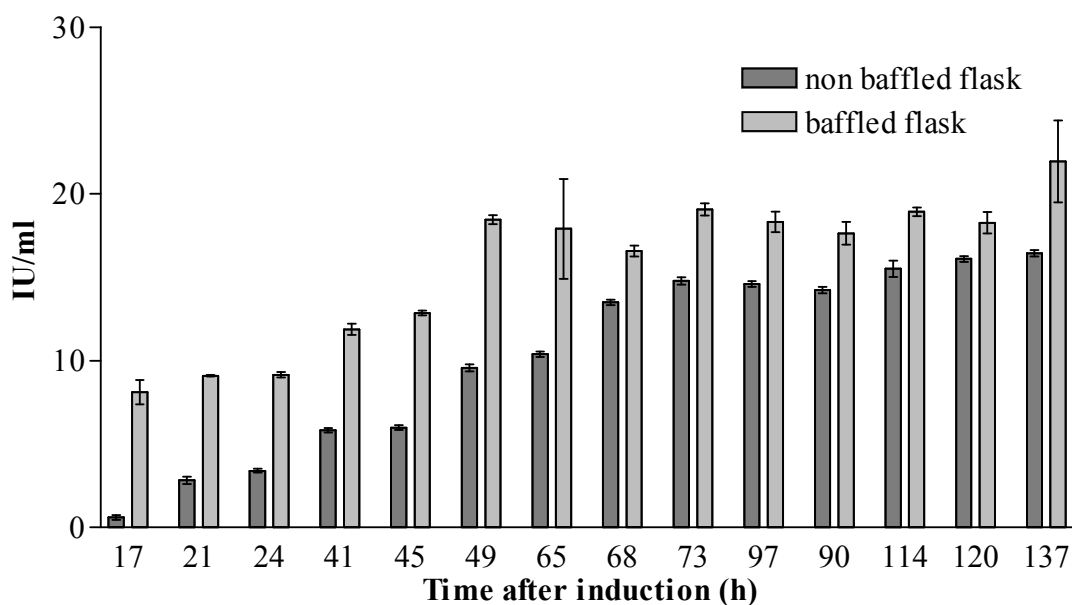


Figure 4-6: Inhibition activities (IU/ml) plotted against the time after the start of the induction (h). Inhibition activities as measured on supernatants of cultures induced in non-baffled flasks and baffled flasks are indicated in dark grey and light grey, respectively. Expressions were performed in duplicate and the inhibition activities were averaged. Error bars indicate differences from the mean value.

4.3.3 Production of rTLXI in *P. pastoris*

rTLXI was expressed under the optimal conditions. Briefly, 10 ml of BMGY medium (pH 6.0) supplemented with 0.35 M sodium chloride was inoculated with a single transformed colony. After 24 hours of incubation (30°C, shaking at 250 rpm), the volume was increased to 500 ml in a 2 l flask covered with 2-3 layers of sterile gauze to

accumulate biomass. After an overnight incubation period (30°C, shaking at 250 rpm), a pre-induction phase was included in which 1/10th volume of 10% glycerol/13.4% yeast nitrogen base (w/o amino acids) was added to the primary culture. The resulting mixture was incubated for an additional 3-5 h until the OD_{600nm} reached 10-12. The cell culture was harvested by centrifugation (2500 *x g*, 10 min, room temperature). To induce protein expression the cells were suspended in BMMY medium pH 6.0 to an OD_{600nm} of 50 and methanol was added to a final concentration of 1.25%, which was added every 24h. The induction was performed between 20°C and 26°C in baffled flasks. After approximately 50 h, the cultures were harvested by centrifugation (2500 *x g*, 10 min, room temperature) and the medium, containing rTLXI, was dialyzed overnight against 25 mM sodium acetate buffer pH 5.0 prior to purification.

4.3.4 Purification of rTLXI with CEC

The dialyzed culture medium was purified using a SP-Sepharose Fast Flow column (Figure 4-7). Eluted fractions were analyzed with protein electrophoresis (Figure 4-7) and pure fractions were pooled, followed by dialysis against 25 mM sodium acetate buffer (pH 5.0) to remove sodium chloride.

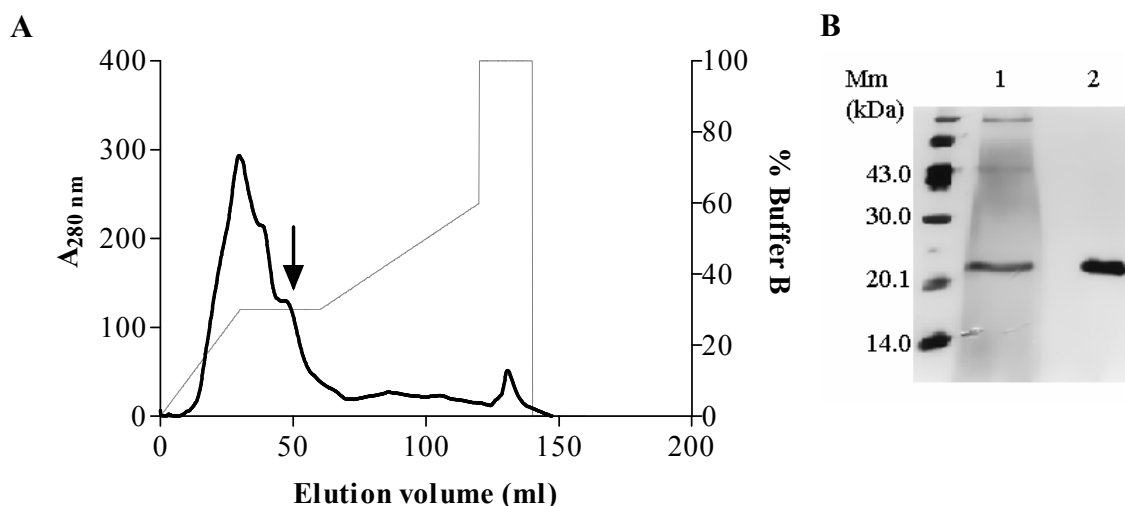


Figure 4-7: Chromatographic elution profile (A) and SDS-PAGE (B) of rTLXI purified with CEC. (A) The A_{280nm} (mAU) and the salt gradient (% buffer B: 25 mM sodium acetate pH 5.0 with 1.0 M NaCl) are plotted against the elution volume (black line and grey line, respectively). The peak containing rTLXI is indicated with an arrow. (B) SDS-PAGE analysis shows non-purified rTLXI (lane 1) and CEC purified rTLXI (lane 2). The LMW marker is loaded on the left side and molecular masses (Mm) are indicated.

To verify whether the purified protein is indeed a TLXI-like protein, western blot (Figure 4-8) was performed with antibodies raised against native TLXI. The results confirm what was already suggested by the inhibition activity assay i.e. that the purified protein is indeed a TLXI-like protein. The difference in molecular mass between native TLXI and rTLXI is caused by a different glycosylation extent as will be shown in chapter 5.

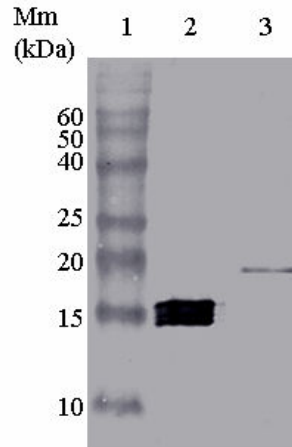


Figure 4-8: Western blot analysis of native TLXI and rTLXI

Lane 1: BenckMark™ Pre-stained Protein Ladder, molecular masses (Mm) are indicated; lane 2: native TLXI, lane 3: rTLXI

4.4 Discussion

The putative TLXI encoding gene was used for recombinant expression to confirm that it indeed codes for a xylanase inhibitor. At first, production in *E. coli* was attempted. Although the inhibitor was expressed as a fusion with thioredoxin, generally known to enhance the solubility of the fusion partner (Baneyx, 1999), all the expressed TLXI protein was present in the insoluble fraction causing the protein to be inactive. Because TLXI contains ten cysteine residues, which are thought to be involved in five disulfide bonds, the presence of the protein in the insoluble fraction, probably caused by protein aggregation leading to the formation of inclusion bodies, is most likely due to the fact that those bonds cannot be formed. Structural disulfide bonds do not form in the cytoplasm of *E. coli* as this environment is reducing and at least five *E. coli* proteins (thioredoxins 1 and 2, and glutaredoxins 1, 2 and 3, the products of the *trxA*, *trxC*, *grxA*, *grxB* and *grxC* genes, respectively) are involved in the reduction of disulfide

bridges that transiently arise in cytoplasmic enzymes (Baneyx, 1999). For this reason, the protein was targeted to the periplasm by cloning the *tlxi* gene downstream of a signal sequence. The periplasm offers several advantages for recombinant expression compared to the cytoplasm. Not only contains the periplasm only 4% of the total cell protein (Nossal and Heppel, 1966), making the recombinant protein easier to purify, the oxidizing environment of the periplasm also facilitates the proper folding of proteins because this compartment contains enzymes, like protein disulfide isomerases, catalyzing the formation and rearrangement of disulfide bonds (Missiakas and Raina, 1997). Nevertheless, no inhibition activity could be measured in the periplasmic protein fraction and no protein band corresponding to rTLXI could be visualized on SDS-PAGE. However, it has been shown that protein transport to the bacterial periplasm is a particularly complex process (Pugsley, 1993), and that the presence of a signal peptide does not always ensure efficient protein translocation through the inner membrane (Makrides, 1996; Lee *et al.*, 1989). Indeed, in some cases, preproteins are not readily exported and either become ‘jammed’ in the inner membrane, accumulate in precursor inclusion bodies, or are rapidly degraded in the cytoplasm. The fact that no protein band, corresponding to rTLXI, could be detected on SDS-PAGE and that no inhibition activity could be measured when the cytoplasmic soluble protein fraction was isolated, suggests that the inhibitor is either stuck in the inner membrane or that it is present in the cytoplasm in the form of inclusion bodies. To examine whether the failure of translocation to the periplasm or the formation of inclusion bodies is not due to the presence of the C-terminal tags that are not properly exposed, a construct without tags was expressed with vector pBAD/gIII B. Once again, no expression product was detected in the periplasm, indicating that the presence of tags is not the primary cause of the failure to express *tlxi*.

The inability to express the inhibitor in *E. coli*, forced us to use another type of expression system. Many proteins, generated as misfolded, insoluble inclusion bodies through expression in *E. coli*, were successfully expressed in the yeast *P. pastoris* as soluble and correctly folded proteins (Li *et al.*, 2001; Mason *et al.*, 1996). This is due to differences in the protein-folding environment between those two organisms and to the inability of *E. coli* and the ability of *P. pastoris* to perform post-translational modifications, like glycosylation. For these reasons and because other plant proteins have successfully been expressed in *P. pastoris* (Juge *et al.*, 1996; Fierens *et al.*, 2004),

we chose to express the TLXI encoding gene in the methylotrophic yeast *P. pastoris*, which is able to use methanol as a sole carbon and energy source (Ogata *et al.*, 1969). Expression systems are based on the observation that the enzymes required for the methanol metabolism are only present at substantial levels when cells are grown on methanol. Hence the promoter regulating the production of alcohol oxidase (AOX) is most frequently used to drive heterologous protein expression in *Pichia*. In this study, we used the pPICZaC vector to express TLXI in *P. pastoris*. Due to the presence of the signal sequence from the *S. cerevisiae* α -factor prepro-peptide, the recombinant protein is targeted to the secretory pathway. The major advantage of expressing heterologous proteins as secreted proteins is that *P. pastoris* secretes very low levels of native proteins, making the protein easy to purify. A second reason to choose a vector for secretion, is that recombinant proteins will be glycosylated if there is a glycosylation site present, as is the case for TLXI. In addition, native TLXI from wheat appeared to be glycosylated (Fierens *et al.*, 2007).

The expression in *P. pastoris* was optimized because for biochemical and structural characterization, considerable amounts of rTLXI will be required. A first parameter that was subjected to optimization was the strain used for expression. The genetic background and the phenotype of the *P. pastoris* strain, and more specifically the Mut (methanol utilization) phenotype, can significantly influence the expression levels. Strains with a disrupted *AOX1* gene, which can only metabolize methanol slowly (Mut^S phenotype), are sometimes better producers of foreign proteins than wild-type strains (Mut⁺ phenotype) (Cos *et al.*, 2005; Pla *et al.*, 2006). By screening the different transformed colonies with respect to their expression levels of active rTLXI, we noticed that expression levels were significantly higher when using a Mut^S strain (KM71H). The slower growth and protein production of Mut^S strains on methanol, can possibly favor proper folding of rTLXI. It is also known that cells of the Mut^S phenotype tend to produce higher amounts of proteins than Mut⁺ cells in shaken-flasks cultures, probably because the flasks supply less oxygen compared to fermentor cultures and the Mut⁺ phenotypes grow limited under these conditions (Cregg *et al.*, 1993). The use of a strain, SMD1168H (Mut⁺), defective in the vacuole peptidase A, did not positively affect the expression levels indicating that rTLXI is not sensitive to this type of proteases. Comparison of expression levels of rTLXI with and without tags (*c-myc* epitope and polyhistidine tag), revealed a tendency towards higher expression levels

when expression is performed without tags. Possibly, the tags can disturb protein folding if they are not properly exposed or they can interfere with protein translocation to the medium, resulting in lower yields of secreted protein. Since propagation of *E. coli* under high osmotic pressures, created by the addition of sorbitol or betaine, was reported to increase production of soluble, heterologous proteins (Blackwell and Horgan, 1991), application of pre-induction osmotic stress on *P. pastoris* cells was also believed to affect soluble protein yields. In this study, addition of 0.35 M sodium chloride to the growth medium resulted in a slight increase of inhibition activities in the culture medium. When microorganisms are exposed to osmotic stress, this will lead to the accumulation of organic osmolytes, like glycine betaine, trehalose, glycerol and proline, to rebalance the cell turgor (Kempf and Bremer, 1998). For some of these compounds a chaperone function was demonstrated (Singer and Lindquist, 1998; Yang *et al.*, 1999). For example proline prevents protein aggregation by binding to folding intermediates (Samuel *et al.*, 2000).

In most cases, buffered medium (BMGY, BMMY) is used for expression of recombinant proteins in *P. pastoris*, particularly if pH is important for the activity of the expressed protein. When the induction medium is buffered between pH 3.0 and 6.0, the amount of proteolysis of the recombinant protein is often reduced (Sreekrishna *et al.*, 1997). Our results show indeed that expression levels are higher in this pH range compared to more elevated pH values. The expression levels at higher pH values (pH 7.0-8.0) are indeed lower, which can be caused by different reasons. First of all, neutral proteases are more active at this pH, leading to possible proteolysis of rTLXI. Secondly, the lower production levels can also be attributed to the instability of rTLXI when exposed for several hours to these pH values or to lower levels of cell growth and viability at these pH values. Nevertheless Shi and coworkers (2003) proved that higher expression levels are not always correlated with highest levels of cell growth.

Induction of the expression culture at temperatures lower than 30°C seemed to positively affect the amount of active protein in the culture medium, although the effect is rather limited. Inducing the cells at lower temperature could reduce the rate of protein synthesis and thus may allow more time for the nascent peptide chain to fold properly (Sarramegna *et al.*, 2002). Although rTLXI seemed to be a protein resistant to extreme temperature conditions (see further), instability of the protein at 30°C could be taken

into account because the induction period lasts for 20 hours, which is a considerably longer time period as the period used to test the temperature stability.

Methanol was used to switch on the *AOXI* promoter and consecutively induce heterologous expression. The optimal methanol concentration (1.25%), is a balance between two factors. On one hand, a high methanol concentration is desirable because it is related to a strong induction of the *AOXI* promoter, resulting in high expression levels. On the other hand, high methanol concentrations are cytotoxic (Guarna *et al.*, 1997). The methanol concentration in this study is 0.75% higher than what is recommended in the Invitrogen manual, but the methanol consumption rate is strongly dependent on culture variables such as cell density (Guarna *et al.*, 1997) and therefore, the optimal methanol level needs to be assessed for each specific protein produced.

Once the optimal expression conditions had been determined, they were applied in an experiment to determine the optimal duration of induction and to examine the effect of aeration on the expression yield. It was very clear that the use of baffled flasks, increasing the amount of oxygen transferred, was by far the most important factor in the improvement of expression yields, which was also demonstrated by Villatte and coworkers (2001). Moreover, they proved that expression levels of heterologous proteins are even influenced by flask design. The better production of rTLXI when more oxygen is supplied, is not due to the fact that cell growth is higher, because for both baffled and non-baffled flasks, cell growth ceases upon induction, which was also shown by Sarramegna *et al.* (2002). Oxygen supply therefore seemed to directly affect protein production. Protein production reached a plateau phase after 49 hours of induction, the optimal time for harvesting of the cells. Following expression, rTLXI was purified with CEC yielding approximately 4 mg of pure rTLXI per liter growth medium. This is a 20-fold lower yield compared to the yield of rTAXI-I expressed in *P. pastoris* (Fierens *et al.*, 2004). The reason why some proteins are expressed to a lower yield than others remains unknown.

4.5 Conclusions

It was confirmed by production of active inhibitor that the isolated *tlxi* gene sequence indeed encodes a xylanase inhibitor. Failure to express the TLXI encoding gene in *E. coli*, due to several reasons like formation of inclusion bodies and improper periplasmic

secretion, forced us to use an alternative expression system. *P. pastoris* was chosen for this purpose and expression was successfully optimized, which resulted in an optimal expression protocol, where good aeration of the cell culture is the most important parameter. Expressed rTLXI was successfully purified using ion exchange chromatography (CEC). One liter growth medium yielded approximately 4 mg rTLXI, a yield rather low compared to rTAXI-I. Inhibition activity measurements and western blot analysis confirmed that the recombinantly expressed protein is a TLXI-like protein that possesses inhibition activity towards XynI. rTLXI, purified and dialyzed against 25 mM sodium acetate buffer (pH 5.0), was used for biochemical characterization (chapter 5). In the light of understanding TLXI protein structure and functionality, *P. pastoris* provides a suitable expression system for further mutational analysis and large-scale production.

Chapter 5

Biochemical characterization of rTLXI

5.1 Introduction

Following the recombinant expression and purification of rTLXI, the present chapter documents the biochemical characterization of rTLXI. First, some general biochemical features like iso-electric point (pI), glycosylation, optimal temperature and pH are presented. Next, the impact of different pH and temperature conditions on the functional stability of rTLXI is explained followed by an analysis of the inhibitor's specificity, thereby focusing on the inhibition of *T. longibrachiatum* xylanase (XynI) and *A. niger* xylanase (ExlA). Finally, this chapter deals with the inhibitor-polysaccharide interaction. The characteristics are compared to those reported for the other cereal xylanase inhibitors, TAXI and XIP. The most striking feature discriminating TLXI from the other inhibitors is its remarkable stability under extreme temperature and pH conditions.

Knowledge of the biochemical characteristics of xylanase inhibitors, especially characteristics concerning enzyme specificity and stability, is instructive for the assessment of the role of these proteins in biotechnological processes and applications. Also in the context of future mutational analysis, an exact idea about the specificity and activity of the inhibitor is desired.

5.2 Materials and methods

5.2.1 Materials

B. subtilis GH11 xylanase (XynA) and an *A. aculeatus* GH10 xylanase were supplied by NV Puratos (Groot-Bijgaarden, Belgium). Two GH11 xylanases from *T. longibrachiatum* (also known as *T. reesei*), XynI (pI 5.5) and XynII (pI 9.0), and GH11 xylanases from *A. niger* (ExlA) and *T. viride* were from Megazyme. *A. niger* GH10 xylanase was purified from an *A. niger* CBS 110.42 culture filtrate at the Laboratory of Food Chemistry and Biochemistry (K.U.Leuven). Xylan and soluble glucan, used in the polysaccharide binding experiment, were from Sigma-Aldrich. Arabinoxylan (Xylazym

AX tablet) and insoluble glucan were from Megazyme. Accession numbers are mentioned in Table 5-2.

5.2.2 Iso-electric focusing and protein electrophoresis

The pI value of the inhibitor protein was determined by iso-electric focusing as described in the GE Healthcare separation technique file 100, using the PhastSystem unit with polyacrylamide gels containing ampholytes (pH 3-9). The broad range pI markers (3.5-9.3) were used.

Protein electrophoresis of deglycosylated samples and control samples was performed on 20% polyacrylamide gels with a PhastSystem unit, as described in the GE Healthcare separation technique file 110. β -Mercaptoethanol (5%) was used as reducing agent. The low molecular mass markers were from GE Healthcare. All gels were silver stained as described in GE Healthcare development technique file 210.

5.2.3 Xylanase inhibition assay

Inhibition activities were determined with a variant of the colorimetric Xylazyme AX-method (Gebruers *et al.*, 2001) using Xylazyme AX tablets (Megazyme). The protocol described in section 4.2.6. was applied, but with a few adaptations. Xylanase solutions were prepared in sodium acetate buffer (25 mM, pH 5.0) supplemented with BSA (0.5 mg/ml) and contained 2.0 U per ml. One enzyme unit corresponds to the amount of enzyme leading to an increase in $A_{590\text{nm}}$ of 1.0 with the Xylazyme AX- method in the absence of inhibitor as described below. For XynI and ExIA, 1.0 U corresponds to 0.011 nmol and 0.007 nmol, respectively. 500 μ l of inhibitor solution, prepared in sodium acetate buffer (25 mM, pH 5.0), was added to an equal volume of xylanase solution and the mixture was incubated at room temperature for 30 min. The mixtures were then kept at 40 °C, unless specified otherwise, and after 10 min an azurine-cross-linked wheat AX tablet (Megazyme) was added. They were then incubated at the same temperature for an additional 60 min. The reaction was terminated by the addition of 1.0% (w/v) Tris solution (pH 9.0) (10.0 ml) and vigorous vortex-mixing. The rest of the procedure was identical to the one described in section 4.2.6. The control was a sample prepared with buffer (25 mM sodium acetate, pH 5.0) instead of inhibitor solution. The blank contained only buffer. Inhibition activities were calculated as mentioned in section 4.2.6.

5.2.3.1 Temperature optimum and functional stability

The optimal temperature for XynI inhibition by rTLXI was determined by performing the xylanase inhibition assay described above at temperatures ranging from 4°C to 70°C (4°C, 20°C, 30°C, 40°C, 50°C and 70°C). The enzyme (2.0 U/ml) and inhibitor (0.2 µM) solutions were prepared in sodium acetate buffer (25.0 mM, pH 5.0), containing BSA (0.5 mg/ml) in the case of the xylanase solution. Measurements were performed in triplicate. The amount of inhibitor used (final concentration of 0.1 µM) was determined in a preliminary test to give about 50% inhibition activity of XynI at pH 5.0 and 40°C. Inhibition activities were expressed relative to the highest inhibition activity. For each incubation temperature, a control was included in which buffer was added to the xylanase instead of inhibitor solution.

Functional temperature stability of the inhibitor was determined by a 40 min incubation step of the inhibitor solutions (0.2 µM) at temperatures ranging from 25°C to 100°C (25°C, 40°C, 50°C, 60°C, 70°C, 80°C and 100°C). Additionally, pre-incubation at 100°C was performed for 2 hours. Next, the solutions were cooled on ice for 10 min and residual inhibition activity was measured towards XynI as described above. Measurements were performed in triplicate and inhibition activities were expressed relative to a sample that was not pre-incubated and stored at 4°C.

5.2.3.2 pH optimum and functional stability

The pH for maximal inhibition activity towards XynI was determined by the method described in section 5.2.3. but at varying pH. For this purpose, xylanase (2.0 U/ml) and inhibitor solutions (0.2 µM) were prepared in universal buffer at different pH values (pH 2.0 to 8.0). Universal buffer is composed of 0.60% citric acid, 0.39% potassium dihydrogen phosphate, 0.18% trihydrogen borate, 0.33% diethyl barbituric acid and 0.05% BSA in water. Aliquots of this solution were adjusted with either 2.0 M hydrogen chloride or 2.0 M sodium hydroxide to obtain the desired pH. Measurements were performed in triplicate and inhibition activities were given relative to the highest inhibition activity. For each pH condition, a control was included in which buffer (with a particular pH) was added to the xylanase instead of inhibitor solution.

To examine the functional stability of rTLXI, residual inhibitory activity was measured after 2 h of incubation of the inhibitor (1.5 µM) in 200 µl of buffer at varying pH. Buffers with a pH ranging from 3.0 to 12.0 were prepared as described above. For the

extreme pH values, potassium chloride/hydrogen chloride buffers (20 mM, 0.5 mg/ml BSA, pH 1.0 and 2.0) and potassium chloride/sodium hydroxide buffers (20 mM, 0.5 mg/ml BSA, pH 13.0) were prepared. After incubation, the pH of the inhibitor solutions was adjusted to pH 5.0 with 1300 μ l sodium acetate buffer (250 mM, pH 5.0). After a 10 min incubation at room temperature, xylanase inhibition activities were determined as described in section 5.2.3. Measurements were performed in triplicate and inhibition activities were expressed relative to a sample that was not pre-incubated and stored in sodium acetate buffer (25.0 mM, pH5) at 4°C.

5.2.3.3 Dose-response relationship

To determine the dose-response relationship of rTLXI towards XynI and ExIA, fixed amounts of xylanases (0.011 nmol and 0.007 nmol, respectively) were incubated with varying amounts of rTLXI according to the method described in section 5.2.3. Non-linear regression, using the GraphPad Prism software (GraphPad Software, Inc., San Diego, USA), was used to create dose-response curves according to the following equation:

$$Y = \frac{B \max \cdot X}{(K_D + X)}$$

in which Y is the inhibition activity (%), X is the molar ratio of inhibitor/enzyme (I/E), Bmax is the maximal inhibition activity (%) and K_D is the molar I/E ratio required to obtain 50% of the maximal inhibition activity. From these curves, the IC_{50} value, i.e. the molar I/E ratio needed to obtain 50% inhibition of the tested xylanase, could be calculated.

5.2.4 Glycosylation analysis

Glycan detection and deglycosylation experiments were performed in collaboration with the Laboratory of Food Chemistry and Biochemistry (K.U.Leuven).

5.2.4.1 Glycan detection

Native TLXI (Fierens *et al.*, 2007) and rTLXI (0.1 mg) were separated by SDS-PAGE in a 12% polyacrylamide gel using the Hoeffler Mighty Small unit (Hoeffler Scientific Instruments, San Francisco, CA, USA). The glycan detection was performed in gel, using the Pro-Q Emerald 300 Glycoprotein Stain Kit for glycan detection, according to the manufacturer's instructions (Invitrogen). The Pro-Q Emerald 300 glycoprotein stain

reacts with periodate-oxidized carbohydrate groups, creating a bright green-fluorescent signal on glycoproteins upon 300 nm UV illumination.

5.2.4.2 Deglycosylation

Enzymic N-deglycosylation was performed with Peptide-N-Glycosidase F (PNGaseF) (Enzymic In-solution N-deglycosylation kit) under reducing and denaturing conditions according to the instructions of the manufacturer (Sigma-Aldrich). The different deglycosylated and control samples were analyzed by SDS-PAGE followed by silver staining (section 5.2.2.).

Native TLXI (Fierens *et al.*, 2007) and rTLXI were also treated with anhydrous trifluoromethane sulfonic acid (TFMSA), which effectively cleaves N- and O-linked glycans from glycoproteins, leaving the primary structure of the protein intact (Edge, 2003). Anisole was used as a scavenger to neutralize reactive groups formed during the deglycosylation reaction. Excess TFMSA was neutralized later by reaction with pyridine. Briefly, the purified inhibitors (100 µg) were freeze-dried in glass-tubes for 24 h to ensure complete dryness. A 10% anisole in TFMSA solution (150 µl) was cooled to 0°C, and then added to the inhibitor samples. The reaction was performed at 0°C. After 3 h, the reaction was placed in a methanol-dry ice bath and neutralized with an equal volume of ice-cold aqueous pyridine (60%). Pyridine was removed by gel filtration on a PD-10 column (GE Healthcare) and, after freeze-drying, the different deglycosylated samples were analyzed by SDS-PAGE followed by silver staining (section 5.2.2.).

5.2.5 Binding to polysaccharides

rTLXI solution (33.0 µg/500 µl) was prepared in sodium acetate buffer (25.0 mM, pH 5.0) and different xylan and glucan polysaccharides were added (Table 5-1) (5 mg/500 µl). The mixtures were shaken at room temperature for 1 h. In the case of the insoluble polysaccharides, the supernatant was removed after centrifugation (13000 rpm, 10 min) and the pellet was washed twice with sodium acetate buffer (25.0 mM, pH 5.0). The inhibition activity in the mixture (for soluble polysaccharides) and in the supernatant (for insoluble polysaccharides) was determined using 30 µl mixture/supernatant and 0.011 nmol XynI according to the Xylazyme AX-method described in section 5.2.3. Inhibition activities were compared to the inhibition activity of a control sample, prepared and treated in the same way but without addition of any polysaccharide. For

insoluble polysaccharides, supernatant and pellet (suspended in 375 μ l water and supplemented with 125 μ l SDS-PAGE loading buffer (section 4.2.7.)) were analyzed by SDS-PAGE.

Table 5-1: Overview of the different polysaccharides used in the binding experiment

polysaccharide	solubility	viscosity	origin	characteristics
xylan	soluble ⁽³⁾	n.s.	birchwood	A/X=0 ⁽¹⁾
	insoluble ⁽³⁾	n.s.	birchwood	A/X=0 ⁽¹⁾
arabinoxylan	insoluble	n.s.	wheat	A/X \approx 0.6 ⁽²⁾
glucan	soluble	n.s.	<i>Laminaria digitata</i>	β -1,3-glucan with some β -1,6 linkages
	insoluble	low	barley	1,3-1,4- β -D-glucan; Mw: 137000
		medium	barley	1,3-1,4- β -D-glucan; Mw: 216000
		high	barley	1,3-1,4- β -D-glucan; Mw: 327000

n.s. not specified

A/X: arabinose/xylose ratio

⁽¹⁾ contains acetyl and 4-O-methylglucuronic acid substituents (Beg *et al.*, 2001; Teleman *et al.*, 2002)

⁽²⁾ Maes and Delcour, 2002

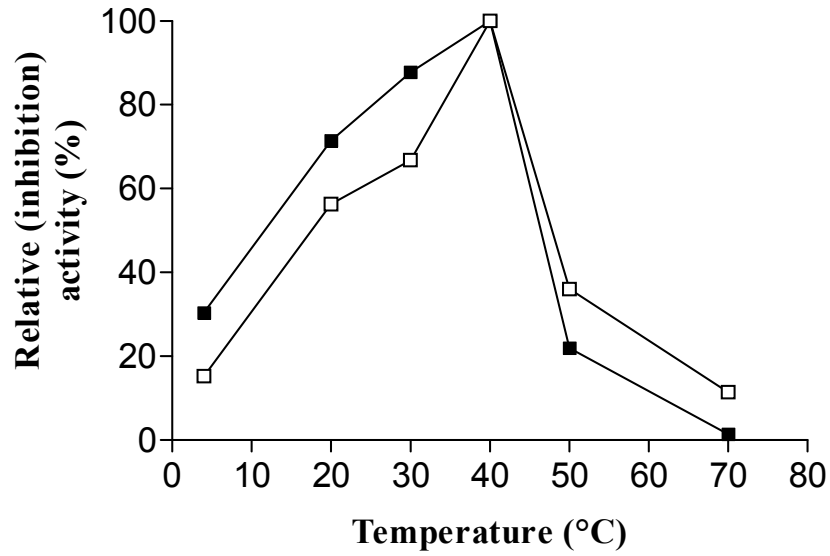
⁽³⁾ separation of the soluble and insoluble fraction was performed by A. Pollet (Laboratory of Food Chemistry and Biochemistry, K.U.Leuven)

5.3 Results

5.3.1 Biochemical characteristics of rTLXI

The experimental molecular mass of rTLXI is approximately 21 kDa, whereas that of the native protein from wheat is approximately 18 kDa. The pI-value of rTLXI is at least 9.3 by iso-electric focusing. Both XynI and rTLXI are maximally active at 40°C (Figure 5-1A). Inhibition activity of rTLXI is significantly reduced at 20°C and 30°C, although the inhibitor still retains more than 70% of its activity at these temperatures. At temperatures lower than 20°C and higher than 40°C, the inhibiting capacity is drastically reduced. The pH at which both proteins display maximal activity on the other hand differs (Figure 5-1B). XynI is maximally active at pH 4.0, whereas rTLXI displays maximal activity at pH 5.0. At pH 6.0, rTLXI retains about 60% of its activity compared to pH 5.0, but at the other pH values tested, inhibition activity is drastically reduced.

A



B

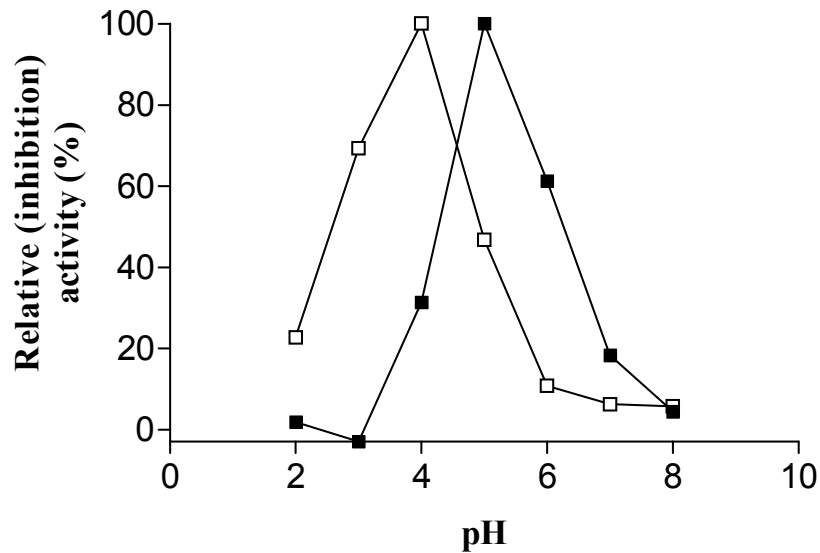


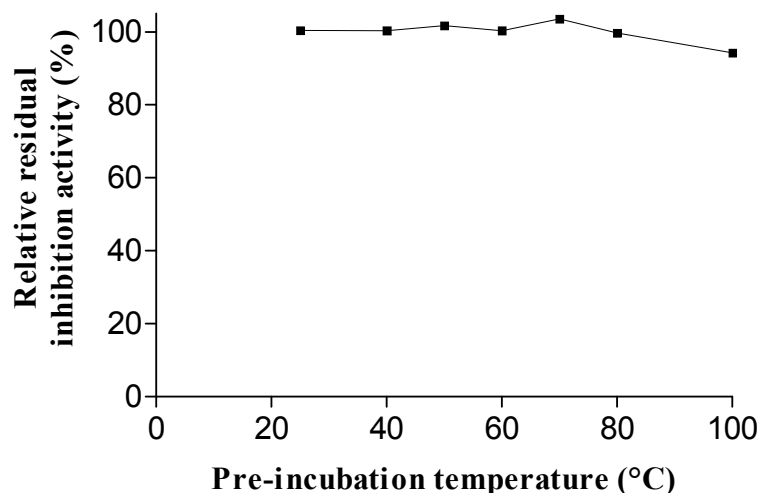
Figure 5-1: Temperature and pH optima of rTLXI (■) and XynI (□).

(A) Relative inhibition and enzymatic activity of rTLXI (against XynI) and XynI, respectively, as a function of temperature (°C). (B) Relative inhibition and enzymatic activity of rTLXI (against XynI) and XynI, respectively, as a function of pH. The activity assays using Xylazyme AX tablets were performed in triplicate (S.D. < 7%). Average (inhibition) activities for each incubation temperature/pH were expressed relative to the highest (inhibition) activity (100%).

rTLXI remains fully active after a 40 min incubation period at temperatures ranging from 25°C to 100°C (Figure 5-2A). Moreover, even after a pre-incubation step of 2 hours at 100°C, inhibition activity was fully recovered after cooling down the samples. rTLXI retains almost its full activity after a 2 h incubation period at pH values ranging

from pH 1.0 to pH 9.0. Pre-incubation at pH 10.0 to 12.0 significantly reduces the activity and the activity is almost completely abolished after incubation at pH 13.0 (Figure 5-2B).

A



B

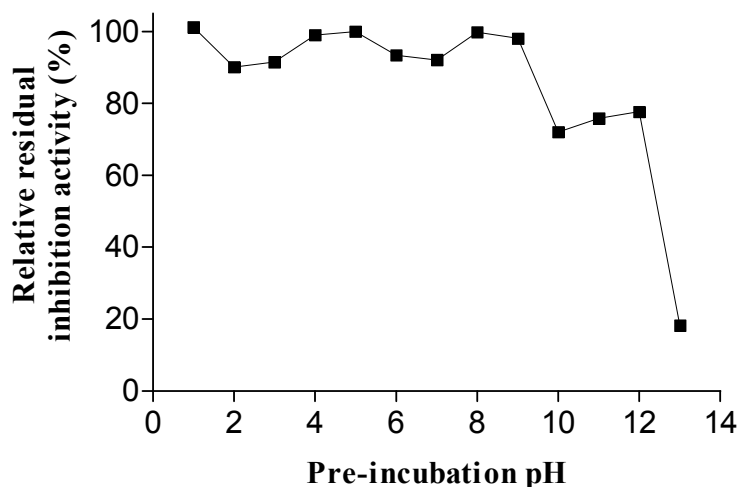


Figure 5-2: Functional stability of rTLXI after pre-incubation at different temperatures (A) and pH values (B).

(A) Relative residual inhibition activity (%) of rTLXI against XynI after a pre-incubation period of 40 min at different temperatures (pH 5.0). Averaged residual inhibition activities for each pre-incubation temperature were expressed relative to a rTLXI sample which was not pre-incubated and stored at 4°C.

(B) Relative residual inhibition activity (%) of rTLXI against XynI after a pre-incubation period of 2 h at different pH values (40°C). Averaged residual inhibition activities for each pre-incubation pH were expressed relative to a rTLXI sample which was not pre-incubated and stored in sodium acetate buffer (25.0 mM, pH 5.0). All measurements were performed in triplicate (S.D. < 8%).

Glycan detection with the Pro-Q Emerald 300 Glycoprotein Gel Stain kit revealed that both native TLXI and rTLXI are glycosylated. To determine whether rTLXI and native TLXI are N- or O-glycosylated or both, deglycosylation experiments were performed. Enzymic deglycosylation with PNGaseF removes only carbohydrate residues linked to an asparagine residue (N-linked glycosylation). The molecular mass of native TLXI only decreased to a small extent, whereas the molecular mass of rTLXI significantly decreased upon PNGaseF treatment (Figure 5-3A). These results indicate that native TLXI is only sparsely N-glycosylated, while rTLXI is extensively N-glycosylated. Chemical treatment with TFMSA, removing both N- and O-bound sugars, clearly reduces the molecular mass of both proteins. Native TLXI appears no longer as multiple bands on SDS-PAGE, indicating that this appearance was caused by different degrees of O-glycosylation (Figure 5-3B). From the results of the deglycosylation experiments, it can be concluded that native TLXI is O-glycosylated and little N-bound sugars are present. rTLXI on the other hand is mainly N-glycosylated and contains little or no O-glycosylation.

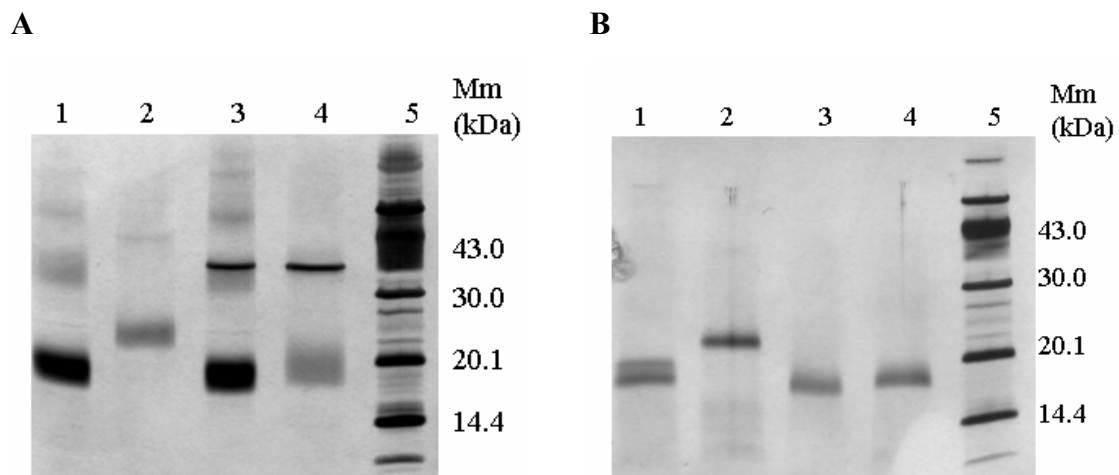


Figure 5-3: SDS-PAGE of the deglycosylation of native TLXI and rTLXI.

Native TLXI and rTLXI were deglycosylated enzymically with PNGaseF (A) and chemically with TFMSA (B). The original TLXI and rTLXI are shown in lane 1 and 2, respectively. Deglycosylated TLXI and rTLXI are shown in lanes 3 and 4, respectively. The enzyme PNGaseF appeared as a fine protein band of 35 kDa. The sizes of the molecular mass (Mm) markers (lane 5) are indicated on the right side of each gel. The gels were silver stained.

5.3.2 Inhibition specificity

rTLXI xylanase inhibition specificity was determined by measuring inhibition activities against several GH10 and GH11 xylanases. The results are shown in Table 5-2. rTLXI

inhibited none of the tested GH10 xylanases but did inhibit GH11 xylanases of *T. viride*, *A. niger* (ExlA) and *T. longibrachiatum* (XynI). Inhibition of *T. viride* xylanase, however, was very weak. GH11 xylanases of *B. subtilis* and *T. longibrachiatum* (XynII) were not inhibited.

Table 5-2: Inhibition specificity of rTLXI towards different GH10 and GH11 xylanases

xylanase	family	pI	pH opt	NCBI Accession no.	inhibition
<i>A. niger</i>	10			CAA03655	-
<i>A. aculeatus</i>	10			AAE69552	-
<i>T. viride</i>	11	9.3 ⁽¹⁾	5.0 ⁽¹⁾	CAB60757	+
<i>B. subtilis</i>	11	9.3 ⁽²⁾	6.0-7.0 ⁽²⁾⁽³⁾	AAA22897	-
<i>T. longibrachiatum</i> (XynI)	11	5.2 ⁽⁴⁾	4.5 ⁽⁵⁾	CAA49294	+
<i>T. longibrachiatum</i> (XynII)	11	9.0 ⁽⁴⁾	6.0 ⁽⁵⁾	CAA49293	-
<i>A. niger</i>	11	3.5 ⁽⁶⁾	3.0 ⁽⁷⁾	CAA01470	+

⁽¹⁾ Ujiie *et al.*, 1991

⁽²⁾ Courtin, 2000

⁽³⁾ Gottschalk *et al.*, 1994

⁽⁴⁾ Törrönen *et al.*, 1992

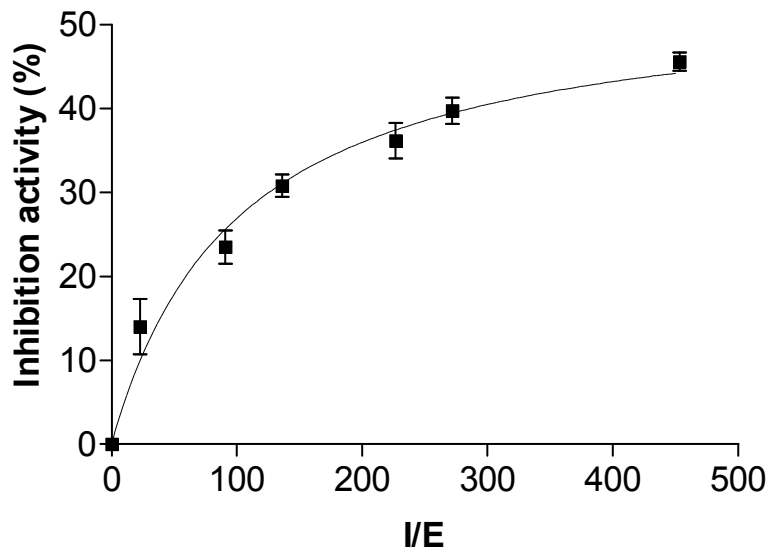
⁽⁵⁾ Tenkanen *et al.*, 1992

⁽⁶⁾ Ito *et al.*, 1992

⁽⁷⁾ Krengel and Dijkstra, 1996

Inhibition activities against ExlA and XynI were studied more in detail. Different amounts of rTLXI were added to a fixed amount of xylanase and the molar I/E ratio was plotted against the inhibition activity (%) (Figure 5-4). From the results, the IC₅₀ value as well as the maximal inhibition activity was calculated using GraphPad Prism Software. Maximal inhibition activity against ExlA and XynI is situated around 55% and 97%, respectively. The IC₅₀ values were determined to be 1063 ± 19 and 8 ± 1 for ExlA and XynI, respectively.

A)



B)

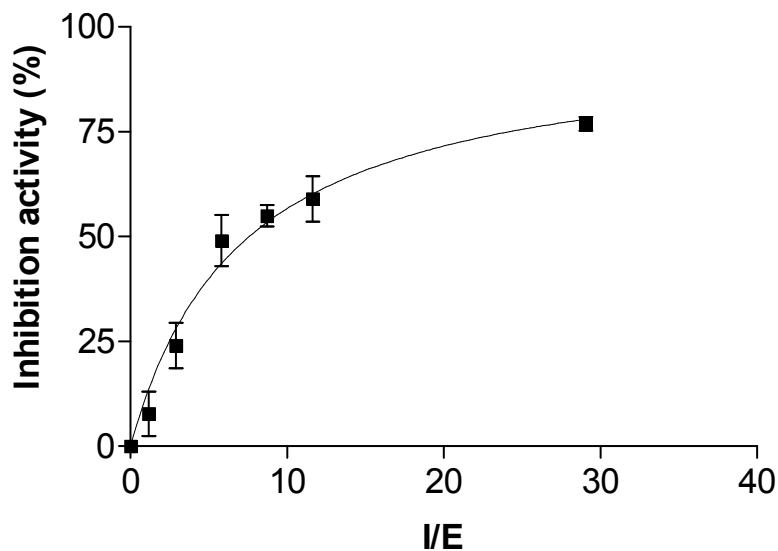


Figure 5-4: Dose-response relationship of rTLXI against ExIA (0.007 nmol) (A) and XynI (0.011 nmol) (B).

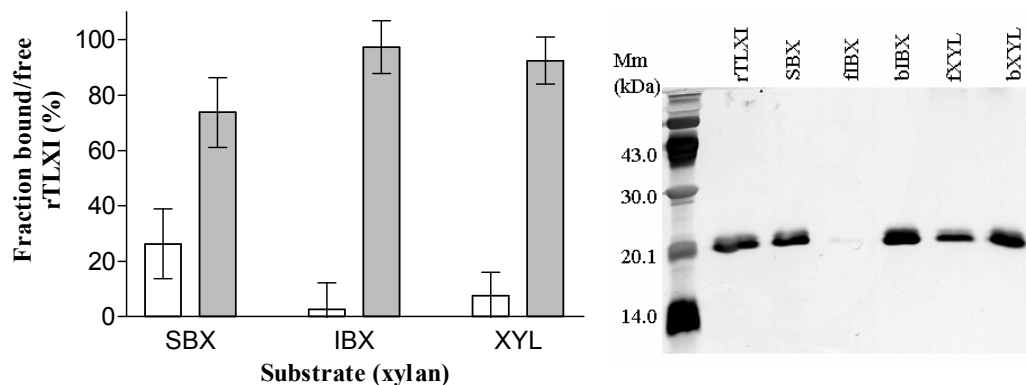
Inhibition activity is plotted as a function of molar I/E ratio. Measurements were performed in triplicate and error bars represent S.D.

5.3.3 Binding of rTLXI to polysaccharides

The interaction of rTLXI with different xylan and glucan polysaccharides (Table 5-1) was investigated by pre-incubating rTLXI with the polysaccharide for 1 hour. The inhibition activity against XynI (0.011 nmol) was measured in the supernatant after centrifugation and compared to a control sample where no polysaccharide was added.

For the soluble polysaccharides, inhibition activity was measured on the inhibitor-polysaccharide mixtures. The dose-response curve (Figure 5-4B) was used to relate the inhibition activity to the amount of rTLXI, present in the supernatant after an hour of incubation with polysaccharide. From these results, the fraction of bound and free inhibitor could be calculated (Figure 5-5).

A



B

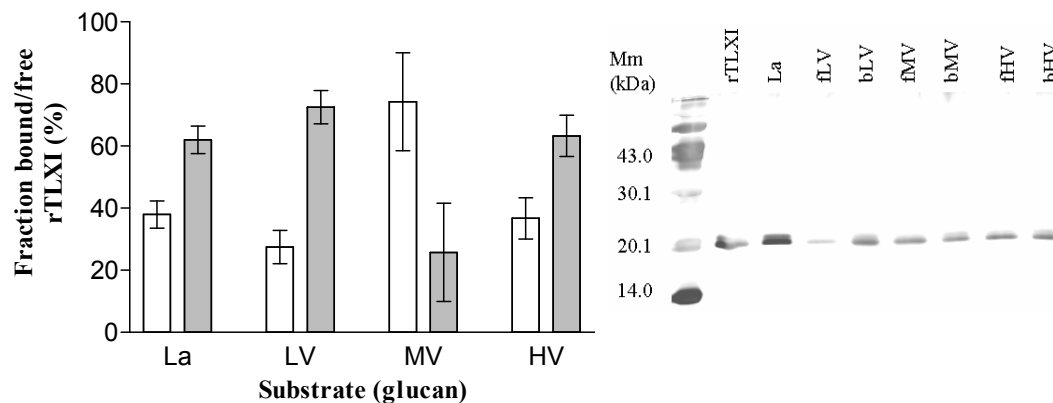


Figure 5-5: Interaction of rTLXI different polysaccharides.

(A) Interaction of rTLXI with soluble birchwood xylan (SBX), insoluble birchwood xylan (IBX) and wheat arabinoxylan (XYL). The fraction of bound (grey) and free (white) rTLXI is given for each substrate. Measurements were performed in triplicate. Error bars represent S.D.

(B) Interaction of rTLXI with laminarin (La; soluble glucan), insoluble barley glucan low viscosity (LV), insoluble barley glucan medium viscosity (MV) and insoluble barley glucan high viscosity (HV). Results are illustrated as above.

SDS-PAGE gels corresponding to each graph are shown on the right. Bound (b) and free (f) fractions for each polysaccharide were loaded. In case of SBX and La, the loaded fractions contain the rTLXI-polysaccharide mixture. A molecular mass (Mm) marker and a rTLXI control sample are included on the left side of each gel. Mm are indicated.

Both inhibition activity measurements and SDS-PAGE experiments indicate that rTLXI binds to every tested polysaccharide, although to different extents. Binding to insoluble birchwood xylan (IBX) and insoluble wheat arabinoxylan (XYL) is most pronounced. Except for MV barley glucan, more than 60% of the added amount of rTLXI interacts with each of the tested polysaccharides in the absence of xylanase.

5.4 Discussion

rTLXI is a basic protein ($pI > 9.3$) which inhibits exclusively microbial GH11 xylanases. Moreover, the inhibitor seems to display a preference for GH11 xylanases with a low pH optimum (Table 5-2), with IC_{50} values of 1063 ± 19 and 8 ± 1 for ExlA and XynI, respectively. Although it seems that only fungal xylanases are inhibited, inhibition activity measurements with native TLXI, performed by Fierens and coworkers (2007), against a more extensive set of xylanases demonstrated the inhibition of a bacterial GH11 xylanase from *Thermobacillus xylanilyticus* (NCBI Accession number CAJ87325) as well. The finding that rTLXI does not inhibit GH10 xylanases, to which the wheat endogenous xylanases belong, suggests again that TLXI is involved in plant defense mechanisms rather than in regulation of plant development.

A striking biochemical feature is that rTLXI is remarkably stable under extreme temperature and pH conditions considering its proteinaceous nature. This stability can probably be attributed to the presence of several disulfide bonds since rTLXI contains 10 cysteine residues. The majority of the TLPs are stabilized by eight disulfide bonds that do not only confer heat and acidic resistance (Grenier *et al.*, 1999) to the proteins, but also resistance against proteolytic degradation (Selitrennikoff, 2001). A first explanation for the observed functional stability is that rTLXI possesses the capacity to refold. While inhibition activity is drastically reduced when the assay was performed at 50°C or even completely abolished when performed at 70°C, probably due to partial or complete unfolding of the protein, respectively, cooling of the sample after a pre-incubation period at higher temperatures led to a complete recovery of the inhibition activity. Only pre-incubation at pH values from 10.0 to 12.0 resulted in an incomplete refolding leading to loss of inhibition capacity after pH adjustment. Pre-incubation at pH 13.0 appears to be pernicious for the protein since less than 20% of its activity was recovered. A second explanation is that the decrease in inhibition activity measured at

temperatures higher than the temperature and pH optimum, could be attributed to a heat- or pH-induced conformational change of the xylanase, hampering the interaction with rTLXI. In this case, rTLXI doesn't necessarily unfold at higher temperatures or pH values but remains properly folded explaining the functional stability. Only at pH values from 10.0 to 13.0, rTLXI would partially or completely unfold since pre-incubation at these pH values does lead to a decreased functionality of the inhibitor.

Deglycosylation experiments showed that rTLXI is mainly N-glycosylated, while O-glycosylation is less extensive. Glycosylation is one of the most common post-translational modifications performed by *P. pastoris*, which is capable of adding both O- and N- linked carbohydrate moieties to secreted proteins (Cereghino and Cregg, 2000). As in other eukaryotic systems the N-glycosylation recognition sequon in *P. pastoris* is Asn-Xaa-Ser/Thr, where Xaa is any amino acid except proline (Shakin-Eshleman *et al.*, 1996). The glycosylation is more readily achieved if the sequon is Asn-Xaa-Thr, as in rTLXI, rather than Asn-Xaa-Ser. It has been shown that the typical outer chain on *P. pastoris*-secreted proteins is Man₈GlcNac₂ or Man₉GlcNac₂. O-linked saccharides on the other hand are assembled onto the hydroxyl groups of serine and threonine. In contrast to higher eukaryotes, lower eukaryotes such as *P. pastoris* add O-oligosaccharides composed solely of mannose residues (Cereghino and Cregg, 2000). It is possible that next to the disulfide bonds, this extensive glycosylation confers the inhibitor its thermostability (Lis and Sharon, 1993) although native TLXI is glycosylated to a lower extent and contains nevertheless a comparable stability (personal communication E. Fierens). However, it has been proven that the position of the oligosaccharide in the protein structure may be more important in thermostability than the amount or length of the group (Olsen and Thomsen, 1991). It is also known that glycosylation of proteins is related to several other physicochemical functions (Lis and Sharon, 1993). For example, glycosylation can also modify solubility of a protein and control protein folding (Mitra *et al.*, 2006). The fact that glycosylation of a protein begins at the onset of synthesis, suggests its importance in protein folding. Inhibition or suppression of glycosylation indeed often results in aggregation or misfolding. These findings lead to the assumption that glycans could affect the fold or folding process of a protein similar to protein chaperones. Thus, this feature of glycosylation can also explain why expression of rTLXI in *E. coli* resulted in the formation of inclusion bodies (chapter 4). The deglycosylation experiments show that native TLXI is less

glycosylated. The type of glycosylation in plants also differs from that in yeast. Whereas glycosylation in *P. pastoris* consists solely of mannose and N-acetylglucosamine residues, plant glycosylation structures also contain saccharides like fucose and xylose (Wilson, 2002).

rTLXI appears to interact with different polysaccharides composed of glucose and xylose moieties, the latter being the substrate for xylanases, which TLXI inhibits. The interaction with the substrate can affect the inhibition activity measurements performed with the Xylazyme AX tablets because upon binding with the substrate, only part of rTLXI is available for interaction with the xylanase. However, in the polysaccharide binding experiments, inhibitor and substrate were incubated first in the absence of xylanase. This is in contrast to the inhibition activity assay. Hence it is not sure whether the interaction with the substrate will be as pronounced when xylanase is competing for binding to rTLXI. Nevertheless, the IC_{50} values determined with Xylazyme AX tablets have to be interpreted carefully, although it can be stated with certainty that rTLXI is a more potent inhibitor of XynI than of ExIA. rTLXI also interacts with laminarin (β -1,3-glucan with some β -1,6-linkages) and β -1,3-1,4-glucan from barley. Interaction with β -1,3-glucan has been demonstrated for other TLPs (Trudel *et al.*, 1998), including TLPs from barley (Osmond *et al.*, 2001). Binding of polysaccharides by TLPs is believed to occur in a long, deep cleft that traverses the surface of the proteins, is negatively charged (Osmond *et al.*, 2001) and is rich in hydrophilic residues (Koiwa *et al.*, 1999), a characteristic fairly typical of carbohydrate-binding sites. Several residues are present along the cleft that might form hydrogen bonds with the bound β -1,3-glucan. However, since TLXI is a smaller protein, it lacks domain II (Koiwa *et al.*, 1999) (Figure 3-8) that takes part in the formation of the cleft making it very unlikely that polysaccharides bind to TLXI in the same way as do other TLPs, especially since the acidic residues are not conserved (chapter 3, discussion). It is known that even the absence of several amino acids, that are located along the cleft and that might form hydrogen bonds with the polysaccharide, can abolish binding (Osmond *et al.*, 2001). The interaction mechanism between rTLXI and polysaccharides still remains to be elucidated. Aromatic residues at the surface of the inhibitor or the polysaccharide structures attached to Asn95 may be involved.

The biological significance of the interaction needs to be addressed. Binding to arabinoxylan would bring the inhibitor in the vicinity of the substrate of the enzyme.

Concentrations of TLXI would therefore be higher close to the enzyme target improving its functionality. An important question is whether TLXI is still able to interact with xylanase when it is bound to arabinoxylan in a natural environment. Although binding to β -glucan has been demonstrated only for β -glucan originating from barley and seaweed (*Laminaria digitata*), one could speculate that rTLXI also interacts with fungal cell walls that contain β -1,3-linked glucan residues as well as β -1,6-glucan (Selitrennikoff, 2001). Again, it can be hypothesized that the function of the interaction is to bring TLXI in close proximity to its target, i.e. the xylanase secreted by the fungus to penetrate the plant cell wall. Hence, TLXI could work more efficiently in preventing the fungus from penetrating the plant cell wall by immediately inhibiting the secreted xylanase. Again, it is not sure whether TLXI can interact simultaneously with glucan and xylanase. Alternatively, binding to the fungal cell wall could sterically hinder the attachment of the fungus to the plant cell.

Table 5-3: Comparison of the three currently known xylanase inhibitor types (TAXI, XIP and TLXI). rTLXI is also included for comparison with native TLXI.

	TAXI-type⁽¹⁾⁽²⁾	XIP-type⁽³⁾⁽⁴⁾	native TLXI⁽⁵⁾	rTLXI
molecular mass (experimental)	form A: 40 kDa form B: 30 kDa + 10 kDa	29 kDa	18 kDa	21 kDa
molecular form	monomer	monomer	monomer	monomer
pI	> 8.8	8.7-8.9	> 9.3	> 9.3
glycosylation	yes (limited)	yes	yes	yes
specificity	GH11 fungal and bacterial	GH10 and GH11 fungal	GH11 fungal and bacterial	GH11 fungal(a)
IC₅₀ (molar ratio)	0.6-1.1	approx. 1.7	6.3-134.7(b)	8.0-1063.0(b)
optimal pH	4.8-5.0	4.5-6.5	5.5	5.0
optimal temperature	20°C-40°C	30°C	40°C	40°C
pH stability	3.0-12.0	3.5-N.D.	1.0-12.0	1.0-12.0
Half-life (100°C)	3.5-4.5 min	< 40 s	> 2h	> 2h

(1) Gebruers, 2002

(2) Fierens, 2004

(3) McLauchlan *et al.*, 1999

(4) Juge *et al.*, 2004

(5) Fierens *et al.*, 2007

(a) rTLXI inhibition activity was only determined against fungal xylanases.

(b) IC₅₀ value for XynI and ExlA, respectively.

A comparison of the biochemical characteristics of the three currently known xylanase inhibitors is given in Table 5-3 including a comparison of native TLXI and rTLXI. Comparative analysis shows that (r)TLXI is the inhibitor with the lowest molecular mass and the highest stability. The inhibition pattern resembles that from TAXI-type inhibitors in that only microbial GH11 xylanases are inhibited. Nevertheless, TAXI-

type inhibitors cover a different spectrum of the GH11 xylanases. For example *B. subtilis* XynA is inhibited by TAXI-type inhibitors but not by (r)TLXI. The IC₅₀ values for (r)TLXI are significantly higher than those for the other inhibitors indicating that (r)TLXI is a less potent xylanase inhibitor. However, the IC₅₀ values for (r)TLXI have to be interpreted carefully because the potential effect of binding to the substrate may result in higher IC₅₀ values.

The biochemical characteristics of native TLXI and rTLXI are much alike. The molecular mass of rTLXI is higher than that of native TLXI, which can mainly be attributed to the higher degree of glycosylation of rTLXI. Additionally, the IC₅₀ values determined for rTLXI are higher compared to those for native TLXI, especially towards ExIA. This apparently lower activity of rTLXI can possibly be caused by a slightly different folding of rTLXI compared to native TLXI due to the 13 extra N-terminal amino acids attached to rTLXI originating from translation of the multiple cloning site of the expression vector. Alternatively, the different glycosylation pattern and extent can be responsible for the difference in IC₅₀ values between rTLXI and native TLXI. This difference may possibly directly interfere with xylanase-(r)TLXI interaction or may result in a different extent of substrate binding. The latter could indeed affect the inhibition activity and the related IC₅₀ value.

5.5 Conclusions

Extensive characterization of the recombinant xylanase inhibitor showed biochemical properties and enzyme specificities similar to those observed for natural TLXI. rTLXI is a 21 kDa protein which is extensively glycosylated and has a basic iso-electric point. The disparity in molecular mass with native TLXI can be attributed to a different extent of glycosylation while the difference in IC₅₀ values is possibly due to a slightly different fold of rTLXI compared to native TLXI or to different substrate binding affinities. The latter is presumably also related to the glycosylation extent and/or pattern. (r)TLXI distinguishes itself from the other xylanase inhibitors by its stability, a feature probably conferred to the inhibitor by the presence of multiple disulfide bonds or by the presence of extensive glycosylation. Stability under extreme temperature and pH conditions might be important in industrial applications.

Chapter 6

Mutational analysis of TLXI to gain insight in its interaction with GH11 xylanases

6.1 Introduction

P. pastoris appeared to be a good expression host for TLXI allowing straightforward purification of sufficient amounts of rTLXI for further analyses, such as mutagenic analysis and subsequent study of the interaction mechanism between TLXI and GH11 xylanases.

Attempts to crystallize TLXI and its complex with xylanases are so far unsuccessful. The interaction mechanism between TLXI and GH11 xylanases remains far from understood. Therefore, a structural model of TLXI was used as a basis for a mutagenic approach to gain insight in the interaction. In first instance, we focused on basic residues on the surface of TLXI because for both TAXI and XIP, basic residues play a key role in the interaction with GH11 xylanases. Among these, two histidine residues (His10 and His22) were selected for mutation based on a comparison with the TAXI-I sequence and with other TLPs, respectively. The mutants were expressed, analyzed for their inhibitory activity and the H22A mutant was also tested for its ability to form a complex with the tested xylanases. To support building of a docking model of TLXI in complex with a GH11 xylanase, two additional mutants, Q23A and L74A, were made. The present docking model is based on the assumption that TLXI, like TAXI and XIP, is a competitive inhibitor since no data were available yet on its competitive or non-competitive character.

6.2 Materials and methods

6.2.1 Standard molecular biology techniques

Agarose gel electrophoresis and DNA sequence analysis were performed as described by Sambrook and Russell (2001) unless specified otherwise. DNA sequences were analyzed on a 377 DNA Sequencer using ABI PRISM Big Dye Terminator chemistry (Applied Biosystems). The Sequencher 4.1 package (Gene Codes Corporation) was used to correct and align obtained DNA sequences. Primers were ordered from Proligo

Primers and Probes unless specified otherwise. All enzymatic reactions, such as restriction digestion, ligation (T4 DNA ligase, Promega) and dephosphorylation (Calf Intestine Phosphatase, Roche Diagnostics), were performed according to the protocol supplied with the enzyme. pPICZ α C ligation mixtures were transferred to chemocompetent *E. coli* TOP10F' cells according to the manufacturer's instructions (Invitrogen). Plasmid DNA (up to 20 μ g) was isolated from *E. coli* cells using the QIAprep Spin Miniprep Kit (Qiagen). Competent *P. pastoris* cells were prepared according to the instructions of the EasySelect *Pichia* Expression kit (Invitrogen).

6.2.2 Molecular biological techniques

PCR reactions were performed with *Pfu* DNA polymerase (Stratagene) on a Biometra TRIO-Thermoblock (Biometra, Goettingen, Germany) applying following temperature program unless specified otherwise: 5 min at 95°C; 1 min at 95°C, 1 min 30s at 58°C, 2 min at 72°C (35 cycles); 15 min at 72°C. PCR products were cloned in a pCR[®]4-TOPO[®] vector (Invitrogen) as described in section 3.2.6. prior to subcloning in the *Bsm*BI (New England Biolabs) restriction site of a pPICZ α C expression vector (Invitrogen) (section 4.2.3.2.). Competent *P. pastoris* X33 cells (Invitrogen) were transformed according to the method discussed in section 4.2.4.2. Recombinant expression was performed using the small scale expression protocol (section 4.2.5.2.) or the expression protocol optimized for rTLXI (section 4.3.2.). Recombinant proteins were purified with CEC (section 4.2.8.). Prior to biochemical characterization, purity of the recombinant proteins was verified by SDS-PAGE (section 5.2.2.). Inhibition activity on the culture supernatant of a small scale culture of rTLXI_[H10A] and rTLXI_[H22A] was performed with Xylazyme AX tablets as described in section 4.2.6. The dose-response relationship of the mutant proteins was determined using Xylazyme AX tablets as described in section 5.2.3.3. To ensure that mutant rTLXI_[H22A] was indeed a TLXI-like protein, western blot was performed for this mutant (section 4.2.10.). For this purpose 0.2 μ g rTLXI and rTLXI_[H22A] and 0.5 μ g native TLXI were used.

6.2.3 Site-directed mutagenesis

Mutations (H10A, H22A, Q23A, L74A) were introduced with the 'megaprimer' method (Smith and Klugman, 1997) (Figure 6-1) using H10Af, H22Af, Q23Af and L74Af (Table 6-1) as mutagenic primers. In a first PCR reaction, the 'megaprimer' was

constructed with the mutagenic primer in combination with XImatrstop (Table 6-1) at an annealing temperature of 58°C. The PCR reaction was performed with *Pfu* DNA polymerase (Fermentas, St. Leon-Rot, Germany) (1.25 U) using a pCR[®]4-TOPO[®] construct containing the *tlxi* gene as a template (1.5 ng), 200 µM of each dNTP, 3 µl commercially supplied (10x) buffer and 0.6 µM of each primer.

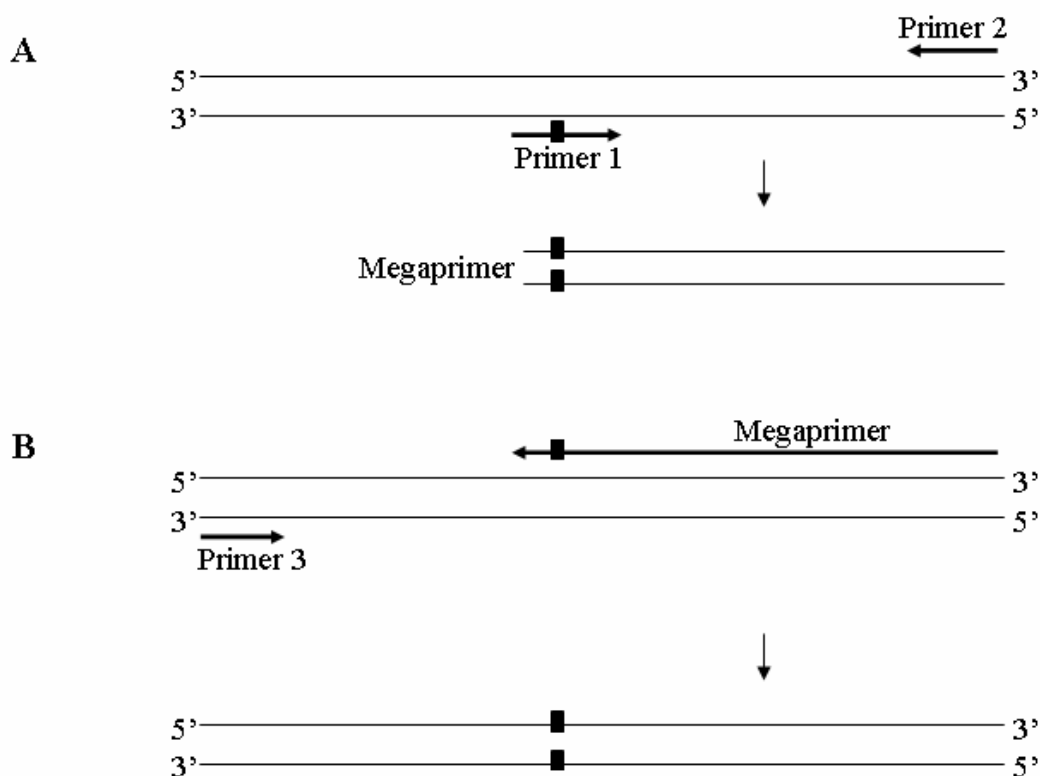


Figure 6-1: Schematic overview of the ‘megaprimer’ method.

(A) The ‘megaprimer’ is generated by PCR using a mutagenic primer (primer 1) and a flanking primer (primer 2). ■ indicates the mutagenic codon. (B) The ‘megaprimer’ is used in combination with the other flanking primer (primer 3) to generate the mutant gene. The flanking primers contain *Bgl*III restriction sites.

This PCR product was purified (Qiagen) and used as ‘megaprimer’ in a subsequent reaction in combination with XImatf or M13r (in case of H10A), the latter annealing to the pCR[®]4-TOPO[®] vector template. The reaction mixtures, containing 1.5 ng template, 200 µM of each dNTP, 3 µl of commercially supplied (10x) buffer, 1.25 U *Pfu* DNA polymerase and 300 ng megaprimer, were subjected to incubation at 95°C for 1 min and 72°C for 3 min (5 cycles). Then the flanking primer (XImatf/M13r) (0.6 µM) was added and 25 cycles at 95°C for 1 min, 58°C for 1 min 30s, 72°C for 1 min were

followed by a final extension at 72°C for 15 min. For H10A an annealing temperature of 60°C was used. Prior to cloning in a pCR[®]4-TOPO[®] vector, PCR products were extracted from agarose gel (QIAquick Gel Extraction kit, Qiagen) and 3′deoxyadenylate-overhangs were added by incubation with *SuperTaq* polymerase (SphaeroQ) (2.5 U, 72°C, 10 min).

Table 6-1: Primers used for mutagenesis.

primer	sequence
H10Af	AACCGTTGCGCCTTCACGGTG
H22Af	CTCGTGCTCGCCCAAGGGGGC
Q23Af	GTGCTCCACGCAGGGGGCGGCGG
L74Af	GGCAGCTCGGCGACTTGCGG
Ximatf	CACAGATCTGCACCGCTCACCATCACGAAC
Ximatrstop	CACAGATCTTCATGGGCAGAAGACGATCTG
M13r	CAGGAAACAGCTATGAC

*Bgl*III restriction sites are indicated in bold. Mutagenic codons are underlined.

6.2.4 Protein content determination

Protein concentrations were determined spectrophotometrically at 280 nm using a specific absorbance value of 1.402 AU, 1.407 AU, 1.407 AU and 1.405 AU for 1 mg/ml rTLXI, rTLXI_[H22A], rTLXI_[Q23A] and rTLXI_[L74A], respectively (1.000 cm UV-cell path length). To calculate the specific absorbance value the formula by Gill and von Hippel (1989) (section 4.2.9.) was used, taking into account that part of multiple cloning site (SMNSRGPAGRLGS) was not cleaved from the protein.

6.2.5 Gel permeation chromatography (GPC)

To assess complex formation, GPC on a Bio-Silect SEC 125-5 column (300 x 7.8 mm) (Bio-Rad) was performed, followed by SDS-PAGE analysis of the protein fractions. Purified rTLXI and rTLXI_[H22A] were freeze-dried and dissolved in 250 mM sodium acetate buffer (pH 5.0). *A. niger* xylanase (ExlA) and *T. longibrachiatum* xylanase (XynI) (Megazyme) were dialyzed overnight against the same buffer. Following samples were loaded separately on the column, dissolved in 150 µl of 250 mM sodium acetate buffer (pH 5.0): ExlA (80 µg), XynI (46.5 µg), rTLXI (20 µg) and rTLXI_[H22A] (17.6 µg). To investigate complex formation, following samples were mixed and incubated for 30 min at room temperature followed by loading on the GPC column (molar ratios are indicated): ExlA and rTLXI (2.8:1), ExlA and rTLXI_[H22A] (3.6:1), XynI and rTLXI (2.4:1), XynI and rTLXI_[H22A] (2.2:1). GPC separation was performed

at a flow rate of 1.0 ml/min and column calibration was done with the Gel Filtration LMW calibration kit (GE Healthcare).

6.2.6 Circular dichroism (CD) measurements

CD spectra of wild type rTLXI and rTLXI_[H22A] were recorded with a JASCO Spectropolarimeter (J-810) (Jasco Benelux, B.V., Maarsse, The Netherlands) at room temperature using a 0.1 mm quartz cell path length. Five scans in the far-UV (200-260 nm) were recorded for each protein sample and averaged. The ellipticities were expressed as mean residue ellipticities. Pure protein samples of rTLXI and rTLXI_[H22A] were prepared in sodium acetate buffer (25 mM, pH 5.0) at concentrations of 15.0 µM.

6.2.7 Modeling

The amino acid sequence of TLXI was used at the Laboratory of Biomolecular Modeling and BioMacS (Department of Chemistry, K.U.Leuven) to generate a molecular model using MOE (The Molecular Operating Environment) (Chemical Computing Group Inc., Montreal, Canada) with the structure of the thaumatin protein from *Thaumatococcus daniellii* (PDB entry 1THV (Ko *et al.*, 1994)) as template. The model was visualized using Pymol (Delano Scientific). The TLXI model was used for automatic protein docking with Ex1A using HADDOCK 1.3 (High Ambiguity Driven protein-protein docking) (Dominguez *et al.*, 2003). The receptor xylanase structure (Ex1A) was taken from the Ex1A-TAXI-I crystal structure (PDB entry 1T6G (Sansen *et al.*, 2004)). The Ambiguous Interaction Restraints for generation of the docking model were set as follows: the catalytic residues of the xylanase as active residues and the solvent accessible neighboring residues of the active site as passive residues for xylanase. For the TLXI protein the results from the mutagenesis studies were used: His22 and Leu74 were set as active residues, except Gln23, which was set as passive residue.

6.3 Results

6.3.1 Three-dimensional model of TLXI

A 3D-model of TLXI was generated by MOE (Chemical Computing Group Inc.) (Figure 6-2) with the structure of the thaumatin protein from *Thaumatococcus daniellii*

as template. TLXI shows 38.8 % sequence identity (EBI services, Align tool, water algorithm) with this sweet-tasting protein. According to the model, visualized with Pymol, the structure of TLXI consists of β -strands only, which was also confirmed by CD analysis (section 6.3.5.). Hence, the α -helix, present in the thaumatin structure, is absent in the smaller TLXI structure. This could be expected because TLXI lacks domain II (Figure 3-8).

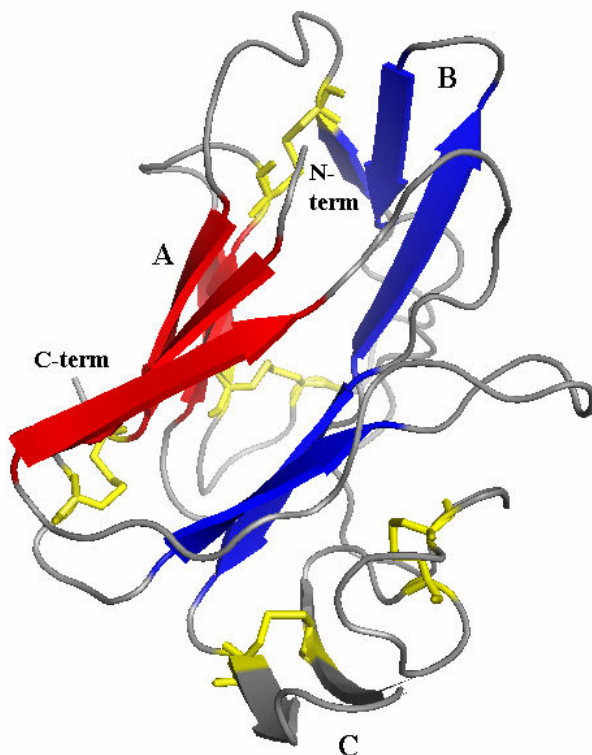


Figure 6-2: Backbone structure of the TLXI model generated with MOE (Chemical Computing Group Inc.).

The main body of the structure, comprising 10 of the 12 β -strands, consists of two β -sheets (indicated as A and B in red and blue, respectively) forming a β -sandwich. A third β -sheet (grey) is labeled with C. The N- and C-terminal parts of the protein are indicated (N-term and C-term, respectively). The five disulfide bridges are in yellow. The structure was visualized with Pymol (Delano Scientific).

The TLXI model has a total of 12 β -strands organized in 3 β -sheets. The main body of the structure consists of 2 β -sheets, A and B, as shown by the topology diagram (Figure 6-3), forming a β -sandwich. Sheet A and B each contain 5 β -strands. Both sheets exhibit a right-handed twist (Chothia, 1973) and the β -strands of one flat sheet are almost parallel to and on top of those of the other sheet. Of the 12 β -strands, each strand is antiparallel to its neighbors with the exception of the N-terminal and the C-terminal

strand, which are parallel to each other. The structure is stabilized by five disulfide bridges (Figure 6-2) between Cys residues 9 and 150, 54 and 64, 69 and 76, 115 and 138, and 123 and 128. The positions of the disulfide bridges are identical to the positions described for other low molecular mass TLP models (PDB entry 2DOV, 2DOW, 2DOX, 2DOZ) (Reiss *et al.*, 2006).

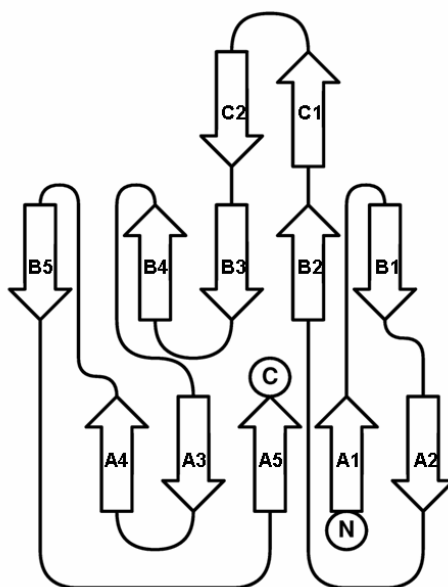


Figure 6-3: Topology diagram of the TLXI model generated with TopDraw (Collaborative Computational Project, Number 4; Bond, 2003).

The TLXI model is composed of 12 β -strands organized in 3 β -sheets (A, B and C). The N- and C-terminal ends of the protein are indicated. All the β -strands are antiparallel except the N- and C-terminal strands, which are parallel.

6.3.2 Selection, construction and recombinant expression of the mutants

For the two currently described xylanase inhibitors, TAXI and XIP, it has been shown that inhibition activity is mainly determined by one single basic residue. In the interaction of TAXI-I with xylanases, a His residue (His374) turned out to be a key residue in the inhibition of xylanases. This was demonstrated by crystallographic analysis of the complex (Sansen *et al.*, 2004) and was confirmed by site-directed mutagenesis (Fierens *et al.*, 2005). Analogously, the interaction of XIP with GH10 and GH11 xylanases is mainly determined by one basic residue, Lys234 and Arg149, respectively (Payan *et al.*, 2004). Based on these results, we speculated that surface located basic residues should be prime candidates as key residues in the interaction of

TLXI with xylanase enzymes. The model generated with MOE revealed the presence of 11 surface exposed basic residues. We focused our attention to His10 and His22. On the one hand, residue His10, residing on loop A1B1 (Figure 6-3), was selected for mutagenesis because the triad His10-Phe11-Thr12 showed a remarkable conservation with the key residue containing TAXI-I segment His374-Phe375-Thr376. On the other hand, according to the 3D-model, residue His22 is located on a loop (B1A2) between β -sheets. This loop extends further compared to the loop of other TLPs like zeamatin or thaumatin and is due to an insert of 4 amino acids (Figure 3-8 and 6-4). Comparison with the corresponding loop of low molecular mass TLPs (Reiss *et al.*, 2006), revealed that this group also possesses a shorter loop.

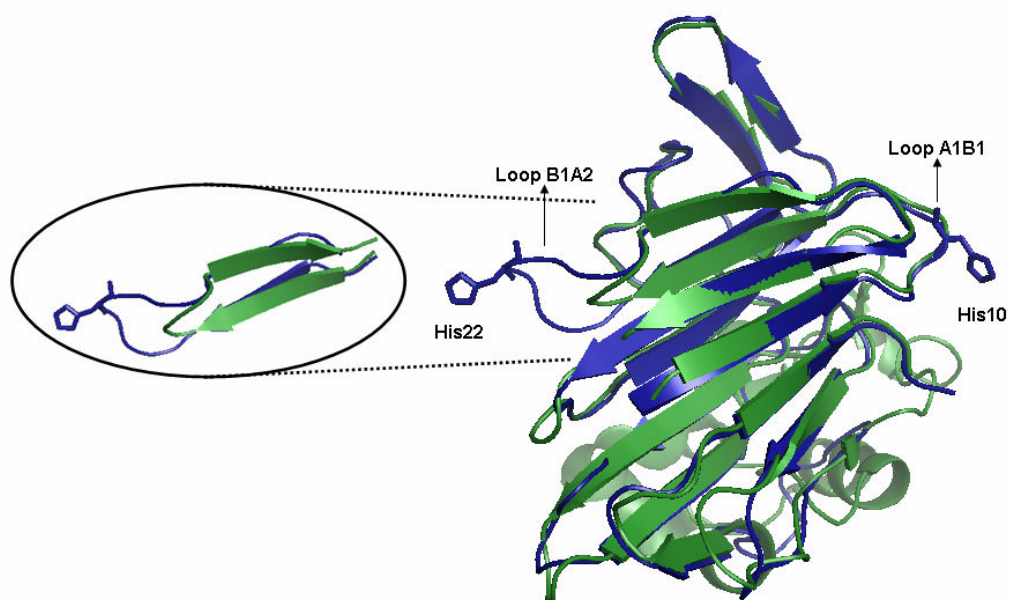


Figure 6-4: Structural alignment of the model of TLXI (blue) and the structure of zeamatin (green).

Ribbon diagram of the 3D-model of TLXI generated by MOE (Chemical Computing Group Inc.) superimposed with the 3D-structure of zeamatin (PDB entry 1DU5). Amino acids histidine 10 and 22, are indicated and the loop region differing between the two structures is enlarged. Loop names were assigned based on the topology diagram generated with TopDraw. Structural alignment was performed with Pymol (Delano Scientific).

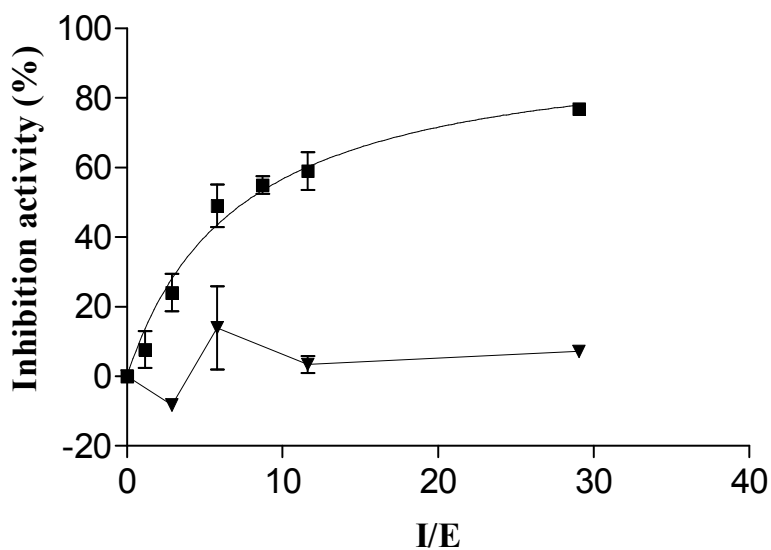
To support building of a docking model, two additional mutants were made. Gln23_{TLXI}, located next to His22_{TLXI}, was mutated to determine the orientation of TLXI relative to the xylanase. Since a Leu residue also plays a crucial role in the ExIA-TAXI interaction, Leu74_{TLXI}, located on a loop neighboring the His22-containing loop, was also mutated.

Mutants H10A, H22A, Q23A and L74A were constructed using the ‘megaprimer’ method as described in the Materials and Methods section. For H10A and H22A, a small scale expression was performed and inhibition activity of rTLXI_[H10A] and rTLXI_[H22A] was determined on the culture supernatant (section 6.3.3.). For mutants H22A, Q23A and L74A, a large scale expression resulted in efficient secretion of the proteins (rTLXI_[H22A], rTLXI_[Q23A] and rTLXI_[L74A]) in the culture medium. Recombinant proteins were purified with CEC and pure fractions were pooled and dialyzed against sodium acetate buffer (25.0 mM, pH 5.0) prior to inhibition activity measurements.

6.3.3 Inhibition activity of the mutants

Determination of inhibition activity of rTLXI_[H10A], measured on the culture supernatant of a small scale culture, led to the conclusion that this mutant is still able to inhibit xylanases and hence that His10 is not the residue essential for inhibition activity. On the other hand, for rTLXI_[H22A] no inhibition activity could be detected in the culture supernatant although SDS-PAGE showed efficient secretion of the mutant protein in the medium. Subsequent large scale expression and purification followed by inhibition activity determination at the optimal conditions for inhibition (section 5.3.1.), confirmed the finding that this residue is critical for xylanase inhibition (Figure 6-5). Mutation of His22 to Ala indeed abolishes the inhibition capacity of rTLXI. Even with an excess of rTLXI_[H22A] (I/E = 380 and 594 for XynI and ExIA, respectively), the mutant still lacks the capacity to inhibit the tested xylanases.

A



B

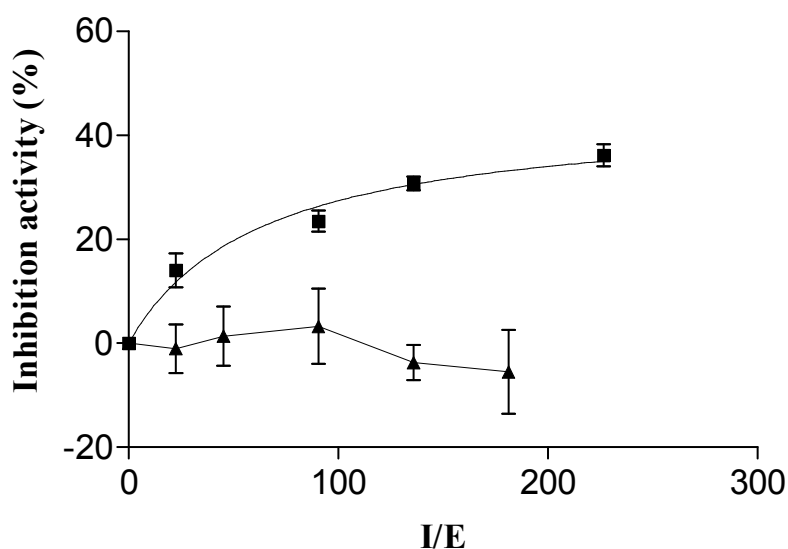


Figure 6-5: Inhibition activity of rTLXI_[H22A] (▲) in comparison with rTLXI (■).

A) Inhibition activity of rTLXI and rTLXI_[H22A] towards XynI.

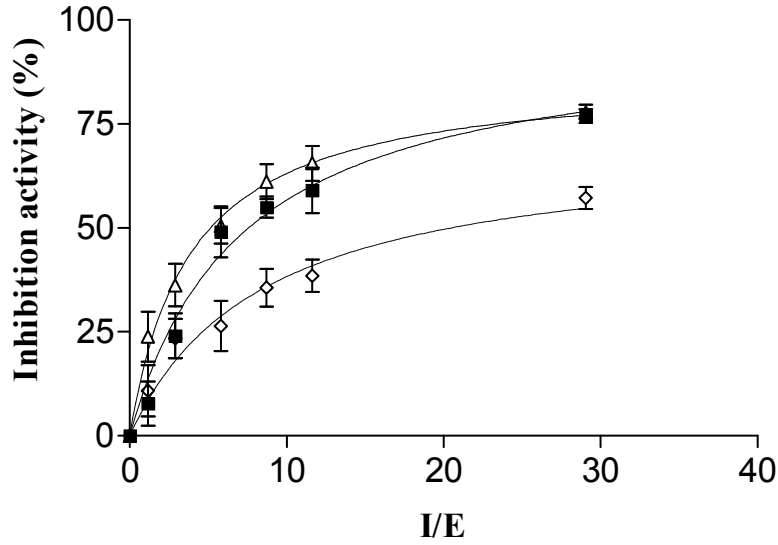
B) Inhibition activity of rTLXI and rTLXI_[H22A] towards ExIA.

1.0 U of XynI (0.011 nmol) or ExIA (0.007 nmol), respectively, was added to different amounts of rTLXI/ rTLXI_[H22A] at pH 5.0 and the corresponding inhibition activity was determined using Xylazyme AX tablets as substrate. Inhibition activity is plotted as a function of molar I/E ratio. Measurements were performed in triplicate and error bars represent S.D. Excess amounts of rTLXI_[H22A] (I/E= 380 and 594 for XynI and ExIA, respectively) are not represented in the figure.

The inhibition activities of CEC purified mutants rTLXI_[Q23A] and rTLXI_[L74A] were determined in the same way as for rTLXI_[H22A]. Whereas rTLXI_[Q23A] showed no

significant difference in inhibition activity towards both tested enzymes, the inhibiting capacity of rTLXI_[L74A] was significantly reduced. Figure 6-6 shows the dose-response relationships of the two latter mutants compared with rTLXI. The corresponding IC₅₀ values are given in Table 6-2.

A



B

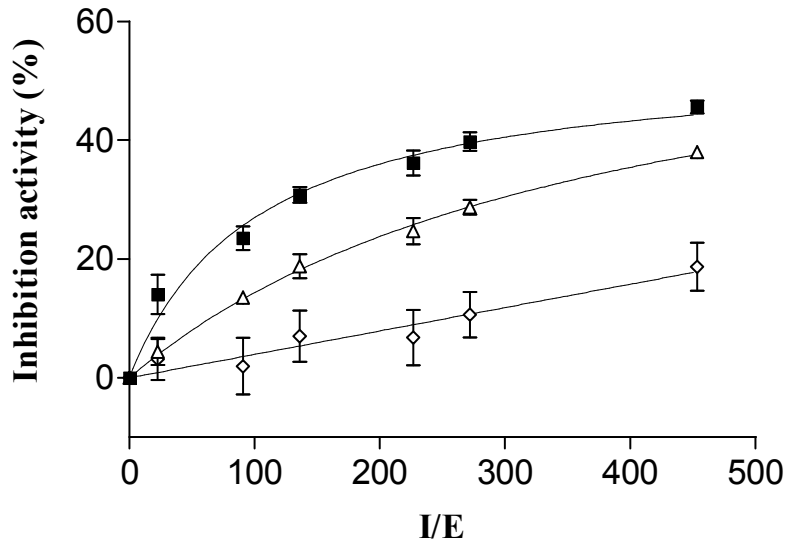


Figure 6-6: Inhibition activity of rTLXI_[Q23A] (△) and rTLXI_[L74A] (◇) in comparison with rTLXI (■).

A) Inhibition activity of rTLXI, rTLXI_[Q23A] and rTLXI_[L74A] towards XynI.

B) Inhibition activity of rTLXI, rTLXI_[Q23A] and rTLXI_[L74A] towards ExlA.

1.0 U of XynI (0.011 nmol) or ExlA (0.007 nmol), respectively, was added to different amounts of rTLXI/mutant at pH 5.0 and the corresponding inhibition activity was determined using Xylazyme AX tablets as substrate. Inhibition activity is plotted as a function of molar I/E ratio. Measurements were performed in triplicate and error bars represent S.D.

Table 6-2: Comparison of the IC₅₀ values of rTLXI and mutants rTLXI_[Q23A] and rTLXI_[L74A] towards XynI and ExIA.

protein	XynI		ExIA	
	IC ₅₀ (I/E)	S.D.	IC ₅₀ (I/E)	S.D.
rTLXI	7.8	1.2	1063.2	19.4
rTLXI _[Q23A]	5.1	1.0	997.0	106.1
rTLXI _[L74A]	19.0	0.6	1288.8	79.4

IC₅₀ values are given as molar I/E ratio. Measurements were performed in triplicate and S.D. is given.

6.3.4 Gel permeation chromatography (GPC)

To determine whether the H22A mutation resulted in the inability to form a complex with both GH11 xylanases, GPC was performed at pH 5.0.

When the ExIA/rTLXI mixture was evaluated with GPC, a peak with a shoulder was eluted (Figure 6-7A). The shoulder peak has an apparent molecular mass of 40 kDa and corresponds to the complex between rTLXI and ExIA (fraction 1 on SDS-PAGE). When rTLXI and ExIA were loaded separately on the GPC column, they eluted at a higher elution volume (corresponding to fraction 2, Figure 6-7A). This shift towards a lower elution volume, and thus a higher molecular mass, is hence caused by complex formation of the two proteins. The major peak corresponds to the excess of ExIA that was added. When the ExIA/ rTLXI_[H22A] mixture was evaluated (Figure 6-7B), only one peak was observed, which contains both free rTLXI_[H22A] and free ExIA, because they have the same apparent molecular mass on GPC. There was no shift towards a higher molecular mass (fraction 1 on SDS-PAGE) and hence, it can be concluded that no detectable complex was formed.

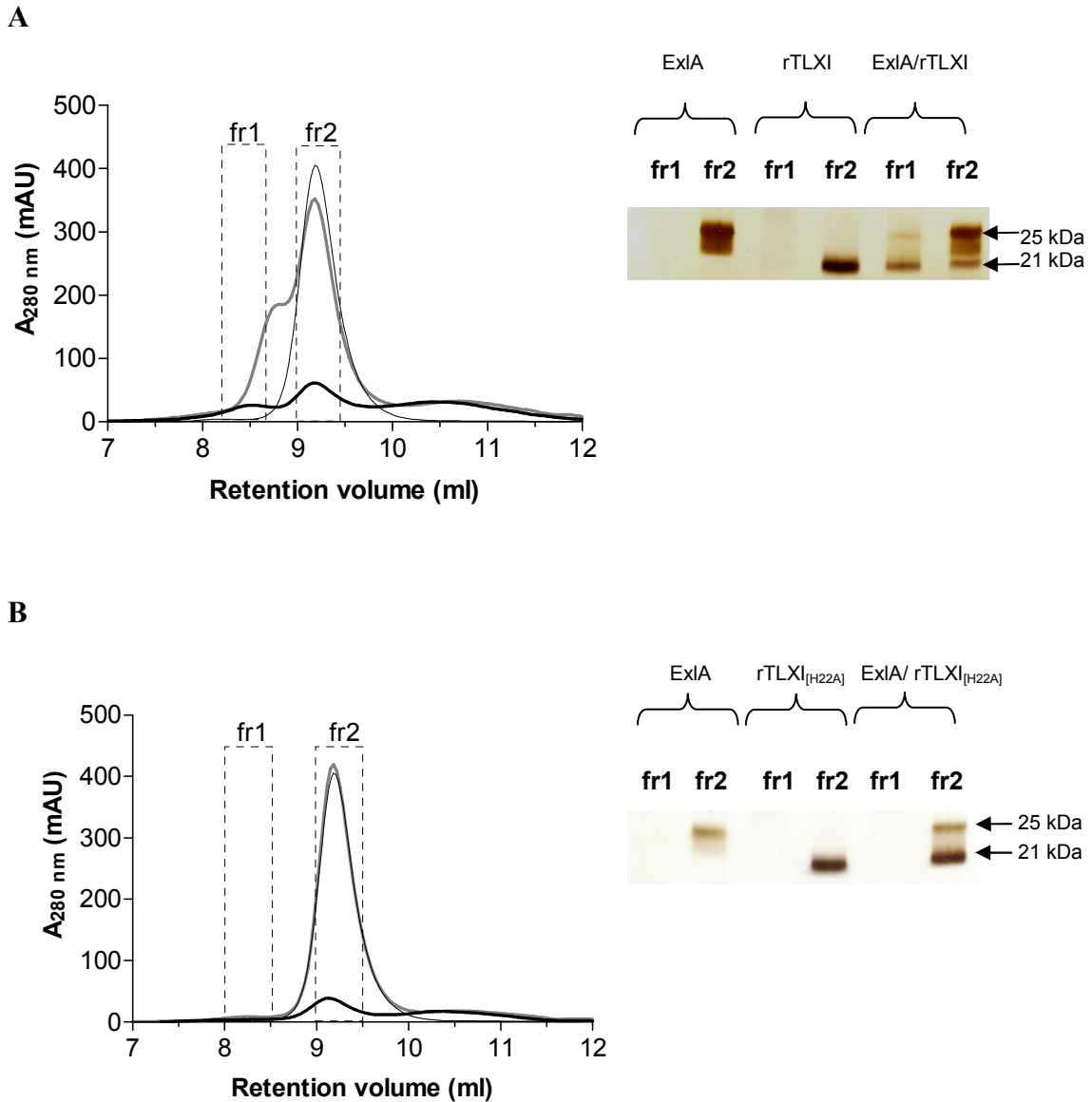


Figure 6-7: GPC chromatograms of rTLXI, rTLXI_[H22A], ExIA, ExIA/rTLXI and ExIA/rTLXI_[H22A].

A) GPC of ExIA (black thin line), rTLXI (black thick line) and ExIA/rTLXI (grey line) (incubated during 30 min at room temperature). The UV absorbance at 280 nm (mAU) was given as a function of the retention volume (ml). Fraction 1 and 2 are boxed. The corresponding SDS-PAGE was shown on the right and loaded fractions are indicated on top. The upper band corresponds to ExIA, the lower band corresponds to rTLXI.

B) GPC of ExIA (black thin line), rTLXI_[H22A] (black thick line) and ExIA/rTLXI_[H22A] (grey line) (incubated during 30 min at room temperature) illustrated as above. The upper band corresponds to ExIA, the lower band corresponds to rTLXI_[H22A].

The same experiment was performed with XynI/rTLXI and XynI/rTLXI_[H22A]. For XynI/rTLXI two peaks appeared (Figure 6-8). The first peak corresponds to an apparent molecular mass of 34 kDa and corresponds to the complex between the two proteins, although the molecular mass is smaller than was expected based on the molecular mass of the separate proteins. Possibly, complex formation of both proteins results in a very compact structure. The second peak corresponds to the excess of XynI. For XynI/rTLXI_[H22A], only one peak could be observed which contains both free rTLXI_[H22A] and free XynI. No SDS-PAGE was shown because rTLXI and XynI comigrate. The GPC results show that rTLXI forms a complex with XynI, while there is no measurable interaction between rTLXI_[H22A] and this xylanase.

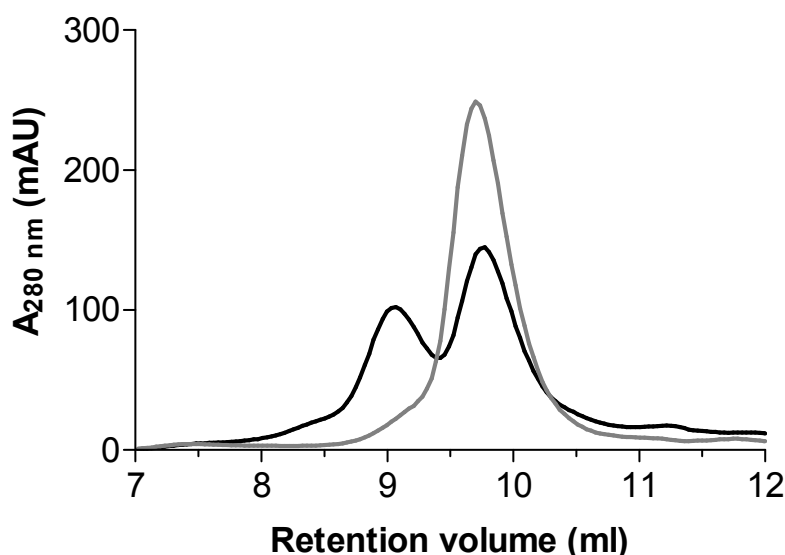


Figure 6-8: Comparison of GPC results of XynI/rTLXI_[H22A] (grey) and XynI/rTLXI (black). The UV absorbance at 280 nm (mAU) was given as a function of the retention volume (ml).

6.3.5 CD analysis

rTLXI and rTLXI_[H22A] were subjected to CD analysis. CD is a form of spectroscopy used to determine the secondary structure of proteins and is based on the differential absorption of left- and right-handed circularly polarized light. In general, this phenomenon will be exhibited by any optically active molecule. A secondary structure will also impart a distinct CD to its respective molecule. The ultraviolet CD spectrum of proteins can predict important characteristics of their secondary structure. CD spectra can be readily used to estimate the fraction of a molecule that is in the α -helix

conformation, the β -sheet conformation, the β -turn conformation, or some other (e.g. random coil) conformation. CD is a valuable tool, especially for showing changes in conformation. Since the CD spectra of rTLXI and rTLXI_[H22A] coincide (Figure 6-9), it can be stated that no clear difference in both protein secondary structures exists, indicating that rTLXI_[H22A] folds properly despite the presence of the mutation. The CD spectra also confirm the absence of α -helices in the rTLXI structure, because the presence of α -helices results in a characteristic CD spectrum with minima at 208 and 222 nm of equal magnitude.

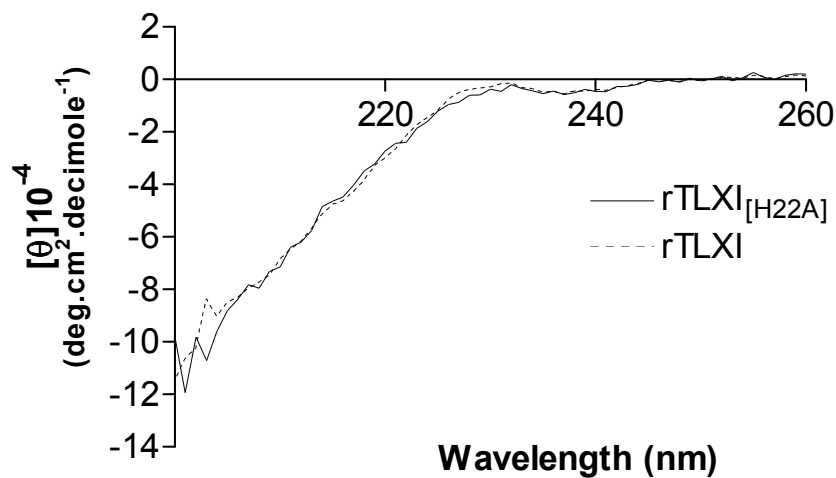


Figure 6-9: CD spectra of rTLXI and rTLXI_[H22A].

Legends are shown on the figure.

6.3.6 Western blot

Western blot analysis with polyclonal antibodies raised against native TLXI confirmed that rTLXI_[H22A] is indeed a TLXI-like protein (Figure 6-10). Hence, the absence of inhibition activity is not caused by the accidental purification of a *P. pastoris* protein of similar molecular mass. The difference in molecular mass between native TLXI and rTLXI is due to the difference in glycosylation extent and pattern (chapter 5).

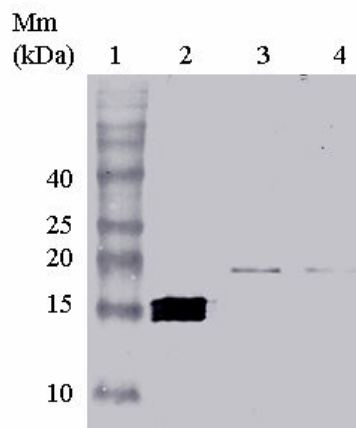


Figure 6-10: Western blot analysis using polyclonal antibodies raised against native TLXI.

Lane 1: BenckMark™ Pre-stained Protein Ladder (Invitrogen), molecular masses (Mm) are indicated; lane 2: native TLXI, lane 3: rTLXI; lane 4: rTLXI_[H22A].

6.3.7 Docking model of the ExIA/TLXI complex

Based on the results of the TLXI mutants and based on the assumption that TLXI, like XIP and TAXI, interacts in the active site of the xylanase, the complex between TLXI and ExIA was modeled using HADDOCK 1.3. with interaction restraints as described in section 6.2.6. The proposed model shows a good complementarity for hydrophobic and polar interactions (Figure 6-11). The interface area of the complex is 1079 Å² and the total energy of the complex comes to -256 kcal/mol, contributed for by Van der Waals (-32 kcal/mol) and electrostatic interactions (-224 kcal/mol). In this model, a double hydrogen bond of His22_{TLXI} with Asp37_{ExIA} and the catalytic residue Glu79_{ExIA} is formed. Furthermore, TLXI residue Leu21 is also buried in the hydrophobic part of the active site cleft (surrounded by ExIA residues Tyr66, Tyr89, Pro91, Phe131 and Trp172), containing substrate binding sites +1/+2 (Phe131_{ExIA} and Trp172_{ExIA}) and +3 (Tyr89_{ExIA}). Thus, the core of the interaction is formed by a hydrophobic protein-protein contact. The position and structure of the 70-80 segment, referred to as loop C2B3 based on the topology diagram of TLXI and containing residue Leu74, is uncertain, since the homology with the template is poor for this segment. Therefore, the exact location of this segment is unknown. Nevertheless, minor rearrangements of this segment suggest several other beneficial interactions. These contacts involve TLXI residue Leu74 with xylanase residues Leu14 and Val34 and ionic interactions at the exterior between xylanase residues Glu31 and Asp32 and TLXI residues Arg58 and Lys61.

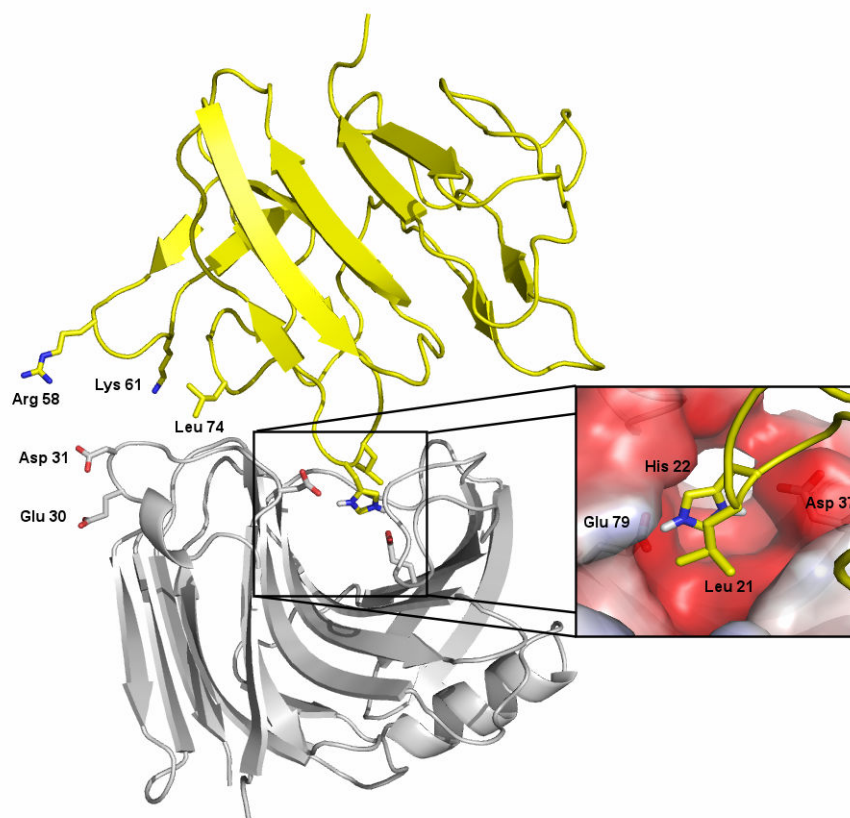


Figure 6-11: 3D-model of TLXI in complex with ExIA as predicted by homology modeling (MOE) and protein-protein docking (HADDOCK 1.3).

Xylanase and TLXI are shown in grey and yellow, respectively. Key interactions in the active site of His22_{TLXI} with Asp37_{ExIA} and Glu79_{ExIA}, and the hydrophobic contact of Leu21_{TLXI} are shown in the blow up inset of the binding cleft. The orientation of the proteins in this inset is rotated 180°. Other interactions involve the contacts between Leu74_{TLXI} (loop C2B3) and Leu14_{ExIA} and Val34_{ExIA}, as well as ionic interactions of Arg58_{TLXI} and Lys61_{TLXI} (loop C1C2) with Glu31_{ExIA} and Asp32_{ExIA}.

6.4 Discussion

The TLXI-xylanase interaction mechanism was studied via a mutagenic approach. Residues of TLXI were selected for mutagenesis based on a 3D-model generated with MOE using the structure of thaumatin as template. This comparative modeling method provided a reliable 3D-model of TLXI since TLXI shows 38.8% sequence identity and 49.3% sequence similarity (Align tool, Smith-Waterman algorithm) with the template sequence. The structure of a protein of unknown structure can be reliably derived by homology modeling if the target sequence has more than 25% to 30% sequence identity with the template sequence (Rost *et al.*, 1997). In addition, the stereochemical quality

of the model was evaluated with PROCHECK (Laskowski *et al.*, 1993). Analysis with 3D-PSSM (Kelley *et al.*, 2000) gives 95% certainty about the fold of the structure. The structural model of TLXI consists of β -strands only organized in three β -sheets, two of which form a β -sandwich analogous to the structure of thaumatin (De Vos *et al.*, 1985) and other TLPs, like zeamatin (Batalia *et al.*, 1996), osmotin (Min *et al.*, 2004), tobacco PR-5d (Koiwa *et al.*, 1999) and Ban-TLP (Leone *et al.*, 2006). The major difference with known TLP structures is the absence of the domain containing one extended α -helix associated with several shorter α -helices (domain II, see chapter 3) resulting in the absence of the cleft region. The subgroup of the TLPs showing low molecular masses (< 18 kDa), analogous to TLXI, also lacks this domain. Crystal structures of this subgroup have not been reported yet, although structures of several shorter TLPs from barley, generated by homology modeling, have recently been published (Reiss *et al.*, 2006) and have become publicly available in the PDB database. The model generated for TLXI is very similar to those obtained for the barley TLPs, with a core consisting of a β -sandwich and containing five disulfide bonds.

The other xylanase inhibitors, TAXI and XIP are structurally unrelated to TLXI since no similarity in the fold could be seen. Both TAXI and XIP are composed of both α -helices and β -strands. β -strands of TAXI are organized in β -sheets, but the β -sheets are not parallel to each other as is the case for TLXI. XIP on the other hand displays a $(\beta/\alpha)_8$ barrel fold. Whereas the structure of TLXI is stabilized by five disulfide bridges, XIP and TAXI contain two and six disulfide bonds, respectively. Although the inhibitors are structurally not related, they seem to have in common that their inhibition capacity is mainly determined by a surface exposed basic residue. Whereas xylanase inhibition by TAXI-I is determined by a C-terminal His residue (His374_{TAXI-I}), the key residues in the inhibition of GH10 and GH11 xylanases by XIP are Lys234_{XIP} and Arg149_{XIP}, respectively. The present study demonstrated that in the case of TLXI, His22_{TLXI}, located on a flexible loop that extends further compared to the loop of other TLPs, fulfills this key role. Indeed, replacement of this residue by Ala, completely abolishes inhibition activity due to the inability of the mutant to form a complex with the xylanase.

Because it was difficult to determine the competitive or non-competitive mode of action of TLXI towards xylanases due to the inhibitor's slow-tight binding nature (Fierens *et al.*, 2007), no data were available on this feature. Based on the similar nature

of the key residues, we therefore assumed that TLXI, like TAXI and XIP, is a competitive inhibitor and hence interacts at the active site of the xylanase. Based on the results obtained for the rTLXI_[H22A] mutant, it can be speculated that the extensive and flexible loop where His22_{TLXI} is located, protrudes in the active site groove of the xylanase. A docking model of the Ex1A-TLXI complex was made based on the results of the H22A mutant and two additional mutants, Q23A and L74A. The interface area of the obtained model is 1079 Å², whereas the interface area of the Ex1A-TAXI complex and the Ex1A-XIP complex are 992 Å² (Sansen, 2005) and 2200 Å² (Juge *et al.*, 2004), respectively.

The docking model allowed us to speculate that His22_{TLXI} binds in a similar manner as the His374 residue of TAXI-I in the Ex1A-TAXI-I complex (Sansen *et al.*, 2004). However, the interaction is not completely the same because a double hydrogen bond with Asp37_{Ex1A} and the catalytic residue Glu79_{Ex1A} is formed, while for TAXI-I a double hydrogen bond is formed with the two catalytic residues Glu79_{Ex1A} and Glu170_{Ex1A}. According to this model, Leu21_{TLXI} fulfils the same role as Leu292_{TAXI-I} interacting with the substrate binding sites. Leu74_{TLXI} on the other hand possibly contributes to the stability of the complex although for the interaction with the xylanase to occur, small rearrangements of the Leu74_{TLXI} containing loop (loop C2B3) have to take place.

It must be noted that some of the residues of Ex1A that, based on the model, are suggested to interact with TLXI, are not conserved in XynI, although this xylanase is inhibited better. In the hydrophobic part of the active site cleft, residues Tyr66_{Ex1A} and Phe131_{Ex1A} are not conserved in XynI but are replaced by other apolar amino acids, i.e. Leu and Ile, respectively. The conserved residues Tyr89_{Ex1A}, Pro91_{Ex1A} and Trp172_{Ex1A} adopt a significantly different orientation in XynI compared to Ex1A. Interacting residues located on the ‘fingers’ of Ex1A (Leu14, Val34, Glu31 and Asp32) are not conserved in XynI, but the ‘fingers’ have a slightly different conformation in XynI compared to Ex1A. Although it is possible that the difference in conformation of particular residues of XynI, in comparison to Ex1A, lead to a more beneficial interaction with TLXI or that TLXI interacts differently with XynI and Ex1A involving different interacting residues, the docking model needs to be verified by additional TLXI mutants or by xylanase mutants (Chapter 8).

6.5 Conclusions

In this chapter, the current insight in the interaction between TLXI and GH11 xylanases is summarized. Like for TAXI-I and XIP, a basic residue, His22_{TLXI}, located on a flexible loop between β -sheets, appeared to be indispensable for inhibition. This loop distinguishes TLXI from other TLPs since, due to an insertion, this loop extends further in case of TLXI suggesting that other known TLPs do not possess xylanase inhibiting activity. The loss of inhibition activity of the mutant is caused by the inability of the mutant to form a complex with GH11 xylanases. To support the building of a docking model, two additional mutants were made, Q23A and L74A, only the latter of which resulted in a significant decrease in activity. The docking model provides a preliminary view on the interaction mechanism between TLXI and GH11 xylanases. Both interaction with the catalytic residues as interaction with the substrate binding sites is suggested. Verification of this model by mutagenic analysis of ExIA is described in chapter 8. Crystals of rTLXI_[H22A] have been obtained recently (E. Vandermarliere, Laboratory for Biocrystallography, Department of Pharmaceutical Sciences) and should provide a new path for structural analysis.

Chapter 7

Recombinant expression and characterization of TLXI variants and related sequences

7.1 Introduction

The identification of *tlxi*-like sequences in the diploid wheat species *A. speltoides* (*as-tlxi*) and in rye (*sc-tlxi*) was described in chapter 3. The present chapter reports their recombinant expression in *P. pastoris*. Both proteins share high sequence similarity with TLXI (90% and 88%, respectively). SC-TLXI lacks the N-glycosylation site present in TLXI. In addition, a gene, homologous to the predominant gene identified in the diploid wheat species *T. urartu* (chapter 3), was amplified from genomic DNA of wheat cv. Chinese Spring and is referred to as *tlp*. An N-glycosylation consensus sequence was introduced by site-directed mutagenesis and the resulting gene (*tlp_{glyc}*) was expressed resulting in a protein displaying 64% identity to TLXI lacking the His₂₂_{TLXI}-containing flexible loop region (chapter 6).

Expression and subsequent characterization of variants of TLXI, differing in a limited amount of amino acids, is interesting because it can provide information about the residues responsible for the inhibition activity and/or specificity and for other biochemical characteristics. The variants described in this chapter are in accordance with the results obtained for the TLXI mutants (rTLXI_[H10A] and rTLXI_[H22A]) in chapter 6. Furthermore, a hypothesis is put forward to explain the decreased functional stability of the rAS-TLXI protein in comparison with rTLXI.

7.2 Materials and methods

7.2.1 Standard molecular biology techniques

The techniques mentioned in section 4.2.1. were applied.

7.2.2 Molecular biology techniques

PCR products were cloned in a pCR[®]4-TOPO[®] vector (Invitrogen) as described in section 3.2.6. prior to subcloning in the *Bsm*BI (New England Biolabs) restriction site of a pPICZαC expression vector (Invitrogen) (section 4.2.3.2.). Expression plasmids

were transferred to competent *P. pastoris* X33 cells (Invitrogen) according to the method discussed in section 4.2.4.2. Site-directed mutagenesis was performed as described in section 6.2.3. using a *tlp*-containing pCR[®]4-TOPO[®] vector as template, BQglycr (Table 7-1) as mutagenic primer and BQmatf and BQmatrstop (Table 7-1) as flanking primers. Small scale expression of *sc-tlxi* and large scale expression of the three described genes, was as mentioned in section 4.2.5.2. and 4.3.3., respectively. Recombinant proteins were purified with CEC at pH 5.0 (rSC-TLXI and rAS-TLXI) or pH 4.0 (rTLP_{glyc}) as described previously (section 4.3.4.). Purity of the recombinant proteins was verified with SDS-PAGE (section 4.2.7.) but gels were silver-stained according to the method described by Shevchenko *et al.* (1996). Xylanase inhibition assays were performed as described in section 5.2.3. Inhibition activity of rAS-TLXI was determined with GH11 xylanases of *T. longibrachiatum* (XynI and XynII), *A. niger* (ExlA), *B. subtilis* (XynA) and *T. viride* and GH10 xylanases of *A. niger* and *A. aculeatus*. Accession numbers, pH optimum and pI of the xylanases are given in Table 5-2. Inhibition activity of rTLP_{glyc} and rSC-TLXI was determined against XynI and ExlA. rAS-TLXI was more profoundly characterized. The dose-response relationship, using XynI as enzyme, and subsequent determination of the IC₅₀ value was studied as described in section 5.2.3.3. The optimal temperature and pH for inhibition activity as well as functional stability after pre-incubation at different temperatures and pH values were determined according to the method described in section 5.2.3.

7.2.3 Isolation of the genes encoding the mature protein

7.2.3.1 sc-tlxi and as-tlxi

The molecular identification of *as-tlxi* and *sc-tlxi* was described in sections 3.3.2.2. and 3.3.2.3., respectively. Amplification of the mature sequence (without signal sequence) was performed with primers containing *Bgl*III restriction sites (Table 7-1) according to the protocol described in section 3.2.4 with genomic DNA of *A. speltoides* and *S. cereale* cv. halo as template, respectively. Primers were designed on the previously identified sequence.

7.2.3.2 tlp

The molecular identification in the *T. urartu* genome of a gene displaying 99% sequence identity with EST BU607139 and 62% with TLXI upon translation was

described in section 3.3.2.2. Since the sequence doesn't contain the start of the mature protein and EST BU607139 doesn't include the translation start, making prediction of the signal sequence and subsequent prediction of the start of the mature protein impossible, expression primers, BQmatf and BQmatrstop (Table 7-1), were designed based on EST BQ838841. This EST displays 97% sequence identity with EST BU607139 but contains a deletion resulting in a translational frame shift. Amplification was performed on genomic DNA of hexaploid wheat cv. Chinese Spring according to the protocol described in section 3.2.4. A sequence verified *tlp*-containing pCR[®]4-TOPO[®] vector was used as template to introduce an N-glycosylation site (*tlp_{glyc}*).

Table 7-1: Primers used in this chapter.

gene	primer name	sequence	reference (section)
<i>as-tlxi</i>	XImatfS	CACAGATCTGCGCCCCTCACCATCACCAAC	7.2.3.1.
	XImatrstopS	CACAGATCTTCATGGGCAGAAGACGACCTG	7.2.3.1.
<i>sc-tlxi</i>	Ximatf	CACAGATCTGCACCGCTCACCATCACGAAC	7.2.3.1.
	SCXImatrstop	CACAGATCTTCATGGGCAGAAGACGACCTG	7.2.3.1.
<i>tlp</i>	BQmatf	CACAGATCTACGTCGACGCTGACGCC	7.2.3.2. and 7.2.2.
	BQmatrstop	AGATCTTCATGGGCAGAAGACGATCTGG	7.2.3.2. and 7.2.2.
	BQglycr	TGATGCCGTAGGTGTAGTTGCCCTCGGAG	7.2.3.2. and 7.2.2.

*Bgl*II restriction sites and mutagenic codons are in bold and underlined, respectively.

7.3 Results

7.3.1 Recombinant expression and purification

Because *as-tlxi*, isolated from the diploid wheat species *A. speltoides* (section 3.3.2.2.), could reveal interesting information concerning structure-function relationship of TLXI because of its 90% protein sequence identity with the inhibitor, the sequence encoding the mature protein was isolated with primers XImatfS and XImatrstopS (Table 7-1) from genomic DNA of *A. speltoides*. The AS-TLXI encoding gene was expressed in *P. pastoris* and the produced protein was purified using CEC (Figure 7-1). Expression levels were somewhat higher than those of rTLXI.

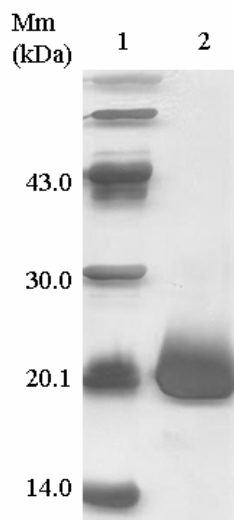


Figure 7-1: SDS-PAGE of purified rAS-TLXI.

Lane 1: LMW marker with molecular masses (Mm) indicated on the right; lane 2: Purified rAS-TLXI.

The *tlxi*-like sequence, identified in rye (*S. cereale* cv. halo), *sc-tlxi*, was also expressed in *P. pastoris* using the pPICZαC vector. The mature sequence was therefore amplified with primers XImatf and SCXImatrstop (Table 7-1) and cloned in the pCR[®] 4-TOPO[®] vector. After sequence verification and subcloning in the *P. pastoris* expression vector, expression was attempted according to the optimized protocol. However, no protein production could be visualized after expression not even after purification with CEC and subsequent concentration.

The *tlp* sequence, amplified with primer combination BQmatf and BQmatrstop (Table 7-1) using genomic DNA of hexaploid wheat cv. Chinese Spring as template, resulted in a sequence displaying 96% nucleotide identity with EST BQ838841. However, the deletion causing the frameshift in the EST sequence was not present in the amplified sequence. Additionally, the resulting sequence displays 97% and 96% sequence identity with EST BU607139 (section 3.3.2.2.), at the nucleotide level and the amino acid level, respectively. Since we failed to express SC-TLXI in *P. pastoris*, which was possibly related to the absence of N-glycosylation, we chose to introduce an N-glycosylation site in the *tlp* sequence to ensure successful expression. For this purpose, the segment ⁹⁶FYH⁹⁸ was mutated with the ‘megaprimer’ method to ⁹⁶NYT⁹⁸, corresponding to the N-glycosylation recognition sequence. The resulting protein, further referred to as TLP_{glyc}, is 64% identical to TLXI (Figure 7-2).

```

TLPglyc      TSTLTPLTITNRCSTVWPVAVA----SAGLGTELHPGANWTVDASAIIDYTADIWGRGTGCS 56
TLXI         ----APLTITNRCHFTVWPVAVALVHQGGGGTELHPGASWSLDTFVIG-SQYIWGRGTGCS 55
              :*****  *****      . * ***** . * : * : * . . : * : * : * : * : *
              :*****  *****      . * ***** . * : * : * . . : * : * : * : * : *

TLPglyc      FDAAGRGRQCQTADCG-SGLRCRSTDPAAPATKAQVAISEGNYTYGIT-LHKGFNLPMDLT 114
TLXI         FDRAGKGRQCQTGDCGSSLTCCG-NPAVPVTMAEVSVLQGNITYGVSTLKGFNLPMDLK 114
              ** *:***** .*** * * * . :** . * * * : * : * : * : * : * : * : * : * : *

TLPglyc      CSSGDALRCREDGCHDAFFYVKYNDHSCTAAGSRLQIVFCP 155
TLXI         CSSGDALPCRKAGCDVVQPYAK----SCSAAGSRLQIVFCP 151
              ***** ** : * . . * . * ** : *****
    
```

Figure 7-2: Sequence alignment of the mature sequences of TLP_{glyc} and TLXI (clustalW).

The introduced N-glycosylation site is shaded.

The TLP_{glyc} protein was expressed in *P. pastoris* (rTLP_{glyc}) and purified with CEC at pH 4.0. Although the protein was not completely pure, the concentration, as estimated on SDS-PAGE (Figure 7-3), was high enough for inhibition activity measurements with excess of rTLP_{glyc}. The molecular mass on SDS-PAGE was estimated around 25 kDa, whereas it was predicted to be 17.7 kDa based on the primary sequence (ProtParam). The increase in molecular mass is most probably related to the N-glycosylation.

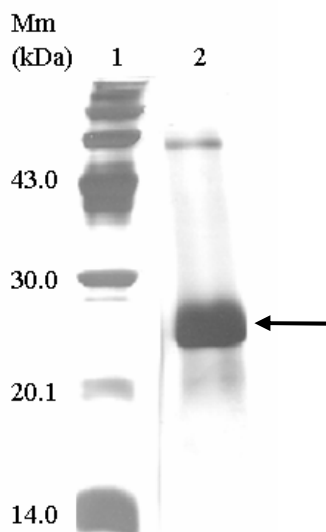


Figure 7-3: SDS-PAGE of purified rTLP_{glyc}.

Lane 1: LMW marker with molecular masses (Mm) indicated on the right; lane 2: Purified TLP_{glyc} (indicated with an arrow).

7.3.2 Biochemical characterization

The inhibition activity of non-diluted purified rTLP_{glyc} was determined against XynI and ExIA. No inhibition activity was detected although the corresponding amount of rTLXI ($\pm 350 \mu\text{g}$) would give maximal inhibition of both enzymes. Since no protein

band could be visualized for rSC-TLXI after expression and purification, inhibition activity was measured directly on medium of a small scale culture and a large scale culture to ensure the absence of an inhibiting protein. Again, no inhibition activity was detected and hence, we can assume that expression failed or resulted in very low expression levels.

To compare the inhibition specificity of rAS-TLXI and rTLXI, the inhibition of different GH10 and GH11 xylanases was evaluated. Of the tested xylanases (section 7.2.2.) only GH11 xylanases from *T. longibrachiatum* (XynI), *A. niger* (ExIA) and *T. viride* were inhibited, whereas the tested GH10 xylanases and GH11 xylanase from *B. subtilis* (XynA) were not. Inhibition of XynI was studied into detail and the dose-response relationship is given in Figure 7-4. The IC_{50} value was calculated to be 10 ± 1 compared to 8 ± 1 for rTLXI.

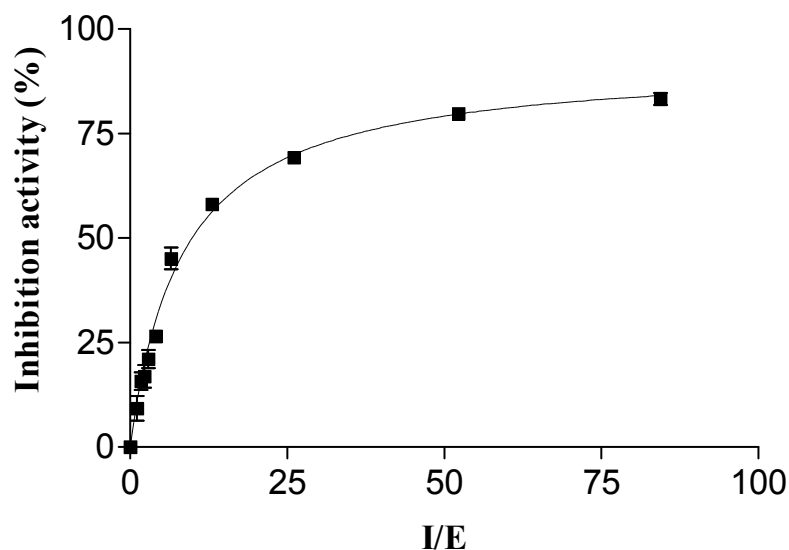


Figure 7-4: Dose-response relationship of rAS-TLXI using XynI (0.011 nmol) as enzyme.

Inhibition activity is plotted as a function of molar I/E ratio. Measurements were performed in triplicate and error bars represent S.D.

The dose-response curve of rAS-TLXI was measured at 40°C and pH 5.0, which were experimentally determined as optimal temperature and pH, respectively, for rAS-TLXI activity. To determine the functional stability of rAS-TLXI, the protein was pre-incubated under different temperature and pH conditions, after which the inhibition activity was measured at the optimal conditions. It appeared that inhibition activity of rAS-TLXI is drastically reduced after a pre-incubation period of 2 hours at pH 12.0.

Only 14% of the activity was recovered after pre-incubation at this pH, while almost full activity was recovered following pre-incubation below pH 12.0. Inhibition activity after pre-incubation under different temperature conditions was decreased over the whole line (Figure 7-5). After incubation at 20°C for 40 min, the residual activity was already reduced to 70% of its initial value. The residual activity drops to zero after pre-incubation at 70°C and higher. Even after 6 min of pre-incubation at 100°C, rAS-TLXI is not able to refold to recover its activity.

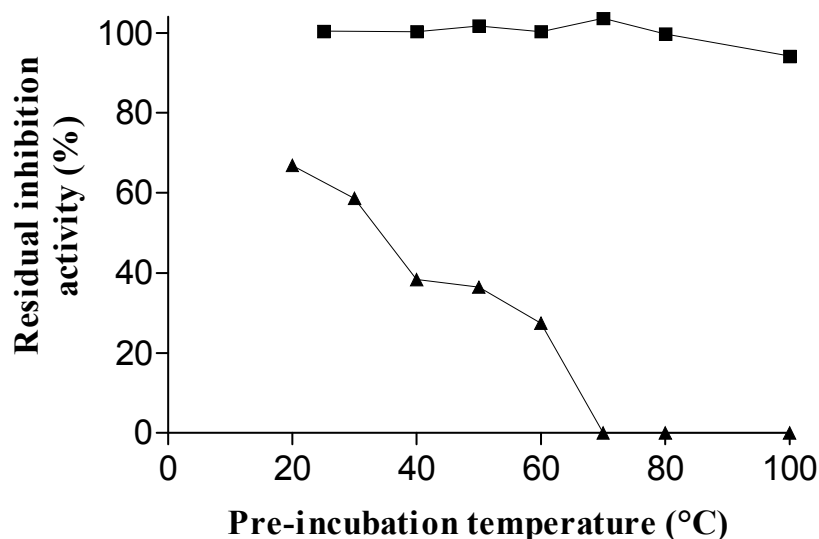


Figure 7-5: Functional stability of rAS-TLXI (▲) compared to rTLXI (■) after pre-incubation at different temperatures.

Residual inhibition activity (%) of rAS-TLXI and rTLXI against XynI after a pre-incubation period of 40 min at different temperatures. Averaged residual inhibition activities for each pre-incubation temperature were expressed relative to a rAS-TLXI or rTLXI sample which was not pre-incubated and stored at 4°C. Measurements were performed in triplicate (S.D. < 10%).

7.4 Discussion

tlxi-like sequences amplified from the diploid wheat species *A. speltoides* (*as-tlxi*), from the hexaploid wheat cv. Chinese spring (*tlp*) and from rye (*sc-tlxi*), were expressed in the yeast *P. pastoris* to gain more insight in the nature of the residues that are important for inhibition activity and/or specificity and possibly in the nature of the residues that are important for other biochemical features. The isolation of the genes encoding AS-TLXI and SC-TLXI was described in chapter 3 and the corresponding proteins each display high sequence identity with TLXI from wheat. The major difference between

TLXI and SC-TLXI is the absence in the latter of a potential N-glycosylation site. The *tlp* sequence was amplified from genomic DNA of wheat cv. Chinese Spring with primers based on EST sequence BQ838841. This EST sequence seemed interesting because of its homology to *tlxi*.

Strikingly, attempts to express *sc-tlxi* in *P. pastoris* failed. Since the amino acid sequences of rTLXI and rSC-TLXI are much alike, we assume that it is the absence of glycosylation that causes the failure to produce the protein in *P. pastoris*. As already mentioned in chapter 5, glycosylation might have an important role in protein folding (Mitra *et al.*, 2006). The N-linked oligosaccharides, already added to the specific consensus sequences when the polypeptide chain enters the lumen of the endoplasmic reticulum (ER) and thus before the protein is folded, may play multiple roles during the conformational maturation of glycoproteins (Hellenius, 1994). They are needed to stabilize folded domains and provide solubility-enhancing polar surface groups that prevent irreversible aggregation of folding intermediates. In addition, they enable newly synthesized glycopolypeptide chains to interact with a set of resident ER enzymes and chaperones that provide assistance to glycoproteins during folding. Mutational elimination of the consensus sequence for N-glycosylation noticeably impaired secretion of a xyloglucan endotransglycosylase from hybrid aspen by *P. pastoris* relative to wild-type enzyme (Kallas *et al.*, 2005). According to the authors this is probably due to incorrect folding or limited solubility of the protein lacking an appendant N-glycan. On the other hand, introduction of an N-glycosylation consensus sequence in a cutinase, increased the secretion by *P. pastoris* (Sagt *et al.*, 2000). A comparison of the hydrophobicity plots (Kyte and Doolittle, 1982) of rTLXI and rSC-TLXI in the vicinity of Asn95 reveals that in both sequences, the region just before this residue is very hydrophobic (residues 81-92, taken into account the window size) (Figure 7-6). Hence, it is possible that the nascent polypeptide chain of rSC-TLXI is prone to aggregation since the hydrophobic residues that might be shielded by the oligosaccharide chain at Asn95 in rTLXI, are exposed. Additionally, in rSC-TLXI Thr75_{TLXI} and Pro83_{TLXI} are replaced by a more hydrophobic Ile and Leu residue, respectively (Figure 3-6), making the region preceding Asn95_{SC-TLXI} even more hydrophobic compared to rTLXI, increasing the probability of aggregation of the polypeptide chain before it is properly folded. The ultimate fate of misfolded, aggregated proteins is degradation in the ER within a few hours after synthesis (Hellenius, 1994). However, it cannot be excluded that other factors can cause the

failure of the expression of *sc-tlxi* in *P. pastoris*, but the presence of rTLXI in the insoluble fraction after expression in *E. coli* (Chapter 4), seems to support this assumption.

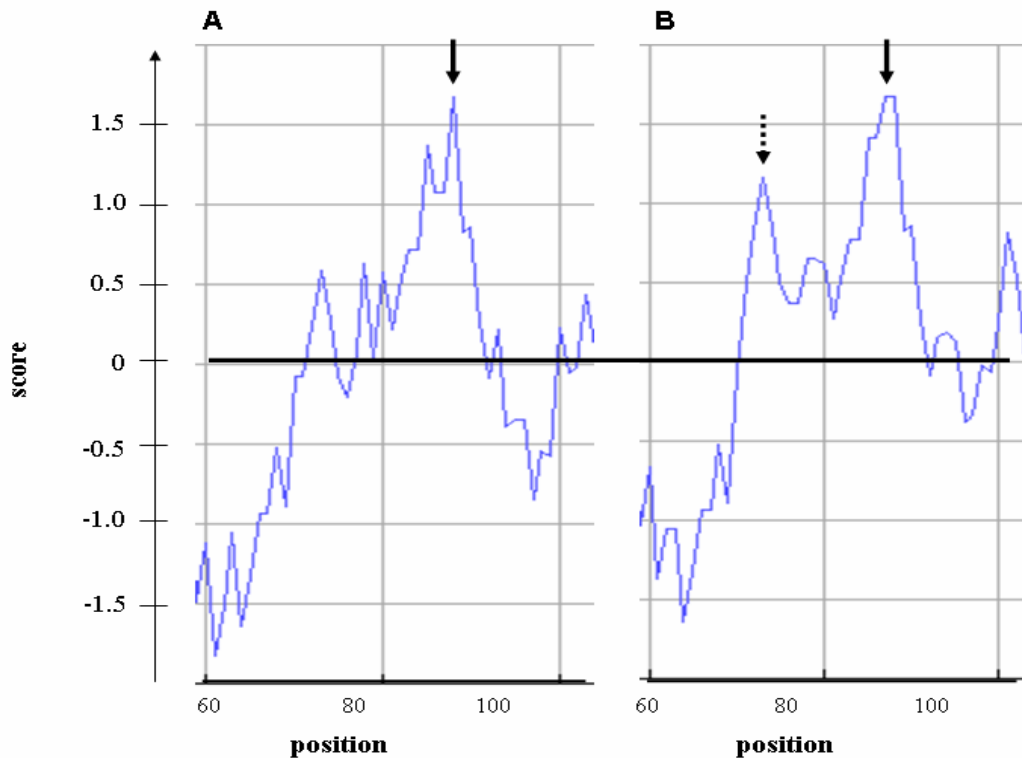


Figure 7-6: Hydrophobicity plot of rTLXI (A) and rSC-TLXI (B) according to Kyte and Doolittle (1982) using Protscale (Gasteiger *et al.*, 2005).

The window size was set at 9. A linear weight variation model was used. Regions with a positive value are hydrophobic. The hydrophobic region surrounding Asn95 is indicated with a solid arrow. The increased hydrophobicity in rSC-TLXI caused by the replacement of Thr75_{TLXI} and Pro83_{TLXI} by Ile and Leu, respectively, is indicated with a dotted arrow.

Because we assumed that the absence of N-glycosylation impaired protein expression of SC-TLXI in *P. pastoris*, we chose to introduce an N-glycosylation consensus sequence in the *tlp* gene (*tlp*_{glyc}) by site-directed mutagenesis as a precautionary measure to avoid failure of expression. Recombinant expression and subsequent purification of rTLP_{glyc} was successful. Inhibition activity measurements demonstrated that rTLP_{glyc} was not active against the tested xylanases. This result was within our expectations because the His22_{TLXI}-containing flexible loop is not present in this protein (Figure 7-2).

The *as-tlxi* gene was also successfully expressed in *P. pastoris* and subsequently purified. The dose-response curve of rAS-TLXI towards XynI shows that the IC₅₀ value

(10 ± 1) is comparable to this from rTLXI (8 ± 1), meaning that none of the amino acids that differ between the two proteins play a crucial role in the inhibition activity. These results confirm the finding that His10_{TLXI} is not the key residue in the inhibition (chapter 6) since this residue is replaced by a Pro in rAS-TLXI (Figure 3-4, numbering of the mature protein). These results are in line with those obtained for the rTLXI_[H10A] mutant (section 6.3.3.). Surprisingly, the functional stability of rAS-TLXI is significantly decreased compared to rTLXI. There is no obvious reason for the significantly decreased thermostability of rAS-TLXI. The N-glycosylation consensus sequence is conserved between both proteins and absence of N-glycosylation can hence not be the cause of the observed decrease in thermostability. The difference in thermostability can also not be explained by a decrease in the number of disulfide bridges since all the cysteine residues are conserved. A close look at the differences in sequence between rTLXI and rAS-TLXI (Figure 3-4), allows us to propose that the substitution of Arg58_{TLXI} and Pro110_{TLXI} by Gly and Ala, respectively, in rAS-TLXI, might contribute to the decreased thermostability of rAS-TLXI. The Gly_{AS-TLXI} residue, located in a β -turn, has more conformational freedom in solution compared to Arg_{TLXI} thereby increasing the entropy of the unfolded form (Matthews *et al.*, 1987). Hence, more free energy is required during the folding process to restrict conformation of glycine. The same is true for the Pro_{TLXI}-Ala_{AS-TLXI} substitution. A Pro residue, especially in a loop region, has been shown to increase thermostability of proteins (Matthews *et al.*, 1987; Watanabe *et al.*, 1996) because few conformations are possible for this residue. As a consequence it is possible that refolding of rAS-TLXI is more difficult due to the higher conformational freedom of Gly58_{AS-TLXI} and Ala110_{AS-TLXI} and the subsequent higher free energy required for refolding.

7.5 Conclusion

The expression of several *tlxi*-like sequences (*as-tlxi*, *sc-tlxi* and *tlp_{glyc}*) in *P. pastoris* was described. Unfortunately, the expression of *sc-tlxi* failed, which can presumably be attributed to the absence of N-glycosylation causing aggregation and subsequent degradation of the protein in the ER of *P. pastoris*. Expression of the TLP_{glyc} protein on the other hand was successful and inhibition activity assays showed that this protein was devoid of inhibition activity suggesting that the His22_{TLXI}-containing flexible loop region is indeed indispensable for its activity. Finally, expression and biochemical

characterization of rAS-TLXI corroborated the finding that His10_{TLXI} is not the crucial residue determining the inhibiting character of TLXI. A surprising feature of the rAS-TLXI protein is its decreased thermostability. Comparison of the TLXI and AS-TLXI sequences reveals that this decrease cannot be attributed to a decrease in the number of disulfide bridges given the conservation of the cysteine residues. Substitution of Arg58_{TLXI} and Pro110_{TLXI} by residues with more conformational freedom (Gly and Ala, respectively) could form the basis for the uncomplete refolding of the protein after pre-incubation at different temperatures.

Chapter 8

Recombinant expression and mutational analysis of *A. niger* xylanase to gain insight in the interaction with TLXI

8.1 Introduction

Whereas in chapter 6 and 7 the inhibitor side of the complex was emphasized, this chapter focuses on the xylanase interaction partner. Mutational analysis of *T. longibrachiatum* xylanase (XynI) would have been most appropriate since this xylanase is best inhibited by rTLXI and changes in IC₅₀ value could hence be measured more accurately. However, attempts to produce this xylanase in *E. coli* (Beliën, 2006) as well as in *P. pastoris* (present study, results not shown) failed up to now. The *A. niger* xylanase encoding gene (*exlA*) was available, but expression in *E. coli* resulted in the formation of inclusion bodies (Beliën, 2006) resulting in low levels of soluble protein. This chapter describes the production of ExlA in *P. pastoris* (rExlA), its subsequent purification and biochemical characterization. Additionally, the produced xylanase was used to optimize a kinetic analysis assay in multiwell plates.

To gain more insight in the mechanism of inhibition by TLXI and to validate the docking model described in chapter 6, a mutant of ExlA was made (D37A) from which it is also known that it abolishes interaction with the other two xylanase inhibitors, TAXI and XIP (Tahir *et al.*, 2004). The docking model of TLXI described in chapter 6 in complex with ExlA suggested an important role of this aspartate residue, also known to influence critically the pH optimum of xylanase activity (Krengel and Dijkstra, 1996), in the interaction. Indeed, xylanases which display a low pH optimum have an aspartate and xylanases with a high pH optimum possess an asparagine at the corresponding position. The fact that TLXI tends to inhibit acidic xylanases (ExlA and XynI) more than basic xylanases (*B. subtilis* XynA and *T. longibrachiatum* XynII), made this residue an interesting candidate for mutagenesis. The ability of this mutant to form a complex with TLXI was investigated by means of GPC. Additionally, kinetic inhibition parameters for rTLXI were assessed using XynI as enzyme.

8.2 Materials and methods

8.2.1 Standard molecular biology techniques

The standard molecular biology techniques described in section 6.2.1. were used.

8.2.2 Molecular biological techniques

The *exlA* coding sequence and the *exlA* coding sequence containing the D37A mutation were cloned in a pCR[®]4-TOPO[®] vector (Invitrogen) as described in section 3.2.6. prior to subcloning in the *Bsm*BI (New England Biolabs) restriction site of a pPICZ α C (Invitrogen) expression vector (section 4.2.3.2.). Expression plasmids were used to transform *P. pastoris* X33 cells (Invitrogen) according to the method discussed in section 4.2.4.2. Recombinant expression was performed using the expression protocol optimized for rTLXI (section 4.3.2.). Purity of the recombinant proteins was verified with SDS-PAGE (section 5.2.2.). The dose-response relationship of rTLXI with rExlA was determined as described in section 5.2.3.3.

8.2.3 Isolation of the *exlA* coding sequence and construction of the expression plasmid

Isolation of the *exlA* coding sequence (Genbank Accession No. X78115) by amplification on genomic DNA of *A. niger*, removal of the intron via ‘splicing by overlap extension’ (SOE) (Horton *et al.*, 1989) and cloning of the resulting gene encoding the mature protein (without signal sequence) in a pCR[®]4-TOPO[®] vector was performed by T. Beliën (2006) and T. Bourgois (personal communication). The resulting sequence differs from the translated GenBank sequence at two amino acid positions (E57D and M167V).

8.2.4 Site-directed mutagenesis

Mutation D37A was introduced using the ‘megaprimer method’ as described in section 6.2.3. (Figure 6-1). An *exlA* gene-containing pCR[®]4-TOPO[®] vector was used as template. In the first PCR reaction D37Af and AnExr02 were used as primers, whereas in the second PCR reaction primer AnExf was used in combination with the ‘megaprimer’, i.e. the product of the first PCR reaction. The annealing temperature in both PCR reactions was 58°C. Sequences of the primers are mentioned in Table 8-1.

8.2.5 Purification with anion exchange chromatography (AEC)

Prior to purification, the culture supernatant containing rExlA or rExlA_[D37A] was dialyzed overnight against 25 mM Tris buffer pH 8.5 with a Spectra/Por[®]4 membrane (MWCO 12000-14000) (Spectrum Laboratories Inc.). Since the pI's of rExlA and rExlA_[D37A] are approximately 4.47 (ProtParam tool) the proteins are negatively charged at this pH allowing AEC purification using a Q-Sepharose Fast Flow column (15 x 160 mm, GE Healthcare) equilibrated with the same buffer. The matrix of the column contains quaternary ammonium groups carrying a positive charge enabling binding of the negatively charged proteins. The proteins were loaded at a flow rate of 2.0 ml/min and after a washing step (200 ml, 2.0 ml/min), the bound proteins were eluted in 2.0 ml fractions using a salt gradient of 0-1.0 M sodium chloride in 210 min (flow rate: 1.0 ml/min unless specified otherwise). The gradient was built up as follows: 0 to 0.15 M NaCl in 0 min; 0.15 to 0.35 M NaCl in 200 min; 0.35 to 1.0 M NaCl in 0 min; 1 M NaCl was kept for 10 min (2.0 ml/min). The purity of the different eluted fractions was verified with SDS-PAGE and the pure fractions were pooled for further experiments.

8.2.6 Protein content determination

Protein concentrations were determined spectrophotometrically at 280 nm using a specific absorbance value of 2.13 AU for 1 mg/ml rExlA and rExlA_[D37A] (1.000 cm UV-cell path length). To calculate the specific absorbance value the formula by Gill and von Hippel (1989) was used (section 4.2.9.), taking into account that part of the multiple cloning site (SMNSRGPAGRLGS) was not cleaved from the protein.

8.2.7 Xylanase activity assay

Xylanase activity measurements were performed using the Xylazyme AX-method (Megazyme). Different dilutions of xylanase were prepared in 1.0 ml sodium acetate buffer (pH 4.0 or pH 5.0) containing 0.5 mg/ml BSA and incubated at 40°C during 10 min. Then a Xylazyme AX tablet (Megazyme) was added and incubation was prolonged for 60 min at 40°C. The reaction was then terminated by the addition of 1% (w/v) Tris solution (10.0 ml) and vigorous vortex-mixing. After 10 min at room temperature the tubes were shaken vigorously and the contents were filtered through a paper filter (VWR International) (diameter 90 mm). The $A_{590\text{nm}}$ values of the filtrates were measured with the Ultrospec II Spectrophotometer (Pharmacia). The amount of

xylanase corresponding to one enzyme unit (U) was determined. One enzyme unit corresponds to an increase in $A_{590\text{nm}}$ of 1.0 with the method described above. The specific activity (U/mg) could hence be calculated.

8.2.7.1 pH optimum determination

The optimal pH for rExIA activity was determined. The procedure was analogous to the xylanase activity assay described above, but instead of sodium acetate buffer (25 mM, pH 5.0), universal buffer (section 5.2.3.2.) was used with a pH ranging from 2.0 to 8.0. 1 U of xylanase, determined at pH 5.0, was dissolved in 1.0 ml of universal buffer.

8.2.8 Kinetic analysis of rExIA

Kinetic parameters were obtained using an adapted form of the dinitrosalicylic (DNS) assay (Bailey *et al.*, 1992). DNS reagent contains 1% DNS, 1.6% sodium hydroxide and 30% sodium potassium tartrate dissolved in water. In first instance birchwood xylan and oat spelt xylan (Sigma-Aldrich) were used as substrate. Since the initial velocities showed great fluctuations, probably due to the poor solubility of the substrates, the soluble fraction of birchwood xylan (prepared by A. Pollet, Laboratory of Food Chemistry and Biochemistry, K.U.Leuven) was used as substrate in further experiments. The reaction was performed in a 96-well plate (Sarstedt, Nümbrecht, Germany). 66.7 μl of different substrate concentrations (0.0 to 25.0 mg/ml in sodium acetate buffer, pH 4.0) were equilibrated at 40°C (10 min) in a thermocycler (Biometra). 13.3 μl of xylanase solution (0.068 nmol/ml in 25 mM sodium acetate, pH 4.0), also equilibrated at 40°C, was then added to the substrate and the reaction was stopped after 10 min by addition of 120 μl DNS solution, boiling for 10 min and centrifugation (2500 xg , 5 min). The $A_{550\text{nm}}$ was measured and, after subtraction of the blank (buffer added to the substrate instead of xylanase solution), related to xylose concentration by measuring the $A_{550\text{nm}}$ of known concentrations of monomeric D-xylose (0.0 to 4.0 mM) (Sigma-Aldrich) after addition of DNS solution, boiling and centrifugation. Hence, the initial velocities could be calculated for each substrate concentration and kinetic parameters could be determined with non-linear regression (Michaelis-Menten equation) using the GraphPad Prism software. The measured velocities are initial velocities since the formation of product still increased linearly with time in this time interval using a substrate concentration of 1 mg/ml (results not shown) indicating that no substrate depletion occurs. The amount of rExIA that was

added, was first optimized. Ultimately, 0.00092 nmol of rExlA was added to each well containing substrate solution.

8.2.9 Gel permeation chromatography (GPC)

To determine whether mutant rExlA_[D37A] is still capable of forming a complex with rTLXI, GPC was performed as mentioned in section 6.2.5., followed by SDS-PAGE analysis of the protein fractions. Purified rExlA_[D37A], rExlA and rTLXI were freeze dried and dissolved in 250 mM sodium acetate buffer (pH 5.0). Following samples were loaded separately on the column, dissolved in 125 μ l of 250 mM sodium acetate buffer (pH5): rExlA (55 μ g), rExlA_[D37A] (94 μ g) and rTLXI (96 μ g). To investigate complex formation, following samples were mixed and incubated for 30 min at room temperature followed by loading on the GPC column (molar ratios are indicated): rTLXI and rExlA (3.7:1); rTLXI and rExlA_[D37A] (3.2:1).

8.2.10 Kinetic analysis of rTLXI

Inhibition kinetic parameters were derived from reaction progress curves with rTLXI and XynI. For this purpose, 4-methylumbelliferyl-beta-D-xylobioside (4-MUX₂) (Figure 8-1), kindly provided by Dr. Wim Nerinckx (Department of Biochemistry, Physiology and Microbiology, UGent), was used as a substrate.

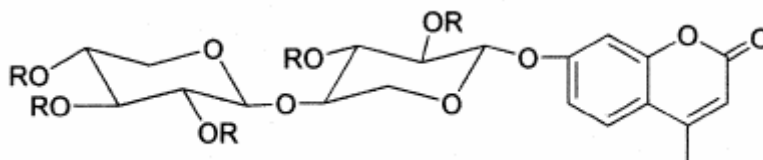


Figure 8-1: Chemical structure of 4-MUX₂ (Kaneko *et al.*, 2000).

R = H

rTLXI (ranging from 100.0 to 200.0 nM) and substrate (22.7 μ M) were mixed and the reaction was started by adding the enzyme (27.1 nM) to a final volume of 150 μ l (in McIlvaine buffer (0.2 M Na₂HPO₄/0.1 M citric acid), pH 5.0). The mixtures were incubated for different periods of time up to 90 min at 40°C. The reaction was stopped by adding 15 μ l of glycine-NaOH buffer (500 mM, pH 13.0) and putting the samples on ice. The hydrolysis products formed were quantified on a fluorimeter (Horiba Jobin Yvon Inc, Edison, Florida, USA) based on a standard curve of 4-methylumbelliferone (0.0-6.0 μ M). Excitation was at 360 nm and the emission was recorded at 446 nm,

during 0.1 s (5 trials, standard error < 1.0%). Both monochromator slit widths were 1 nm. A control was included in which the inhibitor was substituted by McIlvaine buffer (pH 5.0). All measurements were performed in 75 μ l capillaries and were done in triplicate.

8.2.11 Primers used in this chapter

Table 8-1: Primers used in the different sections of this chapter.

primer	sequence	reference (section)
D37Af	GTCAGCTCCGCCTTTGTCGTTG	8.2.4.
AnExr02	CACAGATCTAGAAGAGATCGTGACACTG	8.2.4.
AnExf	CACAGATCTAGTGCCGGTATCAAC	8.2.4.

*Bgl*III restriction sites are indicated in bold. Mutagenic codons are underlined.

8.3 Results

8.3.1 Recombinant expression and purification of rExlA and rExlA_[D37A]

The ExlA encoding gene and the mutant gene (D37A) constructed with the ‘megaprimer’ method were expressed with the *P. pastoris* expression system using the pPICZ α C expression vector. Wild-type rExlA and mutant rExlA_[D37A] were purified from the culture supernatant with AEC at pH 8.5. Pure fractions were pooled and used for subsequent experiments. Expression of both proteins yielded approximately 30 mg per 0.5 liter expression culture.

8.3.2 Xylanase activity assay and pH optimum

To assess xylanase activity, different amounts of xylanase (rExlA/ rExlA_[D37A]) were diluted in 1.0 ml 25 mM sodium acetate buffer (pH 5.0) and the activity was measured as described above. The amount of enzyme needed to obtain an absorbance of 1.0 at 590 nm was calculated using linear regression, resulting in the specific activity (U/mg). Wild-type rExlA specific activity was determined as 10735 U/mg at pH 5.0, whereas the specific activity of the rExlA_[D37A] mutant was decreased to 357 U/mg. Hence, only 3.3% of the activity was retained after mutation of Asp37 to Ala.

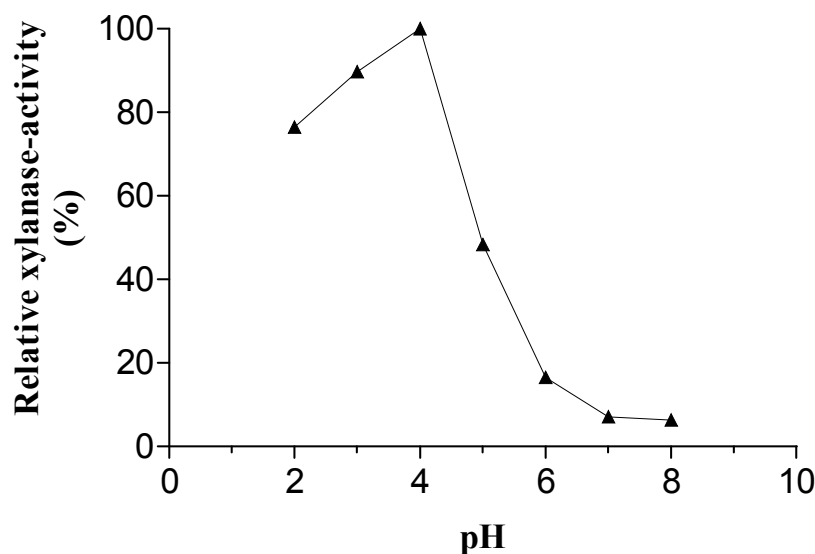


Figure 8-2: pH optimum of rExIA.

Xylanase activities were expressed relative to the highest activity. Measurements were performed in triplicate (S.D.< 10%).

rExIA is most active at pH 2.0 to 4.0, with an optimal activity at pH 4.0 (Figure 8-2). Since the pH optimum of rExIA is pH 4.0, the specific activity was determined at this pH resulting in a specific activity of 26096 U/mg. Hence, rExIA is more than twice as active at pH 4.0 compared to pH 5.0.

8.3.3 Kinetic analysis of rExIA

Kinetic parameters were assessed at the pH optimum of the enzyme (pH 4.0) and with soluble birchwood xylan as substrate. The reaction was performed in a multiwell plate. A monomeric D-xylose standard (0.0 - 4.0 mM) was included in each experiment enabling us to relate absorbance values ($A_{550\text{nm}}$) to amounts of reducing sugars, formed during the enzymatic reaction. Also included in each experiment was a blank in which 13.3 μl of buffer (25 mM sodium acetate, pH 5.0) instead of enzyme was added to 66.7 μl of the various substrate concentrations. The blank was treated analogously to the enzyme samples and was performed because even the presence of non hydrolyzed xylan can lead to low absorbance values at 550 nm after addition of DNS and boiling. For each substrate concentration, the blank $A_{550\text{nm}}$ value was therefore subtracted from the value obtained with the enzyme. The resulting $A_{550\text{nm}}$ values were converted to velocity ($\mu\text{mol xylose}/\text{min}$) by using the following equation:

$$v = \frac{A_{550nm}}{10 \times slope \times 12.5}$$

where 10 is the reaction time (min), slope is the slope of the xylose-standard and 12.5 is a factor to convert mM xylose to μmol xylose. In first instance different amounts of rExIA were tested to determine the optimal enzyme concentration for assessment of the kinetic parameters. 0.00044 nmol, 0.00092 nmol, 0.0014 nmol and 0.0023 nmol rExIA were added to each well and single measurements were performed (Figure 8-3). Data were analyzed with the GraphPad Prism software using the Michaelis-Menten equation:

$$v = \frac{V_{max} [S]}{(K_m + [S])}$$

where V_{max} is the maximal velocity, $[S]$ is substrate concentration and K_m is the Michaelis-Menten constant, i.e. the substrate concentration required to reach half-maximal velocity. The K_m values, determined for the different enzyme concentrations, were comparable ranging from 5.2 mg/ml to 7.3 mg/ml.

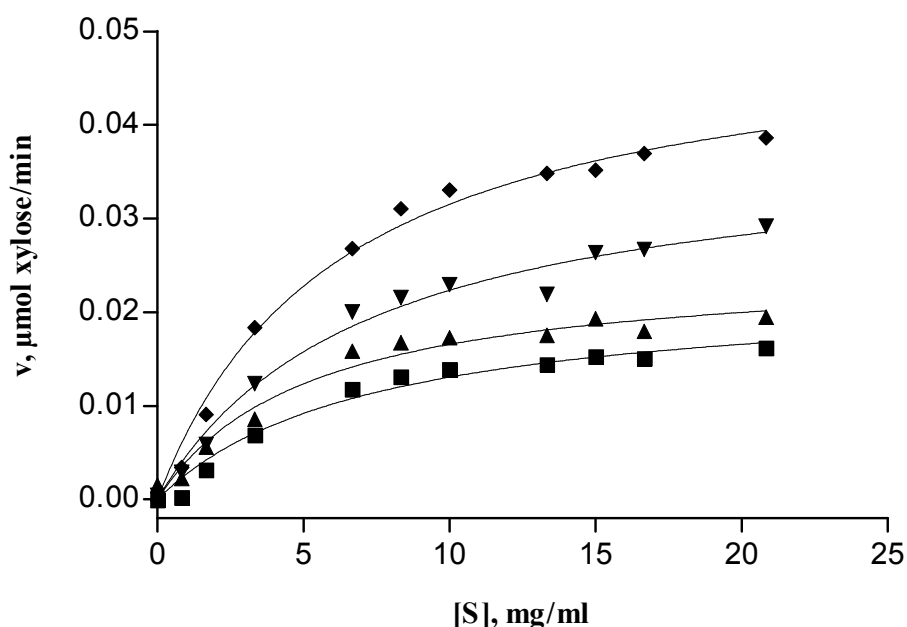


Figure 8-3: Michaelis-Menten kinetics of rExIA using 0.00044 nmol (■), 0.00092 nmol (▲), 0.0014 nmol (▼) and 0.0023 nmol (◆) rExIA.

Initial velocity (μmol xylose/min) was given as a function of the substrate concentration (mg/ml). Data were analyzed with the GraphPad Prism software using the Michaelis-Menten equation.

Based on these results, we chose to perform the kinetic analysis using 0.00092 nmol rExIA, the minimum amount of enzyme giving accurate values differing significantly from the blank. The measurements were performed in triplicate and kinetic parameters (K_m , k_{cat} and k_{cat}/K_m) were determined using the GraphPad Prism software according to the Michaelis-Menten equation (Figure 8-4). The Lineweaver-Burk plot (GraphPad Prism) is given in the inset of Figure 8-4. k_{cat} (s^{-1}) is the catalytic constant and represents the first-order rate constant for the conversion of enzyme-substrate complex in enzyme and product. k_{cat}/K_m ($mg^{-1}.ml.s^{-1}$) is the specificity constant and is a measure of the enzyme's catalytic efficiency.

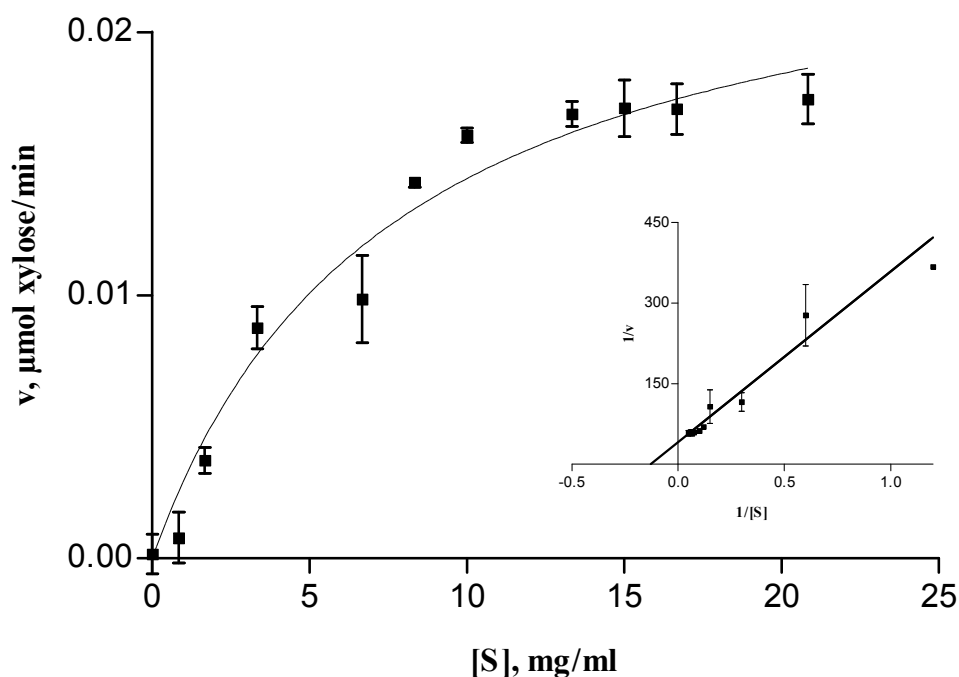


Figure 8-4: Michaelis-Menten kinetics of rExIA using 0.00092 nmol enzyme per reaction.

Measurements were performed in triplicate and error bars represent S.E.M. The inset of the figure shows the Lineweaver-Burk plot.

The kinetic parameters obtained from these results are represented in Table 8-2.

Table 8-2: Kinetic parameters of rEx1A obtained with non-linear regression analysis.

	rEx1A	
	value	S.E.M.
V_{\max} ($\mu\text{mol}\cdot\text{min}^{-1}$)	0.025	0.001
K_m ($\text{mg}\cdot\text{ml}^{-1}$)	7.6	0.9
k_{cat} (s^{-1})	459.3	22.0
k_{cat}/K_m ($\text{mg}^{-1}\cdot\text{ml}\cdot\text{s}^{-1}$)	60.1	4.3

Soluble birchwood xylan was used as substrate and the reactions were performed at pH 4.0 and 40°C.

8.3.4 Xylanase inhibition assay

Inhibition of rEx1A by rTLXI was determined using Xylazyme AX tablets. The dose-response relationship of rTLXI with rEx1A_[D37A] was not determined due to the low activity of this mutant. In each inhibition assay, 1.0 unit of rEx1A (determined at pH 5.0) was used, corresponding to 0.0037 nmol of the enzyme. Molar I/E ratios ranging from 0 to 853 were applied (Figure 8-5). The IC₅₀ value was determined to be 568 ± 23.

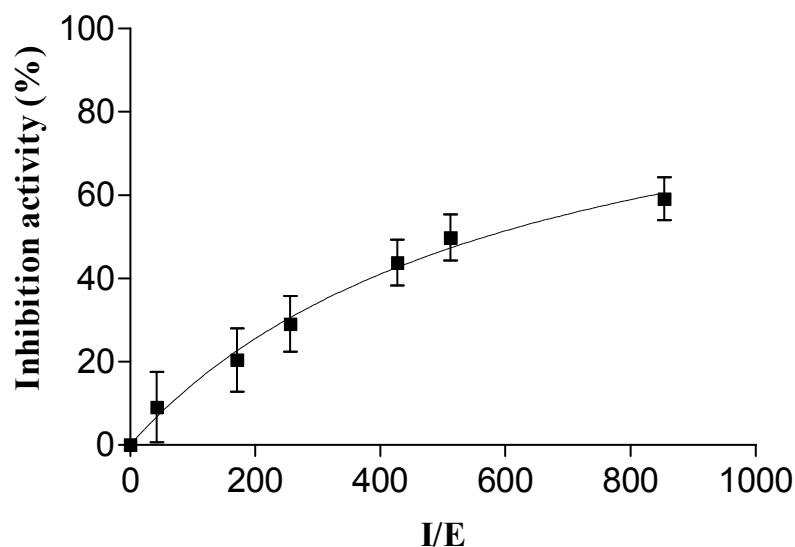


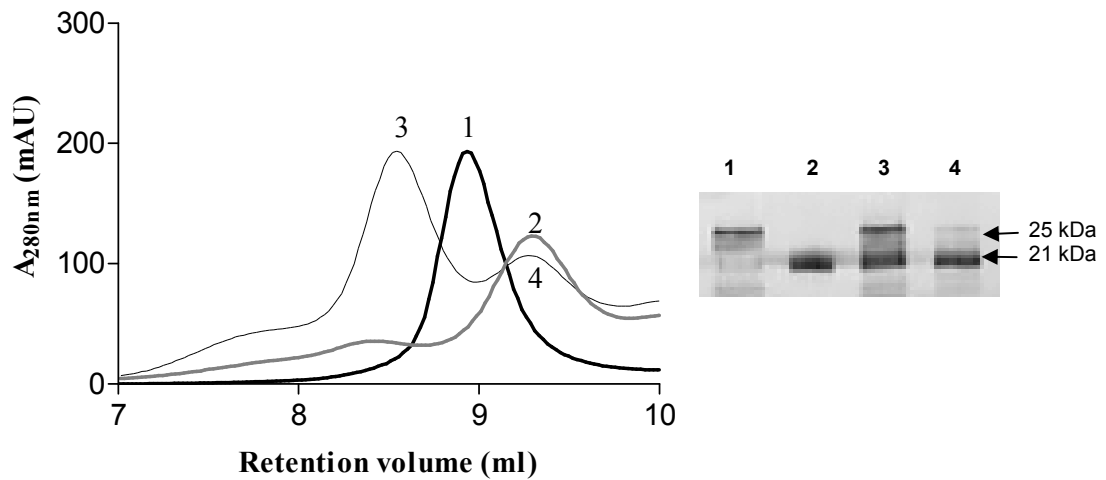
Figure 8-5: Dose-response relationship of rTLXI using rEx1A (0.0037 nmol) as enzyme (pH 5.0, 40°C).

Inhibition activity (%) is plotted as a function of molar I/E ratio. Measurements were performed in triplicate and error bars represent S.D.

8.3.5 Gel permeation chromatography (GPC)

To determine whether mutant rEx1A_[D37A] is still capable of forming a complex with rTLXI, GPC was performed at pH 5.0.

A



B

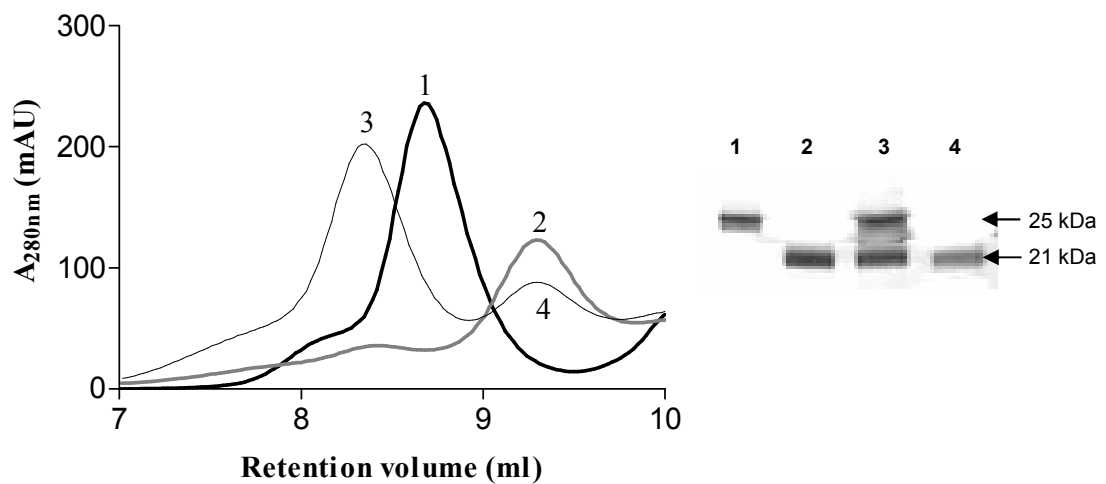


Figure 8-6: GPC of rTLXI, rExIA, rExIA_[D37A], rExIA/rTLXI and rExIA_[D37A] / rTLXI.

A) GPC of rExIA (black thick line), rTLXI (grey thick line) and rExIA/rTLXI (molar ratio: 1/3.7) (thin line) (incubated during 30 min at room temperature). The UV absorbance at 280 nm (mAU) was given as a function of the retention volume (ml). The corresponding SDS-PAGE is shown on the right. Numbers of the loaded fractions correspond to the numbers of the peaks indicated on the graph. The upper band corresponds to rExIA, the lower band corresponds to rTLXI.

B) GPC of rExIA_[D37A] (black thick line), rTLXI (grey thick line) and rExIA_[D37A] / rTLXI (molar ratio: 1/3.2) (thin line) (incubated during 30 min at room temperature) illustrated as above. The upper band corresponds to rExIA_[D37A], the lower band corresponds to rTLXI.

When the rExlA/rTLXI mixture was evaluated with GPC, two peaks eluted (Figure 8-6A). The first peak contains the complex between rExlA and rTLXI according to SDS-PAGE (Figure 8-6A) and corresponds to an apparent molecular mass of 40 kDa. The second peak contains the excess of rTLXI that was added to the reaction mixture. The rExlA_[D37A]/rTLXI mixture was evaluated analogously. Again, two peaks were visible (Figure 8-6B) of which the first one contains the rExlA_[D37A]/rTLXI complex and the second one corresponds to the excess of rTLXI.

8.3.6 Kinetic analysis of rTLXI

Progression curves of rTLXI using 4-MUX₂ as substrate and XynI as enzyme were determined as described above. As shown in Figure 8-7 inhibition by rTLXI shows a clearly time-dependent approach to steady-state whereas the steady-state rate of substrate hydrolysis is reached instantaneously. This inhibition pattern indicates that rTLXI is a slowly binding inhibitor. Additionally, the concentrations of inhibitor which had to be used to obtain significant progress curves (100-200 nM) were of similar order of magnitude as the concentration of enzyme (27.1 nM) indicating that rTLXI is not only a slowly binding but also a tightly binding inhibitor (Morrison and Walsh, 1998). Specifically in the presence of slow-tight binding inhibitors, formation of reaction product, P, as a function of time can be evaluated using the following equation (Cha, 1975) with the GraphPad Prism software:

$$[P] = v_s t + \frac{v_s - v_o}{k} (1 - e^{-kt})$$

where $[P]$ is the product concentration at any time, v_s and v_o are the steady-state and initial velocities, respectively, t is time and k is the apparent first-order rate constant for the interconversion between v_o and v_s . Non-linear regression using this equation (Figure 8-7), results in a value for k , v_s and v_o for each inhibitor concentration.

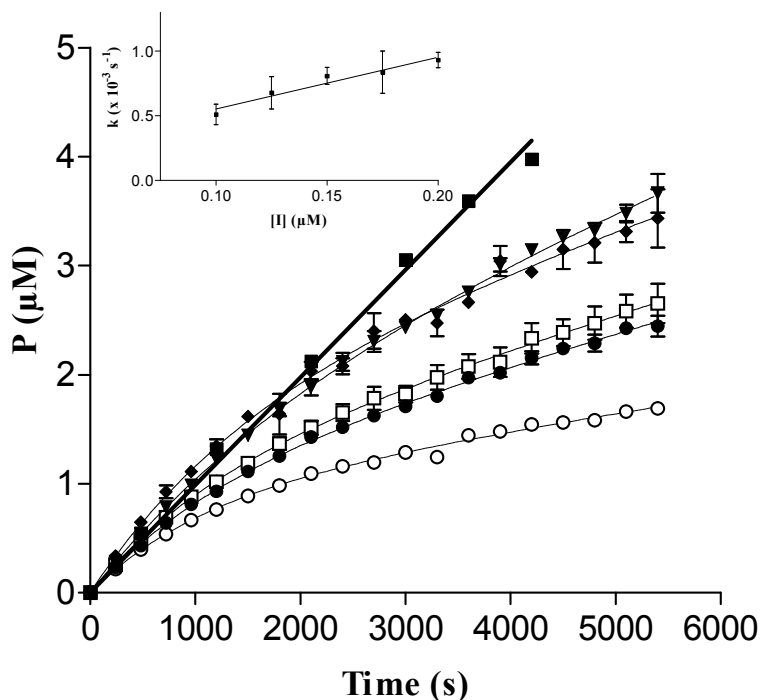


Figure 8-7: Time course of the inhibition of XynI.

For different quantities of rTLXI, progress curves were plotted with XynI xylanase (27.1 nM). 4-MUX₂ (22.7 μM) was used as substrate. The different concentrations were 200.0 nM (○), 175.0 nM (●), 150.0 nM (□), 125.0 nM (◆) and 100.0 nM (▼). The linear relationship between k and $[I]$ is represented in the inset of the graph.

Extensive kinetic analysis of native TLXI at the Laboratory of Food Chemistry and Biochemistry revealed that TLXI is non-competitive inhibitor of XynI. According to Cha (1975) the steady-state velocity of a slow-tight binding inhibitor, following the non-competitive type of inhibition is described by:

$$v_s = \frac{V_{\max} [S]/K_m}{(1+[I]/K_i)(1+[S]/K_m)}$$

where V_{\max} is the maximal velocity of the enzymatic reaction (0.04935 s^{-1}), K_m is the Michaelis-Menten constant of XynI ($577 \pm 102 \text{ μM}$), $[S]$ is the substrate concentration, $[I]$ is the inhibitor concentration and K_i is the inhibition constant. Applied to the results generated for rTLXI, the K_i value determined with this equation is $25.7 \pm 1.6 \text{ nM}$.

When the k value, determined from the progression curves, was plotted against the inhibitor concentration, a linear relationship was observed (inset of Figure 8-7)

described by the following equation (provided that $[S] \ll K_m$, under which these experiments were performed):

$$k = k_{-1} + k_{+1}[I]$$

The slope is the association rate constant for inhibition (k_{+1}) and comes to 0.40 ± 0.06 ($\times 10^4 \text{ M}^{-1} \text{ s}^{-1}$), whereas the intercept is the dissociation rate constant (k_{-1}) for inhibition and comes to 1.54 ± 0.88 ($\times 10^{-4} \text{ s}^{-1}$). The inhibition constant could also be calculated from these two values ($K_i = k_{-1}/k_{+1}$) and comes to $38.7 \pm 16.6 \text{ nM}$, a value comparable to the one obtained by non-linear regression.

8.4 Discussion

The present chapter reports the recombinant expression of the ExlA xylanase encoding gene from *A. niger* using the yeast *P. pastoris* as a host system. The purified xylanase was used to optimize a kinetic analysis assay in multiwell plates. The gene was also used as a template for site-directed mutagenesis.

Expression of *exlA* in *E. coli* has already been reported by Beliën (2006). Since the expression yield in this host system was low and the greater part of the produced xylanase was present in the insoluble fraction of the cytoplasm in the form of inclusion bodies, the use of an alternative host system was required. Berrin *et al.* (2000) already described successful production of *A. niger* xylanase XylA, only differing from the xylanase discussed in this chapter in three amino acids, in *P. pastoris*. The expression yields of purified xylanase (approximately 30 mg/0.5 liter expression culture) were of similar magnitude compared to the yields obtained by Berrin and co-workers (2000) and are much higher than the yields obtained for rTLXI. The produced xylanase, rExlA, is characterized by a low pH optimum (pH 3-4) making it of particular commercial interest. Since this xylanase is used as a supplement in chicken food, a low pH optimum is indeed essential for releasing important nutrients in acidic environments like the chicken stomach. Kregel and Dijkstra (1996) revealed that Asp37 forms the molecular basis for this low pH optimum. The hydrogen bond between Asp37 and the acid-base catalyst, Glu170, is only broken at a low pH due to the protonation of the Asp37 residue. In this way, the proton of Glu170 becomes available for catalysis at low pH.

Purified rExlA was used to optimize a kinetic analysis assay in multiwell plates. The dissociation constant of the *E.S* complex (K_m , Michaelis-Menten constant) using the soluble fraction of birchwood xylan as substrate, was determined as $7.6 \pm 0.9 \text{ mg ml}^{-1}$, a value slightly lower than the one obtained by Berrin *et al.* (2000) ($12.6 \pm 0.4 \text{ mg ml}^{-1}$). However, the specificity constant, k_{cat}/K_m , determined in this study, was approximately 4 times higher, which was mainly accounted for by the higher turnover number of the enzyme (k_{cat}). In this perspective it must be noted that Berrin *et al.* (2000) performed the kinetic study at pH 5.5 and 50°C , non-optimal conditions which lower k_{cat} . They also used xylan from birchwood, although not fractionated, possibly resulting in a different first order rate constant (k_{cat}). It is also interesting to mention that considerable variation of results may occur between -or even within- laboratories using the same enzymes, substrates and methods (Bailey *et al.*, 1992).

As expected, rExlA is inhibited by rTLXI. The IC_{50} value is 568 ± 23 . In this context, it must be remarked that in case of rTLXI, rExlA is not the most suitable target enzyme for mutagenesis and subsequent comparison of IC_{50} values. For this purpose it is better to use enzymes for which the 50% inhibition threshold is located in the linear area of the dose-response curve, which is the case for strongly inhibited xylanases like XynI. Deviations in the measured values, inherent to the assay, have a smaller impact on the IC_{50} value. Unfortunately, attempts to produce XynI in *E. coli* (Beliën, 2006) and *P. pastoris* have not been successful.

Tahir *et al.* (2004) demonstrated the functional importance of Asp37 of ExlA in the binding to two proteinaceous xylanase inhibitors from wheat, TAXI-I and XIP-I. Mutation of this residue to alanine completely abolished the enzyme's capacity to interact with both inhibitors, which was demonstrated by electrophoretic titration and confirmed by surface plasmon resonance. To investigate whether Asp37 plays the same role in the interaction of TLXI with ExlA, the ExlA encoding gene was used as template to mutate Asp37 to alanine. The mutant xylanase was produced in *P. pastoris* yielding approximately the same amount of protein as the wild-type xylanase. The specific activity of rExlA_[D37A] was reduced to 3.3% of the activity of the wild-type xylanase (determined at pH 5.0). Because of the reasons described above, the IC_{50} value is not a reliable parameter to compare inhibition activity of rTLXI towards rExlA and rExlA_[D37A]. For this reason, a biophysical approach, GPC, was used to determine

the complex forming ability of rExlA_[D37A] with rTLXI. Surprisingly, unlike TAXI-I and XIP-I, rTLXI is still able to form a complex with the mutant enzyme. However, the strength of the complex could not be determined using this method. Surface plasmon resonance would be an appropriate, currently used technique to do this. However, because of unclear reasons, attempts to immobilize (r)TLXI to the activated carboxymethylated dextran surface failed (Laboratory for Pharmaceutical Biology, Department of Pharmaceutical Sciences, K.U.Leuven). More specifically, stable binding of sufficient amounts of inhibitor to the surface of the chip could not be achieved. Also electrophoretic titration wasn't successful since rTLXI seems to be rather insensitive to silver staining in its native form.

The results obtained for rExlA_[D37A] indicate that interaction of rExlA with rTLXI does not occur as proposed by the docking model (chapter 6) since in this model the interaction of rTLXI with Asp37_{ExlA} seems even more crucial than in the ExlA-TAXI-I complex. Extensive kinetic analysis of native TLXI at the Laboratory of Food Chemistry and Biochemistry using 4-MUX₂ as substrate revealed that TLXI is a non-competitive inhibitor of xylanases (Fierens *et al.*, 2007). These findings implicate that TLXI interacts with the xylanase outside the active site. However, the precise interaction mechanism is difficult to predict due to the uncertainty in both partners. Moreover, up to now, few crystallographic data have been published about complex structures of enzymes with proteinaceous as well as chemical non-competitive inhibitors (Love *et al.*, 2003; Pallarès *et al.*, 2005; Li *et al.*, 2006). The general concept of a non-competitive inhibitor is that it induces a conformational change in the enzyme via binding to an allosteric site (rather than to the enzyme's active site). The substrate would still be able to bind, but binding of the inhibitor hampers catalysis (V_{\max} decreases) through unfavourable repositioning of the catalytic residues. However, based on crystallographic data of a chemical non-competitive inhibitor in complex with hepatitis RNA-polymerase, Love *et al.* (2003) proposed that a non-competitive inhibitor can also exert its activity by perturbing dynamic properties of a domain or interdomain contacts that are necessary for normal enzymatic function. They also postulate that they can interfere with important protein-substrate interactions.

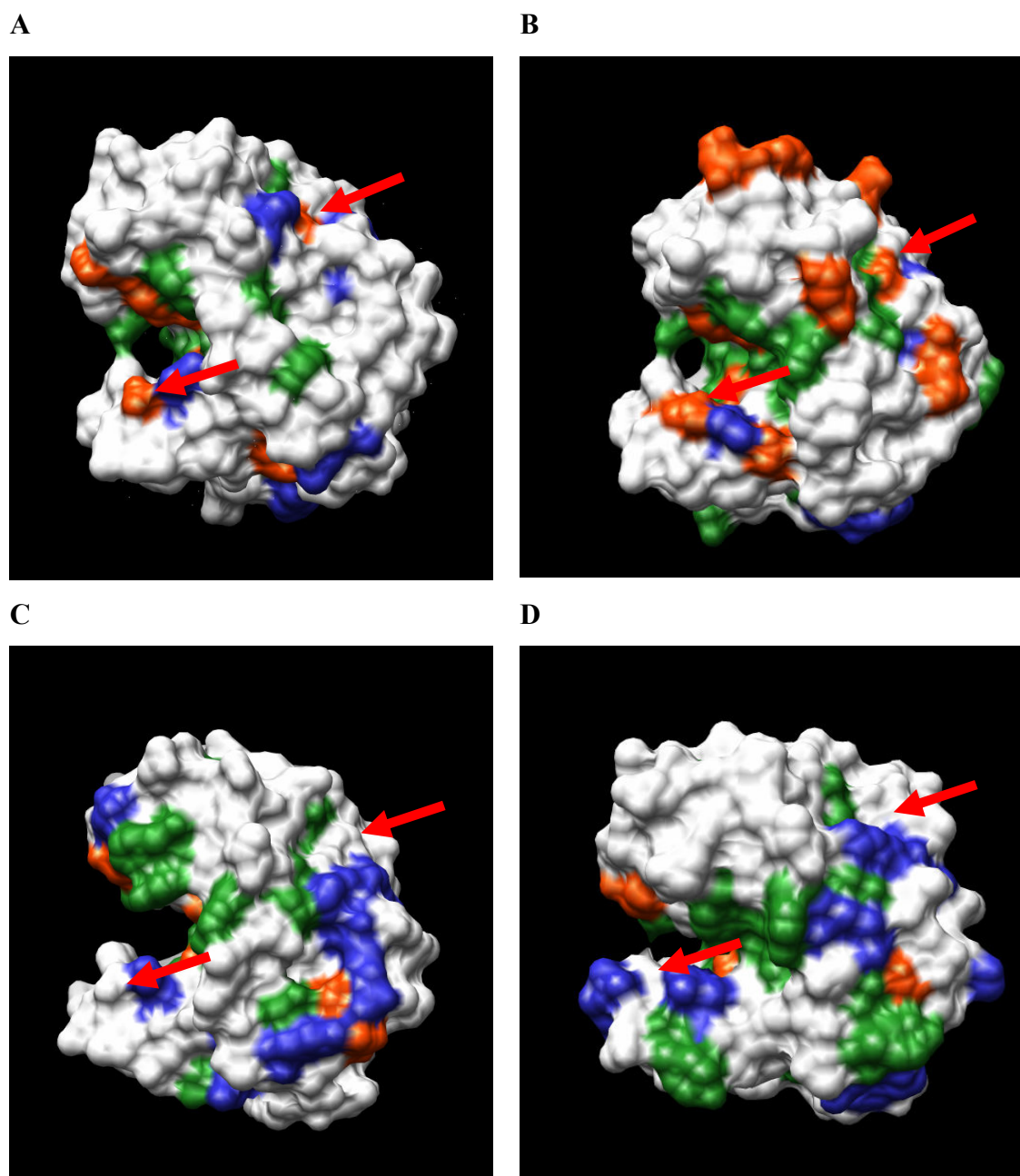


Figure 8-8: Solvent accessible surfaces of GH11 xylanases inhibited (A and B) and uninhibited (C and D) by (r)TLXI.

Negatively charged residues, positively charged residues and aromatic residues are indicated in red, blue and green, respectively. XynI (A) and ExIA (B) are inhibited by (r)TLXI. XynII (C) and XynA (D) are uninhibited by (r)TLXI. The upper arrow on each structure indicates the residues corresponding to Glu118_{ExIA} whereas the lower arrow indicates the residues corresponding to Asp85_{ExIA}. Pictures were made with Chimera (Pettersen *et al.*, 2004) (<http://www.cgl.ucsf.edu/chimera>).

To be able to formulate a hypothesis about the xylanase residues involved in the interaction with TLXI a closer look was taken at the surface charges of two inhibited (XynI and ExIA) and two uninhibited (XynII and XynA) xylanases (Figure 8-8). The

fact that inhibition activity is pH dependent (Figure 5-1B) demonstrates indeed the involvement of electrostatic charges in the interaction. This is in line with the fact that His22, essential for inhibition and complex formation, carries a positive charge. Hence we focused our attention to negatively charged amino acids at the surface of ExlA, located outside the active site and that are neutral or positively charged in the uninhibited xylanases. Two such residues were found: Glu118_{ExlA} (Glu112_{XynI}) and Asp85_{ExlA} (Asp81_{XynI}) (Figure 8-8) which correspond to Ala and Ser in XynA and Gln and Asn in XynII, respectively.

Glu118_{ExlA} is located at the ‘thumb’ of the xylanase. During the catalytic cycle the ‘thumb’ moves significantly. The distance between Tyr10_{ExlA} (‘fingers’) and Pro119_{ExlA} (‘thumb’) shortens when substrate is bound (Havukainen *et al.*, 1996; Muilu *et al.*, 1998). The active site is therefore partly closed. When the reaction proceeds, the ‘thumb’ opens again and allows the reaction product to diffuse away. Binding of TLXI to the ‘thumb’ might hence perturb the dynamic properties of the ‘thumb’ thereby influencing the catalytic mechanism. Alternatively, interaction with the ‘thumb’ region might also sterically block the entrance of substrate without directly interfering with the substrate binding sites. Increasing the substrate concentration wouldn’t decrease inhibition since substrate and inhibitor don’t compete for the same binding sites, which results in a non-competitive inhibition profile. In contrast, Asp85_{ExlA} is located on the ‘finger’ of the xylanase in proximity of the hinge region between ‘palm’ and ‘fingers’ (Muilu *et al.*, 1998). Interaction of TLXI with the ‘fingers’ or the hinge region might perturb flexibility of the ‘fingers’ influencing catalytic activity. However, the movement of the ‘fingers’ during the catalytic cycle is not as pronounced as the movement of the ‘thumb’ (Havukainen *et al.*, 1996). Evidently, it cannot be excluded that TLXI causes a conformational change to occur in the xylanase by interacting with one of these residues. This would also result in a decreased catalytic activity.

TLXI is the first non-competitive inhibitor among the xylanase inhibitors. Slow-tight binding of xylanases, however, has already been reported for the proteinaceous bifunctional aspartic protease inhibitor from an extremophilic *Bacillus* species (Dash *et al.*, 2002). Whereas this inhibitor follows a two-step reaction mechanism, slow binding of TLXI to xylanases occurs through a single-step reaction mechanism, which could be derived from the linear relationship between the apparent first-order rate constant and

the concentration of inhibitor (inset of Figure 8-7). In contrast, a hyperbolic relationship would occur for a two-step mechanism with a rapidly formed initial collision complex, which isomerizes slowly to form the final tight complex (Morrison and Walsh, 1998). Kinetic parameters were assessed taking into account the slow-tight binding non-competitive interaction mechanism. The K_i for rTLXI comes to 25.7 ± 1.6 nM as determined by non-linear regression. The reason why native TLXI is characterized by a higher K_i value (57.2 ± 5.2 nM) remains unclear. The lower K_i value of rTLXI suggests a tighter interaction of rTLXI with xylanases, although the IC_{50} value determined previously for XynI (Table 5-3) suggests the opposite. This indicates that the overestimation of the IC_{50} value made by measurements with the Xylazyme AX-method and probably caused by stronger interaction with the substrate (chapter 5), is bigger for rTLXI than for TLXI.

8.5 Conclusions

This chapter provides a first insight in the xylanase side of the TLXI-xylanase interaction. Asp37_{ExIA} was mutated to Ala because this residue seemed to play, according to the proposed docking model (chapter 6), an important role in the interaction with TLXI. Additionally, the D37A mutation was already shown to abolish interaction with TAXI-I and XIP-I (Tahir *et al.*, 2004). Surprisingly, this mutation didn't affect the complex forming ability of the xylanase with rTLXI although no information could be generated about the strength of the complex. Concurrently, the non-competitive interaction mechanism of native TLXI with xylanases was demonstrated indicating that TLXI interacts, unlike TAXI and XIP, outside the active site of the xylanase. A hypothesis was made about the possible interaction mechanism taking into account that His22_{TLXI} is the main inhibition determinant. However, only crystallographic analysis of the ExIA-TLXI or XynI-TLXI complex would enable to clarify the precise mechanism of the interaction.

General conclusions and future prospects

This dissertation describes the molecular identification and characterization of a recently identified xylanase inhibitor, TLXI. The TLXI encoding sequence is 534 bp long and encodes a mature protein of 151 amino acids preceded by a signal peptide for secretion of 26 amino acids. Analysis of the promoter region revealed the presence of certain motifs suggesting a role in the plant defense mechanism. The calculated molecular mass and pI are 15.6 kDa and 8.38, respectively, and the protein contains a potential N-glycosylation site at Asn95. A database search (InterPro) for the presence of catalogued motifs or patterns in the identified TLXI sequence revealed that the protein belongs to the thaumatin family of proteins, conferring the inhibitor its name, thaumatin-like xylanase inhibitor (TLXI). As a member of this group of proteins, which are classified to group 5 of the pathogenesis-related proteins, its involvement in plant defense is further supported.

A straightforward expression system using *P. pastoris* as a host and a subsequent purification protocol were developed and functional analysis confirmed that the isolated gene was indeed a xylanase inhibitor encoding gene. The recombinant inhibitor (rTLXI) was biochemically characterized and the characteristics were compared to those of the native inhibitor. A striking difference between native TLXI and rTLXI was found in the molecular masses, being 18 kDa and 21 kDa, respectively. This difference could mainly be accounted for by a difference in glycosylation extent. Interaction of rTLXI with the substrate of the reaction causes the IC₅₀ values to be overestimated. Therefore, inhibition assays using arabinoxylan as substrate were only applicable to screen inhibition specificity or to compare mutants to the wild-type inhibitor. rTLXI inhibited only GH11 xylanases and showed a preference for GH11 xylanases displaying a low pH optimum.

Since crystallographic analysis of (r)TLXI and of (r)TLXI in complex with a xylanase remained unsuccessful so far, insight in the interaction mechanism was achieved through a combined molecular modeling and mutagenic approach. A molecular model of TLXI was generated and revealed that TLXI has the general fold of low molecular mass thaumatin-like proteins (TLPs). Two residues, His10 and His22, were selected for

mutagenesis based on a structure and sequence comparison with TLPs and with TAXI, respectively. Mutation of His22_{TLXI}, located on a flexible loop which extends further compared to the loop of other TLPs, completely abolished inhibition activity as well as complex forming ability of rTLXI. In addition, heterologous expression of a sequence displaying 64% sequence identity to TLXI and lacking the flexible His22-containing loop resulted in a protein without inhibition activity corroborating the results obtained with the mutagenesis study. The finding that His10_{TLXI} is not essential for inhibition activity was confirmed by the expression and characterization of rAS-TLXI, a TLXI variant encoded by the S-genome of a diploid wheat species and containing a Pro at the position corresponding to His10_{TLXI}. A docking model of the TLXI-xylanase complex was generated based on the knowledge that His22_{TLXI} is indispensable for inhibition activity and based on the assumption that TLXI is, like TAXI and XIP, a competitive inhibitor. According to this model, His22_{TLXI} hydrogen bonds with Asp37 and with the nucleophile, Glu79, of the xylanase (ExIA). Surprisingly, mutation of Asp37_{ExIA} to Ala didn't abolish complex formation with TLXI and hence questioned the docking model. At the same time it was demonstrated that TLXI is not only a slow-tight inhibitor, but also a non-competitive inhibitor of xylanases. This interaction mechanism suggests that TLXI interacts, unlike TAXI and XIP, outside the active site of the xylanase. Due to the limited capabilities of modeling as it comes to non-competitive inhibitors, a new docking model could not be generated. However, based on our findings and a comparative sequence analysis of inhibited versus uninhibited xylanases, we were able to put forward two candidate interaction sites. We suggest that TLXI could exert its inhibition activity not only by inducing a conformational change of the xylanase, like is common for non-competitive inhibitors, but also by restricting flexibility of the 'thumb' or 'finger' regions of the xylanase or by sterically impeding substrate entrance into the active site of the enzyme (without affecting substrate binding as such). Site-directed mutagenesis of the suggested interaction sites of the xylanase, could be used to validate the proposed interaction mechanism.

Evidently, additional experiments, such as crystallographic analysis of the TLXI-xylanase complex, should be able to give a decisive answer on the precise interaction mechanism and should confirm the non-competitive interaction mechanism. At present, crystals are available yet of rTLXI mutant H22A and should provide a first step towards the elucidation of the interaction.

Considering the fact that TLXI is a completely new and recently identified xylanase inhibitor, displaying no affinity with the previously characterized xylanase inhibitors, much of its biochemical characteristics have now been elucidated. However, many questions concerning its interaction with polysaccharides and its precise role in the plant defense system, remain to be solved and are still a challenge for the future.

Summary

Endo- β -1,4-xylanases (xylanases, EC 3.2.1.8.) are key enzymes in the degradation of heteroxylan, the predominant hemicellulose in the cell walls of plants. Microbial xylanolytic enzymes have attracted a great deal of attention during the last decade because of their biotechnological potential in many industrial processes. Indeed, due to their hydrolytic activity on heteroxylan, they have a profound impact on the functionality of these polysaccharides in several cereal-based industrial processes. Furthermore, being capable to degrade the plant cell wall, xylanases, especially from fungal origin, have a potential role in phytopathogenesis. They also have potential in the production of prebiotic xylooligosaccharides. The presence in cereals of proteins capable of inhibiting xylanases was first demonstrated by the Laboratory of Food Chemistry and Biochemistry of the K.U.Leuven in 1997 (Debyser *et al.*, 1997). Later on, a first type of proteinaceous xylanase inhibitors could be purified from wheat (*Triticum aestivum*) and they were therefore named TAXIs (*T. aestivum* xylanase inhibitor). In 1999, a second class of wheat proteins with xylanase inhibiting activity was identified and named XIPs (xylanase inhibitor protein). At the beginning of this study, a novel type of xylanase inhibitor was purified from wheat. Based on its sequence homology with thaumatin-like proteins (TLPs), proteins classified into group 5 of the pathogenesis-related proteins, this new inhibitor was named TLXI, thaumatin-like xylanase inhibitor. Since no other TLPs are reported to be endowed with xylanase inhibiting activity, TLXI represents a novel protein function within this group of proteins. The molecular identification, recombinant expression, subsequent biochemical characterization, and mutagenesis, form the subject of this dissertation, which is divided in two parts. A first part is an **introduction** providing a background that enables one to understand the framework of this study. A second part outlines the **experimental work** obtained during this research.

Chapter one sketches the context of this study by discussing the three important players: the substrates (xylans), the enzymes (xylanases) and the inhibitors. Since heteroxylans are a heterogeneous group of polysaccharides, their complete degradation requires the action of several enzymes. The xylanases are discussed in more detail. More specifically, their classification system is highlighted and special emphasis is put

on the GH10 and GH11 xylanases. Furthermore, an overview of some industrial applications of microbial xylanases is presented. Since TLXI is a new member of the group of xylanase inhibiting proteins, the current state of the art on the two previously described xylanase inhibitors (TAXI and XIP) is provided.

Whereas TLXI is functionally related to xylanase inhibitors, its sequence is homologous to those of the TLPs, discussed in **chapter two**. This group of proteins all share sequence identity to the sweet tasting protein, thaumatin. The biochemical characteristics, structure and industrial applications of thaumatin are discussed. Further, the activities that have been ascribed to the TLPs are described and explained.

At the beginning of this study, only the first thirty amino acids of TLXI were known. Knowledge of the complete amino acid sequence however is a prerequisite to gain insight in the inhibition determinants of this inhibitor. A molecular biological approach is to pre-eminently identify the nucleotide sequence and subsequently the amino acid sequence of TLXI. Hence, the molecular identification of the TLXI encoding gene in hexaploid wheat forms the subject of **chapter three**. For the first time, the complete amino acid sequence of TLXI was described. The DNA, mRNA and amino acid sequences were deposited in the NCBI database (Accession numbers AJ786602, AJ786601 and CAH10283, respectively). Additionally, analysis of the promoter region of the *tlxi* gene allowed us to make suggestions about the biological function of this inhibitor. Furthermore, *tlxi*-like sequences could be identified in diploid wheat species and in rye.

In order to be able to perform a mutational analysis of TLXI, a recombinant expression system needed to be established first. The optimization of expression in *Pichia pastoris*, by varying different parameters, is outlined in **chapter four**. The optimal expression conditions determined in this chapter were used throughout further experiments to produce TLXI. The biochemical characterization of the recombinantly expressed and purified protein is described in **chapter five** and enabled us to compare recombinant TLXI (rTLXI) with native TLXI.

Because of the novelty of the protein and because of the lack of structural information, the inhibition mechanism of TLXI remained unclear. Difficulties to crystallize TLXI and its complex with a xylanase forced us to follow an alternative approach to gain insight in the inhibition mechanism. **Chapter six** thus describes how, based on a molecular model and based on a comparative analysis of TLXI, TAXI and other TLPs, residues were selected for mutation. Recombinant expression and subsequent inhibition

assays resulted in the identification of His22 as the main inhibition determinant. Based on this finding a docking model of the xylanase-TLXI complex was created under the assumption that TLXI is, like TAXI and XIP, a competitive inhibitor. Another, complementary, approach to identify TLXI residues involved in inhibition activity and specificity is the expression and characterization of related sequences, described in **chapter seven**. The results confirmed the results obtained in the mutagenesis study. Finally, in **chapter eight**, we took a closer look at the xylanase side of the interaction and validated the proposed docking model described in chapter six. First, the *A. niger* xylanase encoding gene (*exlA*) was expressed in *P. pastoris* and the purified protein was used to optimize a kinetic assay in multiwell plates. Mutation of a residue strongly suggested to participate in the interaction with TLXI revealed that the proposed docking model was not correct. Furthermore, TLXI was shown to be a non-competitive inhibitor according to kinetic studies performed at the Laboratory of Food Chemistry and Biochemistry. Due to the limited capabilities of docking as it comes to non-competitive inhibitors, a new model could not be proposed. However, new hypotheses are put forward to explain the inhibition capacity of TLXI.

Samenvatting

Endo- β -1,4-xylanasen (xylanasen, EC 3.2.1.8.) zijn sleutelenzymen in de degradatie van heteroxylan, het belangrijkste hemicellulose in de celwand van planten. Microbiële xylanolytische enzymen hebben gedurende de laatste tien jaar de aandacht getrokken omwille van hun biotechnologisch potentieel in vele industriële processen. Omwille van hun hydrolytische activiteit op heteroxylan hebben ze immers een grote impact op de functionaliteit van deze polysachariden in verschillende graanverwerkende industriële processen. Omdat ze bovendien in staat zijn om de plantencelwand te degraderen, hebben xylanasen, vooral van fungale oorsprong, een mogelijke rol in de fytopathogenese. Ze hebben daarenboven ook potentieel in de productie van xylooligosachariden. De aanwezigheid in graangewassen van proteïnen met xylanase inhiberende capaciteit werd voor het eerst vastgesteld door het Laboratorium voor Levensmiddelenchemie van de K.U.Leuven in 1997 (Debyser *et al.*, 1997). Wat later slaagde men erin om een eerste type xylanase inhibitoren op te zuiveren uit tarwe (*Triticum aestivum*). Deze werden, verwijzend naar hun oorsprong, TAXI's genoemd. In 1999 werd een tweede klasse xylanase inhiberende eiwitten geïdentificeerd die XIPs werden genoemd. Bij de start van deze studie werd een nieuw type xylanase inhibitor opgezuiverd uit tarwe. Op basis van zijn sequentiehomologie met thaumatine-achtige eiwitten (TLPs), eiwitten die ingedeeld worden bij groep 5 van de pathogenesis-gerelateerde eiwitten, werd deze nieuwe inhibitor TLXI, *thaumatin-like xylanase inhibitor*, genoemd. Omdat er tot nu toe geen andere TLPs gekend zijn die xylanase inhiberende activiteit bezitten, vertegenwoordigt TLXI een nieuwe functie binnen deze groep van proteïnen. De moleculaire identificatie, recombinante expressie en daaropvolgende biochemische karakterisering en mutagenese van TLXI vormen het onderwerp van deze thesis die opgedeeld is in twee delen. De **introdunctie** vormt het eerste deel en verschaft een achtergrond die iemand in staat stelt om het kader van deze studie te begrijpen. In een tweede deel worden de **resultaten** van dit werk uiteengezet.

Hoofdstuk één schetst de context van dit werk door de drie belangrijke spelers voor te stellen: de substraten (xylanen), de enzymen (xylanasen) en de inhibitoren. Aangezien heteroxylanen een heterogene groep polysachariden vormen, vereist hun volledige afbraak de inwerking van verschillende enzymen, waarvan de xylanasen in detail

worden besproken. Hun classificatiesysteem wordt toegelicht en de klemtoon wordt gelegd op xylanasen van familie 10 en 11. Bovendien wordt een overzicht gegeven van de belangrijkste industriële toepassingen van xylanasen van microbiële oorsprong. Omdat TLXI een nieuw lid is van de groep van de xylanase inhibitoren wordt de huidige stand van zaken omtrent de reeds beschreven xylanase inhibitoren (TAXI en XIP) gegeven.

Waar TLXI aan de ene kant functioneel verwant is met de xylanase inhibitoren, is hij op sequentieniveau verwant met de TLPs die worden besproken in **hoofdstuk twee**. De gemeenschappelijke factor binnen deze groep eiwitten is dat ze allen sequentiesimilariteit vertonen met het zoetsmakende eiwit thaumatine. De biochemische eigenschappen, structuur en industriële toepassingen van thaumatine worden besproken. Verder worden de activiteiten die worden toegekend aan TLPs beschreven en verklaard.

Bij de aanvang van dit onderzoek waren enkel de dertig eerste aminozuren van TLXI gekend. Kennis van de volledige aminozuursequentie is echter de eerste vereiste om inzicht te krijgen in de inhibitiedeterminanten van een eiwit. Een moleculair biologische benadering is de benadering bij uitstek om de nucleotidesequentie en bijgevolg de aminozuursequentie te achterhalen van TLXI. De moleculaire identificatie van het TLXI coderende gen in hexaploide tarwe vormt dan ook het onderwerp van **hoofdstuk drie**. De volledige aminozuursequentie van TLXI werd voor de eerste keer beschreven. De DNA, mRNA en aminozuursequenties kunnen worden teruggevonden in de NCBI databank onder *Accession numbers* AJ786602, AJ786601 en CAH10283, respectievelijk. Verder liet een analyse van de promoterregio ons toe om suggesties te formuleren omtrent de biologische functie van deze inhibitor. Bovendien konden er ook *tlxi*-achtige sequenties geïdentificeerd worden in diploide tarwesoorten en in rogge.

Om een mutationale analyse uit te kunnen voeren op TLXI, moest er eerst een expressiesysteem ontwikkeld worden. De optimalisatie van de expressie in *Pichia pastoris* door verschillende parameters te variëren, wordt uiteengezet in **hoofdstuk vier**. De optimale expressiecondities die hier werden bepaald, werden in volgende experimenten gebruikt voor de productie van TLXI. De biochemische karakterisering van het recombinant aangemaakte en opgezuiverde eiwit wordt beschreven in **hoofdstuk vijf**. Deze karakterisering bevestigde dat inderdaad een xylanase inhibitor geïsoleerd werd en stelde ons in staat om de eigenschappen van recombinant TLXI (rTLXI) te vergelijken met deze van natief TLXI.

Door de nieuwheid van het eiwit en door het gebrek aan structurele informatie, bleef het inhibitiemechanisme van TLXI onduidelijk. Moeilijkheden om TLXI en zijn complex met een xylanase te kristalliseren dwongen ons om een alternatieve route te volgen om inzicht te verwerven in het inhibitiemechanisme. **Hoofdstuk zes** beschrijft hoe, gebaseerd op een moleculair model en op een vergelijkende analyse van TLXI, TAXI en TLPs, residu's werden geselecteerd voor mutagenese. Recombinante expressie van de mutanten en daaropvolgende inhibitietesten worden beschreven en resulteerden in de identificatie van His22 als de belangrijkste inhibitiedeterminant. Gebaseerd op deze bevindingen werd een docking model gecreëerd van het xylanase-TLXI complex in de veronderstelling dat TLXI, zoals TAXI en XIP, een competitieve inhibitor is. Een andere, complementaire, benadering om residu's te identificeren die betrokken zijn in de inhibitieactiviteit en -specificiteit is de expressie en karakterisering van gerelateerde sequenties, beschreven in **hoofdstuk zeven**. De resultaten bevestigden de resultaten verkregen door de mutagenese studie. Tenslotte bekijken we in **hoofdstuk acht** de xylanase kant van de interactie om het docking model, voorgesteld in hoofdstuk zes, te valideren. Vooreerst werd het gen coderend voor *A. niger* xylanase (*exlA*) tot expressie gebracht in *P. pastoris* en werd het opgezuiverde eiwit gebruikt om een kinetische test te optimaliseren in multiwell platen. Mutatie van een aminozuur dat werd gesuggereerd deel te nemen aan de interactie met TLXI toonde aan dat het voorgestelde docking model niet correct is. Bovendien werd door kinetische studies op het Laboratorium voor Levensmiddelenchemie aangetoond dat TLXI aan niet-competitieve inhibitor is. Door de beperkte capaciteit van docking programma's wat betreft niet-competitieve inhibitoren, kon er geen nieuw model worden voorgesteld. Er worden wel nieuwe hypothesen geformuleerd om de inhiberende capaciteit van TLXI te verklaren.

References

- Abad, L.R., D'Urzo, M.P., Liu, D., Narasimhan, M.L., Reuveni, M., Zhu, J.K., Niu, X., Singh, N.K., Hasegawa, P.M. and Bressan, R.A. (1996). Antifungal activity of tobacco osmotin has specificity and involves plasma membrane permeabilization. *Plant Sci.* 118, 11-23.
- Altschul, S.F., Madden, T.L., Schaffer, A.A., Zhang, J., Zhang, Z., Miller and Lipman, D.J. (1997). Gapped BLAST and PSI-BLAST: a new generation of protein database search programs. *Nucleic Acids Res.* 25, 3389-3402.
- Anand, A., Zhou, T., Trick, H.N., Gill, B.S., Bockus, W.W. and Muthukrishnan, S. (2003). Greenhouse and field testing of transgenic wheat plants stably expressing genes for thaumatin-like protein, chitinase and glucanase against *Fusarium graminearum*. *J. Exp. Bot.* 54, 1101-1111.
- Anzlovar, S., Dalla Serra, M., Dermastia, M. And Menestrina, G. (1998). Membrane permeabilizing activity of pathogenesis-related protein linusitin from flax seed. *Mol. Plant-Microb. Interact.* 11, 610-617.
- Bailey, M.J., Biely, P. and Poutanen, K. (1992). Interlaboratory testing of methods for assay of xylanase activity. *J. Biotechnol.* 23, 257-270.
- Baneyx, F. (1999). Recombinant expression in *E. coli*. *Curr. Opin. Biotechnol.* 10, 411-421.
- Barre, A., Peumans, W.J., Menu-Bouaouiche, L., Van Damme, E.J.M., May, G.D., Fernandez Herrera, A., Van Leuven, F. and Rougé, P. (2000). Purification and structural analysis of an abundant thaumatin-like protein from ripe banana fruit. *Planta* 211, 791-799.
- Bartoszewski, G., Niedziela, A., Szwacka, M. and Niemirowicz-Szczytt, K. (2003). Modification of tomato taste in transgenic plants carrying a thaumatin gene from *Thaumatococcus daniellii* Benth. *Plant Breeding* 122, 347-351.
- Batalia, M.A., Monzingo, A.F., Ernst, S., Roberts, W. and Robertus, J.D. (1996). The crystal structure of the antifungal protein zeamatin, a member of the thaumatin-like, PR-5 protein family. *Nat. Struct. Biol.* 3, 19-23.
- Beaugrand, J., Gebruers, K., Ververken, C., Fierens, E., Croes, E., Goddeeris, B., Courtin, C.M. and Delcour, J.A. (2006). Antibodies against wheat xylanase inhibitors as tools for the selective identification of their homologues in other cereals. *J. Cereal Sci.* 44, 59-67.
- Bedford, M.R. and Classen, H.L. (1992). The influence of dietary xylanase on intestinal viscosity and molecular weight distribution of carbohydrates in rye-fed broiler chick. In "Xylans and xylanases", Visser, J., Beldman, G., vanSomeren, M.A.K. and Voragen, A.G.J. (eds). Elsevier, Amsterdam, 361-370.
- Beg, Q.K., Kapoor, M., Mahajan, L. and Hoondal, G.S. (2001). Microbial xylanases and their industrial applications: a review. *Appl. Microbiol. Biotechnol.* 56, 326-338.
- Beliën, T. (2006). Study of molecular interactions between endoxylanases and their inhibitors by phage display technology and mutagenesis. PhD dissertation, Katholieke Universiteit Leuven, Leuven, Belgium.
- Bellincampi, D., Camardella, L., Delcour, J.A., Desseaux, V., D'Ovidio, R., Durand, A., Elliot, G., Gebruers, K., Giovane, A., Juge, N., Sørensen, J.F., Svensson, B. and Vairo, D. (2004). Potential physiological role of plant glycosidase inhibitors. *Biochim. Biophys. Acta.* 1696, 265-274.
- Bendtsen, J.D., Nielsen, H., von Heijne, G and Brunak, S. (2004). Improved prediction of signal peptides: SignalP 3.0. *J. Mol. Biol.* 340, 783-795.
- Berrin, J., Williamson, G., Puigserver, A., Chaix, J., McLauchlan, W.R. and Juge, N. (2000). High-level production of recombinant fungal endo- β -1,4-xylanase in the methylotrophic yeast *Pichia pastoris*. *Protein Expr. Purif.* 19, 179-187.
- Biely, P., Kratky, Z. and Vrsanska, M. (1981). Substrate-binding site of endo-1,4-beta-xylanase of the yeast *Cryptococcus albidus*. *Eur. J. Biochem.* 119, 559-564.
- Biely, P., Vrsanska, M., Tenkanen, M. And Kluepfel, D. (1997). Endo- β -1,4-xylanase families: differences in catalytic properties. *J. Biotechnol.* 57, 151-166.
- Bishop, J.G., Dean, A.M. and Mitchell-Olds, T. (2000). Rapid evolution in plant chitinases: molecular targets of selection in plant-pathogen coevolution. *Proc. Natl. Acad. Sci. U.S.A.* 97, 5322-5327.

- Black, G.W., Hazlewood, G.P., Millward-Sadler, S.J., Laurie, J.I. and Gilbert, H.J. (1995). A modular xylanase containing a novel non-catalytic xylan-specific binding domain. *Biochem J.* 307, 191–195.
- Blackwell, J.R. and Horgan, R. (1991). A novel strategy for production of a highly expressed recombinant protein in an active form. *FEBS Lett.* 295, 10-12.
- Bond, C.S. (2003). TopDraw: a sketchpad for protein structure topology cartoons. *Bioinformatics* 19, 311-312.
- Bourgois, T., Nguyen, D.V., Sansen, S., Raedschelders, G., Fierens, K., Rombouts, S., Beliën, T., Courtin, C.M., Delcour, J.A., Rabijns, A., Van Campenhout, S. and Volckaert, G. (2006). Targeted molecular engineering of a family 11 endoxylanase to decrease its sensitivity towards *Triticum aestivum* endoxylanase inhibitor types. Submitted.
- Brandazza, A., Angeli, S., Tegoni, M., Cambillau, C. and Pelosi, P. (2004). Plant stress proteins of the thaumatin-like family discovered in animals. *FEBS Lett.* 572, 3-7.
- Breiteneder, H. (2004). Thaumatin-like proteins – a new family of pollen and fruit allergens. *Allergy* 59, 479-481.
- Brennan, C.S. (2005). Dietary fibre, glycaemic response, and diabetes. *Mol. Nutr. Food Res.* 49, 560-570.
- Breton, G., Danyluk, J., Ouellet, F. and Sarhan, F. (2000). Biotechnological applications of plant freezing associated proteins. *Biotechnol. Annu. Rev.* 6, 59-101.
- Bretthauer, R.K. and Castellino, F.J. (1999). Glycosylation of *Pichia pastoris*-derived proteins. *Biotechnol. Appl. Biochem.* 30, 193-200.
- Brown, L., Rosner, B., Willett, W.W. and Sacks, F.M. (1999). Cholesterol-lowering effects of dietary fiber: a meta-analysis. *Am. J. Clin. Nutr.* 69, 30-42.
- Brutus, A., Reça, I.B., Herga, S., Mattei, B., Puigserver, A., Chaix, J.C., Juge, N., Bellincampi, D. and Giardina, T. (2005). A family 11 xylanase from the pathogen *Botrytis cinerea* is inhibited by plant endoxylanase inhibitors XIPI and TAXI-I. *Biochem. Biophys. Res. Commun.* 337, 160-166.
- Bryngelsson, T. and Green, B. (1989). Characterization of a pathogenesis-related, thaumatin-like protein isolated from barley challenged with an incompatible race of mildew. *Physiol. Mol. Plant Pathol.* 35, 45-52.
- Campbell, J.M., Fahey, G.C. and Wolf, B.W. (1997). Selected indigestible oligosaccharides affect large bowel mass, cecal and fecal short-chain fatty acids, pH and microflora in rats. *J. Nutr.* 127, 130-136.
- Cereghino, J.L. and Cregg, J.M. (2000). Heterologous protein expression in the methylotrophic yeast *Pichia pastoris*. *FEMS Microbiol. Rev.* 24, 45-66.
- Cha, S. (1975) Tight-binding inhibitors-I: Kinetic behavior. *Biochem. Pharmacol.* 24, 2177-2185.
- Chan, Y. W., Tung, W.L., Griffith, M. and Chow, K. (1999). Cloning of a cDNA encoding the thaumatin-like protein of winter rye (*Secale cereale* L. Musketeer) and its functional characterization. *J. Exp. Bot.* 50, 1627-1628.
- Charalampopoulos, D., Wang, R. Pandiella, S.S. and Webb, C. (2002). Application of cereals and cereal components in functional foods: a review. *Int. J. Food Microbiol.* 79, 131-141.
- Charnock, S.J., Spurway, T.D., Xie, H., Beylot, M.H., Virden, R., Warren, R.A., Hazlewood, G.P. and Gilbert, H.J. (1998). The topology of the substrate binding clefts of glycosyl hydrolase family 10 xylanases are not conserved. *J. Biol. Chem.* 273, 32187-32199.
- Chen, W.P., Chen, P.D., Liu, D.J., Kynast, R., Friebe, B., Velazhahan, R., Muthukrishnan, S. and Gill, B.S. (1999). Development of wheat scab symptoms is delayed in transgenic wheat plants that constitutively express a rice thaumatin-like protein gene. *Theor. Appl. Gen.* 99, 755-760.
- Chothia, C. (1973). Conformation of twisted β -pleated sheets in proteins. *J. Mol. Biol.* 75, 295-302.
- Christensen, A.B., Ho Cho, B., Næsby, M., Gregersen, P.L., Brandt, J., Madriz-Ordeñana, K., Collinge, D.B. and Thordal-Christensen, H. (2002). The molecular characterization of two barley proteins establishes the novel PR-17 family of pathogenesis-related proteins. *Mol. Plant Pathol.* 3, 135-144.
- Collaborative Computational Project Number 4. The CCP4 suite: programs for protein crystallography (1994). *Acta Crystallogr. D*50, 760-763.

- Collins, T., Gerday, C. and Feller, G. (2005). Xylanases, xylanase families and extremophilic xylanases. *FEMS Microbiol. Rev.* 29, 3-23.
- Cortegano, I., Civantos, E., Aceituno, E., del Moral, A., López, E., Lombardero, M., del Pozo, V. and Lahoz, C. (2004). Cloning and expression of a major allergen from *Cupressus arizonica* pollen, Cup a 3, a PR-5 protein expressed under polluted environment. *Allergy* 59, 485-490.
- Cos, O., Serrano, A., Montesinos, J.L., Ferrer, P., Cregg, J.M. and Valero, F. (2005). Combined effect of the methanol utilization (Mut) phenotype and gene dosage on recombinant protein production in *Pichia pastoris* fed-batch cultures. *J. Biotechnol.* 116, 321-335.
- Courtin, C.M. and Delcour, J.A. (1998). Physicochemical and bread-making properties of low molecular weight wheat-derived arabinoxylans. *J. Agric. Food Chem.* 46, 4066-4073.
- Courtin, C.M., Roelants, A. and Delcour, J.A. (1999). Fractionation-reconstitution experiments provide insight into the role of endoxylanases in bread-making. *J. Agric. Food Chem.* 47, 1870-1877.
- Courtin, C.M. (2000). Arabinoxylan and endoxylanase functionality in bread-making. PhD Dissertation, Katholieke Universiteit Leuven, Leuven, Belgium.
- Courtin, C. M., Gelders, G.G. and Delcour, J.A. (2001). Use of two endoxylanases with different substrate selectivity for understanding arabinoxylan functionality in wheat flour breadmaking. *Cereal Chem.* 78, 564-571.
- Courtin, C.M., Gys, W., Gebruers, K. and Delcour, J.A. (2005). Evidence for the involvement of arabinoxylan and xylanases in refrigerated dough syruing. *J. Agric. Food Chem.* 53, 7623-7629.
- Courtin, C.M., Gys, W. and Delcour, J.A. (2006). Arabinoxylans and endoxylanases in refrigerated dough syruing. *J. Sci. Food Agr.* 86, 1587-1595.
- Coutinho, P.M. and Henrissat, B. (1999). Carbohydrate-active enzymes: an integrated database approach. In "Recent Advances in Carbohydrate Bioengineering", H.J. Gilbert, G. Davies, B. Henrissat and B. Svensson (eds.), The Royal Society of Chemistry, Cambridge, 3-12.
- Cregg, J.M., Vedvick, T.S. and Raschke, W.C. (1993). Recent advances in the expression of foreign genes in *Pichia pastoris*. *BioTechnology* 11, 905-910.
- Cudney, B., Patel, S. Weisgraber, K., Newhouse, Y. and McPherson, A. (1994). Screening and optimization strategies for macromolecular crystal growth. *Acta Cryst. D* 50, 414-423.
- Dash, C., Vathipadikal, V., George, S.P. and Rao, M. (2002). Slow-tight binding inhibition of xylanase by an aspartic protease inhibitor: kinetic parameters and conformational changes that determine the affinity and selectivity of the bifunctional nature of the inhibitor. *J. Biol. Chem.* 277, 17978-17986.
- Datta, K., Velazhahan, R., Oliva, N., Ona, I., Mew, T., Khush, G.S., Muthukrishnan, S. and Datta, S.K. (1999). Over-expression of the cloned rice thaumatin-like protein (PR-5) gene in transgenic rice plants enhances environmental friendly resistance to *Rhizoctonia solani* causing sheath blight disease. *Theor. Appl. Genet.* 98, 1138-1145.
- Davidson, M.H. and McDonald, A. (1998). Fiber: forms and functions. *Nutr. Res.* 18, 617-624.
- Davies, G.J., Wilson, K.S. and Henrissat, B. (1997). Nomenclature for sugar-binding subsites in glycosyl hydrolases. *Biochem. J.* 321, 557-559.
- Debyser, W., Derdelinckx, G. and Delcour, J.A. (1997). Arabinoxylan solubilisation and inhibition of the barley malt xylanolytic system by wheat during brewing with wheat wholemeal adjunct: evidence for a new class of enzyme inhibitors. *J. Am. Soc. Brew. Chem.* 55, 153-156.
- Debyser, W. and Delcour, J.A. (1998). Inhibitors of xylanolytic and β -glucanolytic enzymes. *Patent application* WO 98/49278.
- Debyser, W. Arabinoxylan solubilisation during the production of Belgian white beer and a novel class of wheat proteins that inhibit endoxylanases (1999). PhD dissertation, Katholieke Universiteit Leuven, Leuven, Belgium.
- Debyser, W., Peumans, W.J., Van Damme, E.J.M. and Delcour, J.A. (1999). *Triticum aestivum* xylanase inhibitor (TAXI), a new class of enzyme inhibitor affecting breadmaking performance. *J. Cereal Sci.* 30, 39-43.

- Dekker, R.F.H. and Richards, G.N. (1976). Hemicellulases: their occurrence, purification, properties, and mode of action. *Adv. Carbohydr. Chem. and Biochem.* 32, 277-352.
- De Lemos Esteves, F., Ruelle, V., Lamotte-Brasseur, J., Quinting, B. and Frere, J.M. (2004). Acidophilic adaptation of family 11 endo-beta-1,4-xylanases: modeling and mutational analysis. *Protein Sci.* 13, 1209-1218.
- De Vos, A.M., Hatada, M., van der Wel, H., Krabbendam, H., Peerdeman, A.F. and Kim, S.H. (1985). Three-dimensional structure of thaumatin I, an intensely sweet protein. *Proc. Natl. Acad. Sci. U.S.A.* 82, 1406-1409.
- Dominguez, C., Boelens, R. and Bonvin, A.M. (2003). HADDOCK: a protein-protein docking approach based on biochemical or biophysical information. *J. Am. Chem. Soc.* 125, 1731-1737.
- Drenth, J., Low, B.W., Richardson, J.S. and Wright, C.S. (1980). The toxin-agglutinin fold. A new group of small protein structures organized around a four-disulfide core. *J. Biol. Chem.* 255, 2652-2655.
- Eastwood, M.A. and Passmore, M. (1983). Dietary fibre. *Lancet.* 23, 202-206.
- Edens, L., Heslinga, L., Klok, R., Ledebouer, A.M., Maat, J., Toonen, M.Y., Visser, C. and Verrips, C.T. (1982). Cloning of cDNA encoding the sweet-tasting plant protein thaumatin and its expression in *Escherichia coli*. *Gene* 18, 1-12.
- Edens, L. and van der Wel, H. (1985). Microbial synthesis of the sweet-tasting plant protein thaumatin. *Trends Biotechnol.* 3, 61-64.
- Edge, A.S. (2003). Deglycosylation of glycoproteins with trifluoromethanesulphonic acid: elucidation of molecular structure and function. *Biochem J.* 376, 339-350.
- Elliott, G.O. (2002). Molecular and biochemical studies into wheat xylanase inhibitor proteins. PhD Dissertation, University of East Anglia, Norwich, UK.
- Elliott, G.O., Hughes, R.K., Juge, N., Kroon, P.A. and Williamson, G. (2002). Functional identification of the cDNA coding for a wheat endo-1,4- β -D-xylanase inhibitor. *FEBS Lett.* 519, 66-70.
- Elliott, G.O., McLauchlan, W.R., Williamson, G. and Kroon, P.A. (2003). A wheat xylanase inhibitor protein (XIP-I) accumulates in the grain and has homologues in other cereals. *J. Cereal Sci.* 37, 187-194.
- Enkerli, J., Felix, G. and Boller, T. (1999). The enzymatic activity of fungal xylanase is not necessary for its elicitor activity. *Plant Physiol.* 121, 391-397.
- Faus, I., Patiño, C., del Río, J.L., del Moral, C., Barroso, H.S., Bladé, J. and Rubio, V. (1997). Expression of a synthetic gene encoding the sweet-tasting protein thaumatin in the filamentous fungus *Penicillium roquefortii*. *Biotechnol. Lett.* 19, 1185-1191.
- Faus, I. (2000). Recent developments in the characterization and biotechnological production of sweet-tasting proteins. *Appl. Microbiol. Biotechnol.* 53, 145-151.
- Fierens, K., Brijs, K., Courtin, C.M., Gebruers, K., Goesaert, H., Raedschelders, G., Robben, J., Van Campenhout, S., Volckaert, G. and Delcour, J.A. (2003). Molecular identification of wheat endoxylanase-inhibitor TAXI-I, member of a new class of plant proteins. *FEBS Lett.* 540, 259-263.
- Fierens, K. (2004). Molecular cloning, expression and mutational analysis of wheat endoxylanase inhibitor TAXI-I. PhD dissertation, Katholieke Universiteit Leuven, Leuven, Belgium.
- Fierens, K., Geudens, N., Brijs, K., Courtin, C.M., Gebruers, K., Robben, J., Van Campenhout, S., Volckaert, G. and Delcour, J.A. (2004). High-level expression, purification, and characterization of recombinant wheat xylanase inhibitor TAXI-I secreted by the yeast *Pichia pastoris*. *Protein Expr. Purif.* 37, 39-46.
- Fierens, K., Gils, A., Sansen, S., Brijs, K., Courtin, C.M., Declerck, P.J., De Ranter, C.J., Gebruers, K., Rabijns, A., Robben, J., Van Campenhout, S., Volckaert, G. and Delcour, J.A. (2005). His374 of wheat endoxylanase inhibitor TAXI-I stabilizes complex formation with glycoside hydrolase family 11 endoxylanases. *FEBS J.* 272, 5872-5882.
- Fierens, E., Rombouts, S., Gebruers, K., Goesaert, H., Brijs, K., Beaugrand, J., Volckaert, G., Van Campenhout, S., Proost, P., Courtin, C.M. and Delcour, J.A. (2007). TLXI, a novel type of xylanase inhibitor from wheat (*Triticum aestivum*) belonging to the thaumatin family. *Biochem. J.*, doi:10.1042/BJ20061291.

- Fincher, G.B. (1989). Molecular and cellular biology associated with endosperm mobilization in germinating cereal grains. *Annu. Rev. Plant Physiol. Plant Mol. Biol.* 40, 305-346.
- Flatman, R., McLaughlan, W.R., Juge, N., Furniss, C., Berrin, J.-G., Hughes, R.K., Manzanares, P., Ladbury, J.E., O'Brien, R. and Williamson, G. (2002). Interactions defining the specificity between fungal xylanases and the xylanase-inhibiting protein XIP-I from wheat. *Biochem. J.* 365, 773-781.
- Frederix, S.A., Courtin, C.M. and Delcour, J.A. (2003). Impact of xylanases with different substrate selectivity on gluten-starch separation of wheat flour. *J. Agric. Food Chem.* 51, 7338-7345.
- Frederix, S.A., Van Hoeymissen, K.E., Courtin, C.M. and Delcour, J.A. (2004). Water-extractable and water-unextractable arabinoxylans affect gluten agglomeration behavior during wheat flour gluten-starch separation. *J. Agric. Food Chem.* 52, 7950 -7956.
- Fujimura, H. and Sakuma, Y. (1993). Simplified isolation of chromosomal and plasmid DNA from yeasts. *Biotechniques* 14, 538-540.
- Furniss, C.S., Belshaw, N.J., Alcocer, M.J., Williamson, G., Elliott, G.O., Gebruers, K., Haigh, N.P., Fish, N.M. and Kroon, P.A. (2002). A family 11 xylanase from *Penicillium funiculosum* is strongly inhibited by three wheat xylanase inhibitors. *Biochim. Biophys. Acta.* 1598, 24-29.
- Gasteiger, E., Hoogland, C., Gattiker, A., Duvaud, S., Wilkins, M.R., Appel, R.D., Bairoch, A. (2005). Protein Identification and Analysis Tools on the ExPASy Server. (In) John M. Walker (ed): *The Proteomics Protocols Handbook*, Humana Press, 571-607.
- Gattiker, A., Gasteiger, E. and Bairoch, A. (2002). ScanProsite: a reference implementation of a PROSITE scanning tool. *Appl. Bioinformatics* 1, 107-108.
- Gavrovic-Jankulovic, M., Cirkovic, T., Vuckovic, O., Atanaskovic-Markovic, M., Petersen, A., Gojgic, G., Burazer, L. and Jankov, R.M. (2002). Isolation and biochemical characterization of a thaumatin-like kiwi allergen. *J. Allergy Clin. Immunol.* 110, 805-810.
- Gebler, J., Gilkes, N.R., Claeysens, M., Wilson, D.B., Beguin, P., Wakarchuk, W.W., Kilburn, D.G., Miller, R.C. Jr, Warren, R.A. and Withers, S.G. (1992). Stereoselective hydrolysis catalyzed by related beta-1,4-glucanases and beta-1,4-xylanases. *J. Biol. Chem.* 267, 12559-12561.
- Gebruers, K., Debyser, W., Goesaert, H., Proost, P., Van Damme, J. And Delcour, J.A. (2001). *Triticum aestivum* L. endoxylanase inhibitor (TAXI) consists of two inhibitors, TAXI I and TAXI II, with different specificities. *Biochem. J.* 353, 239-244.
- Gebruers, K. (2002). Endoxylanase inhibitors in wheat (*Triticum aestivum* L.): isolation, characterization and use for endoxylanase purification. PhD dissertation, Katholieke Universiteit Leuven, Leuven, Belgium.
- Gebruers, K., Goesaert, H., Brijs, K., Courtin, C.M. and Delcour, J.A. (2002a). Purification of TAXI-like endoxylanase inhibitors from wheat (*Triticum aestivum* L.) whole meal reveals a family of iso-forms. *J. Enzyme Inhib. Med. Chem.* 17, 61-68.
- Gebruers, K., Goesaert, H., Brijs, K., Courtin, C.M. and Delcour, J.A. (2002b). Affinity chromatography with immobilized endoxylanases separates TAXI- and XIP-type endoxylanase inhibitors from wheat (*Triticum aestivum* L.). *J. Cereal Sci.* 36, 367-375.
- Gebruers, K., Brijs, K., Courtin, C.M., Fierens, K., Goesaert, H., Rabijns, A., Raedschelders, G., Robben, J., Sansen, S., Sorensen, J.F., Van Campenhout, S., Delcour, J.A. (2004). Properties of TAXI-type endoxylanase inhibitors. *Biochim Biophys Acta.* 1696, 213-221.
- Gilbert, H.J. and Hazlewood, G.P. (1993). Bacterial cellulases and xylanases. *J. Gen. Microbiol.* 139, 187-194.
- Gill, S.C. and von Hippel, P.H. (1989). Calculation of protein extinction coefficients from amino acid sequence data. *Anal. Biochem.* 182, 319-326.
- Goesaert, H., Debyser, W., Gebruers, K., Proost, P., Van Damme, J. And Delcour, J.A. (2001). Purification and partial characterization of an endoxylanase-inhibitor from barley. *Cereal Chem.* 78, 453-457.
- Goesaert, H. (2002). Occurrence, purification and properties of endoxylanase inhibitors in different cereals. PhD dissertation, Katholieke Universiteit Leuven, Leuven, Belgium.
- Goesaert, H., Gebruers, K., Courtin, C.M., Proost, P., Van Damme, J. and Delcour, J.A. (2002). A family of 'TAXI'-like endoxylanase inhibitors in rye. *J. Cereal Sci.* 36, 177-185.

- Goesaert, H., Gebruers, K., Brijs, K., Courtin, C.M. and Delcour, J.A. (2003). XIP-type endoxylanase inhibitors in different cereals. *J. Cereal Sci.* 38, 317-324.
- Goesaert, H., Elliott, G., Kroon, P.A., Gebruers, K., Courtin, C.M., Robben, J., Delcour, J.A. and Juge, N. (2004). Occurrence of proteinaceous endoxylanase inhibitors in cereals. *Biochim Biophys Acta.* 1696, 193-202.
- Gomez-Gomez, E., Ruiz-Roldan, M.C., Di Pietro, A., Roncero, M.I. and Hera, C. (2002). Role in pathogenesis of two endo-beta-1,4-xylanase genes from the vascular wilt fungus *Fusarium oxysporum*, *Fungal Genet. Biol.* 35, 213-222.
- Gottschalk, M., Schuster, E. and Sprössler, B. (1994). Bacterial xylanase, method for its production, bacteria producing a xylanase, DNA fragment encoding a xylanase, plasmid containing the DNA fragment, baking agents containing a xylanase and a method for producing bread and baked goods using the xylanase. *US Patent* N°5,306,633.
- Greenstein, S., Shadkchan, Y., Jadoun, J., Sharon, C., Markovich, S. and Oshero, N. (2006). Analysis of the *Aspergillus nidulans* thaumatin-like cetA gene and evidence for transcriptional repression of pyr4 expression in the cetA-disrupted strain. *Fungal Genet. Biol.* 43, 42-53.
- Grenier, J., Potvin, C., Trudel, J. and Asselin, A. (1999). Some thaumatin-like proteins hydrolyse polymeric β -1,3-glucans. *Plant J.* 19, 473-480.
- Grenier, J., Potvin, C. and Asselina, A. (2000). Some fungi express β -1,3-glucanases similar to thaumatin-like proteins. *Mycologia* 92, 841-848.
- Griffith, M. and Ewart, K.V. (1995). Properties of antifreeze proteins. *Biotechnol. Adv.* 13, 375-402.
- Guarna, M.M., Lesnicki, G.J., Tam, B.M., Robinson, J., Radziminski, C.Z., Hasenwinckle, D., Boraston, A., Jervis, E., MacGillivray, R.T.A., Turner, R.F.B. and Kilburn, D.G. (1997). On-line monitoring and control of methanol concentration in shake-flask cultures of *Pichia pastoris*. *Biotechnol. Bioeng.* 56, 279-286.
- Gys, W., Courtin, C.M. and Delcour, J.A. (2003). Refrigerated dough syruing in relation to the arabinoxylan population. *J. Agric. Food Chem.* 51, 4119-4125.
- Hanselle, T., Ichinoseb, Y. and Barz, W. (2001). Biochemical and molecular biological studies on infection (*Ascochyta rabiei*)-induced thaumatin-like proteins from chickpea plants (*Cicer arietinum* L.). *Zeitschr. Naturforsch. C* 56, 1095-1107.
- Havukainen, R., Törrönen, A., Laitinen, T. and Rouvinen, J. (1996). Covalent binding of three epoxyalkyl xylosides to the active site of endo-1,4-xylanase II from *Trichoderma reesei*. *Biochemistry* 35, 9617-9624.
- Hejgaard, J., Jacobsen, S. and Svendsen, I. (1991). Two antifungal thaumatin-like proteins from barley grain. *FEBS Lett.* 291, 127-131.
- Hellenius, A. (1994). How N-linked oligosaccharides affect glycoprotein folding in the endoplasmic reticulum. *Mol. Biol. Cell* 5, 253-265.
- Henrissat, B. (1991). A classification of glycosyl hydrolases based on amino acid sequence similarities. *Biochem. J.* 280, 309-316.
- Henrissat, B. and Davies, G. (1997). Structural and sequence-based classification of glycoside hydrolases. *Curr. Opin. Struc. Biol.* 7, 637-644.
- Henry, R. J. (1985). Comparison of the non-starch carbohydrates in cereal grains. *J. Sci. Food Agric.* 36, 1243-1253.
- Hertveldt, K., Robben, J. and Volckaert, G. (2002). In vivo selectively infective phage as tool to detect protein interactions: evaluation of a novel vector system with yeast Ste7p-Fus3p interacting proteins. *Yeast* 19, 499-508.
- Hoffmann-Sommergruber, K. (2000). Plant allergens and pathogenesis-related proteins. *Int. Arch. Allergy Immunol.* 122, 155-166.
- Holloway, W.D., Tasman-Jones, C. and Bell, E. (1980). The hemicellulose component of dietary fiber. *Am. J. Clin. Nutr.* 33, 260-263.
- Hon, W., Griffith, M., Mlynarz, A., Kwok, Y.C. and Yang, D.S.C. (1995). Antifreeze proteins in winter rye are similar to pathogenesis-related proteins. *Plant Physiol.* 109, 879-889.

- Horton, R.M., Hunt, H.D., Ho, S.N., Pullen, J.K. and Pease, L.R. (1989). Engineering hybrid genes without the use of restriction enzymes: gene splicing by overlap extension. *Gene* 77, 61-68.
- Hrmova, M. and Fincher, B.G. (1993). Purification and properties of three (1-->3)-beta-D-glucanase isoenzymes from young leaves of barley (*Hordeum vulgare*). *Biochem. J.* 289, 453-461.
- Hrmova, M. and Fincher, B.G. (2001). Plant Enzyme Structure. Explaining substrate specificity and the evolution of function. *Plant Physiol.* 125, 54-57.
- Hsieh, L.S., Moos, M. Jr and Lin, Y. (1995). Characterization of apple 18 and 31 kd allergens by microsequencing and evaluation of their content during storage and ripening. *J. Allergy Clin. Immunol.* 96, 960-970.
- Hsu, C.K., Liao, J.W., Chung, Y.C., Hsieh, C.P. and Chan, Y.C. (2004). Xylooligosaccharides and fructooligosaccharides affect the intestinal microbiota and precancerous colonic lesion development in rats. *J. Nutr.* 134, 1523-1528.
- Huynh, Q.K., Borgmeyer, J.R. and Zobel, J.F. (1992). Isolation and characterization of a 22 kDa protein with antifungal properties from maize seeds. *Biochem. Biophys. Res. Commun.* 182, 1-5.
- Igawa, T., Ochiai-Fukuda, T., Takahashi-Ando, N., Ohsato, S., Shibata, T., Yamaguchi, I. and Kimura, M. (2004). New TAXI-type xylanase inhibitor genes are inducible by pathogens and wounding in hexaploid wheat. *Plant Cell Physiol.* 45, 1347-1360.
- Igawa, T., Tokai, T., Kudo, T., Yamaguchi, I. and Kimura, M. (2005). A wheat xylanase inhibitor gene, xip-I, but not taxi-I, is significantly induced by biotic and abiotic signals that trigger plant defense. *Biosci. Biotechnol. Biochem.* 69, 1058-1063.
- Illingworth, C., Larson, G. and Hellekant, G. (1988). Secretion of the sweet-tasting plant protein thaumatin by *Bacillus subtilis*. *Biotechnol. Lett.* 10, 587-592.
- Illingworth, C., Larson, G. and Hellekant, G. (1989). Secretion of the sweet-tasting plant protein thaumatin by *Streptomyces lividans*. *J. Ind. Microbiol. Biotechnol.* 4, 37-42.
- Ingelbrecht, J.A., Moers, K., Abecassis, J., Rouau, X., and Delcour, J.A. (2001). Influence of arabinoxylans and endoxylanases on pasta processing and quality. Production of high-quality pasta with increased levels of soluble fiber. *Cereal chem.* 78, 721-729.
- Inschlag, C., Hoffmann-Sommergruber, K., O'Riordain, G., Ahorn, H., Ebner, C., Scheiner, O. and Breiteneder, H. (1998). Biochemical characterization of Pru a 2, a 23-kD thaumatin-like protein representing a potential major allergen in cherry (*Prunus avium*). *Int. Arch. Allergy Immunol.* 116, 22-28.
- Ito, K., Ogasawara, H., Sugimoto, T. and Ishikawa, T. (1992). Purification and properties of acid stable xylanases from *Aspergillus kawachii*. *Biosci. Biotechnol. Biochem.* 56, 547-550.
- Iyengar, R.B., Smits, P., van der Ouderaa, F., van der Wel, H., van Brouwershaven, J., Ravestein, P., Richters, G. and van Wassenaar, P.D. (1979). The complete amino-acid sequence of the sweet protein thaumatin I. *Eur. J. Biochem.* 96, 193-204.
- Jancarik, J. and Kim, S.H. (1991). Sparse matrix sampling: a screening method for crystallization of proteins. *J. Appl. Cryst.* 24, 409-411.
- Jeffries, T.W. (1996). Biochemistry and genetics of microbial xylanases. *Curr. Opin. Biotech.* 7, 337-342.
- Jenkins, J., Lo Leggio, L., Harris, G. and Pickersgill, R. (1995). Beta-glucosidase, beta-galactosidase, family A cellulases, family F xylanases and two barley glucanases form a superfamily of enzymes with 8-fold beta/alpha architecture and with two conserved glutamates near the carboxy-terminal ends of beta-strands four and seven. *FEBS Lett.* 362, 281-285.
- Johal, J., Gianibelli, M.C., Rahman, S., Morell, M.K. and Gale, K.R. (2004). Characterization of low-molecular-weight glutenin genes in *Aegilops tauschii*. *Theor. Appl. Genet.* 109, 1028-1040.
- Joshi, M.D., Sidhu, G., Pot, I., Brayer, G.D., Withers, S.G. and McIntosh, L.P. (2000). Hydrogen bonding and catalysis: a novel explanation for how a single amino acid substitution can change the pH optimum of a glycosidase. *J. Mol. Biol.* 299, 255-279.

- Juge, N., Andersen, J.S., Tull, D., Roepstorff, P. and Svensson, B. (1996). Overexpression, purification, and characterization of recombinant barley alpha-amylases 1 and 2 secreted by the methylotrophic yeast *Pichia pastoris*. *Protein Expr. Purif.* 8, 204-214.
- Juge, N., Payan, F. and Williamson, G. (2004). XIP-I, a xylanase inhibitor protein from wheat: a novel protein function. *Biochim Biophys Acta.* 1696, 203-211.
- Kallas, A.M., Piens, K., Henriksson, H., Fäldt, J., Johansson, P., Brumer, H. and Teeri, T.T. (2005). Enzymatic properties of native and deglycosylated hybrid aspen (*Populus tremula x tremuloides*) xyloglucan endotransglycosylase 16A expressed in *Pichia pastoris*. *Biochem. J.* 390, 105-113.
- Kaneko, S., Kitaoka, M., Kuno, A. and Hayashi, M. (2000). Syntheses of 4-methylumbelliferyl- β -D-xylobioside and 5-bromo-3-indolyl- β -D-xylobioside for sensitive detection of xylanase activity on agar plates. *Biosci. Biotechnol. Biochem.* 64, 741-745.
- Kaneko, R. and Kitabatake, N. (2001). Structure-sweetness relationship in thaumatin: importance of lysine residues. *Chem. Senses* 26, 167-177.
- Kelley, L.A., MacCallum, R.M. and Sternberg, M.J.E. (2000). Enhanced Genome Annotation using Structural Profiles in the Program 3D-PSSM. *J. Mol. Biol.* 299, 499-520.
- Kempf, B. and Bremer, E. (1998). Uptake and synthesis of compatible solutes as microbial stress responses to high-osmolality environments. *Arch. Microbiol.* 170, 319-330.
- Kettner, J. and Dörffling, K. (1995). Biosynthesis and metabolism of abscisic acid in tomato leaves infected with *Botrytis cinerea*. *Planta* 196, 627-634.
- Kim, S.H. and Weickmann, J.L. (1994). Crystal structure of thaumatin I and its correlation to biochemical and mutational studies. In "Thaumatococcus", Witty, M. and Higginbotham, J.D. (eds). CRC Press, Boca Raton, FL, 135-149.
- Ko, T.P., Day, J., Greenwood, A. and McPherson, A. (1994). Structures of three crystal forms of the sweet protein thaumatin. *Acta Crystallogr. D Biol. Crystallogr.* 50, 813-825.
- Koiwa, H., Kato, H., Nakatsu, T., Oda, J., Yamada, Y. and Sato, F. (1997). Purification and characterization of tobacco pathogenesis-related protein PR-5d, an antifungal thaumatin-like protein. *Plant Cell Physiol.* 38, 783-791.
- Koiwa, H., Kato, H., Nakatsu, T., Oda, J., Yamada, Y. and Sato, F. (1999). Crystal structure of tobacco PR-5d protein at 1.8 Å resolution reveals a conserved acidic cleft structure in antifungal thaumatin-like proteins. *J. Mol. Biol.* 286, 1137-1145.
- Krengel, U. and Dijkstra, B.W. (1996). Three-dimensional structure of endo-1,4- β -xylanase I from *Aspergillus niger*: molecular basis for its low pH optimum. *J. Mol. Biol.* 263, 70-78.
- Kulkarni, N., Shendye, A. and Rao, M. (1999). Molecular and biotechnological aspects of xylanases. *FEMS Microbiol. Rev.* 23, 411-456.
- Kyte, J. and Doolittle, R.F. (1982). A simple method for displaying the hydropathic character of a protein. *J. Mol. Biol.* 157, 105-132.
- Laemmli, U.K. (1970). Cleavage of structural proteins during the assembly of the head of bacteriophage T4. *Nature* 227, 680-685.
- Laskowski, R.A., McArthur, M.W., Moss, D.S. and Thornton, J.M. (1993). PROCHECK: a program to check the stereochemical quality of protein structures. *J. Appl. Cryst.* 26, 283-291.
- Ledeboer, A.M., Verrips, C.T. and Dekker, B.M.M. (1984). Cloning of the natural gene for the sweet-tasting plant protein thaumatin. *Gene* 30, 23-32.
- Lee, J., Weickmann, J.M., Koduri, R.K., Ghosh-Dastidar, P., Saito, K., Blair, L.C., Date, T., Lai, J.S., Hollenberg, S.M. and Kendall, R.L. (1988). Expression of synthetic thaumatin genes in yeast. *Biochemistry* 27, 5101-5107.
- Lee, C., Li, P., Inouye, H., Brickman, E.R. and Beckwith, J. (1989). Genetic studies on the inability of 3-galactosidase to be translocated across the *Escherichia coli* cytoplasmic membrane. *J. Bacteriol.* 171, 4609-4616.
- Leitner, A., Jensen-Jarolim, E., Grimm, R., Wuthrich, B., Ebner, H., Scheiner, O., Kraft, D. and Ebner, C. (1998). Allergens in pepper and paprika. Immunologic investigation of the celery-birch-mugwort-spice syndrome. *Allergy* 53, 36-41.

- Leone, P., Menu-Bouaouiche, L., Peumans, W.J., Payan, F., Barre, A., Roussel, A., Van Damme, E.J.M. and Rougé, P. (2006). *Biochimie* 88, 45-52.
- Lescot, M., Dehais, P., Thijs, G., Marchal, K., Moreau, Y., Van de Peer, Y., Rouze, P. and Rombauts, S. (2002). PlantCARE, a database of plant cis-acting regulatory elements and a portal to tools for in silico analysis of promoter sequences. *Nucleic Acids Res.* 30, 325-327.
- Li, K., Azadi, P., Collins, R., Toland, J., Kim, J.S. and Eriksson, K.L. (2000). Relationships between activities of xylanases and xylan structures. *Enzyme Microb. Tech.* 27, 89-94.
- Li, Z.J., Xiong, F., Lin, Q.S., d'Anjou, M., Daugulis, A.J., Yang, D.S.C. and Hew, C.L. (2001). Low-temperature increases the yield of biologically active herring antifreeze protein in *Pichia pastoris*. *Protein Express. Purif.* 21, 438-445.
- Li, H., Tatlock, J., Linton, A., Gonzalez, J., Borchardt, A., Dragovich, P., Jewell, T., Prins, T., Zhou, R., Blazel, J., Parge, H., Love, R., Hickey, M., Doan, C., Shi, S., Dugall, R., Lewis, C. and Fuhrman, S. (2006). Identification and structure-based optimization of novel dihydropyrones as potent HCV RNA polymerase inhibitors. *Bioorg. Med. Chem. Lett.* 16, 4834-4838.
- Lis, H. and Sharon, N. (1993). Protein glycosylation. Structural and functional aspects. *Eur. J. Biochem.* 218, 1-27.
- Liu, D., Raghothama, K.G., Hasegawa, P.M. and Bressan, R.A. (1994). Osmotin Overexpression in potato delays development of disease symptoms. *PNAS* 91, 1888-1892.
- Liu, Y.G. and Whittier, R.F. (1995). Thermal asymmetric interlaced PCR: automatable amplification and sequencing of insert end fragments from P1 and YAC clones for chromosome walking. *Genomics* 25, 674-681.
- Liu, Y.G., Mitsukawa, N., Oosumi, T. and Whittier, R.F. (1995). Efficient isolation and mapping of *Arabidopsis thaliana* T-DNA insert junctions by thermal asymmetric interlaced PCR. *Plant J.* 8, 457-463.
- Love, R.A., Parge, H.E., Yu, X., Hickey, M.J., Diehl, W., Gao, J., Wriggers, H., Ekker, A., Wang, L., Thomson, J.A., Dragovich, P.S. and Fuhrman, S.A. (2003). Crystallographic identification of a noncompetitive inhibitor binding site on the hepatitis C virus NS5B RNA polymerase enzyme. *J. Virol.* 77, 7575-7581.
- Mackintosh, C.A., Lewis, J., Radmer, L.E., Shin, S., Heinen, S.J., Smith, L.A., Wyckoff, M.N., Dill-Macky, R., Evans, C.K., Kravchenko, S., Baldrige, G.D., Zeyen, R.J. and Muehlbauer, G.J. (2006). Overexpression of defense response genes in transgenic wheat enhances resistance to *Fusarium* head blight. *Plant Cell. Rep.* [Epub ahead of print].
- Maes, C. and Delcour, J.A. (2002). Structural characterization of water-extractable and water-unextractable arabinoxylans in wheat bran. *J. Cereal Sci.* 35, 315-326.
- Makrides, S.C. (1996). Strategies for achieving high-level expression of genes in *Escherichia coli*. *Microbiol. Rev.* 60, 512-538.
- Marentes, E., Griffith, M., Mlynarz, A. and Brush, R.A. (1993). Proteins accumulate in the apoplast of winter rye leaves during cold acclimation. *Physiol. Plant.* 87, 499-507.
- Mason, A.B., Woodworth, R.C., Oliver, R.W.A., Green, B.N., Lin, L.N., Brandts, J.F., Tam, B.M., Maxwell, A. and Macgillivray, R.T.A. (1996). Production and isolation of the recombinant N-lobe of human serum transferrin from the methylotrophic yeast *Pichia pastoris*. *Protein Express. Purif.* 8, 119-125.
- Masuda, T., Tamaki, S., Kaneko, R., Wada, R., Fujita, Y., Mehta, A. and Kitabatake, N. (2004). Cloning, expression and characterization of recombinant sweet-protein thaumatin II using the methylotrophic yeast *Pichia pastoris*. *Biotechnol. Bioeng.* 85, 761-769.
- Matthews, B.W., Nicholson, H. and Becktel, W.J. (1987). Enhanced protein thermostability from site-directed mutations that decrease the entropy of unfolding. *Proc. Natl. Acad. Sci. USA* 84, 6663-6667.
- McLauchlan, W.R., Garcia-Conesa, M.T., Williamson, G., Roza, M., Ravestein, P. and Maat, J. (1999). A novel class of protein from wheat which inhibits xylanases. *Biochem. J.* 338, 441-446.
- Menu-Bouaouiche, L., Vriet, C., Peumans, W.J., Barre, A., Van Damme, E.J.M. and Rougé, P. (2003). A molecular basis for the endo- β 1,3-glucanase activity of the thaumatin-like proteins from edible fruits. *Biochimie* 85, 123-131.

- Midoro-Horiuti, T., Goldblum, R.M., Kurosky, A., Wood, T.G. and Brooks, E.G. (2000). Variable expression of pathogenesis-related protein allergen in mountain cedar (*Juniperus ashei*) pollen. *J. Immunol.* 164, 2188-2192.
- Min, K., Ha, S.C., Hasegawa, P.M., Bressan, R.A., Yun, D. and Kim, K.K. (2004). Crystal structure of osmotin, a plant antifungal protein. *Proteins* 54, 170-173.
- Missiakas, D. and Raina, S. (1997). Protein folding in the bacterial periplasm. *J. Bacteriol.* 179, 2465-2471.
- Mitra, N., Sinha, S., Ramya, T.N.C. and Surolia, A. (2006). N-linked oligosaccharides as outfitters for glycoprotein folding, form and function. *Trends Biochem Sci.* 31, 156-163.
- Moers, K., Courtin, C.M., Brijs, K. and Delcour, J.A. (2003). A screening method for endo- β -1,4-xylanase substrate selectivity. *Anal. Biochem.* 319, 73-77.
- Moralejo, F.J., Cardoza, R.E., Gutierrez, S. and Martin, J.F. (1999). Thaumatin production in *Aspergillus awamori* by use of expression cassettes with strong fungal promoters and high gene dosage. *Appl. Environ. Microbiol.* 65, 1168-1174.
- Moralejo, F.J., Cardoza, R.E., Gutierrez, S., Sisniega, H., Faus, I. and Martin, J.F. (2000). Overexpression and lack of degradation of thaumatin in an aspergillopepsin A-defective mutant of *Aspergillus awamori* containing an insertion in the pepA gene. *Appl. Microbiol. Biotechnol.* 54, 772-777.
- Moralejo, F.J., Watson, A.J., Jeenes, D.J., Archer, D.B. and Martin, J.F. (2001). A defined level of protein disulfide isomerase expression is required for optimal secretion of thaumatin by *Aspergillus awamori*. *Mol Genet. Genomics* 266, 246-253.
- Moralejo, F.J., Cardoza, R.E., Gutierrez, S., Lombrana, M., Fierro, F. and Martin, J.F. (2002). Silencing of the aspergillopepsin B (pepB) gene of *Aspergillus awamori* by antisense RNA expression or protease removal by gene disruption results in a large increase in thaumatin production. *Appl. Environ. Microbiol.* 68, 3550-3559.
- Morrison, J.F. and Walsh, C.T. (1998). The behavior and significance of slow-binding enzyme inhibitors. *Adv. Enzymol.* 59, 201-301.
- Muilu, J., Törrönen, A., Perakyla, M. and Rouvinen, J. (1998). Functional conformational changes of endo-1,4-xylanase II from *Trichoderma reesei*: a molecular dynamics study. *Proteins* 31, 434-444.
- Nossal, N.G. and Heppel, L.A. (1966). The release of enzymes by osmotic shock from *Escherichia coli* in exponential phase. *J. Biol. Chem.* 241, 3055-3062.
- Ogata, K., Nishikawa, H. and Ohsugi, M. (1969). A yeast capable of utilizing methanol. *Agric. Biol. Chem.* 33, 1519-1520.
- Ogata, C.M., Gordon, P.F., de Vos, A.M. and Kim, S.H. (1992). Crystal structure of a sweet tasting protein thaumatin I, at 1.65 Å resolution. *J. Mol. Biol.* 228, 893-908.
- Olsen, O. and Thomsen, K. (1991). Improvement of bacterial beta-glucanase thermostability by glycosylation. *J. Gen. Microbiol.* 137, 579-585.
- Osmond, R.I.W., Hrmova, M., Fontaine, F., Imberty, A. and Fincher, G.B. (2001). Binding interactions between barley thaumatin-like proteins and (1,3)- β -D-glucans. *Eur. J. Biochem.* 268, 4190-4199.
- Pallares, I., Bonet, R., Garcia-Castellanos, R., Ventura, S., Aviles, F.X., Vendrell, J. and Gomis-Ruth, F.X. (2005). Structure of human carboxypeptidase A4 with its endogenous protein inhibitor, latexin. *Proc. Natl. Acad. Sci. U. S. A.* 102, 3978-3983.
- Payan, F., Flatman, R., Porciero, S., Williamson, G., Juge, N. and Roussel, A. (2003). Structural analysis of xylanase inhibitor protein I (XIP-I), a proteinaceous xylanase inhibitor from wheat (*Triticum aestivum*, var. Soisson). *Biochem. J.* 372, 399-405.
- Payan, F., Leone, P., Porciero, S., Furniss, C., Tahir, T., Williamson, G., Durand, A., Manzanares, P., Gilbert, H.J., Juge, N. and Roussel, A. (2004). The dual nature of the wheat xylanase protein inhibitor XIP-I: structural basis for the inhibition of family 10 and family 11 xylanases. *J. Biol. Chem.* 279, 36029-36037.
- Pell, G., Szabo, L., Charnock, S.J., Xie, H., Gloster, T.M., Davies, G.J. and Gilbert, H.J. (2004). Structural and biochemical analysis of *Cellvibrio japonicus* xylanase 10C: how variation in substrate-binding cleft influences the catalytic profile of family GH-10 xylanases. *J. Biol. Chem.* 279, 11777-11788.

- Pettersen, E.F., Goddard, T.D., Huang, C.C., Couch, G.S., Greenblatt, D.M., Meng, E.C. and Ferrin, T.E. (2004). UCSF Chimera - A visualization system for exploratory research and analysis. *J. Comput. Chem.* 25, 1605-1612.
- Pla, I.A., Damasceno, L.M., Vannelli, T., Ritter, G., Batt, C.A. and Schuller, M.L. (2006). Evaluation of Mut⁺ and Mut^S *Pichia pastoris* phenotypes for high level extracellular scFv expression under feedback control of the methanol concentration. *Biotechnol. Prog.* 22, 881-888.
- Polizeli, M.L.T.M., Rizzatti, A.C.S., Monti, R., Terenzi, H.F., Jorge, J.A. and Amorim, D.S. (2005). Xylanases from fungi: properties and industrial applications. *Appl. Microbiol. Biotechnol.* 67, 577-591.
- Pugsley, A.P. (1993). The complete general secretory pathway in gram-negative bacteria. *Microbiol. Rev.* 57, 50-108.
- Raedschelders, G., Debeve, C., Goesaert, H., Delcour, J.A., Volckaert, G. and Van Campenhout, S. (2004). Molecular identification and chromosomal localization of genes encoding *Triticum aestivum* xylanase inhibitor-I proteins in cereals. *Theor. Appl. Genet.* 109, 112-121.
- Raedschelders, G., Fierens, K., Sansen, S., Rombouts, S., Gebruers, K., Robben, J., Rabijns, A., Courtin, C.M., Delcour, J.A., Van Campenhout, S. and Volckaert, G. (2005). Molecular identification of wheat endoxylanase inhibitor TAXI-II and the determinants of its inhibition specificity. *Biochem. Biophys. Res. Commun.* 335, 512-522.
- Reimann, C. and Dudler, R. (1993). cDNA cloning and sequence analysis of a pathogen-induced thaumatin-like protein from rice (*Oryza sativa*). *Plant Physiol.* 101, 1113-1114.
- Reiss, E., Schlesier, B. and Brandt, W. (2006). cDNA sequences, MALDI-TOF analyses, and molecular modelling of barley PR-5 proteins. *Phytochemistry* 67, 1856-1864.
- Roberts, W. and Selitrennikoff, C.P. (1990). Zeamatin, an antifungal protein from maize with membrane-permeabilizing activity. *J. Gen. Microbiol.* 136, 1771-1778.
- Rost, B., Schneider, R. and Sander, C. (1997). Protein fold recognition by prediction-based threading. *J. Mol. Biol.* 270, 471-480.
- Rouau, X., El-Hayek, M-L. and Moreau, D. (1994). Effect of an enzyme preparation containing pentosanases on the bread-making quality of flours in relation to changes in pentosan properties. *J. Cereal Sci.* 19, 259-272.
- Sagt, C.M.J., Kleizen, B., Verwaal, R., De Jong, M.D.M., Müller, W.H., Smits, A., Visser, C., Boonstra, J., Verkleij, A.J. and Verrips, C.T. (2000). Introduction of an N-glycosylation site increases secretion of heterologous proteins in yeast. *Appl. Environ. Microbiol.* 66, 4940-4944.
- Sambrook, J. and Russell, D.W. (2001). *Molecular cloning: a Laboratory Manual*, Cold Spring Harbor Laboratory Press, Cold Spring Harbor, New York, USA.
- Samuel, D., Kumar, T.K., Ganesh, G., Jayaraman, G., Yang, P.W., Trivedi, V.D., Wang, S.L., Hwang, K.C., Chang, D.K. and Yu, C. (2000). Proline inhibits aggregation during protein refolding. *Protein Sci.* 9, 344-352.
- Sancho, A.I., Faulds, C.B., Svensson, B., Bartolomé, B., Williamson, G. and Juge, N. (2003). Cross-inhibitory activity of cereal protein inhibitors against α -amylases and xylanases. *Biochim. Biophys. Acta* 1650, 136-144.
- Sansen, S., Verboven, C., De Ranter, C.J., Gebruers, K., Brijs, K., Courtin, C.M., Delcour, J.A. and Rabijns, A. (2003). Crystallization and preliminary X-ray diffraction study of wheat (*Triticum aestivum* L.) TAXI-type endoxylanase inhibitor. *Acta Crystallogr. D Biol. Crystallogr.* 60, 555-557.
- Sansen, S., De Ranter, C.J., Gebruers, K., Brijs, K., Courtin, C.M., Delcour, J.A. and Rabijns, A. (2004). Structural basis for inhibition of *Aspergillus niger* xylanase by *Triticum aestivum* xylanase inhibitor-I. *J. Biol. Chem.* 279, 36022-36028.
- Sansen, S. (2005). Towards a better understanding of xylanase inhibition by TAXI-type proteins: a crystallographic study. PhD dissertation, Katholieke Universiteit Leuven, Leuven, Belgium.
- Sarramegna, V., Demange, P., Milon, A. and Talmont, F. (2002). Optimizing functional versus total expression of the human μ -opioid receptor in *Pichia pastoris*. *Protein Exp. Purif.* 24, 212-220.
- Schimoler O'Rourke, R., Richardson, M. and Selitrennikoff, C.P. (2001). Zeamatin inhibits trypsin and α -amylase activities. *Appl. Environ. Microb.* 67, 2365-2366.
- Selitrennikoff, C.P. (2001). Antifungal proteins. *Appl. Environ. Microbiol.* 67, 2883-2894.

- Shakin-Eshleman, S.H., Spitalnik, S.L. and Kasturi, L. (1996). The amino acid at the X position of an Asn-X-Ser sequon is an important determinant of N-Linked core-glycosylation efficiency. *J. Biol. Chem.* 271, 6363-6366.
- Shatters, R.G., Boykin, L.M., Lapointe, S.L., Hunter, W.B. and Weathersbee, A.A. (2006). Phylogenetic and structural relationships of the PR5 gene family reveal an ancient multigene family conserved in plants and select animal taxa. *J. Mol. Evol.* 63, 12-29.
- Shen, Q.J., Casaretto, J.A., Zhang, P. and Ho, T.D. (2004). Functional definition of ABA-response complexes: the promoter units necessary and sufficient for ABA induction of gene expression in barley (*Hordeum vulgare* L.). *Plant Mol. Biol.* 54, 111-124.
- Shevchenko, A., Wilm, M., Vorm, O. and Mann, M. (1996). Mass spectrometric sequencing of proteins silver-stained polyacrylamide gels. *Anal. Chem.* 68, 850-858.
- Shi, X., Karkut, T., Chamankhah, M., Alting-Mees, M., Hemmingsen, S.M. and Hegedus, D. (2003). Optimal conditions for the expression of a single-chain antibody (scFv) gene in *Pichia pastoris*. *Protein Expres. Purif.* 28, 321-330.
- Simpson, D.J., Fincher, G.B., Huang, A.H.C. and Cameron-Mills, V. (2003). Structure and function of cereal and related higher plant (1,4)-b-xylan endohydrolases. *J. Cereal Sci.* 37, 111-127.
- Singer, M.A. and Lindquist, S. (1998). Multiple effects of trehalose on protein folding in vitro and in vivo. *Molecular Cell* 1, 639-648.
- Smith, A.M. and Klugman, K.P. (1997). "Megaprimer" method of PCR-based mutagenesis: the concentration of megaprimer is a critical factor. *Biotechniques* 22, 438-442.
- Soman, K.V., Midoro-Horiuti, T., Ferreon, J.C., Goldblum, R.M., Brooks, E.G., Kurosky, A., Braun, W. and Schein, C.H. (2000). Homology modeling and characterization of IgE binding epitopes of mountain cedar allergen Jun a 3. *Biophys. J.* 79, 1601-1609.
- Sørensen, J.F. and Sibbesen, O. (2006). Mapping of residues involved in the interaction between the *Bacillus subtilis* xylanase A and proteinaceous wheat xylanase inhibitors. *Protein Eng. Des. Sel.* 19, 205-210.
- Sprössler, B.G. (1997). Xylanases in baking. In "The first European symposium on enzymes and grain processing" (S.A.G.F. Angelino *et al.*, eds.), TNO Nutrition and Food Research Institute, Zeist, The Netherlands, 177-187.
- Sreekrishna, K., Brankamp, R.G., Kropp, K.E., Blankenship, D.T., Tsay, J., Smith, P.L., Wierschke, J.D., Subramaniam, A. and Birkenberger, L.A. (1997). Strategies for optimal synthesis and secretion of heterologous proteins in the methylotrophic yeast *Pichia pastoris*. *Gene* 190, 55-62.
- Stevens, D.A., Calderon, L., Martinez, M., Clemons, K.V., Wilson, S.J. and Selitrennikoff, C.P. (2002). Zeamatin, clotrimazole and nikkomyein Z in therapy of a *Candida* vaginitis model. *J. Antimicrob. Chemother.* 50, 361-364.
- Subramaniyan, S. and Prema, P. (2002). Biotechnology of microbial xylanases: enzymology, molecular biology and application. *Crit. Rev. Biotechnol.* 22, 33-64.
- Suomäki, A., Tenkanen, M., Buchert, J. and Viikari, L. (1997). Hemicellulases in the bleaching of chemical pulps. *Adv. Biochem. Eng. Biotechnol.* 57, 261-287.
- Tahir, T.A., Berrin, J.G., Flatman, R., Roussel, A., Roepstorff, P., Williamson, G. and Juge, N. (2002). Specific characterization of substrate and inhibitor binding sites of a glycosyl hydrolase family 11 xylanase from *Aspergillus niger*. *J. Biol. Chem.* 277, 44035-44043.
- Tahir, T.A., Durand, A., Gebruers, K., Roussel, A., Williamson, G. and Juge, N. (2004). Functional importance of Asp37 from a family 11 xylanase in the binding to two proteinaceous xylanase inhibitors from wheat. *FEMS Microbiol. Lett.* 239, 9-15.
- Takeda, S., Sato, F., Ida, K. and Yamada, Y. (1991). Nucleotide sequence of a cDNA for osmotin-like protein from cultured tobacco cells. *Plant Physiol.* 97, 844-846.
- Teleman, A., Tenkanen, M., Jacobs, A. and Dahlman, O. (2002). Characterization of O-acetyl-(4-O-methylglucuronoxylan isolated from birch and beech. *Carbohydr. Res.* 337, 373-377.
- Temussi, P.A. (2002). Why are sweet proteins sweet? Interaction of brazzein, monellin and thaumatin with the T1R2-T1R3 receptor. *FEBS Lett.* 526, 1-4.

- Tenkanen, M., Puls, J. and Poutanen, K. (1992). Two major xylanases from *Trichoderma reesei*. *Enzyme Microb. Technol.* 14, 566-574.
- Törrönen, A., Mach, R.L., Messner, R., Gonzalez, R., Kalkkinen, N., Harkki, A. and Kubicek, C.P. (1992). The two major xylanases from *Trichoderma reesei*: characterization of both enzymes and genes. *Biotechnology* 10, 1461-1465.
- Törrönen, A., Harkki, A. and Rouvinen, J. (1994). Three-dimensional structure of endo-1,4-beta-xylanase II from *Trichoderma reesei*: two conformational states in the active site. *EMBO J.* 13, 2493-2501.
- Törrönen, A. and Rouvinen, J. (1995). Structural comparison of two major endo-1,4-xylanases from *Trichoderma reesei*. *Biochemistry* 34, 847-856.
- Törrönen, A. and Rouvinen, J. (1997). Structural and functional properties of low molecular weight endo-1,4- β -xylanases. *J. Biotechnol.* 57, 137-149.
- Towbin, H., Staehelin, T. and Gordon, J. (1979). Electrophoretic transfer of proteins from polyacrylamide gels to nitrocellulose sheets: procedure and some applications. *Proc. Natl. Acad. Sci. U S A.* 76, 4350-4354.
- Tronsmo, A.M. (1984). Predisposing effects of low temperature on resistance to winter stress factors in grasses. *Acta Agric. Scand.* 34, 210-220.
- Trudel, J., Grenier, J., Potvin, C. and Asselin, A. (1998). Several thaumatin-like proteins bind to beta-1,3-glucans. *Plant Physiol.* 118, 1431-1438.
- Tung, W.L. and Chow, K.C. (1995). A modified medium for efficient electrotransformation of *E. coli*. *Trends Genet.* 11, 128-129.
- Tuomi, T., Ilvesoksa, J., Laakso, S. and Rosenqvist, H. (1993). Interaction of abscisic acid and indole-3-acetic acid-producing fungi with *Salix* leaves. *J. Plant Growth Regul.* 12, 149-156.
- Ujiié, M., Roy, C. and Yaguchi, M. (1991). Low-molecular-weight xylanase from *Trichoderma viride*. *Appl. Environ. Microbiol.* 57, 1860-1862.
- Urao, T., Yamaguchi-Shinozaki, K., Urao, S. and Shinozaki, K. (1993). An *Arabidopsis* myb homolog is induced by dehydration stress and its gene product binds to the conserved MYB recognition sequence. *Plant Cell.* 5, 1529-1539.
- Van der Wel, H. and Loeve, K. (1972). Isolation and characterization of thaumatin I and II, the sweet-tasting proteins from *Thaumatococcus daniellii* Benth. *Eur. J. Biochem.* 31, 221-225.
- Van der Wel, H., Iyengar, R.B., van Brouwershaven, J., van Wassenaar, P.D., Bel, W.J. and van der Ouderaa, F.J. (1984). Assignment of the disulphide bonds in the sweet-tasting protein thaumatin I. *Eur. J. Biochem.* 144, 41-45.
- Van Herpen, T.W., Goryunova, S.V., Van der Schoot, J., Mitreva, M., Salentijn, E., Vorst, O., Schenk, M.F., Van Veelen, P.A., Koning, F., Van Soest, L.J., Vosman, B., Bosch, D., Hamer, R.J., Gilissen, L.J. and Smulders, M.J. (2006). Alpha-gliadin genes from the A, B, and D genomes of wheat contain different sets of celiac disease epitopes. *BMC Genomics* 10, 7:1.
- Van Loon, L.C. (1985). Pathogenesis-related proteins. *Plant Mol. Biol.* 4, 111-116.
- Van Loon, L.C. and Van Strien, E.A. (1999). The families of pathogenesis-related proteins, their activities, and comparative analysis of PR-1 type proteins. *Physiol. Mol. Plant Pathol.* 55, 85-97.
- Villatte, F., Hussein, A.S., Bachmann, T.T. and Schmid, R.D. (2001). Expression level of heterologous proteins in *Pichia pastoris* is influenced by flask design. *Appl. Microbiol. Biotechnol.* 55, 463-465.
- Walton, J.D. (1994). Deconstructing the cell wall. *Plant Physiol.* 104, 1113-1118.
- Watanabe, K., Kitamura, K. and Suzuki, Y. (1996). Analysis of the critical sites for protein thermostabilization by proline substitution in oligo-1,6-glucosidase from *Bacillus coagulans* ATCC 7050 and the evolutionary consideration of proline residues. *Appl. Environ. Microbiol.* 62, 2066-2073.
- Wierenga, R.K. (2001). The TIM-barrel fold: a versatile framework for efficient enzymes. *FEBS Lett.* 492, 193-198.
- Wiese, J., Kranz, T. and Schubert, S. (2004). Induction of pathogen resistance in barley by abiotic stress. *Plant Biol. (Stuttg)* 6, 529-536.

- Wilson, I.B.H. (2002). Glycosylation of proteins in plants and invertebrates. *Curr. Opin. Struct. Biol.* 12, 569-577.
- Witty, M. (1990). Preprothaumatin II is processed to biological activity in *Solanum tuberosum*. *Biotechnol. Lett.* 12, 131-136.
- Witty, M. and Harvey, W. (1990). Sensory evaluation of transgenic *Solanum tuberosum* producing recombinant thaumatin II. *NZJ Crop Hortic. Sci.* 18, 77.
- Woloshuk, C.P., Meulenhoff, J.S., Sela-Buurlage, M., van den Elzen, P.J. and Cornelissen, B.J. (1991). Pathogen-induced proteins with inhibitory activity toward *Phytophthora infestans*. *Plant Cell* 3, 619-628.
- Yang, D., Yip, C.M., Huang, T.H.J., Chakrabartty, A. and Fraser, P.E. (1999). Manipulating the amyloid- β aggregation pathway with chemical chaperones. *J. Biol. Chem.* 274, 32970-32974.
- Yang, Y. and Klessig, D.F. (1996). Isolation and characterization of a tobacco mosaic virus-inducible *myb* oncogene homolog from tobacco. *Proc. Natl. Acad. Sci.* 93, 14972-14977.
- Yu, X. and Griffith, M. (1999). Antifreeze proteins in winter rye leaves form oligomeric complexes. *Plant Physiol.* 119, 1361-1369.
- Yu, X. and Griffith, M. (2001). Winter rye antifreeze activity increases in response to cold and drought, but not abscisic acid. *Physiol. Plant.* 112, 78-86.
- Yu, X., Griffith, M. and Wiseman, S.B. (2001). Ethylene induces antifreeze activity in winter rye leaves. *Plant Physiol.* 126, 1232-1240.
- Yun, D., Zhao, Y., Pardo, J.M., Narasimhan, M.L., Damsz, B., Lee, H., Abad, L.R., D'Urzo, M.P., Hasegawa, P.M. and Bressan, R.A. (1997). Stress proteins on the yeast cell surface determine resistance to osmotin, a plant antifungal protein. *Proc. Natl. Acad. Sci. USA* 94, 7082-7087.

Curriculum Vitae

Sigrid Rombouts (born 1977, Turnhout, Belgium) attended secondary high school (Latin-Sciences) at the 'St. Jozefcollege' in Turnhout, Belgium from 1989-1995. She studied Pharmaceutical Sciences at the Katholieke Universiteit Leuven, Belgium and graduated in 2000. In 2001, she obtained a degree in the Advanced studies in Cellular Biotechnology at the same institute after which she started as a researcher for the 'Microbial Malting Technology (MMT)' project under the guidance of Prof. Delcour (Faculty of Bioscience Engineering, K.U.Leuven). In 2002, she continued her research work at the Division of Gene Technology of the same faculty for the 'Xylafun' project. She was awarded a 2-year doctoral grant by the IWT-Vlaanderen (Institute for the Promotion of Innovation through Science and Technology in Flanders) in 2002, which was extended in 2004 for another 2 years. Her PhD training was fulfilled in the Division of Gene Technology, under the guidance of Prof. Volckaert (Faculty of Bioscience Engineering, K.U.Leuven) and Prof. Rabijns (Faculty of Pharmaceutical Sciences, K.U.Leuven).

List of publications

Raedschelders, G., Fierens, K., Sansen, S., **Rombouts, S.**, Gebruers, K., Robben, J., Rabijns, A., Courtin, C.M., Delcour, J.A., Van Campenhout, S. and Volckaert, G. (2005). Molecular identification of wheat endoxylanase inhibitor TAXI-II and the determinants of its inhibition specificity. *Biochem. Biophys. Res. Commun.* 335, 512-522.

Moers, K., Bourgois, T., **Rombouts, S.**, Beliën, T., Van Campenhout, S., Volckaert, G., Robben, J., Brijs, K., Delcour, J.A. and Courtin, C.M. (2006). Alteration of *Bacillus subtilis* XynA endoxylanase substrate selectivity by site-directed mutagenesis. *Enzyme Microb. Tech.*, doi:10.1016/j.enzmictec.2006.12.019.

Fierens, E.¹, **Rombouts, S.**¹, Gebruers, K., Goesaert, H., Brijs, K., Beaugrand, J., Volckaert, G., Van Campenhout, S., Proost, P., Courtin, C.M. and Delcour, J.A. (2007). TLXI, a novel type of xylanase inhibitor from wheat (*Triticum aestivum*) belonging to the thaumatin family. *Biochem. J.*, doi:10.1042/BJ20061291.

Bourgois, T.M., Nguyen, D.V., Sansen, S., **Rombouts, S.**, Beliën, T., Fierens, K., Raedschelders, G., Rabijns, A., Courtin, C.M., Delcour, J.A., Van Campenhout, S. and Volckaert, G. (2007). Targeted molecular engineering of a family 11 endoxylanase to decrease its sensitivity towards *Triticum aestivum* endoxylanase inhibitor types. *J. Biotechnol.*, doi:10.1016/j.jbiotec.2007.02.011.

Beliën, T., Van Campenhout, S., Vanden Bosch, A., Bourgois, T.M., **Rombouts, S.**, Robben, J., Courtin, C.M., Delcour, J.A. and Volckaert, G. (2007). Engineering molecular recognition of endoxylanase enzymes and their inhibitors through phage display. *J. Mol. Recognit.*, accepted for publication.

Van Campenhout, S., Pollet, A., Bourgois, T.M., **Rombouts, S.**, Beaugrand, J., Gebruers, K., De Backer, E., Courtin, C.M., Delcour, J.A. and Volckaert, G. (2007). Unprocessed barley aleurone endo- β -1,4-xylanase X-I is an active enzyme. *Biochem. Biophys. Res. Commun.*, accepted for publication.

¹ Contributed equally